DEPARTAMENTO DE BIOLOGÍA MOLECULAR
FACULTAD DE CIENCIAS
UNIVERSIDAD AUTÓNOMA DE MADRID

TESIS DOCTORAL

PAPEL DE SPRY1 EN LA PATOGÉNESIS DEL SARCOMA DE EWING: IMPLICACIONES PRONÓSTICAS Y TERAPÉUTICAS

Memoria presentada por **Florencia Cidre Aranaz**,
Licenciada en Biotecnología, Máster en Biociencias Moleculares,
para optar al grado de Doctor por la Universidad Autónoma de Madrid.

Director de Tesis: Dr. Fco. Javier Alonso García de la Rosa.

Instituto de Investigación en Enfermedades Raras
Instituto de Salud Carlos III
Madrid, 2016

MINISTERIO
DE ECONOMÍA
Y COMPETITIVIDAD

30 ANIVERSARIO (1986-2016)
Instituto de Salud Carlos III

D. Francisco Javier Alonso García de la Rosa, Doctor en Biología y Científico Titular del Instituto de Salud Carlos III,

CERTIFICA:

que **Florencia Cidre Aranaz**, Licenciada en Biotecnología por la Universidad Francisco de Vitoria, Máster en Biociencias Moleculares por la Universidad Autónoma de Madrid, ha realizado bajo mi dirección el trabajo que lleva por título:

"**Papel de SPRY1 en la patogénesis del sarcoma de Ewing: Implicaciones pronósticas y terapéuticas"**

el cual considero satisfactorio y apto para ser presentado como Tesis Doctoral en el Departamento de Biología Molecular de la Universidad Autónoma de Madrid.

Y para que conste, expido el siguiente certificado en Madrid, a 1 de septiembre de 2016.

Fdo. Fco. Javier Alonso García de la Rosa
Investigador del ISCIII

Cuando emprendas tu viaje a Ítaca
pide que el camino sea largo,
lleno de aventuras, lleno de experiencias. [….]
Ten siempre a Ítaca en tu mente.
Llegar allí es tu destino.
Mas no apresures nunca el viaje.
Mejor que dure muchos años
y atracar, viejo ya, en la isla,
enriquecido de cuanto ganaste en el camino
sin aguardar a que Ítaca te enriquezca.

K. Kavafis. Antología poética, 1999.

A mamá

Agradecimientos

Estos últimos 4 años han estado llenos de experiencias y grandes aprendizajes. Nada de esto habría sido posible sin aquellos que de una forma u otra me han ayudado a llegar hasta aquí y por ello les estoy profundamente agradecida.

En primer lugar quiero agradecer al Dr. Javier Alonso por haber puesto a mi disposición los recursos y conocimientos necesarios para el desarrollo de esta Tesis y por su labor de supervisión a lo largo de estos años.

A las instituciones que me han acogido, el Instituto de Salud Carlos III de Madrid (ISCIII) y el Institut Curie de París, cuyas infraestructuras me han permitido desarrollar estos estudios. A la Red Temática de Investigación Cooperativa en Cáncer (RTICC) por la financiación concedida (RD12/0036/0027). Me gustaría agradecer en especial a la Asociación Pablo Ugarte por su fantástica labor, por haber depositado su confianza en nosotros y por haber financiado de forma sostenida este proyecto (TPY-M 1149/13). Espero que esta Tesis haya contribuido a avanzar un pasito más hacia la consecución de vuestro objetivo.

A la Dra. Sonsoles Hortelano, por haberme dado la oportunidad de descubrir este maravilloso mundo y por todo lo que me ha enseñado a lo largo de los años, tanto a nivel profesional como personal. Para mí siempre serás un gran ejemplo. Al Dr. Alfonso Luque, por abrirme las puertas de su laboratorio en mis inicios y por su infinita paciencia a lo largo de los años, siempre dispuesto a enseñar. He sido muy afortunada de haber podido contar con vosotros. Gracias.

Al Dr. Thomas Grüenewald, que me enseñó a convertir resultados en historias. Las discusiones científicas que hemos mantenido estos últimos años han sido esenciales para mi formación. Al Dr. Olivier Delattre, por haberme aceptado en su laboratorio en el Institut Curie y por haber hecho todo lo posible porque mi estancia allí fuese una gran experiencia formativa.

Al personal de las unidades centrales del ISCIII, en especial a Fernando y Silvia de Microscopía Confocal y a Raquel de Histología cuyas aportaciones han enriquecido el contenido de esta Tesis.

A todos aquellos con los que he tenido la suerte de compartir estos años en el laboratorio y que tanto me han ayudado. A Lau, por todo lo que me ha enseñado, por su dedicación y por las risas compartidas. Para mí siempre serás estrella dorada en culti. A Carlos, por las charlas, la complicidad y por haber podido contar siempre con su apoyo. A Gema, por haberme animado a seguir y por sus buenos consejos. A Lidia y Sandra por todos los buenos momentos dentro y fuera del laboratorio y por haberme ayudado tanto. A Ana, Leti, Patri, Bea, Laura Gon y Cristina de nuestro laboratorio y a Javi Castro, Stefano, Isa, MA, Tere, Ander, Patri, Andrés, Irmina, Fernando, Rafa y Nerea del pasillo. A Anneliene y Frank, que iluminaron mi estancia en París con su alegría. Todos vosotros habéis hecho que este periodo haya sido mucho más fácil y, sin duda, mucho más divertido.

A todos los que me habéis acompañado fuera del ámbito científico. A David, por las aventuras vividas, que han sido muchas y memorables. A Pati, por todos los años de sincera amistad y por todo lo que hemos vivido juntas. A Mónica, por regalarme su música y también por haberme metido en más de un berenjenal.

A Javi, por quererme tan bien. Por haber compartido la escritura conmigo y haberla hecho tan dulce.

A mi familia, por haberme enseñado el valor del esfuerzo y haber sabido apoyarme siempre en cada uno de mis proyectos.

A mi Yoyoyo, por haberme acompañado hasta aquí con sus palabras y su recuerdo. Para mí siempre hay un colibrí en el jardín.

A mamá, por el amor y alas, por haber sido siempre ejemplo de rectitud y coraje y por haberme inculcado los valores que me han permitido culminar esta etapa.

A todos vosotros, mi más sincero agradecimiento.

Resumen

El sarcoma de Ewing se caracteriza por la presencia de translocaciones cromosómicas que originan genes de fusión entre el gen *EWSR1* y diferentes miembros de la familia de factores de transcripción *ETS*, principalmente *FLI1*. El gen de fusión resultante, *EWS-FLI1*, es un factor de transcripción aberrante que desempeña un papel central en el origen del sarcoma de Ewing a través de la regulación transcripcional de otros genes diana.

En esta Tesis mostramos que *Sprouty 1 (SPRY1)*, un inhibidor *downstream* de los receptores del factor de crecimiento fibroblástico (FGFRs) y otros receptores activadores de Ras, es un gen regulado negativamente por EWS-FLI1 en células de sarcoma de Ewing A673. El análisis de la expresión de SPRY1 en una selección de células de sarcoma de Ewing mostró que SPRY1 no se expresa en estas líneas celulares, lo que sugiere que SPRY1 podría actuar como un supresor tumoral en células de sarcoma de Ewing. En concordancia con estos resultados, la re-expresión de SPRY1 inhibió la proliferación, el crecimiento clonogénico y la migración en tres líneas celulares diferentes de sarcoma de Ewing. Además, la re-expresión de SPRY1 inhibió la ruta de señalización de Ras/MAPK/ERK inducida por suero o FGFb. Por otro lado, al tratar las células de sarcoma de Ewing con el inhibidor de FGFR PD173074, se redujo la proliferación inducida por FGFb, la formación de colonias y el crecimiento de tumores *in vivo* de forma dependiente de dosis.

Aunque la expresión de SPRY1 en células de sarcoma de Ewing es baja, SPRY1 se expresa de forma variable en las muestras de tumores primarios. El análisis de una cohorte grande de pacientes indica que los pacientes con tumores que presentaron una expresión mayor de SPRY1 tuvieron un mejor pronóstico.

En resumen, los resultados mostrados en esta Tesis indican que la regulación negativa de SPRY1 mediada por EWS-FLI1 produce una desregulación de la proliferación celular inducida por FGFb, lo que sugiere que la ruta de señalización de FGFR/Ras/MAPK/ERK podría ser una diana interesante para el desarrollo de nuevas aproximaciones terapéuticas para esta devastadora enfermedad.

Summary

Ewing sarcoma is characterized by chromosomal translocations fusing the *EWSR1* gene with various members of the *ETS* family of transcription factors, most commonly *FLI1*. EWS-FLI1 is an aberrant transcription factor driving Ewing sarcoma tumorigenesis by either transcriptionally inducing or repressing specific target genes.

Herein, we showed that *Sprouty 1* (*SPRY1*), which is a physiological negative feedback inhibitor downstream of fibroblast growth factor (FGF) receptors (FGFRs) and other Ras-activating receptors, is an EWS-FLI1 repressed gene. EWS-FLI1 knock-down specifically increased the expression of SPRY1 while other *Sprouty* family members remained unaffected. Analysis of SPRY1 expression in a panel of Ewing sarcoma cells showed that SPRY1 was not expressed in Ewing sarcoma cell lines, suggesting that it could act as a tumor suppressor gene in these cells. In agreement, induction of SPRY1 in three different Ewing sarcoma cell lines functionally impaired proliferation, clonogenic growth and migration. In addition, SPRY1 expression inhibited ERK/MAPK signalling induced by serum and basic FGF (bFGF). Moreover, treatment of Ewing sarcoma cells with the potent FGFR inhibitor PD173074 reduced bFGF-induced proliferation, colony formation and *in vivo* tumor growth in a dose-dependent manner, thus mimicking SPRY1 activity in Ewing sarcoma cells.

Although the expression of SPRY1 was low when compared to other tumors, SPRY1 was variably expressed in primary Ewing sarcoma tumors and higher expression levels were significantly associated with improved outcome in a large patient cohort.

Taken together, our data indicate that EWS-FLI1-mediated repression of SPRY1 leads to unrestrained bFGF-induced cell proliferation, suggesting that targeting the FGFR/Ras/MAPK/ERK pathway can constitute a promising therapeutic approach for this devastating disease.

Índice

Abreviaturas

5-aza	**5-aza**-2'-deoxicitidina
abs	**Abs**orbancia
AD	Dominio activador *(**A**ctivation **d**omain)*
ATRT	Tumor teratoideo/rabdoide atípico (*Atypical **t**eratoid **r**habdoid **t**umor)*
BG-98	NVP-**BG**J3**98** (inhibidor FGFR)
BrdU	**Br**omo**d**esoxi**u**ridina
BSA	Albúmina sérica bovina *(**B**ovine **s**erum **a**lbumin)*
Ca-	**Car**cinoma
c-Cbl	***C**anonical **C**asitas **B**-lineage **l**ymphoma*
CCK	Colecistoquinina (*Chole**c**ysto**k**inin)*
CCLE	***C**ancer **C**ell **L**ine **E**ncyclopedia*
CRD	Dominio rico en cisteínas *(**C**ysteine-**r**ich **d**omain)*
Ct	Ciclo umbral *(**C**ycle **T**hreshold)*
DBD	Dominio de unión al ADN *(**D**NA **B**inding **D**omain)*
DOX	**Dox**iciclina
EAD	Dominio de regulación de secuencia potenciadora *(**E**nhancer **a**ctivation **d**omain)*
EBI	***E**uropean **B**ioinformatics **I**nstitute*
EGF	Factor de crecimiento epidérmico *(**E**pidermal **G**rowth **F**actor)*
EGFR	Receptor de factor de crecimiento epidérmico (*Epidermal **G**rowth **F**actor **R**eceptor)*
ERK1/2	Quinasa regulada por señales extracelulares *1/2 (**E**xtracellular signal-**r**egulated **k**inase 1/2)*
EWS	Sarcoma de Ewing *(**E**wing **s**arcoma)*
ETS	Factor específico de transformación E26 *(**E**26 **t**ransformation-**s**pecific)*
ETS-DBD	Dominio ETS de unión al ADN *(**ETS** **D**NA **b**inding **d**omain)*
EWSR1	Proteína de unión al ARN de sarcoma de Ewing *(**Ew**ing **S**arcoma **R**NA-binding protein **1**)*
FGFb	Factor de crecimiento fibroblástico básico *(**F**ibroblast **G**rowth **F**actor **b**asic)*
FGFR	Receptor de factor de crecimiento fibroblástico básico *(**F**ibroblast **g**rowth **f**actor **r**eceptor)*
FITC	Isotiocianato de fluoresceína *(**F**luorescein **i**so**t**io**c**yanate)*
FOXM1	***Fo**rkhead bo**x** protein **M1***
GEO	***G**ene **E**xpression **O**mnibus*
GIST	Tumor estromal gastrointestinal *(**G**astro**i**ntestinal **s**tromal **t**umor)*
GLI1	Oncogén asociado a glioma, homólogo 1 *(**Gli**oma-Associated Oncogene Homolog **1**)*
GTEx	***G**enotype-**T**issue **Ex**pression*
Grb2	Proteína unida a factor de crecimiento 2 *(**G**rowth factor **r**eceptor-**b**ound protein **2**)*
HDAC	Desacetilasa de histonas *(**H**istone **deac**etylase)*
HGFR	Factor de crecimiento de hepatocitos *(**H**epatocyte **g**rowth **f**actor **r**eceptor)*

HNRNPH1	Ribonucleoproteína nuclear heterogénea H1, *(**H**eterogeneous **N**uclear **R**ibo**n**ucleo**p**rotein **H1**)*
IFN	**I**nter**f**eró**n**
IGF-1	*Factor de crecimiento insulínico 1 (**I**nsulin **G**rowth **F**actor **1**)*
IGF-1R	Receptor de factor de crecimiento insulínico tipo 1 *(**I**nsulin **G**rowth **F**actor **1** **R**eceptor)*
IGFBP-3	Proteína de unión al factor de crecimiento insulínico 3 *(**I**nsulin **G**rowth **F**actor **B**inding **P**rotein **3**)*
IR	Receptor de insulina *(**I**nsulin **r**eceptor)*
LOX	Lisil oxidasa *(**L**ysyl-**ox**idase)*
MAPK	Proteína quinasa activada por mitógenos *(**M**itogen-**A**ctivated **P**rotein **K**inase)*
MSC	Célula madre mesenquimal *(**M**esenchymal **s**tem **c**ell)*
NGF	Factor de crecimiento nervioso *(**N**erve **g**rowth **f**actor)*
NR0B1	Receptor nuclear, subfamilia 0, grupo B, miembro 1 *(**N**uclear **R**eceptor Subfamily **0**, Group **B**, Member **1**)*
NSCLC	Carcinoma de pulmón no microcítico *(**N**on-**s**mall **c**ell **l**ung **c**ancer)*
PD-66	**PD**166**66** (inhibidor de FGFR)
PD-74	**PD**173**74** (inhibidor de FGFR)
PDGFR	Receptor de factor de crecimiento derivado de plaquetas *(**P**latelet-**d**erived **g**rowth **f**actor **r**eceptor)*
PI3K	Fosfatidilinositol 3-quinasa *(**P**hosphatidyl**i**nositide **3**-**k**inases)*
AKT (o PKB)	Proteína quinasa B *(**P**rotein **k**inase **B**)*
PNET	Tumor neuroectodérmico primitivo *(**P**rimitive **N**euro**e**ctodermal **T**umor)*
PRKCB	Proteína quinasa C-ß *(**Pr**otein **k**inase **C-ß**)*
Ras	***Ra**t **S**arcoma Viral Oncogene Homolog*
Rho	Homólogo de Ras *(**R**as **ho**molog)*
RMS	**R**abdo**m**io**s**arcoma
RRM	Motivo de reconocimiento de ARN *(**R**NA **r**ecognition **m**otif)*
RTK	Receptor de tirosina quinasa *(**R**eceptor **T**yrosine **K**inase)*
SFB	**S**uero **f**etal **b**ovino
SFB-TET	**S**uero **f**etal **b**ovino sin **tet**raciclina
SPRED	Proteínas relacionadas con Sprouty con dominio EVH-1 *(**S**prouty-related **pr**oteins with an **E**VH-1 **d**omain)*
SPRY	***Spr**outy*
SRM	Motivo rico en serinas *(**S**erine-**r**ich **m**otif)*
Src	***S**tored **r**esponse **c**hain*
STR	Secuencias cortas repetitivas en serie *(**S**hort **t**andem **r**epeat**s**)*
SU54	**SU54**02 (inhibidor de FGFR)
TAF15	Factor 15 asociado a la proteína de unión a secuencias TATA *(**T**ATA-binding protein-**a**ssociated **f**actor **15**)*
TBP	Proteína de unión a secuencias TATA *(**T**ATA **B**inding **P**rotein)*
TCR	Receptor de células T *(**T** **c**ell **r**eceptor)*
TGFβ	Factor de crecimiento transformante β *(**T**ransforming **G**rowth **F**actor **β**)*
TKB	Dominio de unión a tirosina *(**T**yrosine **k**inase-**b**inding domain)*
TLS	Translocado en liposarcoma *(**T**ranslocated in **l**ipo**s**arcoma)*

TLS/FUS	Translocado en liposarcoma/Fusión *(**T**ranslocated in **L**ipo**s**arcoma/**Fu**sion)*
TR	Represor de tetraciclina *(**T**etracycline **r**epressor*)
uPAR	Receptor del activador de plasminógeno de tipo uroquinasa *(**U**rokinase **p**lasminogen **a**ctivator **r**eceptor)*
VDC/IE	**V**incristina, **D**oxorrubicina, **C**iclofosfamida/**I**fosfamida-**E**topósido
VEGFR	Receptor de factor de crecimiento endotelial vascular *(**V**ascular **e**ndothelial **g**rowth **f**actor **r**eceptor)*
VIDE	**V**incristina, **I**fosfamida, **D**oxorrubicina, **E**topósido
VT	**V**ariante **t**ranscripcional

1. Introducción

Introducción

1.1. Sarcoma de Ewing: características clínicas.

El sarcoma de Ewing es la segunda neoplasia ósea más frecuente en niños y adolescentes, por detrás del osteosarcoma (Gaspar *et al.* 2015). Presenta una incidencia de 3 casos por millón de individuos menores de 15 años y aparece en una proporción ligeramente superior en varones frente a mujeres (3:2). Además, la incidencia es mayor en la población caucásica en comparación con la población asiática o africana (Khoury 2005, Esiashvili *et al.* 2008, Beck *et al.* 2012). Según datos de la Sociedad Española de Hemato-Oncología Pediátricas (SEHOP) y el Registro Español de Tumores Infantiles (RETI) se diagnostican en España aproximadamente 30 nuevos casos al año.

El sarcoma de Ewing aparece normalmente como masas destructivas asociadas a hueso que suelen extenderse al tejido circundante, aunque en un 15% de los casos se desarrollan en tejidos blandos sin asociación a tejidos óseos (Grier 1997). Los huesos más frecuentemente afectados son la pelvis (31%,), el fémur (20%) y la tibia (11%). Entre un 15-30% de los casos presentan metástasis al diagnóstico, localizadas principalmente en el pulmón (50%), huesos (25%) y en médula ósea (25%) (Arvand and Denny 2001).

Desde un punto de vista histológico, el sarcoma de Ewing está formado por una población homogénea de células pequeñas, redondeadas e indiferenciadas con escaso citoplasma y núcleos redondos e hipercromáticos. El sarcoma de Ewing comparte características histopatológicas similares con otras entidades como el tumor de Askin y el tumor neuroectodérmico primitivo (PNET, *Primitive Neuroectodermal Tumor*). Por esta razón, todas estas variantes se las englobaron tradicionalmente bajo el nombre de tumores de la familia Ewing.

El sarcoma de Ewing presenta características histológicas similares a otros tipos de tumores pediátricos como los neuroblastomas, rabdomiosarcomas, los tumores desmoplásicos de células redondas y pequeñas y algunos linfomas (Triche 1988). Por ello, el diagnóstico diferencial se realizaba por exclusión, de forma que los tumores de Ewing se definían como neoplasias de células redondas y pequeñas que carecieran de las características bioquímicas y estructurales de neuroblastos (neuroblastomas), músculo esquelético primitivo (rabdomiosarcoma), células epiteliales (carcinoma) o

células linfoides (linfoma), fundamentalmente presentes en niños y con menor frecuencia en adultos. Actualmente, el diagnostico histológico diferencial se realiza empleando marcadores inmunohistoquímicos como MIC2/CD99, presente en la mayoría de los sarcomas de Ewing (Kovar *et al.* 1990, Perlman *et al.* 1994), aunque no es totalmente específico dado que también se expresa en otros tipos de tumores de células redondas y pequeñas como los rabdomiosarcomas o los sarcomas sinoviales poco diferenciados (Hibshoosh and Lattes 1997, Folpe *et al.* 2000).

A pesar de las mejoras en los tratamientos que se consiguieron en los años 70-80 con la incorporación de la quimioterapia a los regímenes de tratamiento (revisado en Grohar and Helman 2013), los niveles de supervivencia siguen siendo hoy en día inadmisiblemente bajos, especialmente en pacientes con metástasis óseas al diagnóstico o que experimentan una recaída: la supervivencia libre de eventos a 5 años es del 85% en pacientes con enfermedad localizada, mientras que en el caso de presentar metástasis la supervivencia es inferior al 25% (revisado en Hamilton *et al.* 2015, Jackson *et al.* 2016).

Actualmente el sarcoma de Ewing se trata con protocolos complejos que constan de una fase de quimioterapia de inducción, seguida por tratamiento local del tumor mediante cirugía y/o radioterapia y una fase de quimioterapia de consolidación (Rodriguez-Galindo *et al.* 2003). Los protocolos de tratamiento se han ido perfeccionando gracias a la organización de ensayos clínicos cooperativos internacionales. En 1999 se lanzó el programa Euro Ewing para poner en marcha en el contexto de la Unión Europea ensayos clínicos de carácter coordinado, colaborativo e internacional en pacientes con sarcoma Ewing, con el objetivo de contribuir a mejorar la supervivencia de los pacientes. En la actualidad hay dos grandes ensayos clínicos en marcha: el ensayo *Euro Ewing 2012* (EudraCT 2012-002107-17) para nuevos casos diagnosticados y *rEE Cur* (EudraCT 2014-000259-99) para casos recurrentes o refractarios al tratamiento. En el caso de *Euro Ewing 2012*, se está comparando por un lado la combinación VIDE (Vincristina, Ifosfamida, Doxorrubicina, Etopósido) frente a la combinación VDC/IE (Vincristina, Doxorrubicina, Ciclofosfamida e Ifosfamida-Etopósido) y por otro la adición del ácido zoledrónico al tratamiento quimioterapéutico de consolidación. En paralelo se están realizando estudios biológicos para buscar nuevos marcadores

pronósticos para obtener una mejor estratificación de los pacientes y detectar potenciales intolerancias a las terapias.

1.2. Biología celular de los sarcomas de Ewing

La célula de origen del sarcoma de Ewing sigue siendo en la actualidad un tema controvertido para el que, a pesar de los esfuerzos conjuntos, todavía no se ha llegado a un consenso definitivo (Kovar *et al.* 2016). Históricamente, la hipótesis más aceptada era que los tumores de Ewing derivaban de células puripotenciales de la cresta neural, dado que algunos tumores de Ewing presentaban características de tipo neuronal, como la expresión de la enzima catecol acetil transferasa y de la enolasa específica de neurona. Por otro lado, ciertas líneas celulares de Ewing forman dendritas primitivas y expresan proteínas asociadas a neuronas en respuesta a agentes diferenciadores y comparten un perfil de expresión génico semejante al de las células derivadas de la cresta neural (Cavazzana *et al.* 1987, Noguera *et al.* 1992, O'Regan *et al.* 1995, Arvand *et al.* 2001, Staege *et al.* 2004). Recientemente se ha descrito que las células derivadas de la cresta neural son permisivas a la expresión de EWS-FLI1 y son susceptibles a la inmortalización mediada por este oncogén, lo que apoyaría la hipótesis de que las células de sarcoma de Ewing podrían provenir de la transformación de células derivadas de la cresta neural (von Levetzow *et al.* 2011).

Sin embargo, en otros estudios se ha propuesto un posible origen mesenquimal. Según esta teoría, las células madre mesenquimales adultas (MSC; *mesenchymal stem cells*) sufrirían un bloqueo de la diferenciación promovido por EWS-FLI1, que unido a la inducción de otras características tumorigénicas, desencadenaría el desarrollo del sarcoma de Ewing. Hay varios trabajos experimentales que apoyarían esta teoría. Por ejemplo, el silenciamiento de EWS-FLI1 induce la re-expresión de marcadores de MSC (CD44, CD54, CD59 y CD73) así como la diferenciación a adipocitos, osteoblastos y condrocitos, que es una de las principales características de las células madre mesenquimales (Tirode *et al.* 2007). Además, las MSC humanas son permisivas a la expresión de EWS-FLI1 y su sobre-expresión en estas células induce la expresión de marcadores específicos de células de Ewing (Riggi *et al.* 2008) además de conferirles un fenotipo similar al observado en las células de sarcoma de Ewing (Miyagawa *et al.* 2008). Por otro lado, recientemente se ha descrito que en MSC humanas la expresión

ectópica de EWS-FLI1 induce la expresión de genes de células madre embrionarias como *OCT4*, *SOX2*, y *NANOG* (Riggi *et al.* 2010) y del represor *EZH2* (Richter *et al.* 2009). Esto sugiere que EWS-FLI1 podría estar contribuyendo al mantenimiento de un estado indiferenciado en sarcoma de Ewing al regular estos genes propios de células madre (Lessnick and Ladanyi 2012).

Finalmente, dado que por un lado en la médula ósea existen MSC que derivan de progenitores neurales y que las células de la cresta neural presentan la plasticidad propia del linaje mesenquimal, Riggi y colaboradores han sugerido que los dos posibles orígenes (mesenquimal y neural) no tendrían por qué ser excluyentes (Riggi *et al.* 2009).

1.3. Biología molecular de los sarcomas de Ewing.

1.3.1. Características oncogénicas de la proteína de fusión.

Desde un punto de vista molecular, la principal característica de los sarcomas de Ewing es la presencia de una translocación cromosómica que da lugar a la fusión del gen *EWSR1* (*Ewing Sarcoma RNA-binding protein 1*), que pertenece a la familia de proteínas TET (formada por las proteínas *Translocated in liposarcoma (TLS)*, *Ewing sarcoma* (EWS) y *TATA-binding protein-associated factor 15 (TAF15)*) con alguno de los genes que codifican para factores de transcripción de la familia *ETS (E26 transformation-specific)*, como *FLI1*, *ERG*, *FEV*, *E1AF y ETV1*. Asimismo, se ha descrito la fusión del gen *TLS/FUS (Translocated in Liposarcoma/Fusion*), también de la familia TET, con el gen que codifica para el factor de transcripción ERG (**Tabla 1**).

Como se muestra en la **Figura 1**, la proteína EWS tiene un dominio de unión al ARN (RRM: *RNA recognition motif*) en la zona C-terminal y un dominio de activación transcripcional (EAD; *Enhancer activation domain*) en la región N-terminal que contiene múltiples repeticiones de hexapéptidos degenerados (Lessnick *et al.* 1995). FLI1 (al igual que el resto de factores de transcripción ETS) tiene un dominio de unión al ADN (DBD, *DNA Binding Domain*) que reconoce específicamente secuencias GGAA/T en el ADN (Donaldson *et al.* 1994, Truong and Ben-David 2000) y un dominio de transactivación en el N-terminal (AD). Al formarse la proteína de fusión, el

dominio de transactivación de FLI1 es reemplazado por la región N-terminal de EWS que contiene el dominio de transactivación, dando lugar a EWS-FLI1, que tiene una capacidad de activación transcripcional muy superior a la de FLI1 nativo (May *et al.* 1993b).

Tabla 1. Tipos de translocaciones y los genes de fusión correspondientes encontrados más frecuentemente en sarcoma de Ewing

Tipo de Translocación	Gen de fusión	Frecuencia	Referencia
t(11;22)(q24;q12)	EWS-FLI1	90-95 %	Delattre *et al.* 1992
t(21;22)(q22;q12)	EWS-ERG	5-10 %	Zucman *et al.* 1993, Sorensen *et al.* 1994
t(7;22)(p22;q12)	EWS-ETV1	< 1 %	Jeon *et al.* 1995
t(2;22)(q33;q12)	EWS-FEV	< 1 %	Peter *et al.* 1997
t(17;22)(q12;q12)	EWS-E1AF	< 1 %	Kaneko *et al.* 1997, Urano *et al.* 1998
t(16;21)(p11;q22)	FUS-ERG	< 1 %	Shing *et al.* 2003

Por otro lado, la implicación de diferentes combinaciones de exones da lugar a distintos tipos de fusiones. La fusión denominada de tipo I es la más frecuente y consiste en la fusión del exón 7 de *EWSR1* con el exón 6 de *FLI1*. Se han descrito 12 tipos más de fusiones EWS-FLI1 y al menos 5 tipos de fusiones EWS-ERG (Zucman *et al.* 1993, Zoubek *et al.* 1994, Ginsberg *et al.* 1999).

Actualmente se sabe que las proteínas de fusión EWS-ETS se localizan en el núcleo y se unen al ADN a través del reconocimiento de secuencias específicas, actuando como activadores o represores de la transcripción (Erkizan *et al.* 2010). Sin embargo, estos factores de transcripción quiméricos requieren también de la participación de otras proteínas para desempeñar su función, como el factor de transcripción AP-1 (Kim *et al.* 2006) o la ARN helicasa A, que actúa como un cofactor transcripcional (Toretsky *et al.* 2006). Además, en los tumores de la familia Ewing, estas translocaciones características pueden ir acompañada de otras alteraciones genéticas como la deleción en homocigosis del locus p16, presente en el 20-30% de los tumores de Ewing (Kovar *et al.* 1997), la translocación t(1;16) en el 20% de los casos, deleciones en 1p36 en el 18% de los casos,

ganancias cromosómicas del cromosoma 8 (trisomía) en el 35-55% de los casos y del cromosoma 12 en el 25% de los casos (Armengol *et al.* 1997, Hattinger *et al.* 1999) y ganancias en 1q (1qG) (Mackintosh *et al.* 2012).

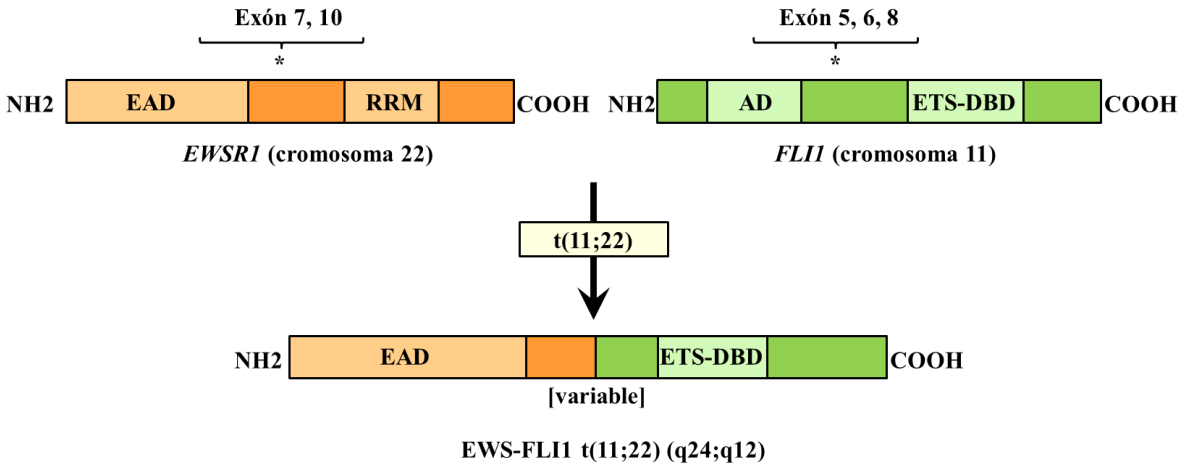

Figura 1. Esquema de la fusión EWS-FLI1 producida por la translocación t(11;22)(q24;q12) en sarcomas de Ewing. La fusión EWS-FLI1 se genera por la unión del dominio activador de *EWSR1 (EAD)* localizado en la región N-terminal, que contiene múltiples repeticiones de hexapéptidos degenerados, y el dominio ETS de unión al ADN en la región C-terminal (ETS-DBD; *ETS DNA binding domain*) de *FLI1*. El motivo de reconocimiento a ARN de EWS (RRM; *RNA recognition motif*) y el dominio activador de FLI1 (AD; *activation domain*) no forman parte de la fusión. Los diferentes tipos de fusiones se generan por variaciones en los puntos de ruptura de los cromosomas, que dan lugar a la fusión de diferentes exones de cada una de las proteínas que originan la fusión (asteriscos) (Modificado de Anderson *et al.* 2012).

El mantenimiento del fenotipo tumoral en el sarcoma de Ewing depende fundamentalmente de la expresión de EWS-FLI1. Este hecho ha quedado suficientemente demostrado a lo largo de los últimos años mediante el empleo de diferentes estrategias experimentales. Así, varios estudios han demostrado que la inhibición de EWS-FLI1 en células de Ewing mediante la utilización de ARN antisentido o ARN de interferencia inhibía la proliferación, aumentaba la susceptibilidad a la apoptosis y limitaba la capacidad transformante *in vitro* e *in vivo* (Ouchida *et al.* 1995, Kovar *et al.* 1996, Tanaka *et al.* 1997, Toretsky *et al.* 1997, Lambert *et al.* 2000, Hu-Lieskovan *et al.* 2005). Por otro lado, la expresión de la proteína de fusión EWS-FLI1 en fibroblastos normales de ratón resulta suficiente para desencadenar la adquisición de características propias de las células tumorales como el crecimiento independiente de anclaje o la formación de tumores histológicamente similares al sarcoma de Ewing en ratones inmunodeprimidos, mientras que la expresión

de FLI1 nativo carece de ese efecto (May *et al.* 1993a, May *et al.* 1993b, Yi *et al.* 1997, Thompson *et al.* 1999).

Como hemos mencionado anteriormente, las propiedades oncogénicas de EWS-FLI1 dependen de su capacidad de unión al ADN, que reside en la región C-terminal derivada del miembro de la familia ETS que forma parte de la proteína de fusión. De hecho, la inactivación de este dominio provoca una reducción de la capacidad transformante de la proteína quimérica (May *et al.* 1993b, Jaishankar *et al.* 1999). Por otro lado, EWS-FLI1 es capaz de activar la transcripción a través del dominio N-terminal de EWS (May *et al.* 1993a, Ohno *et al.* 1993, Bailly *et al.* 1994, Mao *et al.* 1994) dado que la deleción de este dominio transactivador reduce el potencial oncogénico de EWS-ETS (Lessnick *et al.* 1995).

La regulación de la transcripción de otros genes es determinante para el desarrollo de los tumores de Ewing y puede ocurrir de forma directa o indirecta. Cuando la regulación es directa, EWS-FLI1 se une a motivos ETS o a repeticiones de elementos GGAA de determinados microsatélites que se localizan cerca de los promotores de los genes que regula. Estos microsatélites se encuentran en mayor proporción cerca de los genes inducidos por EWS-FLI1. Por el contrario, estos elementos de respuesta GGAA no se encuentran cerca de los promotores de los genes reprimidos por EWS-FLI1. Además, se ha visto que la activación de la transcripción depende del número de repeticiones GGAA presentes en el promotor de los genes regulados y que una unión cooperativa o un aumento en la probabilidad de unión debido a la alta concentración de sitios de unión podrían explicar esta correlación (Gangwal *et al.* 2008, Garcia-Aragoncillo *et al.* 2008, Guillon *et al.* 2009, Gangwal *et al.* 2010, Bilke *et al.* 2013, Grunewald *et al.* 2015).

Por otro lado, aunque EWS-FLI1 y FLI1 poseen el mismo dominio de unión al ADN, en realidad se unen a regiones diferentes del genoma. Esto se debe a que EWS-FLI adquiere la capacidad de alterar la cromatina, generando una depleción de nucleosomas de ciertas regiones genómicas diana que da lugar a la desregulación transcripcional característica del sarcoma de Ewing (Patel *et al.* 2012). Estos eventos de remodelación de la cromatina mediados por EWS-FLI1 pueden consistir en el desplazamiento de otros factores de transcripción nativos más activos, en el caso de genes reprimidos; o bien en abrir la cromatina y reclutar complejos de remodelación de la cromatina a zonas que

previamente carecían de función reguladora para el caso de genes inducidos por EWS-FLI1 (Riggi *et al.* 2014).

Recientemente se ha descrito que EWS-FLI1 posee un efecto sobre el epigenoma de la célula de Ewing: mediante técnicas de ChIP-seq (*Chromatin Immunoprecipitation-sequencing*) se ha demostrado que la inhibición de la expresión de EWS-FLI1 en células de sarcoma de Ewing genera cambios importantes en las marcas epigenéticas de promotores, *enhancers* y *super enhancers*, siendo la acetilación de la histona H3K27 la marca más afectada (Tomazou *et al.* 2015).

En resumen, existen varios mecanismos, tanto directos como indirectos a través de los cuales EWS-FLI1 es capaz de modular la expresión génica y, en consecuencia, regular el proceso tumoral.

1.3.2. Genes diana de EWS-FLI1: oportunidades terapéuticas

Actualmente existe una necesidad acuciante de encontrar nuevas terapias dirigidas que ofrezcan una mayor eficacia y menores efectos adversos que las terapias convencionales centradas en la quimio y radioterapia usadas hasta el momento. En este sentido, resulta clave ampliar el conocimiento de las bases moleculares implicadas en la patogénesis del sarcoma de Ewing con el objetivo de diseñar nuevas terapias biológicas dirigidas.

EWS-FLI1 induce una desregulación masiva de la expresión génica en sarcoma de Ewing mediante la inducción o inhibición a nivel transcripcional de numerosos genes diana, muchos de los cuales están implicados en el proceso oncogénico (revisado en Lessnick and Ladanyi 2012, Kovar 2014, Cidre-Aranaz and Alonso 2015). Por ejemplo, EWS-FLI1 induce la expresión de *NR0B1* (*DAX1*), *TOPK*, *EGR2*, *NKX2.2*, *CCK*, *PRKCB* y *STEAP1* (Smith *et al.* 2006, Carrillo *et al.* 2007, Garcia-Aragoncillo *et al.* 2008, Herrero-Martin *et al.* 2009, Grunewald *et al.* 2012, Grunewald *et al.* 2015, Surdez *et al.* 2012), mientras que inhibe la expresión de otros genes como *IGFBP3*, *LOX*, *DKK1* o *TGF-beta RII* (Hahm *et al.* 1999, Prieur *et al.* 2004, Navarro *et al.* 2010, Agra *et al.* 2013).

A continuación se describen algunos genes diana de EWS-FLI1 que podrían emplearse como punto de partida para el desarrollo de abordajes terapéuticos más específicos:

- La opción posiblemente más evidente consistiría en bloquear la expresión del factor de transcripción EWS-FLI1 o inhibir su actividad. Este abordaje se ha llevado a cabo con éxito *in vitro* y en modelos animales mediante la utilización de tecnologías de ARN de interferencia o similares (Ouchida *et al.* 1995, Kovar *et al.* 1996, Tanaka *et al.* 1997, Toretsky *et al.* 1997, Yi *et al.* 1997, Lambert *et al.* 2000, Prieur *et al.* 2004, Hu-Lieskovan *et al.* 2005). Sin embargo, su aplicación clínica requiere el desarrollo de tecnologías más seguras y efectivas. Por otro lado, el desarrollo de fármacos contra EWS-FLI1 es una tarea compleja debido a que se trata de un factor de transcripción y por tanto de localización nuclear. En este sentido, Barber-Rotenberg y colaboradores han demostrado recientemente que otra de las funciones oncogénicas de EWS-FLI1 es la alteración del *splicing* de ARN y que este efecto puede ser inhibido por una molécula pequeña llamada YK-4-279 que interacciona con la ARN helicasa A (Barber-Rotenberg *et al.* 2012). Sin embargo, actualmente se desconoce su sitio de unión exacto a EWS-FLI1 y no se ha visto que su utilización tenga un impacto en la regulación transcripcional de otros genes dianas de EWS-FLI1 (Kovar *et al.* 2016). Recientemente se ha analizado también el efecto de los análogos de mitramicina, un antineoplásico que ya se había testado previamente en sarcoma de Ewing con buenos resultados pero elevada toxicidad en ensayos clínicos en fase II, y se ha visto que dos de ellos (EC-8105 y EC-8042) inhiben la actividad transcripcional de EWS-FLI1 y la formación de tumores en modelos de xenotransplante *in vivo*, por lo que podrían representar buenas aproximaciones terapéuticas (Osgood *et al.* 2016). También se ha estudiado el efecto de la trabectedina (ET-743, Yondelis), ya aprobado en Europa para el tratamiento de sarcomas de tejido blando. En sarcoma de Ewing se ha visto que la trabectedina inhibe la actividad transcripcional de EWS-FLI1 (Grohar *et al.* 2011). Este compuesto ha sido estudiado en un ensayo clínico de fase II en pacientes en recaída y se ha visto que la trabectedina no presentaba suficiente actividad como para ser empleado como agente único (Baruchel *et al.* 2012). Sin embargo, recientemente se ha descrito que su uso en combinación con olaparib (un inhibidor de PARP) podría aumentar la sensibilidad *in vitro* e *in vivo* al tratamiento en sarcoma de Ewing (Ordonez *et al.* 2015), lo que podría suponer una nueva posibilidad para la

utilización de este fármaco. Por otro lado, Grohar y colaboradores identificaron que el *splicing* de los transcritos primarios de EWS-FLI1 mediado por elementos de la maquinaria de *splicing* como HNRNPH1 (ribonucleoproteína nuclear heterogénea H1) es necesario para la correcta expresión de EWS-FLI1 y que el *knock-down* de HNRNPH1 altera la expresión de la proteína EWS-FLI1 y la posterior transcripción regulada por ella (Grohar *et al.* 2016). Esto sugiere que el procesamiento del ARNm de EWS-FLI1 podría ser una interesante diana en sarcoma de Ewing.

- La ruta del **IGF-1** (*Insulin Growth Factor 1*) es clave para la supervivencia celular de los tumores de Ewing y algunos de sus elementos, como la IGFBP-3 (*Insulin Growth Factor Binding Protein 3*), son regulados por EWS-FLI1 (Yee *et al.* 1990, Mitsiades *et al.* 2004, Prieur *et al.* 2004, Kim *et al.* 2005). Varios estudios preclínicos han evaluado el efecto terapéutico de la quimioterapia convencional en combinación con anticuerpos específicos dirigidos contra el receptor de IGF-1 (IGF-1R) (Kolb *et al.* 2008, Olmos *et al.* 2010) o inhibidores de su actividad tirosina quinasa como NVP-AEW541 o NVP-ADW742 (Benini *et al.* 2001, Scotlandi *et al.* 2002b, Martins *et al.* 2006, Manara *et al.* 2007). Lamentablemente, los buenos resultados obtenidos en estos estudios, no se han visto reproducidos en los ensayos clínicos en pacientes (Gaspar *et al.* 2015).
- ***NR0B1*** (*Nuclear Receptor Subfamily 0, Group B, Member 1*), es una diana directa de EWS-FLI1 que se expresa a elevados niveles en sarcoma de Ewing y cuya inhibición reduce la proliferación celular y el crecimiento tumoral *in vivo* (Garcia-Aragoncillo *et al.* 2008). Por ello, una posible estrategia podría consistir en la inhibición farmacológica de *NR0B1* (Cidre-Aranaz and Alonso 2015).
- ***CCK*** (*Cholecystokinin*) es un neuropéptido inducido por EWS-FLI1 que actúa como un factor autocrino para las células de sarcoma de Ewing. Un antagonista de los receptores de CCK (*Devazepide*) mostró ciertos efectos antitumorigénicos *in vitro* e *in vivo* (Carrillo *et al.* 2007, Carrillo *et al.* 2009).
- ***LOX*** (Lisil-oxidasa), es un gen fuertemente reprimido por EWS-FLI1 (Agra *et al.* 2013), expresado a muy bajos niveles en sarcoma de Ewing. Uno de los fragmentos de la proteína, denominado propéptido de LOX (LOX-PP) posee actividad antitumoral en sarcoma de Ewing (Agra *et al.* 2013). Este péptido podría administrarse solo o en combinación con quimioterapia tradicional (Cidre-Aranaz and Alonso 2015).

- ***PRKCB*** (*protein kinase C-ß*) es una diana directa de EWS-FLI1 inducida en sarcoma de Ewing y responsable de la fosforilación de la histona H3T6 cuya inhibición induce apoptosis *in vitro* e inhibe el desarrollo tumoral *in vivo* de esta neoplasia (Surdez *et al.* 2012). Se ha observado que el tratamiento con el inhibidor de PRKCB enzastaurina o la inhibición de su expresión mediante ARN de interferencia disminuye significativamente el tamaño de los tumores en modelos de xenotransplante (Surdez *et al.* 2012).
- ***FOXM1*** (*Forkhead box protein M1*), es un gen inducido por EWS-FLI1 y su inhibición reduce la tumorigenicidad de las células de sarcoma de Ewing *in vitro* (Gartel 2011). Desde un punto de vista terapéutico, se ha visto que el tratamiento con tiostreptona, un antibiótico natural, bloquea la expresión de FOXM1 en las células de sarcoma de Ewing, disminuyendo así sus características oncogénicas (Gartel 2011).

En resumen, el estudio de genes diana de EWS-FLI1 ha contribuido a aumentar el conocimiento sobre esta devastadora enfermedad y ha posibilitado el análisis de nuevas terapias que podrían ser de utilidad para el tratamiento del sarcoma de Ewing.

1.4. La vía de señalización RTK/Ras/ERK en cáncer

El mantenimiento y la proliferación de las células tumorales depende en gran medida de la activación autocrina o paracrina de receptores de factores de crecimiento. Los receptores de tirosina quinasa (RTK; *Receptor Tyrosine Kinase*) son una familia de proteínas de la membrana celular que actúan como receptores de factores de crecimiento, hormonas, citoquinas, factores neurotróficos y otras moléculas extracelulares (revisado en Regad 2015). Los RTK son mediadores de vías de señalización involucradas en proliferación celular, diferenciación, supervivencia y migración celular (revisado en Lemmon and Schlessinger 2010).

La familia de RTK incluye varias subfamilias: los receptores de los factores de crecimiento epidérmicos (*epidermal growth factor receptors* (EGFR)), receptores de los factores de crecimiento fibroblástico (*fibroblast growth factor receptors* (FGFR)), receptores de insulina y de factores de crecimiento insulínicos (*insulin* y *insulin-like growth factor receptors* (IR y IGFR)), receptores de los factores de crecimiento derivados de plaquetas (*platelet-derived growth factor receptors* (PDGFR)), receptores

de los factores de crecimiento vascular endotelial (*vascular endothelial growth factor receptors* (VEGFR)), receptores de los factores de crecimiento de hepatocitos (*hepatocyte growth factor receptors* (HGFR)), y el proto-oncogén c-KIT (Li and Hristova 2006, Hubbard and Miller 2007).

Muchos tumores presentan mutaciones que afectan a la actividad de RTKs o a los componentes *downstream* de la vía de señalización, como las MAP quinasas (MAPK; *Mitogen-Activated Protein Kinases*) o PI3K/AKT *(phosphatidylinositide 3-kinases/Protein kinase B)*, desregulando la proliferación, supervivencia, capacidad invasiva y metastásica de las células y desencadenando la transformación maligna (revisado en Low and Zhang 2016).

En el caso particular del sarcoma de Ewing, uno de los efectos de la translocación EWS-FLI1 es la desregulación de la ruta de señalización mediada por IGF-1R (*insulin growth factor 1 receptor*), lo que contribuye en gran medida al mantenimiento del fenotipo tumoral de estas neoplasias (Karnieli *et al.* 1996, Scotlandi *et al.* 1998, Scotlandi *et al.* 2002a, Leavey and Collier 2008, Herrero-Martin *et al.* 2009). Esto ha convertido a la ruta de IGF-1R en una posible diana terapéutica en el sarcoma de Ewing que ha sido testada en numerosos ensayos clínicos mediante el empleo de diferentes drogas, incluyendo anticuerpos monoclonales contra IGF-1R y antagonistas específicos, aunque de momento los resultados no han sido tan favorables como se esperaba (Olmos *et al.* 2010, Naing *et al.* 2012, Schoffski *et al.* 2013, Pappo *et al.* 2014).

Por otro lado, ERK1/2 (*Extracellular signal-regulated kinase 1/2*), otro de los componentes fundamentales de la ruta RTK/Ras/ERK, se encuentra activado de forma aberrante en un tercio de los cánceres humanos (Schubbert *et al.* 2007). Es interesante destacar además que la mayoría de los eventos pro-oncogénicos que dan lugar a la activación constitutiva de la señalización de ERK1/2 ocurren *upstream* ERK1/2, a nivel del RTK o de mutaciones en Ras (revisado en Schubbert *et al.* 2007). Por ello, tanto ERK1/2 como sus moduladores se mantienen bajo una estricta regulación positiva y negativa.

Uno de los activadores de esta ruta de MAPK es FGF (*Fibroblast Growth Factor*). En los últimos años han surgido varios estudios que están poniendo de manifiesto la

importancia de las rutas de señalización mediadas por FGF en la patogénesis del sarcoma de Ewing. Por ejemplo, se ha visto que FGFb (*basic Fibroblast Growth Factor*) aumenta la proliferación de las células de Ewing *in vitro* y que *EGR2*, un componente *downstream* de la ruta de FGF, es un gen inducido por EWS-FLI1 (Grunewald *et al.* 2015). En otros estudios se ha demostrado que FGFb regula la movilidad e invasividad de las células de Ewing en el microentorno óseo (Kamura *et al.* 2010) y que la deleción constitutiva de *FGFR1* inhibe la implantación de xenotransplantes de sarcoma de Ewing en ratones (Agelopoulos *et al.* 2015). Finalmente, cerca del 75% de las biopsias de sarcoma de Ewing presentan niveles de fosforilación de FGFR1 moderados o altos (Kamura *et al.* 2010), a pesar de que las mutaciones activadoras de FGFR1 son muy infrecuentes en esta enfermedad (Agelopoulos *et al.* 2015). Estos estudios indican que la ruta del FGF puede ser una de las rutas de RTKs más relevantes en sarcoma de Ewing.

Uno de los reguladores negativos fundamentales de la señalización mediada por FGF es la familia de proteínas *Sprouty* (SPRY) (Masoumi-Moghaddam *et al.* 2014b) (**Figura 2**). La unión de FGF a su receptor genera una activación de la familia de quinasas Src, que a su vez activan a SPRY por fosforilación (Mason *et al.* 2004). Una vez activado, SPRY secuestra a la molécula adaptadora Grb2 *(Growth factor receptor-bound protein 2)*, que interacciona con SOS (*Son of Sevenless*). SOS es un factor encargado del intercambio GDP-GTP en Ras, generando así la transducción de la señalización de los receptores RTK hacia la activación de la ruta MAPK (Casci *et al.* 1999, Gross *et al.* 2001, Hanafusa *et al.* 2002). Dado que la activación de Ras es esencial para la señalización por MAPK, al interrumpir la señalización de RTKs a nivel de la activación de Ras, SPRY actúa como un inhibidor de la ruta de MAPK.

La relación entre SPRY1 y la activación de esta ruta de MAPK por FGF en mamíferos ha sido descrita en varios estudios donde se ha visto, por ejemplo, que durante la organogénesis SPRY1 y -2 antagonizan la señalización por FGF durante el desarrollo embrionario del oído limitando su crecimiento (Mahoney Rogers *et al.* 2011). Además, SPRY1 está implicado en el control de la proliferación y la diferenciación celular en cáncer. Por ejemplo, en cáncer de próstata, donde hay una sobreexpresión de FGF, se cree que los bajos niveles de SPRY1 favorecen una traducción descontrolada de la señal de este factor de crecimiento, fomentando así la progresión tumoral (Kwabi-Addo *et al.*

2004). En muestras clínicas de mama se ha observado que en tejido sano SPRY1 y FGF8 mantienen sus niveles de expresión y que en el tejido tumoral cercano, la expresión de FGF8 incrementa mientras que la de SPRY1 baja drásticamente (Lo *et al.* 2004). Es interesante mencionar también que durante la embriogénesis su expresión coincide espacialmente con la de los centros de señalización de FGF (de Maximy *et al.* 1999, Minowada *et al.* 1999, Chambers and Mason 2000), lo que vuelve a poner de manifiesto la relación entre las proteínas SPRY y las rutas de señalización dependientes de FGF.

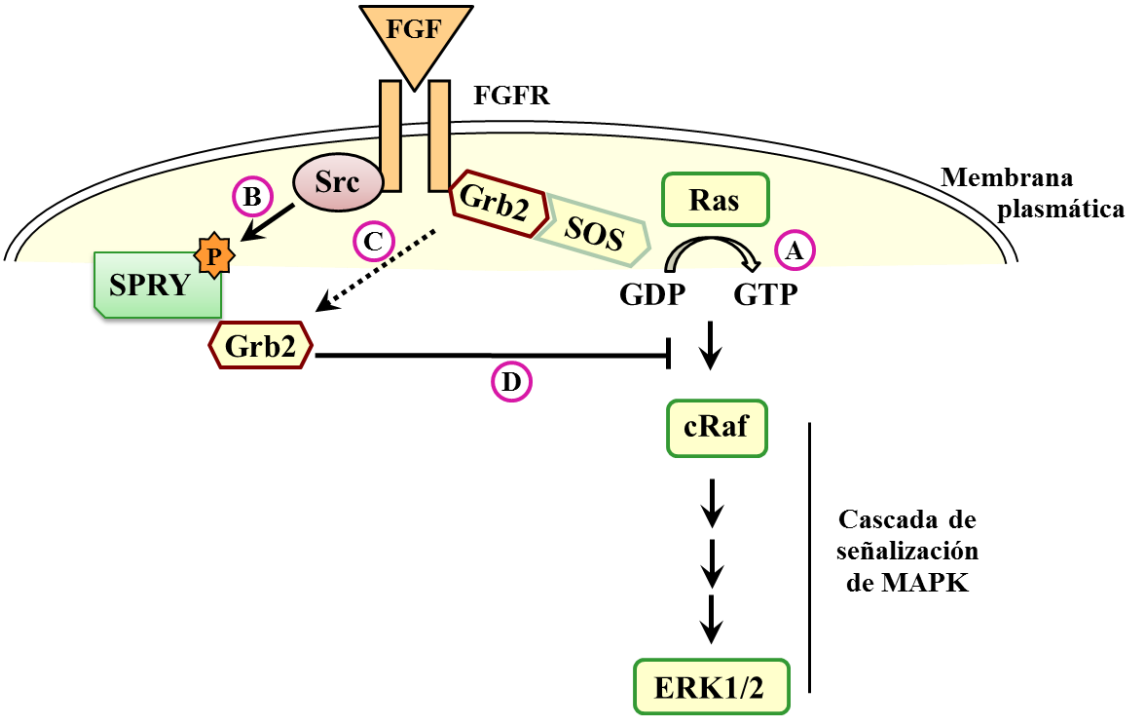

Figura 2. Regulación negativa de la ruta de señalización Ras/MAPK/ERK inducida por FGF mediante SPRY1. (A) La activación del receptor de tirosina quinasa (FGFR) por su ligando (FGF) da lugar a la activación de Grb2 por fosforilación que permite el acoplamiento de SOS. SOS convierte Ras-GDP en Ras-GTP, generando la consiguiente activación de la cascada de MAPK. **(B)** Por otro lado, la activación de FGFR también genera la activación Src, que a su vez activa SPRY por fosforilación (P). **(C)** SPRY1 activado secuestra Grb lo que produce **(D)** la inhibición de la cascada de señalización de la ruta de MAPK activada por FGF. Modificado de Assinder *et al.* (Assinder *et al.* 2015).

Se puede concluir entonces que existe una relación importante entre SPRY1 y FGF y que esta podría ser relevante en la patogénesis del sarcoma de Ewing.

A continuación vamos a describir en detalle las características de la proteína SPRY1, así como sus funciones fisiológicas y su rol en cáncer.

1.5. *Sprouty 1* (SPRY1)

1.5.1. Características moleculares de SPRY1 y otros miembros de la familia de proteínas *Sprouty*.

El primer miembro de la familia de proteínas *Sprouty* se descubrió en 1998 mientras se realizaba una búsqueda de los genes implicados en el desarrollo y la formación de la tráquea durante la fase embrionaria en *Drosophila* (Hacohen *et al.* 1998), observándose que las moscas deficientes en dSpry presentaban excesivas ramificaciones de la tráquea, de ahí el nombre. Posteriormente se demostró que se trataba de una proteína intracelular asociada a membrana que actuaba como un inhibidor de la ruta de señalización RTK/Ras/ERK *downstream* de varios factores de crecimiento como FGF y EGF (*Epidermal Growth Factor*) (Casci *et al.* 1999).

En mamíferos, la familia de proteínas *Sprouty* está compuesta por 4 miembros (SPRY1-4) que comparten varias regiones conservadas (Minowada *et al.* 1999): un dominio rico en cisteínas muy conservado (CRD, *cysteine-rich domain*) de aproximadamente 110 residuos, que contiene 22 cisteínas en la región C-terminal; un motivo de unión a tirosina quinasa (TKB, *tyrosine kinase-binding*) de c-Cbl (*canonical Casitas B-lineage lymphoma*) en torno a una tirosina (Y53 en SPRY1, Y55 en SPRY2, Y27 en SPRY3 y Y53 en SPRY4); y un dominio rico en serinas (SRM, *serine-rich motif*) en la región N-terminal (Guy *et al.* 2009) (**Figura 3**). El dominio rico en cisteínas también está presente en otra familia de proteínas llamadas SPRED (*Sprouty-related proteins with an EVH-1 domain*), que en mamíferos está formada por 4 miembros (SPRED1-3 y EVE-3) y que también actúan como inhibidores de la fosforilación de ERK mediada por FGF o NGF (*nerve growth factor*) (Wakioka *et al.* 2001). La función del dominio CDR es mediar la homo y heterodimerización entre los miembros de la familia (Ozaki *et al.* 2005) y favorecer la localización de las proteínas en la membrana, influenciando así su función (Casci *et al.* 1999, Lim *et al.* 2000). De hecho, se ha observado que si bien las proteínas no dimerizadas son capaces de inhibir la ruta Ras/MAPK/ERK, el efecto inhibitorio es aún mayor cuando las proteínas forman heterodímeros (y en menor medida homodímeros) (Ozaki *et al.* 2005). En cuanto a la tirosina del dominio de activación, se sabe que su actividad depende de la fosforilación mediada por la tirosina quinasa Src (*Stored response chain)* y que esta fosforilación es necesaria para inhibir la señalización a través de la ruta Ras/MAPK/ERK (Li *et al.* 2004). Finalmente, el

dominio rico en serinas forma una "bisagra" implicada en el mantenimiento de la estructura tridimensional de las proteínas de la familia Sprouty (Guy *et al.* 2009).

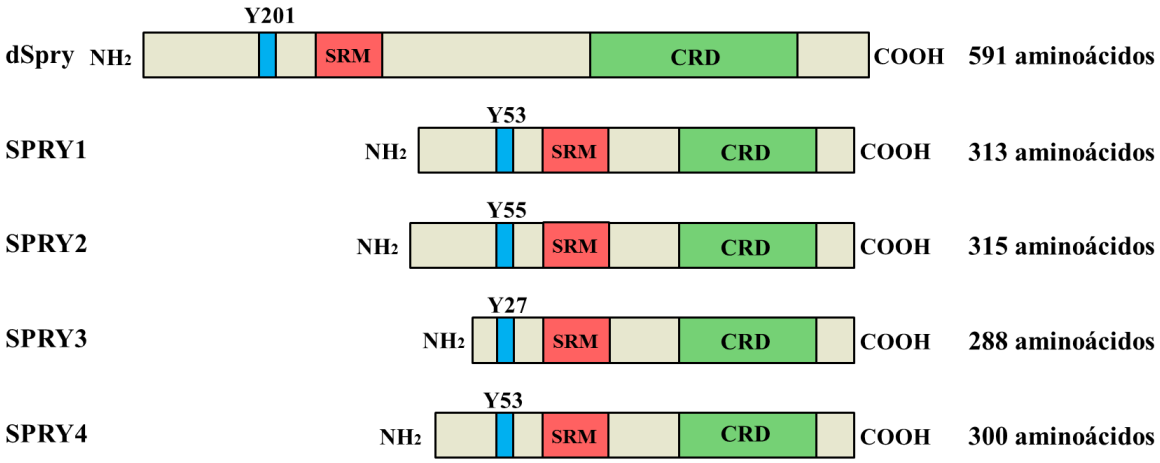

Figura 3. Estructura de la familia de proteínas Sprouty en *Drosophila* y en mamíferos. Se muestra una representación esquemática de los dominios conservados en la familia de proteínas Sprouty incluida la tirosina (Y), que se fosforila por Src en respuesta a factores de crecimiento y el motivo rico en serinas (SRM; *serine-rich motif*) conservados en el N-terminal. En la región C-terminal se muestra el dominio conservado rico en cisteinas (CRD; *cysteine-rich domain*). Se indica también el tamaño en aminoácidos de cada una de las proteínas.

Los diferentes miembros de la familia difieren en su distribución tisular y en las proteínas con las que interaccionan, como c-Cbl, Grb2, Raf1, FRS2, caveolina-1, TESK1 y PTP1B (Christofori 2003).

1.5.2. SPRY1: funciones fisiológicas

Las proteínas *Sprouty* son inhibidoras de la señalización mediada por factores de crecimiento. Así, la deleción de *SPRY* en modelos murinos da lugar a una serie de anormalidades fenotípica relacionadas con la hiperactivación de la señalización por RTKs, que confirman la importancia de estas proteínas durante la organogénesis. De este modo, la deleción de *SPRY1* genera defectos en el tracto urinario y un aumento de la activación de ERK (Basson *et al.* 2005, Basson *et al.* 2006), la deleción de *SPRY2* provoca alteraciones en el desarrollo del oído interno (Shim *et al.* 2005) y la deleción de *SPRY4* genera un retraso en el crecimiento y polisindactilia (Taniguchi *et al.* 2007). Asimismo, en otros estudios se ha descrito que SPRY2 y -4 están relacionados con la

formación de diastemas debido a la inhibición de la señalización de FGF (Klein *et al.* 2006). Por otro lado, las proteínas de la familia *Sprouty* también regulan negativamente la señalización mediada por interferón (IFN) y se ha descrito que al inhibir su expresión se genera un aumento del efecto antileucémico dependiente de IFN tipo I (Sharma *et al.* 2012).

Además de los estudios realizados en ratones *knock-out* para *SPRY1* mencionados anteriormente, existen otros muchos sistemas en los que se ha descrito su actividad. SPRY1 y -2 tienen roles importantes en la diferenciación temprana de varios órganos: regulan la diferenciación cortical en el cerebro mediante la inhibición de la señalización FGF/MAPK/ERK (Faedo *et al.* 2010), la diferenciación de la córnea, el cierre del párpado del ojo (Kuracha *et al.* 2011, Kuracha *et al.* 2013), el desarrollo de los genitales externos (Ching *et al.* 2014) y de la articulación temporomandibular (Purcell *et al.* 2012). Además, son reguladores negativos de TGFβ (*Transforming Growth Factor β*) en el contexto de la transición epitelio-mesénquima, y su ausencia genera la formación de fibrosis en enfermedades como las cataratas (Shin *et al.* 2012). Se ha descrito que SPRY1 y -4 tienen efectos antagónicos en las células de músculo liso vascular, siendo SPRY1 el que mantiene el fenotipo diferenciado regulando la ruta AKT/FOXO/Miocardina (Yang *et al.* 2013).

En el contexto hematopoyético, SPRY1 actúa favoreciendo la diferenciación osteoblástica de progenitores hematopoyéticos en detrimento de la formación de adipocitos (Urs *et al.* 2010), de modo que la expresión específica de SPRY1 en adipocitos reduce la grasa corporal y aumenta la masa ósea, generando un efecto protector sobre ratones alimentados con dietas altas en grasas (Urs *et al.* 2010, Urs *et al.* 2012). SPRY1 también ha demostrado ser un regulador de la eritropoyesis en modelos de anemia (Sathyanarayana *et al.* 2012).

En el sistema inmune, se ha descrito que el efecto de SPRY1 sobre la señalización por TCR (*T cell receptor*) de células T depende de su estado de diferenciación. Así, SPRY1 inhibe la señalización mediada por TCR y la proliferación en células diferenciadas, mientras que en células T *naïve* presenta el efecto opuesto (Choi *et al.* 2006). SPRY1 regula también la respuesta efectora de células T $CD4^+$ y $CD8^+$ dotándolas de una mayor actividad antitumoral (Collins *et al.* 2012).

Además, SPRY1 participa en la reparación tisular regulando el estado de quiescencia de células madre musculares adultas durante el proceso de regeneración (Shea *et al.* 2010) y la hipermetilación del promotor de SPRY1 debido al envejecimiento se ha propuesto como una de las causas de la disminución de la capacidad de regeneración tisular asociadas a la edad (Bigot *et al.* 2015). Finalmente, SPRY1 tiene un efecto inhibidor de la angiogénesis y de la proliferación celular en células endoteliales (Lee *et al.* 2010, Sabatel *et al.* 2010).

En la **Tabla 2** se resumen las funciones fisiológicas de la proteína SPRY1 que acabamos de describir.

Tabla 2. Funciones fisiológicas de la proteína SPRY1.

Organogénesis y diferenciación	Referencias
Regula la diferenciación cortical del cerebro mediante la represión de la señalización de FGF.	Faedo *et al.* 2010
Favorece la diferenciación de la córnea e inhibe la proliferación de las células epiteliales de la córnea.	Kuracha *et al.* 2011
Permite el desarrollo de la estructura para el cierre del párpado en el ojo.	Kuracha *et al.* 2013
Participa en el desarrollo de los genitales externos mediante la regulación de la señalización de FGF.	Ching *et al.* 2014
SPRY1 es una diana de WT1, un factor de transcripción implicado en el desarrollo del riñón y es necesario para la correcta organogénesis.	Gross *et al.* 2003
SPRY1 es necesario para la regulación de la señalización de FGF y el correcto desarrollo de la articulación temporomandibular.	Purcell *et al.* 2012
SPRY1 regula la transición epitelio-mesénquima mediante la inhibición de TGFβ.	Shin *et al.* 2012
Mantenimiento de la diferenciación en músculo liso vascular.	Yang *et al.* 2013
SPRY1 favorece la diferenciación osteoblástica de precursores hematopoyéticos.	Urs *et al.* 2010
Regulación de células T	**Referencias**
Inhibición de la señalización TCR y la proliferación en células T diferenciadas.	Choi *et al.* 2006
SPRY1 favorece la señalización TCR en células T *naïve.*	Choi *et al.* 2006
Regulación respuesta efectora de células T CD4+ y CD8+.	Collins *et al.* 2012
Regeneración y proliferación celular	**Referencias**
Regulación de la quiescencia en células madre musculares adultas durante la regeneración tisular.	Shea *et al.* 2010, Bigot *et al.* 2015
Inhibición de la angiogénesis y proliferación celular en células endoteliales por regulación de p21 y p27.	Lee *et al.* 2010, Sabatel *et al.* 2010

1.5.3. SPRY1 en cáncer

Dado que SPRY1 es un regulador negativo de la señalización mediada por Ras y que aproximadamente un tercio de los cánceres en humanos presentan mutaciones activadoras en Ras (Zhao *et al.* 2010), se ha sugerido que SPRY1 podría actuar como un supresor tumoral. Además, varios estudios han puesto de manifiesto que SPRY1 se expresa a niveles bajos en diferentes tipos de cáncer, como el cáncer de mama, ovario o próstata (Lo *et al.* 2004, Fritzsche *et al.* 2006, Kwabi-Addo *et al.* 2009, Moghaddam *et al.* 2012). Por otro lado, la sobreexpresión de SPRY1 en células tumorales inhibe sus características tumorigénicas como la proliferación, la migración y el crecimiento independiente de anclaje *in vitro* en cáncer de próstata, cáncer de mama, de ovario, melanoma y en células de carcinoma medular de tiroides (Kwabi-Addo *et al.* 2004, Lo *et al.* 2004, Macia *et al.* 2012, Masoumi-Moghaddam *et al.* 2014a, Liu *et al.* 2015). Por último, se ha descrito que SPRY1 es además, diana de varios supresores de tumores conocidos, como WT1 (Gross *et al.* 2003), el agente angiostático prolactina 16K (Sabatel *et al.* 2010) y miR-21 (Xu *et al.* 2014).

Debido a la relación entre los niveles altos de expresión de SPRY1 y la inhibición de la tumorigenicidad en diferentes tipos de cáncer, se ha valorado la posibilidad de emplear los niveles de expresión de SPRY1 como factor pronóstico en varios tipos de cáncer. Por ejemplo, la expresión de SPRY1 es superior en los casos de cáncer hepático sin cirrosis en comparación con los casos que sí la presentan (Sirivatanauksorn *et al.* 2012). En cáncer de mama, la expresión de SPRY1 se reduce drásticamente en las células tumorales en relación al tejido epitelial normal circundante (Lo *et al.* 2004). En cáncer de ovario, la expresión de SPRY1 correlaciona negativamente con características de malignidad (estadio del tumor, recaída, invasión linfovascular) y la expresión de ERK y Ki-67 y positivamente con mejores valores de supervivencia global (Masoumi-Moghaddam *et al.* 2015). En cáncer de tiroides, la expresión de SPRY1 es más baja en tejido tumoral que en el tejido normal (Macia *et al.* 2014). Por último, en cáncer de próstata, donde las alteraciones en FGF o FGFR contribuyen a la progresión de la enfermedad, se han descrito niveles más bajos de SPRY1 en el 40% de los tumores con respecto al tejido normal (Kwabi-Addo *et al.* 2004) y niveles de SPRY1 incluso más bajo en los casos de pacientes con recaídas (Fritzsche *et al.* 2006, Terada *et al.* 2014).

En la **Tabla 3** se muestra un resumen de las funciones de SPRY1 en cáncer descritas hasta el momento.

Tabla 3. Funciones de la proteína SPRY1 en cáncer.

Cáncer de próstata	**Referencias**
La re-expresión de SPRY1 inhibe la proliferación de células de cáncer de próstata *in vitro*.	Kwabi-Addo *et al.* 2009
Bajos niveles de expresión de SPRY1 en cáncer de próstata.	Fritzsche *et al.* 2006
Cáncer de ovario	**Referencias**
La expresión de SPRY1 correlaciona inversamente con el crecimiento, la proliferación y la migración de células de cáncer de ovario.	Masoumi-Moghaddam *et al.* 2014a
Niveles bajos de expresión de SPRY1 en tumores de ovario.	Moghaddam *et al.* 2012
Cáncer de mama	**Referencias**
La inhibición de SPRY1 en células de cáncer de mama genera un fenotipo tumoral más acusado *in vitro* e *in vivo*.	Lo *et al.* 2004
Niveles bajos de expresión de SPRY1 en tumores de mama.	Lo *et al.* 2004
Melanoma	**Referencias**
La re-expresión de SPRY1 inhibe la proliferación de células de melanoma *in vitro* e *in vivo*.	Liu *et al.* 2015
Cáncer de tiroides	**Referencias**
La deleción de SPRY1 genera lesiones precancerosas en un modelo murino de carcinoma medular de tiroides. La re-expresión de SPRY1 inhibe la proliferación de las células tumorales.	Macia *et al.* 2012

En resumen, varios estudios indican que hay una asociación entre la baja expresión de SPRY1 con las características tumorigénicas en varios tipos de cáncer; y viceversa, una alta expresión de SPRY1 se correlaciona con mejores pronósticos en diversas neoplasias. Es por ello que SPRY1 constituye una diana de estudio muy interesante en otros tipos de cáncer como el sarcoma de Ewing.

2. Objetivos

Objetivos

El sarcoma de Ewing se caracteriza por la presencia de translocaciones cromosómicas que dan lugar a un factor de transcripción quimérico, el más frecuente de los cuales es EWS-FLI1. EWS-FLI1 regula la expresión de numerosos genes implicados en la patogénesis de este tumor. Por ello es importante estudiar los genes regulados por EWS-FLI1 para ampliar así nuestro conocimiento sobre la biología de los tumores de Ewing e identificar nuevas dianas terapéuticas.

Esta Tesis está centrada en el estudio de *SPRY1*, un gen que regula la actividad de la ruta de las MAPK y que actúa como un gen supresor de tumores en varios tipos de cáncer. El papel de este gen en el sarcoma de Ewing no ha sido estudiado hasta el momento.

Los objetivos concretos planteados en esta Tesis son:

1) **Caracterizar el perfil de expresión de SPRY1 en células y tumores de sarcoma de Ewing y su regulación por EWS-FLI1.**

   Para ello se emplearán sistemas de ARN de interferencia inducible contra EWS-FLI1 en células de Ewing y se analizará el efecto del silenciamiento de EWS-FLI1 sobre la expresión de *SPRY1*. También se analizará la expresión de SPRY1 en tumores primarios y líneas celulares derivadas de sarcoma de Ewing, tejidos normales y líneas celulares procedentes de otros tumores pediátricos.

2) **Estudiar el papel funcional de SPRY1 en el desarrollo de los tumores de Ewing.**

   Para ello se establecerán modelos de expresión inducible de SPRY1 en líneas celulares de sarcoma de Ewing y se estudiará el efecto de su expresión sobre las características transformantes y tumorigénicas de estas células.

3) **Estudiar el efecto de SPRY1 sobre la ruta de señalización FGFR/Ras/MAPK/ERK en sarcoma de Ewing.**

   Para ello se analizará el efecto de la re-expresión de SPRY1 sobre la ruta de señalización de FGFR/Ras/MAPK/ERK en líneas celulares de sarcoma de Ewing.

4) **Valorar la utilidad de los inhibidores de los receptores de FGF en el tratamiento del sarcoma de Ewing.**

   Se estudiará el efecto de diferentes inhibidores de FGFR sobre las células de sarcoma de Ewing y sobre modelos de xenotransplantes murinos, así como el posible efecto sinérgico entre SPRY1 y los inhibidores de FGFR.

5) **Estudiar el posible papel pronóstico de SPRY1 en sarcoma de Ewing.**

   Para ello se analizarán los niveles de expresión de SPRY1 en relación con la supervivencia global, la supervivencia libre de eventos y la presencia de metástasis al diagnóstico en una cohorte grande de pacientes.

3. Materiales y Métodos

Materiales y Métodos

3.1. Material biológico

3.1.1. Líneas celulares

En las **Tablas 4 y 5** se enumeran las líneas celulares utilizadas en la realización de esta Tesis así como sus características más relevantes y el medio de cultivo utilizado en cada una.

El medio de cultivo se suplementó con suero fetal bovino (SFB) (10-20% según la línea celular), o con suero fetal bovino sin tetraciclina (SFB-TET) en el caso de las líneas celulares con los sistemas de expresión inducibles por tetraciclina. Todos los medios de cultivo fueron suplementados con penicilina (100 UI/ml) y estreptomicina (100 µg/ml). Las líneas celulares se cultivaron a 37 ºC en atmósfera al 5% de CO2 y 95% de humedad. Todas las líneas celulares se testaron de forma rutinaria para detectar contaminaciones de micoplasma utilizando el kit comercial *Mycoalert mycoplasma detection kit* (#LT07-318, Lonza, Basilea, Suiza) y se autentificaron por análisis del perfil de STRs *(short tandem repeat*s) en la Unidad de Genómica del Instituto de Investigaciones Biomédicas-CSIC (Madrid, España).

3.1.2. Cohortes de pacientes y tumores primarios

En esta Tesis se han utilizado datos procedentes de dos cohortes de pacientes. En ambas cohortes se analizaron las muestras tumorales con *arrays* de expresión y se obtuvieron los datos clínicos. Los protocolos de tratamiento en ambas cohortes fueron similares. La primera cohorte está formada por 117 pacientes analizados con *microarrays* HG-U133 plus2.0 (Affymetrix, California, EEUU) y ha sido previamente publicada (Postel-Vinay *et al.* 2012). La segunda cohorte está formada por 45 pacientes cuyos tumores se habían analizado previamente en nuestro laboratorio utilizando un *microarray Uniset Human 20K* (Codelink Amersham Bioscience, GE Healthcare, Reino Unido). Todos los procedimientos fueron aprobados por los comités de ética de las instituciones correspondientes.

Para los estudios de expresión por RT-PCR cuantitativa se utilizó una selección de muestras tumorales de pacientes que presentaban diferentes tipos de fusión EWS-FLI1.

Tabla 4. Lista de líneas celulares utilizadas

Línea Celular	Tipo celular*	Características**	Medio de cultivo	Referencia
A673	SE	t(11;22); EWS-FLI1 tipo I	DMEM	Frolik *et al.* 1984, Dauphinot *et al.* 2001
SKES	SE	t(11;22); EWS-FLI1 tipo II	DMEM	Giovanini *et al.* 1994, Dauphinot *et al.* 2001
SKNMC	SE	t(11;22); EWS-FLI1 tipo I	IMDM	Bastida *et al.* 1985
SKPNDW	SE	t(11;22); EWS-FLI1 tipo I	IMDM	Potluri *et al.* 1987
TC-71	SE	t(11;22); EWS-FLI1 tipo I	IMDM	Whang-Peng *et al.* 1984
A4573	SE	t(11;22); EWS-FLI1 10/6	RPMI	Cavazzana *et al.* 1987
RDES	SE	t(11;22); EWS-FLI1 tipo II	RPMI	Giovanini *et al.* 1994, Dauphinot *et al.* 2001
TTC466	SE	t(21;22); EWS-ERG tipo I	RPMI	Sorensen *et al.* 1994
POE	SE	t(11;22); EWS-FLI1 tipo I	RPMI	Generadas en el Instituto Curie, París, Francia
U2OS	OS	pRb+, p53+	RPMI	Ponten and Saksela 1967
SAOS-2	OS	pRb-, p53-	RPMI	Fogh *et al.* 1977
SH-SH5Y	NB	NMA-	DMEM	Biedler *et al.* 1978
IMR-32	NB	1p-, NMA+	RPMI	Tumilowicz *et al.* 1970, Brodeur *et al.* 1977
SK-N-SH	NB	1p-, 1q+	RPMI	Brodeur *et al.* 1977, Seeger *et al.* 1977
CW9019	RMS	t(1;13) PAX7/FKHR	RPMI	Edwards *et al.* 1997
SK-N-AS	NB	1p-	RPMI	Sugimoto *et al.* 1984
293 FT	HEK	Células transformadas con adenovirus 5	DMEM	Invitrogen
IMR90	FB	p53-	DMEM	Nichols *et al.* 1977

Tabla 5. Lista de líneas celulares modificadas genéticamente utilizadas

Línea Celular Modificada Genéticamente	Tipo celular*	Características**	Medio de cultivo	Referencia
A673/TR	SE	t(11;22); EWS-FLI1 tipo I. Expresan el represor de tetraciclina (TR) de forma constitutiva	DMEM + 3 µg/ml blasticidina	Carrillo *et al.* 2007
SKES/TR	SE	t(11;22); EWS-FLI1 tipo II. Expresan el represor de tetraciclina (TR) de forma constitutiva	DMEM + 3 µg/ml blasticidina	Carrillo *et al.* 2007
SKNMC/TR	SE	t(11;22); EWS-FLI1 tipo I. Expresan el represor de tetraciclina (TR) de forma constitutiva	IMDM + 3 µg/ml blasticidina	Carrillo *et al.* 2007
A673/TR/shEF	SE	t(11;22); EWS-FLI1 tipo I. Estas células expresan un shARN dirigido contra EWS-FLI1 cuando se estimulan con doxiciclina.	DMEM + 100 µg/ml zeocina + 3 µg/ml blasticidina	Carrillo *et al.* 2007
A673/TR/SPRY1	SE	t(11;22); EWS-FLI1 tipo I. Estas células re-expresan el cDNA de SPRY1 en respuesta a estimulación con doxiciclina.	DMEM + 100 µg/ml zeocina + 3 µg/ml blasticidina	Esta Tesis y Cidre-Aranaz *et al.* 2016
SKES/TR/SPRY1	SE	t(11;22); EWS-FLI1 tipo II. Estas células re-expresan el cDNA de SPRY1 en respuesta a estimulación con doxiciclina.	DMEM + 100 µg/ml zeocina + 3 µg/ml blasticidina	Esta Tesis y Cidre-Aranaz *et al.* 2016
SKNMC/TR/SPRY1	SE	t(11;22); EWS-FLI1 tipo I. Estas células re-expresan el cDNA de SPRY1 en respuesta a estimulación con doxiciclina.	DMEM + 100 µg/ml zeocina + 3 µg/ml blasticidina	Esta Tesis y Cidre-Aranaz *et al.* 2016

*SE: Sarcoma de Ewing; NB: Neuroblastoma; OS: Osteosarcoma; FB: Fibroblasto; RMS: Rabdomiosarcoma; HEK: *Human Embryonic Kidney*.
**Se indican algunas de las características moleculares más relevantes de las líneas celulares empleadas, como el tipo de translocación y de proteína quimérica en las líneas de sarcoma de Ewing, la existencia de amplificación (NMA+) del oncogén *N-myc* en las líneas de neuroblastoma, así como el estatus funcional del gen *pBb* y *p53*. En las líneas celulares modificadas genéticamente se incluye la adición del sistema represor de tetraciclina (TR) que controla la expresión de las construcciones añadidas a continuación mediante la adición de doxiciclina al medio de cultivo.

3.2. Plásmidos

En la **Tabla 6** se muestran los plásmidos utilizados para la realización de esta Tesis, así como sus principales características.

Tabla 6. Plásmidos empleados y sus características.

Plásmido	Características	Casa comercial
pENTR2B	Plásmido de entrada del ADNc del gen de interés que permite la recombinación posterior con un plásmido lentiviral de destino.	Invitrogen
pLenti4/TO/V5-DEST	Plásmido lentiviral de destino, que permite la expresión regulada del gen de interés en respuesta a doxiciclina.	Invitrogen

3.3. Establecimiento de líneas celulares de sarcoma de Ewing con expresión inducible de SPRY1

El primer paso para obtener las líneas celulares de sarcoma de Ewing (A673, SKES y SKNMC) con un sistema de re-expresión inducible de SPRY1 por doxiciclina, un análogo de la tetraciclina, fue el clonaje del ADNc de SPRY1 en el vector de expresión lentiviral pLenti4/TO/V5-DEST. Para ello se amplificó la región codificante completa de *SPRY1* mediante RT-PCR utilizando ARN total procedente de células A673/TR/shEF tratadas durante 72 horas con doxiciclina (1 µg/ml) que expresan niveles elevados de SPRY1. Los cebadores utilizados (**Tabla 7**) contienen las dianas de restricción *SalI* y *NotI* que se emplearon posteriormente para realizar el clonaje.

Tabla 7. Cebadores para SPRY1 y localización de las dianas de restricción.

Cebador	Secuencia
SPRY1 F	5'-GCG**GTCGAC**GAGATCACTACACATGGATCC-3' ***SalI***
SPRY1 R	5'-CG**GCGGCCGC**TCATCATCATGATGGTTTACCCTGACC-3' ***NotI***

Los productos de PCR se digirieron con las enzimas de restricción *SalI* y *NotI* y se clonaron en el plásmido de entrada pENTR2B (Invitrogen, Massachusetts, EEUU). Una vez confirmada la identidad de la secuencia mediante secuenciación, el ADNc de SPRY1 se transfirió por recombinación al vector lentiviral pLenti4/TO/V5-DEST (Invitrogen) inducible por doxiciclina, obteniéndose el plásmido pLenti4/TO/V5-DEST-SPRY1 que se utilizó a continuación para la generación de lentivirus.

Para producir los lentivirus se transfectaron células 293FT (Invitrogen) con pLenti4/TO/V5-DEST-SPRY1. Para la transfección, se preparó una mezcla compuesta por 12 µl de plásmidos empaquetadores (*ViraPower Packaging Mix*, Invitrogen) y 4 µg del vector que contenía el ADNc de SPRY1, diluidos en 2 ml de medio de cultivo OptiMEM I sin suero. En otro tubo, se añadieron 46 µl de lipofectamina 2000 a 2 ml de medio OptiMEM I sin suero. Después de incubar 5 minutos a temperatura ambiente, se mezclaron ambas soluciones añadiendo el ADN sobre la mezcla de lipofectamina y se incubaron 20 minutos más a temperatura ambiente para que se formasen los complejos ADN-lipofectamina 2000.

Una vez formados los complejos, la solución con los complejos ADN-lipofectamina 2000 (4 ml) se añadió a 8 millones de células 293FT en 6,5 ml de medio OptiMEM con suero en un frasco T75. Después de 24 horas, las células 293FT transfectadas se incubaron en medio DMEM suplementado con 10% de suero, sodio-piruvato y 0,1% de aminoácidos no esenciales para incrementar la producción de lentivirus. A las 48 horas se recogió el sobrenadante con los virus, se clarificó a través de un filtro de 0,45 µm, se alicuotó y se congeló rápidamente en nieve carbónica, conservándose a -80 ºC hasta su utilización.

Para la obtención de células de sarcoma de Ewing que expresaran SPRY1 en respuesta a doxiciclina se infectaron las células A673/TR, SKES/TR y SKNMC/TR, que expresaban altos niveles del represor de tetraciclina (TR) de forma constitutiva, con lentivirus que contenían el vector pLenti4/TO/V5-DEST-SPRY1. Las células control se infectaron con lentivirus que contenían el vector vacío (*Empty*). Para la infección se sembraron células A673/TR, SKES/TR y SKPNDW/TR a 150.000 células/pocillo en placas de 6 pocillos. Tras 48 horas se incubaron con 1 ml de sobrenadante viral en presencia de 1 µg/ml de polibreno (#AL-118, Sigma-Aldrich, Missouri, EEUU) durante

24 horas. Al día siguiente se cambió el medio por DMEM suplementado con 10% de suero fetal bovino libre de tetraciclina. A las 48 horas se cambió nuevamente el medio por DMEM suplementado con suero y blasticidina (5 µg/ml, resistencia asociada al pLenti6/TR) y zeocina (100 µg/ml, resistencia asociada al vector pLenti4/TO/V5-DEST-SPRY1 o pLenti4/TO/V5-DEST-Empty). Una vez obtenidos los cultivos policlonales resistentes, se aislaron 20-25 clones por cada línea celular. Cada uno de los clones estables se estimularon con doxiciclina (1 µg/ml, Ibian Technologies, Zaragoza, España) y se analizaron los niveles de expresión de SPRY1 por western blot. Los clones con niveles más altos de expresión de SPRY1 se seleccionaron para ser utilizados en los estudios posteriores. Todas las manipulaciones con lentivirus se llevaron a cabo en las instalaciones de nivel de bioseguridad 2 (P2), exclusivamente por personal autorizado.

3.4. Estudios de expresión

3.4.1. Extracción de ARN

La extracción de ARN total de células en cultivo se realizó mediante el método de fenol-cloroformo empleando el reactivo TRI Reagent (Sigma-Aldrich) y siguiendo las instrucciones del fabricante. El ARN obtenido se cuantificó empleando un sistema Nanodrop (Thermo Scientific, Massachusetts, EEUU) y se conservó a -80 ºC hasta su utilización.

3.4.2. RT-PCR cuantitativa a tiempo real

La retrotranscripción del ARN a ADNc se llevó a cabo en un volumen final de 20 µl donde se incluyó 1 µg de ARN, 1 mM dNTPs, 10 mM DTT, 2,5 µM de cebadores hexámeros (Promega, Wisconsin, EEUU) y tampón de transcripción reversa 1x. La reacción se incubó 10 minutos a 70 °C para desnaturalizar el ARN y se enfrió en hielo. Posteriormente se añadieron 2 U/µl de inhibidor de ribonucleasas (RNasin, Promega) y 10 U/µl de transcriptasa reversa MMLV (Invitrogen). La mezcla se incubó 10 minutos a 25 ºC, 30 minutos a 42 ºC, y finalmente 5 minutos a 95 ºC. Como controles negativos se incluyeron muestras sin la enzima transcriptasa reversa.

La PCR cuantitativa con sondas Taqman se realizó en un volumen final de 20 µl donde se incluyeron 800 µM dNTPs, 4 mM $MgCl_2$, 1 µl de solución cebadores/sonda Taqman (20x) (Applied Biosystems, California, EEUU), 0,5 U Taq polimerasa (Biotools, Madrid, España) y tampón de reacción 1x. El programa de PCR tuvo los siguientes pasos:

1	96 ºC	120 segundos
40 ciclos	96 ºC	15 segundos
	60 ºC	30 segundos

Se emplearon los canales verde (FAM, para el gen de interés) y amarillo (HEX, para la TBP) y la adquisición se realizó a 510 nm y 555 nm respectivamente a 60 ºC en un equipo *Rotor Gene 6000* (Corbett, Qiagen, Venlo, Holanda). El análisis de los resultados se realizó empleando el programa *RotorGene versión 6.0* (Qiagen).

En todos los ensayos se amplificó en paralelo el ARN mensajero del gen TBP (*TATA binding protein*), que se utilizó como control de referencia interno para la normalización de los niveles de expresión de los genes de interés.

La secuencia de los cebadores y sondas Taqman empleados se muestran en la **Tabla 8**.

Tabla 8. Cebadores y sondas empleadas en la técnica de RT-PCR cuantitativa mediante sondas Taqman

Gen	Cebadores-sonda Taqman
TBP	Sonda Taqman 5'- HEX-CTGCCACCTTACGCTCAGGGCTTGG-TAMRA- 3' TBP-F2 5' -GAACATCATGGATCAGAACAACAG -3' TBP-R2 5' -ATTGGTGTTCTGAATAGGCTGTG -3'
EWS-FLI1	Sonda Taqman 5'-FAM-AACAGAGCAGCAGCTACGGGCAGCA-TAMRA-3' EWS-F2 5' –AGCCAAGCTCCAAGTCAATATAG- 3' FLI1-R3 5' –TCCTCTTCTGACTGAGTCATAAG- 3'
SPRY1	Sonda Taqman Hs00398096_m1 (Applied Biosystems)
SPRY2	Sonda Taqman Hs00183386_m1 (Applied Biosystems)
SPRY3	Sonda Taqman Hs00538856_m1 (Applied Biosystems)
SPRY4	Sonda Taqman Hs00540086_m1 (Applied Biosystems)

Para el estudio de las variantes transcripcionales de SPRY1 se empleó la técnica de PCR cuantitativa con *SYBR green*. La reacción de PCR se realizó en un volumen final de 20 µl donde se incluyeron 10 µl de Quantimix Easy Kit (Biotools), que contiene la ADN polimerasa, los cuatro dNTPs, $MgCl_2$, buffer de reacción y *SYBR Green* I (Biotools), 0,2 µl del cebador F y R (10 µM), 7,6 µl de H_2O y 2 µl de la reacción de transcripción reversa.

El programa de PCR tuvo los siguientes pasos:

1 ciclo	95 °C	120 segundos
40 ciclos	95 °C	10 segundos
	60 ºC	15 segundos
	72 °C	40 segundos
	75 °C	10 segundos
	80 °C	10 segundos

Se empleó el canal verde (FAM) y la adquisición se realizó a 510 nm a 72 y 80 ºC en un equipo *Rotor Gene 6000* (Corbett). El análisis de los resultados se realizó empleando el programa *RotorGene versión 6.0*.

Las secuencias de los cebadores utilizados para las RT-PCR cuantitativas con *SYBR Green* se muestran en la **Tabla 9**.

Tabla 9. Cebadores empleados en la técnica de RT-PCR cuantitativa para las variantes transcripcionales de SPRY1 con *SYBR Green*.

Gen	Cebadores-sonda Taqman
SPRY1 VT 1F	5’- ACCTCACTCTCTTCACTCCTC - 3’
SPRY1 VT 2F	5’- GTCGCTGTTAAATGTGCCTG - 3’
SPRY1 VT 3F	5’- ATATGGTGATGGGATTGTCCG - 3’
SPRY1 VT 4F	5’- CCGCTTCGGCCTAGGAT - 3’
SPRY1 R común	5’- ACAACTAACGAACTGCCACTG - 3’
SPRY1 R_2	5’- GCAATCTTTGCATTAGGATTTCAGAT - 3’

Para cada gen se obtuvieron los datos de Ct (*Cycle threshold*), usando el programa *RotorGene versión 6.0*. Para comparar los niveles de expresión de un mismo gen en dos muestras diferentes se usó el método de ΔΔCt (Livak *et al.* 2001). Para el análisis de

resultados el nivel de expresión de cada gen se normalizó frente al control interno (TBP).

En primer lugar se calculó el valor de ΔCt de la muestra de interés y de la muestra control usando la fórmula $\Delta Ct = Ct_{\text{gen muestra de interés}} - Ct_{TBP}$. Posteriormente se calculó el valor $\Delta\Delta Ct = \Delta Ct_{\text{muestra de interés}} - \Delta Ct_{\text{muestra control}}$. El valor del cociente (veces de incremento o inhibición) entre las dos muestras se calculó como $2^{-\Delta\Delta Ct}$.

3.4.3. Estudios de regulación epigenética

Para el estudio de la regulación epigenética de SPRY1 se empleó un inhibidor de la desacetilación de histonas (SAHA, también llamado Vorinostat; # S1047, Selleckchem, Texas, EEUU) y un inhibidor de ADN metiltransferasa (5-Aza-2′-deoxycytidine, abreviado "5-aza", #A3656, Sigma-Aldrich) a una concentración de 1 µM. Se incubaron las células A673 en presencia o ausencia de SAHA durante 24 horas o de 5-aza durante 96 horas. Pasado ese tiempo se extrajo el ARNm y se realizó una RT-PCR cuantitativa para determinar la expresión de SPRY1.

3.4.4. Western blot

Para la extracción de proteína total, las células se lavaron con PBS 1x y se lisaron en solución RIPA (PBS 1x, 1% Igepal, 0,1% SDS, 0,5% desoxicolato sódico) suplementada con inhibidores de proteasas libres de EDTA 1x (Sigma-Aldrich), de fosfatasas (por cada mililitro de RIPA se añadieron 50 µl de pirofosfato sódico pH 7,4 0,2 M, 40 µl de ortovanadato sódico 0,1 M y 1 µl de fluoruro sódico 0,5 M) y EDTA 1 µM. El lisado se pasó varias veces por una jeringuilla de 25 G para lisar las células y se incubó en hielo durante 30 minutos. Finalmente se centrifugó a 12.000 rpm durante 10 minutos a 4 ºC para precipitar los restos celulares y el sobrenadante se alicuotó y se congeló a -20 ºC.

Para calcular la concentración de las proteínas extraídas se utilizó el método del ácido bicinconínico (BCA, Pierce, Massachusetts, EEUU) utilizando una curva patrón de albúmina sérica bovina. Para cada muestra se cargaron entre 10-20 µg de proteínas en

un gel de poliacrilamida vertical al 10% (acrilamida: bisacrilamida 37,5:1) y se realizó la electroforesis a 80 V para la fase concentradora y 120 V para la fase separadora.

Tras la electroforesis, las proteínas se transfirieron a una membrana de PVDF (Thermo Scientific) usando el método de transferencia semi-seca (*Trans-Blot SD Semi-Dry Electrophoresis Transfer Cell Instruction Manual*; Bio-Rad Laboratories, California, EEUU) a un amperaje constante de 3 mA por cm^2. Los lavados de la membrana se hicieron con tampón TTBS (Tris 20 mM, NaCl 136 mM, pH 7,5 y Tween 20 0,5%) y el bloqueo se realizó con tampón TTBS y leche desnatada al 5%.

Los anticuerpos utilizados, diluciones y casas comerciales aparecen detallados en la **Tabla 10**.

Tabla 10. Relación de los anticuerpos utilizados durante la realización de esta Tesis

Anticuerpo	Características	Dilución	Referencia	Casa comercial
anti-FLI1	Anticuerpo primario policlonal	1:250	RB-9295-P	NeoMarkers
anti-SPRY1	Anticuerpo primario monoclonal	1:200	SC-100861	Santa Cruz Biotechnology
Anti-tubulina	Anticuerpo primario monoclonal	1:10000	T9026	Sigma-Aldrich
anti-fosfo-p44/42 (pERK)	Anticuerpo primario monoclonal	1:1000	9106	Cell Signaling
anti-p44/42 (ERK_{total})	Anticuerpo primario policlonal	1:1000	9102	Cell Signaling
anti-mouse IgG	Anticuerpo secundario conjugado con peroxidasa de rábano picante	1:5000 – 1:10000	SC-2055	Santa Cruz Biotechnology
anti-rabbit IgG	Anticuerpo secundario conjugado con peroxidasa de rábano picante	1:5000 – 1:10000	SC-2054	Santa Cruz Biotechnology

Tras las incubaciones con el anticuerpo primario y secundario, se realizaron 4 lavados de 15 minutos cada uno con TTBS 1x. Finalmente se visualizaron las proteínas utilizando el sistema ECL (Amersham, Amersham, Reino Unido) y el sistema Chemidoc XRS+ Molecular Imager (BioRad). La cuantificación de las bandas se realizó con el programa ImageLab Software (BioRad).

Las membranas fueron re-hibridadas varias veces con diferentes anticuerpos. Antes de cada hibridación se sometieron a un tratamiento con una solución compuesta por SDS 10% (p/v), β-mercaptoetanol 5 mM y Tris HCl 50 mM pH 8,8 a 65 ºC durante 30 minutos en rotación con el objetivo de eliminar los anticuerpos hibridados previamente.

3.5. Estudios funcionales

3.5.1. Estudios de proliferación celular

3.5.1.1. xCELLigence

Para determinar el efecto de la re-expresión de SPRY1 sobre la proliferación celular se utilizó el sistema bioeléctrico xCELLigence (Roche, Basilea, Suiza) que mide periódicamente la impedancia celular, la cual es proporcional al número de células presentes en la placa de cultivo. En estos experimentos se sembraron por triplicado 3-4x10^3 células por pocillo, en una placa de 96 pocillos específica para este ensayo que incluye micro-electrodos en el fondo (e-plate, Roche). Las células se cultivaron en ausencia o presencia de doxiciclina (1 µg/ml) para inducir la expresión de SPRY1. El medio se cambió una vez a las 72 horas.

3.5.1.2. Ensayos de proliferación celular por incorporación de bromodesoxiuridina (BrdU) al ADN

La proliferación celular se midió utilizando el kit comercial *BrdU chemiluminescent assay* (Roche). La BrdU se incorpora al ADN de nueva síntesis permitiéndonos así determinar la proliferación. En estos experimentos se sembraron 10^3 células/pocillo por octuplicado en una placa de 96 pocillos en 200 µl de medio en ausencia o presencia de doxiciclina (1 µg/ml). Para determinar el efecto del suero, las células se incubaron con medio de cultivo suplementado con 10% o 1% de SFB libre de tetraciclina. Después del periodo de incubación con el estímulo, las células se incubaron con la solución de BrdU, se fijaron y se incubaron con una solución anti-BrdU-POD que tras el lavado fue incubada con el sustrato para dar la reacción que genera quimioluminiscencia. La señal se cuantificó midiendo los fotones emitidos usando una placa blanca en el luminómetro con tecnología de fotomultiplicador Infinite M200 (Tecan, Zúrich, Suiza). La relación

de unidades relativas de luz/segundo (rlu/s) correlaciona directamente con la cantidad de ADN sintetizado y, por lo tanto, con el número de células que han proliferado en el cultivo.

3.5.1.3. Determinación de la viabilidad celular mediante reducción de resazurina

La viabilidad celular se midió utilizando un ensayo con resazurina (Sigma-Aldrich), que es un compuesto no fluorescente que al ser reducido por las células vivas metabólicamente activas se convierte en resorufina, que emite fluorescencia roja.

En el caso de los ensayos con células A673/TR/SPRY1, SKES/TR/SPRY1 y SKNMC/TR/SPRY1, las células se sembraron por octuplicado a una densidad de $2{,}5x10^3$ células por pocillo en placas de 96 pocillos y se cultivaron en presencia o ausencia de doxiciclina (1 µg/ml) o el estímulo correspondiente (SFB libre de tetraciclina a 1% o 10%, o 10 ng/ml de FGFb) durante 72 horas.

Para analizar el efecto de los inhibidores de los receptores de FGF (FGFR) se utilizaron células A673, SKNMC, SKES, POE e IMR90 cultivadas en presencia de dosis crecientes de cada uno de los inhibidores durante 72 horas. Los inhibidores empleados se detallan en la **Tabla 11**.

Tabla 11. Inhibidores de FGFR empleados para la realización de esta Tesis.

Inhibidor	Características	Casa comercial	Referencia
PD173074	Inhibidor de FGFR1	Selleckchem	#S1264
PD166866	Inhibidor de FGFR1	Sigma-Aldrich	# PZ0114
SU5402	Inhibidor de FGFR1	Selleckchem	# S7667
NVP-BGJ398	Inhibidor de FGFR1, -2 y -3	Selleckchem	# S2183

Una vez finalizados los periodos de incubación correspondientes se añadió resazurina (Sigma-Aldrich) al medio de cultivo a 0,15 µg/ml y se incubó durante 2 horas a 37 ºC. Finalmente se midió la fluorescencia a 560 nm de excitación y 590 nm emisión en un lector de placas Infinite M200 (Tecan).

3.5.1.4. Análisis de las fases del ciclo celular mediante citometría de flujo empleando yoduro de propidio

Para determinar las fases del ciclo celular se llevaron a cabo experimentos de citometría de flujo con yoduro de propidio. Para ello, se sembraron las líneas celulares A673/TR/SPRY1, SKES/TR/SPRY1 y SKNMC/TR/SPRY1 en placas p100 y se cultivaron en presencia o ausencia de doxiciclina durante 72 horas. Pasado ese tiempo, se recogió el sobrenadante para recuperar las células en suspensión y se tripsinizaron las células adheridas, juntándose todas en el mismo tubo. Las células se lavaron dos veces con PBS 1x y se fijaron en etanol al 70% a 4 ºC durante un mínimo de 2 horas.

A continuación las células se lavaron con PBS 1x, se resuspendieron en PBS 1x que contenía ribonucleasa A 100 µg/ml (#R6148, Sigma-Aldrich) y yoduro de propidio 40 µg/ml (#P4170, Sigma-Aldrich) y se incubaron durante 30 minutos en oscuridad a 37 ºC.

Para cada condición se analizaron 10.000 células en un citómetro MACS Quant Analyzer (Miltenyi Biotec, Colonia, Alemania). Los datos se procesaron con el programa Flowing Software (Cell Imaging Core, Turku Centre for Biotechnology, Finlandia).

3.5.1.5. Cuantificación del crecimiento clonogénico en placa

Para estudiar el crecimiento en placa a muy baja densidad, las células A673/TR/SPRY1, SKES/TR/SPRY1 y SKNMC/TR/SPRY1 se sembraron por triplicado a $0{,}5x10^3$, 10^3 y $2x10^3$ células por pocillo respectivamente en placas de 24 pocillos. Posteriormente fueron cultivadas en ausencia o presencia de doxiciclina (1 µg/ml) y mantenidas en medio de cultivo suplementado con 5% de SFB libre de tetraciclina durante 9 días. Durante este tiempo el medio se cambió cada 72 horas. Para analizar el efecto de los inhibidores de FGFR sobre las células de sarcoma de Ewing y las células control (IMR90), se sembraron $3x10^3$ células por pocillo por triplicado en medio con suero y se les añadió el inhibidor correspondiente durante 12-15 días, renovando el medio y el tratamiento cada 72 horas.

Al finalizar el periodo de incubación correspondiente se fijaron las colonias con paraformaldehído al 3%, se lavaron con metanol al 2% en PBS 1x y se tiñeron con cristal violeta al 0,5% en 20% de metanol. Se tomaron 10 fotografías representativas de cada pocillo. El colorante se liberó utilizando una solución de etanol al 50% y 0,1 M de citrato sódico (pH 4,2) y se cuantificó la absorbancia de la disolución resultante a 550 nm utilizando un lector de placas Infinite M200 (Tecan).

3.5.1.6. Ensayo de crecimiento libre de anclaje en medio semisólido

Para los experimentos de formación de focos de crecimiento independiente de anclaje se prepararon placas de 6 pocillos con una base de 2 ml de agar noble al 0,5 % (p/v) (Sigma-Aldrich) en medio DMEM/Hepes, suplementado con SFB sin tetraciclina, glutamina (4 mM), penicilina (100 UI/ml), estreptomicina (100 µg/ml), fungizona (3 µg/ml) y baycip (25 µg/ml). Una vez solidificado, se sembraron 50.000 células (A673/TR/SPRY1, SKES/TR/SPRY1 o SKNMC/TR/SPRY1) por pocillo resuspendidas en 0,5 ml de agar noble al 0,3% (p/v) preparado en medio de cultivo suplementado. Las células se mantuvieron a 37 ºC durante 4 semanas, añadiendo medio fresco (aproximadamente 200 µl) cada 2 o 3 días (DMEM suplementado con 10% suero fetal bovino libre de tetraciclina, antibióticos y doxiciclina a 1 µg/ml cuando correspondiese).

Las colonias se tiñeron con cristal violeta al 0,005 % (p/v) y se seleccionaron 3 campos de las placas aleatoriamente para tomar fotografías con aumento 4X. El número y el área de las colonias por campo se cuantificaron con el programa ImageJ (NIH, Maryland, EEUU).

3.5.2. Estudios de migración celular

3.5.2.1. Ensayos de migración por cierre de herida

Este ensayo se basa en la observación de la progresión de la migración celular en una monocapa confluente de células a la que previamente se le ha realizado una “herida”. Las células en el borde de la “herida” (frente) migrarán hasta establecer nuevos contactos célula-célula, cerrando así la “herida” y permitiendo cuantificar el avance de este frente y determinar así su capacidad migratoria.

Para este ensayo, las células A673/TR/SPRY1, SKES/TR/SPRY1 o SKNMC/TR/SPRY1 se sembraron por triplicado a una densidad de $3x10^4$ células por pocillo en placas de 24 pocillos y se incubaron en ausencia o presencia de doxiciclina (1 µg/ml) durante 72 horas hasta obtener un cultivo confluente al 90% en monocapa. Tras este periodo, se utilizó la punta de una pipeta de 200 µl para efectuar una "herida" en la monocapa de células. Posteriormente se señaló en la base de la placa aleatoriamente las zonas de la "herida" destinadas a ser fotografiadas periódicamente para observar la evolución. Se realizaron fotografías cada 6 o 12 horas. La cuantificación de la migración celular relativa se realizó empleando el programa ImageJ donde cada una de las fotografías obtenidas fue convertida a imagen binaria para resaltar la diferencia entre la zona con presencia de células y la zona de la "herida". Posteriormente se obtuvo el área de la "herida" utilizando la herramienta de dibujo de área del mismo programa.

3.5.2.2. Ensayo de migración a través de membrana porosa

Para estudiar la migración a través de membrana se utilizaron células A673/TR/SPRY1, SKES/TR/SPRY1 y SKNMC/TR/SPRY1 cultivadas durante 24 horas en ausencia o presencia de doxiciclina (1 µg/ml) para inducir la expresión de la proteína SPRY1. A continuación las células se deplecionaron de suero (0,5% suero libre de tetraciclina) durante 24 horas más, manteniendo la estimulación con doxiciclina en los casos en los que correspondiese. Pasado ese tiempo, las células se tripsinizaron y se resuspendieron a razón de $3x10^5$ células en 2 ml del medio de cultivo suplementado con 0,5% de suero libre de tetraciclina y se añadieron a la parte superior de una cámara transwell con un tamaño de poro de 8,0 µm (Corning, Carolina del Norte, EEUU). Como quimioatrayente, en el compartimento inferior se añadió medio de cultivo con suero al 10%. Las células se incubaron durante 6 horas a 37 ºC. Pasado ese tiempo se retiró el inserto que contenía la membrana porosa, se fijaron las células con formaldehído al 4% y se tiñeron con cristal violeta, retirando las células que no habían migrado, y por lo tanto se encontraban en la cara superior de la membrana, con un bastoncillo de algodón.

El colorante absorbido por las células adheridas a la parte inferior de la membrana (células migratorias), se liberó con PBS 1x, 2% SDS durante 10 minutos y se midió la

absorbancia de la disolución obtenida a 570 nm en el lector de placas Infinite M200 (Tecan).

3.5.2.3. Estudio de la morfología celular por inmunofluorescencia

Las células se sembraron a una densidad de 2.500 células por pocillo sobre cristales redondos de 12 mm dentro de placas de cultivo multipocillo de 24 pocillos y se cultivaron en presencia o ausencia de doxiciclina durante 72 horas. Después, los cristales se lavaron con PBS 1x y las células se fijaron con etanol al 70% frío durante 10 minutos a -20 ºC. Posteriormente las células se permeabilizaron con Tritón 0,1% en PBS y se bloquearon con una solución de albúmina sérica bovina (BSA, *bovine serum albumin*) al 1% en PBS. Las preparaciones se incubaron con los anticuerpos primarios correspondientes preparados en BSA al 1% en PBS durante 1 hora a 37 ºC y luego con los anticuerpos secundarios conjugados con isotiocianato de fluoresceína (FITC, *fluorescein isotiocyanate*) durante 30 minutos a 37 ºC. Los núcleos se contratiñeron con DAPI (1 µg/µl; #D1306, Life Technologies). Finalmente los cristales se lavaron y se montaron con Mowiol (#475904, Merk Millipore, Massachusetts, EEUU). Las células se visualizaron y fotografiaron en un microscopio confocal de fluorescencia Leica TC5 SP5. Finalmente se cuantificó la circularidad celular con ayuda del programa de análisis de imagen ImageJ (National Institutes of Health, EEUU).

Los anticuerpos empleados aparecen detallados en la **Tabla 12**.

Tabla 12. Relación de los anticuerpos empleados para inmunocitoquímica en esta Tesis.

Reactivo	Dilución o concentración	Referencia, Casa comercial
Anti-Vimentina anticuerpo primario	1:200	#ab92547, Abcam
Anti-Faloidina-FITC	10 µg/ml	#P5282, Sigma-Aldrich
Anti-Rabbit-FITC anticuerpo secundario	1:100	#111-096-047, Jackson ImmunoResearch

3.5.3. Estudios de formación de tumores en ratones *in vivo*

Las células de sarcoma de Ewing POE o SKES se tripsinizaron y lavaron con PBS 1x frío. A continuación se resuspendieron en una disolución (1:1) de PBS/matrigel libre de

rojo fenol (#356237, Corning, Nueva York, EEUU) a razón de $5x10^7$ células/mililitro. Se inyectaron $5x10^6$ células subcutáneamente en un volumen de 100 µl en el flanco de ratones C.B17/SCID de 6-8 semanas.

Se realizó un seguimiento del peso de los ratones utilizando una báscula y el tamaño tumoral utilizando un calibre durante todo el experimento. Cuando el tumor alcanzó un tamaño de 150-200 mm^3 (calculado utilizando la fórmula $L*A^2*\pi/6$, donde L es el lado más largo del tumor y A es en lado más corto), se inició el tratamiento que consistió en una dosis intraperitoneal diaria de 5, 10 o 20 mg/Kg de PD173074 disuelto en DMSO 10% - aceite de maíz 90% (Sigma-Aldrich) o placebo en el caso de los grupos control según el siguiente esquema:

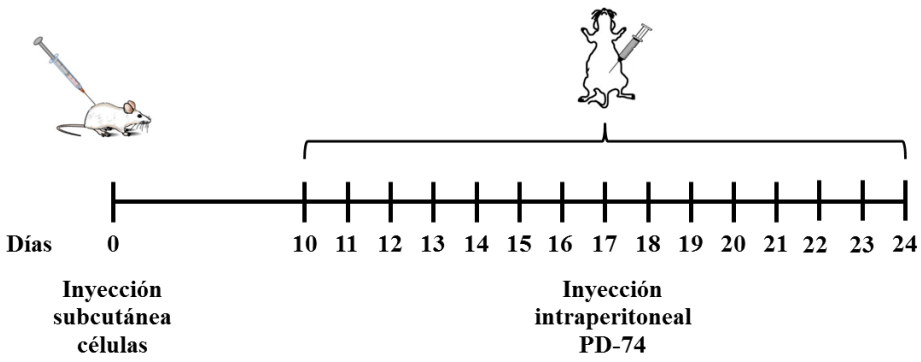

Los ratones fueron sacrificados cuando el tumor alcanzó un volumen de 1.500 mm^3. Todos los tumores fueron fijados en formalina y analizados mediante histología e inmunohistoquímica para determinar el número de células en mitosis y la presencia de apoptosis.

Los experimentos con animales fueron aprobados por los Comités de Ética y Bienestar Animal de las instituciones correspondientes.

3.5.4. Histología y estudios inmunohistoquímicos (IHQ)

Las muestras de tejido tumoral obtenidas se fijaron en formalina durante 24 horas y posteriormente se mantuvieron en etanol al 70% hasta que fueron embebidas en parafina.

Para el análisis inmunohistoquímico se realizaron cortes de 4 µm. El desenmascaramiento antigénico se realizó en microondas con la solución *Target Retrieval Solution* (#S2369, Dako, California, EEUU). Como anticuerpos primarios se utilizaron anti-cleaved caspase-3a policlonal de conejo (1:1000, #9661, Cell Signaling, Massachusetts, EEUU) a temperatura ambiente durante 60 minutos o anti-Ki67 monoclonal de conejo (1:200, #275R-15 clon SP6, Cell Marque, California, EEUU). Para la detección antigénica se utilizó el kit ImmPRESS Reagent Kit IgG anti-conejo (#MP-7401, VectorLabs, California, EEUU).

Las secciones cortadas se contra-tiñeron con hematoxilina/eosina (#H-3401, Vector laboratories). El número medio de células positivas se estableció analizando 10 campos a un aumento de 40X.

3.6. Análisis estadísticos

Para la comparación de dos grupos, se usó el test *T de Student* de dos colas asumiendo una distribución normal. Para la comparación del tamaño tumoral entre el grupo de animales control y el tratado, se usó un test de ANOVA de dos variables basado en el método Student-Newman-Keuls. Los estudios *in situ*, incluyendo la supervivencia global y la probabilidad de supervivencia libre de eventos, se analizaron con el test de log-rank. Para el análisis de proporciones se utilizó el test exacto de Fisher. Para todos los análisis, se consideraron diferencias significativas aquellas con $P < 0,05$. Los datos se presentan como media ± desviación estándar. Todos los análisis estadísticos se realizaron utilizando el programa GraphPad Prism versión 6.0 (*GraphPad Software*, California, EEUU).

4. Resultados

Resultados

4.1. Perfil de expresión de SPRY1 en sarcoma de Ewing: regulación por EWS-FLI1

EWS-FLI1 regula negativamente la expresión de SPRY1 en células de sarcoma de Ewing A673.

Uno de los principales intereses de nuestro laboratorio durante los últimos años ha sido la identificación de los genes regulados por el factor de transcripción quimérico EWS-FLI1, característico del sarcoma de Ewing. Para ello, se estableció previamente una línea celular de sarcoma de Ewing (A673) que expresaba un ARN de interferencia contra EWS-FLI1 de manera condicional en respuesta a doxiciclina (Carrillo *et al.* 2007) (**Figura 4A**). Como puede observarse en la **Figura 4B**, la adición de doxiciclina a estas células provoca una reducción muy significativa de los niveles de EWS-FLI1, lo que convierte a este modelo celular en un sistema idóneo para la identificación de genes dependientes de EWS-FLI1.

Para identificar los genes regulados por EWS-FLI1 en las células A673/TR/shEF, se caracterizó el perfil de expresión génica mediante *microarrays* de expresión en células cultivadas en ausencia (niveles elevados de EWS-FLI1) o presencia de doxiciclina (niveles bajos de EWS-FLI1) durante 72 horas. En la **Figura 4C** se muestran los genes que experimentaron los mayores niveles de inducción o inhibición tras la reducción de los niveles de EWS-FLI1. Algunos de estos son genes regulados por EWS-FLI1 que han sido estudiados previamente por nuestro grupo como *DAX1* (*NR0B1*), *CCK* o *LOX* (Carrillo *et al.* 2007, Garcia-Aragoncillo *et al.* 2008, Agra *et al.* 2013). Como puede observarse en esta figura, *SPRY1* resultó ser uno de los genes más fuertemente reprimidos por EWS-FLI1 en estos experimentos.

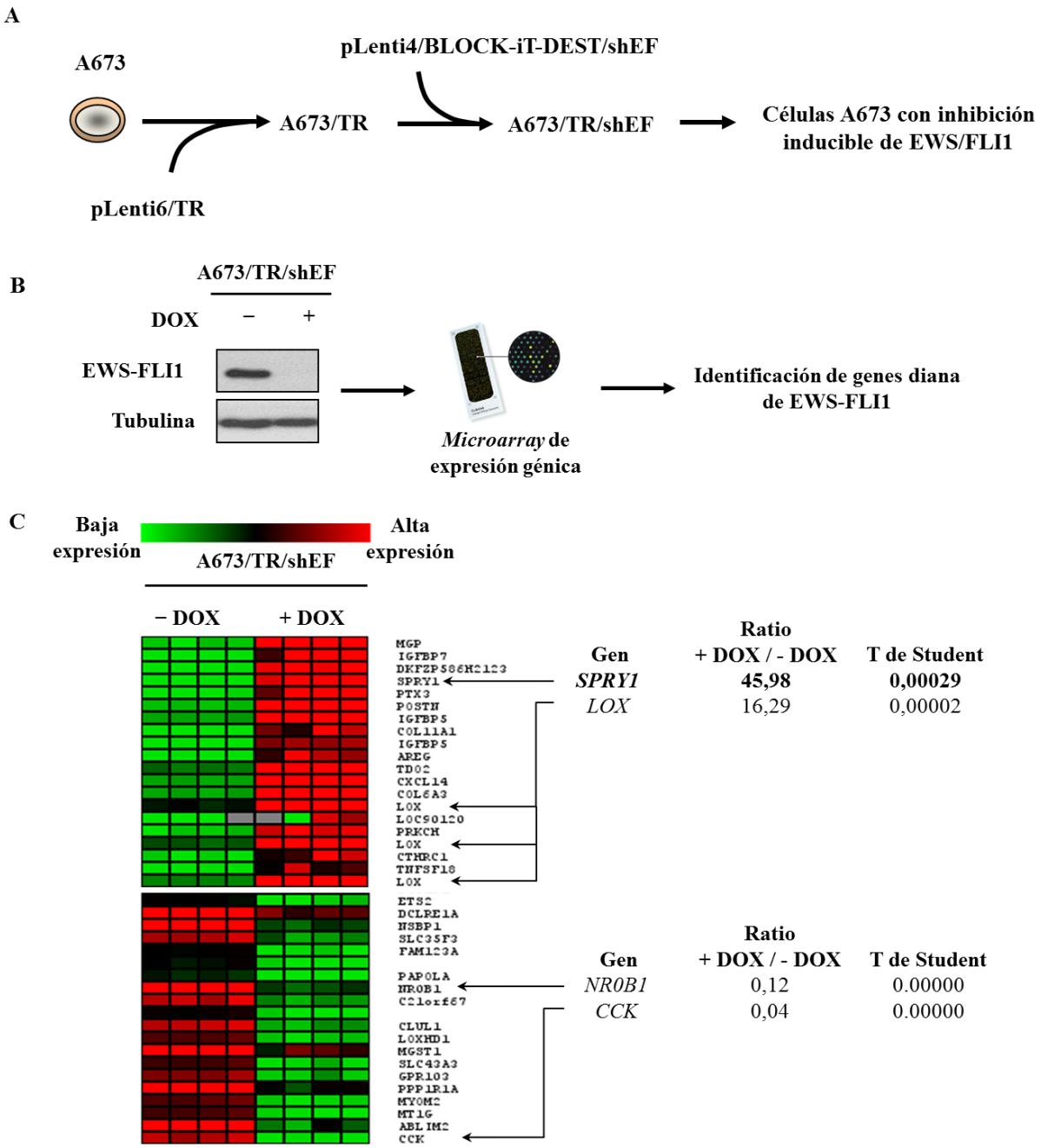

Figura 4. Identificación de genes regulados por EWS-FLI1 en células de sarcoma de Ewing A673. **A.** Establecimiento de la línea celular A673/TR/shEF. Esta línea expresa de manera condicional un shARN dirigido contra EWS-FLI1 (descrito en detalle en Carrillo *et al.* 2007). **B.** Se cultivaron células A673/TR/shEF en ausencia o presencia de doxiciclina (1 µg/ml) durante 72 horas para inducir la expresión del ARN de interferencia dirigido contra EWS-FLI1. Esas muestras fueron analizadas con un *microarray* de expresión génica. La figura muestra un esquema del planteamiento experimental así como un western blot donde se observa la inhibición de EWS-FLI1 en las células A673/TR/shEF tras el tratamiento con doxiciclina. **C.** La figura muestra un *heatmap* con los resultados del *array* y los principales genes reprimidos por EWS-FLI1 (top 20), como *SPRY1* o *LOX* (Agra *et al.* 2013). También se muestran los principales genes inducidos por EWS-FLI1 (top 20) como *CCK* (Carrillo *et al.* 2007) y *NR0B1* (Garcia-Aragoncillo *et al.* 2008). Cada columna corresponde a una muestra diferente de cuatro experimentos independientes. El color verde significa niveles bajos de expresión y el rojo niveles altos de expresión de cada gen.

Para confirmar los resultados obtenidos en los experimentos llevados a cabo con *microarrays* de expresión, realizamos un análisis por RT-PCR cuantitativa. En estos experimentos cultivamos la línea celular A673/TR/shEF en ausencia o presencia de doxiciclina (1 µg/ml) durante 24, 48 o 72 horas y analizamos la expresión del ARNm de SPRY1. Como se puede observar en la **Figura 5A**, los niveles del ARNm de SPRY1 se indujeron más de 1000 veces en las células cultivadas con doxiciclina durante 72 horas y por tanto con niveles bajos de EWS-FLI1. Dado que existen otros 3 miembros de la familia de proteínas *Sprouty* llamados SPRY2, -3 y -4, decidimos estudiar si el efecto inhibidor de EWS-FLI1 sobre SPRY1 se observaba también en el resto de miembros de la familia de proteínas *Sprouty*. En la **Figura 5A** comprobamos como EWS-FLI1 ejerce una inhibición selectiva de SPRY1 con respecto al resto de miembros de su familia de proteínas. En la **Tabla 13** se muestra una comparativa de los resultados obtenidos en los *arrays* de expresión y los análisis de RT-PCR cuantitativa para los genes de la familia *Sprouty* donde se observa el mismo patrón de expresión empleando las dos técnicas. Se muestran también los valores obtenidos para *LOX* y *NR0B1*, dos genes diana de EWS-FLI1 previamente descritos por nuestro grupo (Mendiola *et al.* 2006, Agra *et al.* 2013).

Además, comprobamos mediante western-blot que la re-expresión de SPRY1 se observaba también a nivel de proteína (**Figura 5B**).

SPRY1 presenta cuatro variantes transcripcionales (VT 1-4) que difieren en el número de exones o bien se transcriben a partir de promotores alternativos (**Figura 6A**): la variante 1 (VT1) contiene 3 exones, la variante 2 (VT2) carece del exón 2 y las variantes 3 y 4 (VT3, VT4) también carecen del exón 2 pero presentan un exón nuevo cada una, con promotores alternativos. En las 4 variantes transcripcionales el último exón es el codificante y por lo tanto todas las variantes transcripcionales dan lugar a la misma proteína.

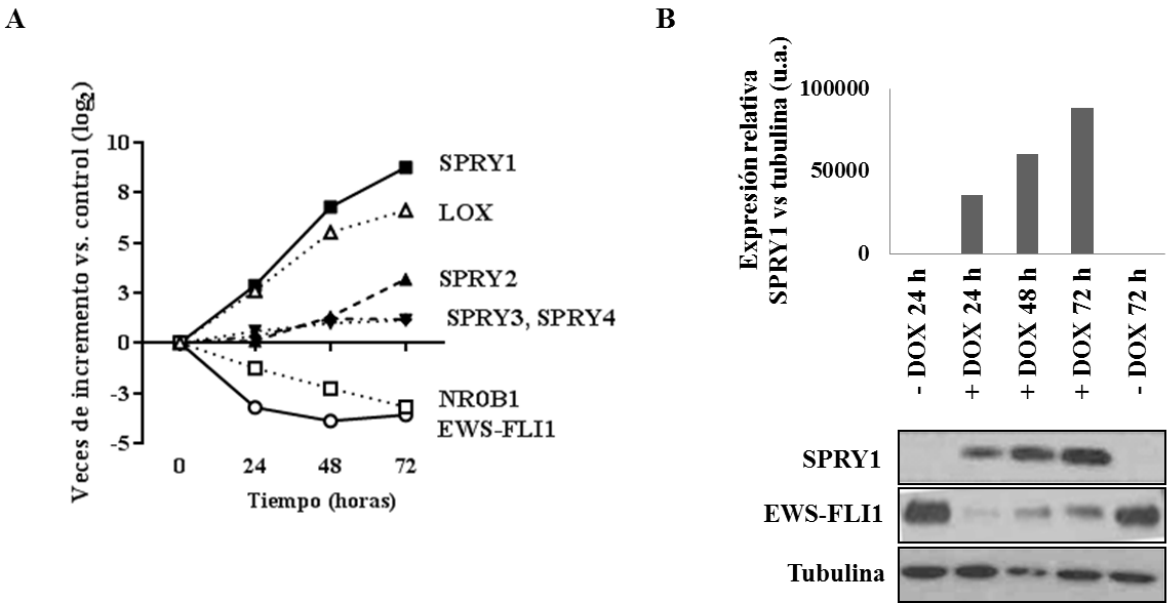

Figura 5. El silenciamiento de EWS-FLI1 induce un fuerte incremento de la expresión de SPRY1 a nivel de ARNm y proteína. A. Las células A673/TR/shEF se estimularon con doxiciclina durante periodos de 0, 24, 48 y 72 hs y se extrajo ARN total. Los niveles de ARNm de SPRY1 y EWS-FLI1 se cuantificaron mediante RT-PCR cuantitativa usando sondas Taqman específicas. La figura muestra los niveles relativos de expresión de *SPRY1, -2, -3 y -4* tras la inhibición de EWS-FLI1 inducida con doxiciclina. Se incluyeron como controles EWS-FLI1 y dos de sus genes diana conocidos (*NR0B1* y *LOX*). En la figura se observa como la inhibición de EWS-FLI1 genera un incremento en los niveles de ARNm de SPRY1 de 1000 veces con respecto al control. Como era esperado, LOX aparece inducido y NR0B1 reprimido tras la inhibición de EWS-FLI1. La figura muestra los resultados de un experimento independiente de un total de tres realizados. **B.** Células A673/TR/shEF testadas por western blot con anticuerpos específicos para SPRY1 y EWS-FLI1 a 24, 48 y 72 horas del tratamiento con doxiciclina. La figura muestra como el tratamiento con doxiciclina genera un fuerte incremento de SPRY1 dependiente del tiempo, que correlaciona con la inhibición de EWS-FLI1 a nivel de proteína. La gráfica muestra los niveles relativos de expresión de la proteína SPRY1 vs tubulina, que fue usado como control de carga (u.a., unidades arbitrarias de densitometría).

Tabla 13. Comparación de los ratios de expresión de cada gen tras la inhibición de EWS-FLI1 analizados mediante *microarrays* de expresión o RT-PCR cuantitativa.

	Ratio + DOX / - DOX			
	Microarray		RT-PCR cuantitativa	
SPRY1	45,98 ± 13,3	(*P* = 0,0002)	430,5 ± 11,35	(*P* = 0,0003)
SPRY2	5,73 ± 1,51	(*P* = 0,0016)	9,1 ± 2,37	(*P* = 0,0002)
SPRY3	0,97 ± 1,12	(*P* = 0,79)	2,1 ± 0,3	(*P* = 0,0002)
SPRY4	2,09 ± 0,76	(*P* = 0,018)	2,2 ± 0,32	(*P* = 0,0001)
LOX	21,16 ± 4,42	(*P* < 0,0001)	97,7 ± 12,1	(*P* = 0,0012)
NR0B1	0,12 ± 0,01	(*P* < 0,0001)	0,1 ± 0,02	(*P* = 0,0003)

Para determinar si la inhibición de EWS-FLI1 afectaba a la expresión de estas variantes de SPRY1 de forma diferente, analizamos el perfil de expresión de cada una de las variantes mediante RT-PCR cuantitativa utilizando cebadores específicos de cada isoforma. En la **Figura 6B** observamos como las variantes 2, -3 y -4 de SPRY1 experimentan un incremento de aproximadamente 40-60 veces tras la inhibición de EWS-FLI1 con respecto al control. La isoforma 1, por el contrario, presenta una menor regulación por EWS-FLI1, alcanzando 20 veces de incremento tras la inhibición de EWS-FLI1 al comparar la muestra tratada frente al control. Además, en la **Figura 6C** vemos un patrón similar al cargar esas muestras en un gel de agarosa. Por lo tanto, concluimos que las isoformas 2, -3 y -4 de SPRY1 son las isoformas preferentemente inducidas tras la inhibición de EWS-FLI1.

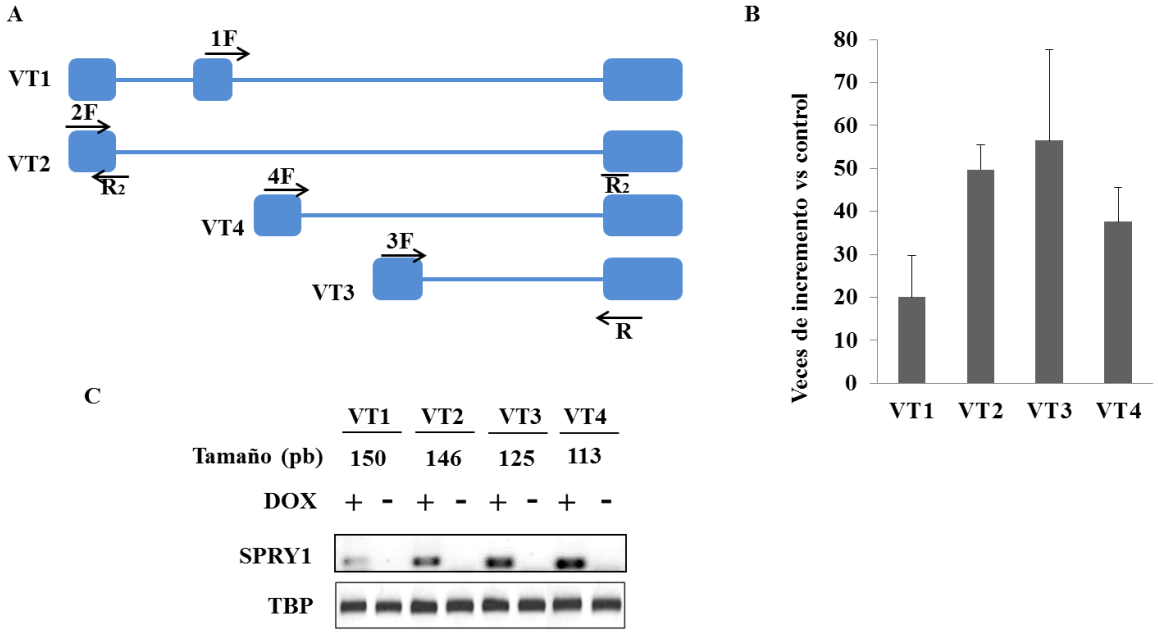

Figura 6. Efecto del silenciamiento de EWS-FLI1 sobre la expresión de las 4 variantes transcripcionales de SPRY1. **A.** SPRY1 presenta 4 variantes transcripcionales. El esquema muestra cada una de las variantes transcripcionales (VT1-4) así como la localización de los cebadores empleados (flechas), donde el cebador R_2 se emplea para diferenciar la VT1 de la VT2. **B.** RT-PCR cuantitativa con cebadores específicos para cada una de las 4 variantes transcripcionales de SPRY1 tras 72 horas de tratamiento con doxiciclina en células A673/TR/shEF para inducir la expresión del ARN de interferencia contra EWS-FLI1. La gráfica muestra la inducción de los niveles de ARNm de las 4 variantes transcripcionales de SPRY1. Las variantes 2, -3 y -4 se inducen mayoritariamente al inhibir EWS-FLI1. **C.** Gel de agarosa en el que se muestran los niveles de expresión de las 4 variantes de SPRY1. Se indica el tamaño en pares de bases (pb) de cada una de las variantes. TBP (*TATA binding protein*) se empleó como control de carga.

Los resultados mostrados hasta ahora indican que EWS-FLI1 inhibe la expresión de SPRY1 en la célula de sarcoma de Ewing A673 y que los niveles de expresión de SPRY1, tanto a nivel de ARNm como de proteína son muy bajos. A continuación, por tanto, decidimos estudiar los niveles de expresión de SPRY1 y el resto de miembros de la familia *Sprouty* en otras líneas celulares derivadas de sarcoma de Ewing. Para ello, se seleccionó un panel de 8 líneas celulares de sarcoma de Ewing (A4573, RDES, SKPNDW, TTC466, SKES, TC71, SKNMC y células A673 parentales).

En la **Figura 7A** se observa que SPRY1 presenta el nivel más bajo de expresión en comparación con el resto de miembros de la familia *Sprouty* en las células de sarcoma de Ewing estudiadas. Además, mediante western blot comprobamos que los niveles de expresión de SPRY1 eran muy bajos o indetectables en todas estas células (**Figura 7B**).

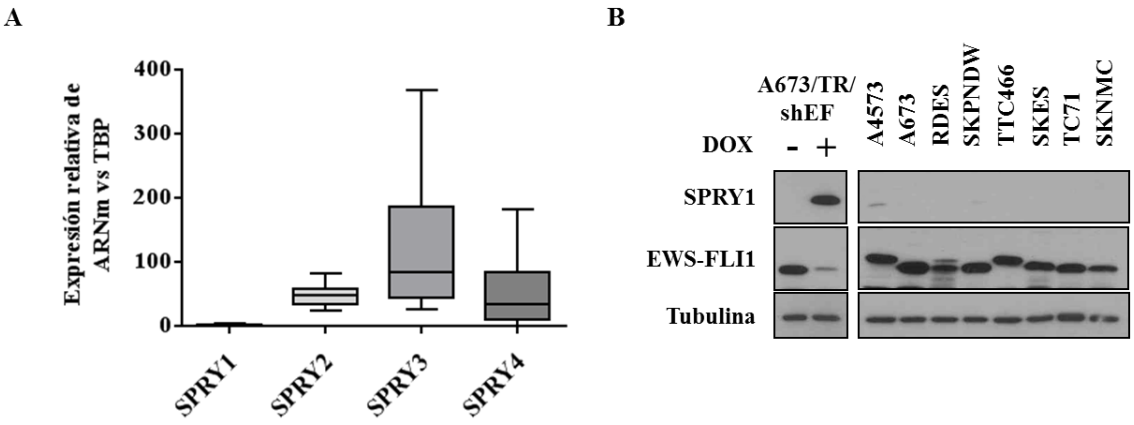

Figura 7. Los valores de expresión de SPRY1 son bajos en relación con el resto de miembros de la familia de proteínas *Sprouty* en líneas celulares de sarcoma de Ewing. A. Se extrajo ARNm de una selección de 8 líneas celulares de sarcoma de Ewing (A4573, A673, RDES, SKPNDW, TTC466, SKES, TC71 y SKNMC) y se analizó por RT-PCR cuantitativa utilizando sondas Taqman específicas para SPRY1, -2, -3 y -4. La figura muestra como SPRY1 es el miembro de la familia de proteínas *Sprouty* que presenta una expresión más baja en líneas de sarcoma de Ewing. La gráfica muestra la media ± desviación estándar. **B.** Se realizó un western blot de la proteína extraída de líneas celulares de sarcoma de Ewing con diferentes fusiones de EWS-FLI1 (A4573, A673, RDES, SKPNDW, TTC466, SKES, TC71 y SKNMC) utilizando anticuerpos específicos contra SPRY1 y EWS-FLI1. Se utilizaron células A673/TR/shEF tratadas con doxiciclina (+ DOX) como controles positivos para la expresión de SPRY1. La tubulina se utilizó como control de carga. La figura muestra como SPRY1 no se expresa en las células de sarcoma de Ewing.

Para comprobar si los resultados obtenidos en nuestro laboratorio concordaban con los datos disponibles en las bases de datos públicas, se compararon los niveles de expresión de SPRY1 en líneas celulares de diferentes tipos tumorales procedentes de la base de datos pública *Cancer Cell Line Encyclopedia* (CCLE, Broad Institute, http://www.broadinstitute.org/ccle) que contiene datos de expresión procedentes de más de 1000 líneas celulares de 37 tumores diferentes. Como se puede observar en la **Figura Suplementaria 1**, las células de sarcoma de Ewing presentan los niveles de expresión de SPRY1 más bajos.

A continuación, analizamos los niveles de expresión de SPRY1 mediante RT-PCR cuantitativa y del resto de miembros de la familia *Sprouty* en una selección de muestras tumorales de Ewing (n=11). Como se muestra en la **Figura 9**, los niveles de expresión de SPRY1 fueron mucho más bajos en comparación con los niveles de SPRY2, -3 y -4.

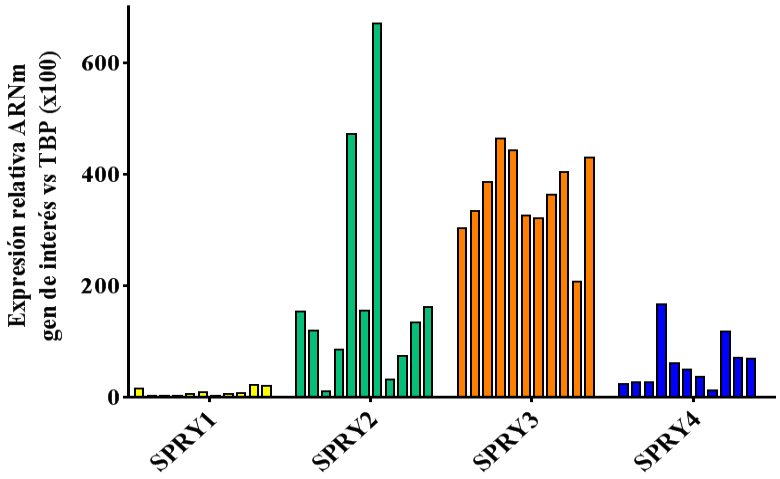

Figura 9. SPRY1 se expresa a niveles inferiores en tumores primarios de sarcoma de Ewing en comparación con el resto de miembros de la familia de proteínas *Sprouty*. Se analizaron los niveles de expresión de SPRY1, -2, -3 y -4 en una selección de tumores primarios de sarcoma de Ewing (n=11). Los niveles de ARNm se cuantificaron por RT-PCR cuantitativa utilizando sondas Taqman específicas. La gráfica muestra la expresión relativa de cada gen con respecto a TBP.

Posteriormente analizamos los perfiles de expresión de SPRY1 y del resto de miembros de la familia *Sprouty* en una serie de líneas celulares procedentes de otros tumores pediátricos, para determinar si estos genes presentaban niveles diferentes de expresión en función del tipo de tumor. La selección incluía células de neuroblastoma (IMR32,

SKNSH, SHSY5Y y SKNAS), rabdomiosarcoma (CW9019) y osteosarcoma (SAOS-2 y U2OS). En la **Figura 10** se observa que SPRY1 no se expresa en las células estudiadas a excepción de la línea celular de neuroblastoma SKNAS, donde SPRY1 presenta niveles elevados de expresión tanto a nivel de ARNm (**Figura 10A**) como a nivel proteína (**Figura 10B**). Este resultado concuerda con los datos publicados en la *Cancer Cell Line Encyclopedia*, donde la célula SKNAS ocupa la segunda posición entre las líneas celulares de cáncer con la mayor expresión de SPRY1 (**Tabla Suplementaria 1**).

En cuanto a los niveles de expresión comparativos de ARNm de los diferentes miembros de la familia de proteínas *Sprouty* en líneas de otros tumores pediátricos, se observa una gran variabilidad en la expresión de SPRY1, -2 y -4, mientras que los niveles de SPRY3 permanecen muy bajos (**Figura 10A**).

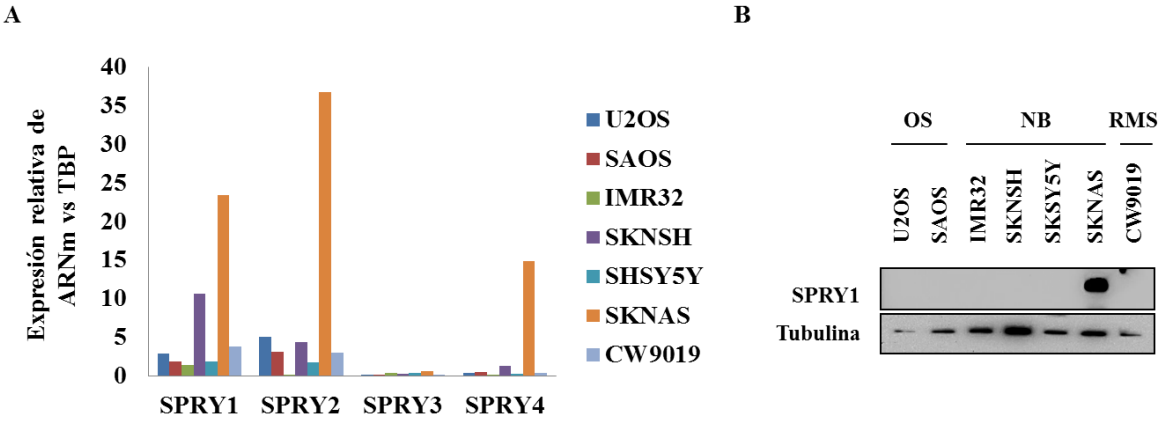

Figura 10. Expresión de SPRY1 en líneas celulares de otros tumores sólidos pediátricos. **A.** Se extrajo ARN total de una selección de líneas celulares de diferentes tumores sólidos pediátricos (neuroblastoma (NB; IMR32, SKNSH, SHSY5Y y SKNAS), rabdomiosarcoma (RMS; CW9019) y osteosarcoma (OS; U2OS y SAOS) y se analizó por RT-PCR cuantitativa utilizando sondas Taqman específicas para SPRY1, -2, -3 y -4. **B.** La proteína SPRY1 no se expresa en ninguna de las líneas de tumores sólidos estudiados excepto en la línea celular de neuroblastoma SKNAS. La figura muestra un análisis por western blot de proteína extraída de una colección de líneas celulares de diferentes tumores sólidos pediátricos (neuroblastoma (IMR32, SKNSH, SHSY5Y y SKNAS)), rabdomiosarcoma (CW9019) y osteosarcoma (U2OS y SAOS) analizada con un anticuerpo específico para la proteína SPRY1. La tubulina se utilizó como control de carga.

Finalmente analizamos los niveles de expresión de SPRY1, -2, -3 y -4 mediante RT-PCR cuantitativa en tejidos normales y lo comparamos con lo observado en las líneas celulares y muestras tumorales. Como se puede observar en la **Figura 11**, en general los tejidos normales presentan niveles bajos de expresión en comparación con el resto de miembros de la familia *Sprouty*. El tejido que presenta mayor expresión de SPRY1 es el tejido adiposo, seguido por vejiga, útero, esófago, colon, corazón, pulmón, próstata, músculo y tráquea (**Figura 11**). Estos resultados concuerdan con los datos presentes en el proyecto *Genotype-Tissue Expression* (GTEx), que agrupa una colección de múltiples tejidos humanos que han sido genotipados y analizados con *arrays* de expresión, donde el tejido no tumoral con mayor expresión de SPRY1 es el adiposo (**Figura Suplementaria 2**).

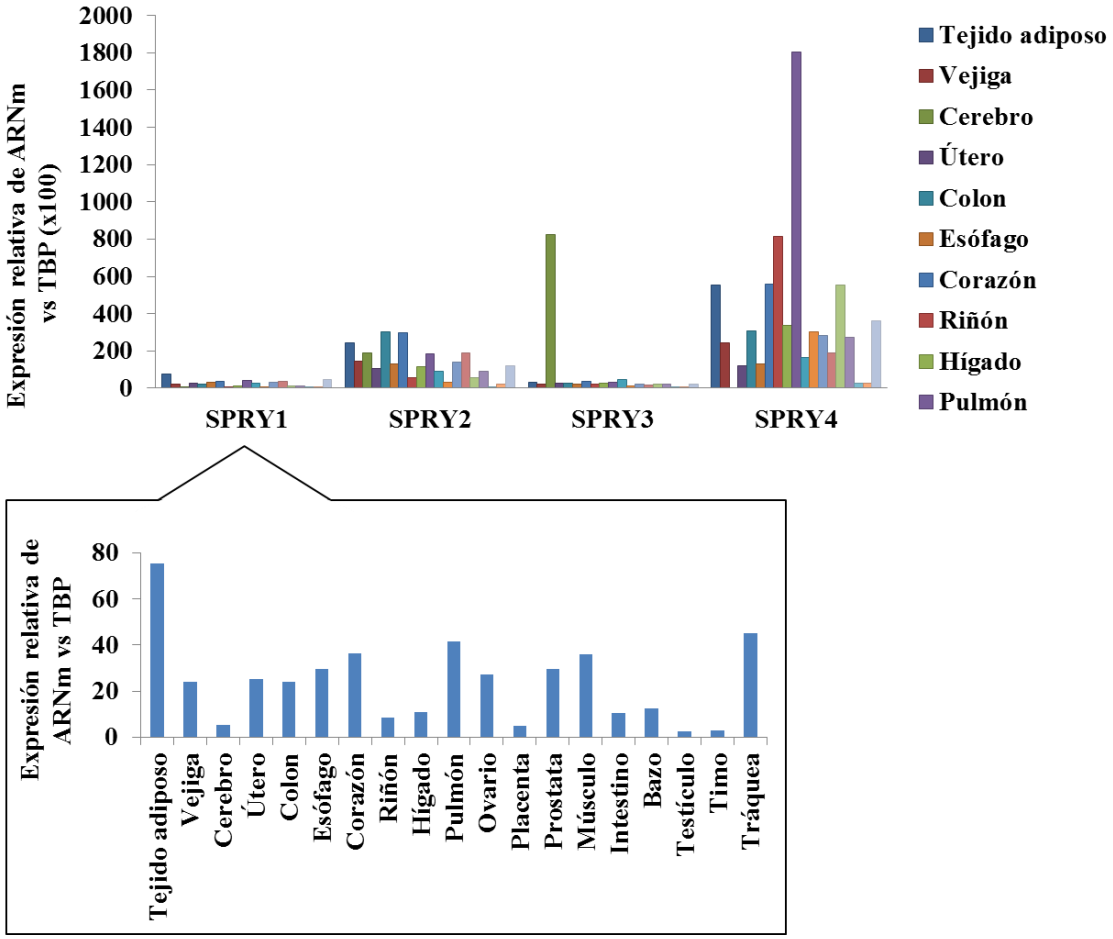

Figura 11. Expresión de SPRY1 en tejidos no tumorales. Se empleó ARN comercial de una batería de tejidos no tumorales (Clontech) y se analizó la expresión de SPRY1-4 por RT-PCR cuantitativa utilizando una sonda Taqman específica. En la gráfica superior se puede observar como SPRY1 se expresa a niveles relativamente bajos en comparación con el resto de miembros de la familia *Sprouty*. En la ampliación se observa como SPRY1 se expresa a niveles más elevados en tejido adiposo mientras que timo y testículos son los tejidos donde hay una expresión más reducida.

La regulación de SPRY1 por EWS-FLI1 en células A673 podría estar mediada por un mecanismo epigenético

Los resultados mostrados hasta el momento en esta Tesis indican que *SPRY1* es un gen regulado selectiva y negativamente por EWS-FLI1, pero no demuestran si esta regulación es directa o indirecta. Con el objeto de avanzar en esta cuestión analizamos tres experimentos de ChIP-seq publicados previamente (Bilke *et al.* 2013, Riggi *et al.* 2014, Tomazou *et al.* 2015). En estos trabajos los autores realizaron experimentos de ChIP-seq para identificar los sitios de unión de EWS-FLI1 en el genoma así como la distribución de las marcas epigenéticas de histonas. En los tres estudios se utilizó como modelo la línea celular A673, comparando los resultados obtenidos en células con expresión alta o baja de EWS-FLI1 (Bilke *et al.* 2013, Riggi *et al.* 2014, Tomazou *et al.* 2015). Además, en dos de estos estudios (Bilke *et al.* 2013, Tomazou *et al.* 2015) se utilizó la línea celular A673/TR/shEF desarrollada en nuestro laboratorio (Carrillo *et al.* 2007) y que se ha empleado para los estudios descritos en esta Tesis.

En la **Figura 12A** se muestran los resultados obtenidos a partir de los datos publicados en los trabajos de Bilke *et al.* y Tomazou *et al.* (Bilke *et al.* 2013, Tomazou *et al.* 2015). Como se puede ver en esta figura, EWS-FLI1 no se une de forma directa al promotor de *SPRY1* o a regiones colindantes. De hecho, las marcas de unión de EWS-FLI1 al genoma más cercanas al gen de *SPRY1* se encuentran a una distancia de más de 120 kb (no mostrado). Estos resultados sugieren que EWS-FLI1 no se une directamente al promotor de *SPRY1*, aunque no es posible descartar totalmente que regiones lejanas puedan estar implicadas en su regulación.

Por otro lado, en las **Figuras 12A,B** se puede ver como la inhibición de EWS-FLI1 genera un incremento en las marcas de histona H3K27ac localizadas en la región promotora putativa de *SPRY1*, que comprende el exón 1 y el intrón 1. Esto sugiere que la inhibición transcripcional de *SPRY1* por EWS-FLI1 podría estar relacionada con un mecanismo epigenético que involucrase modificaciones de histonas, en vez de una unión directa de EWS-FLI1 al promotor de *SPRY1*.

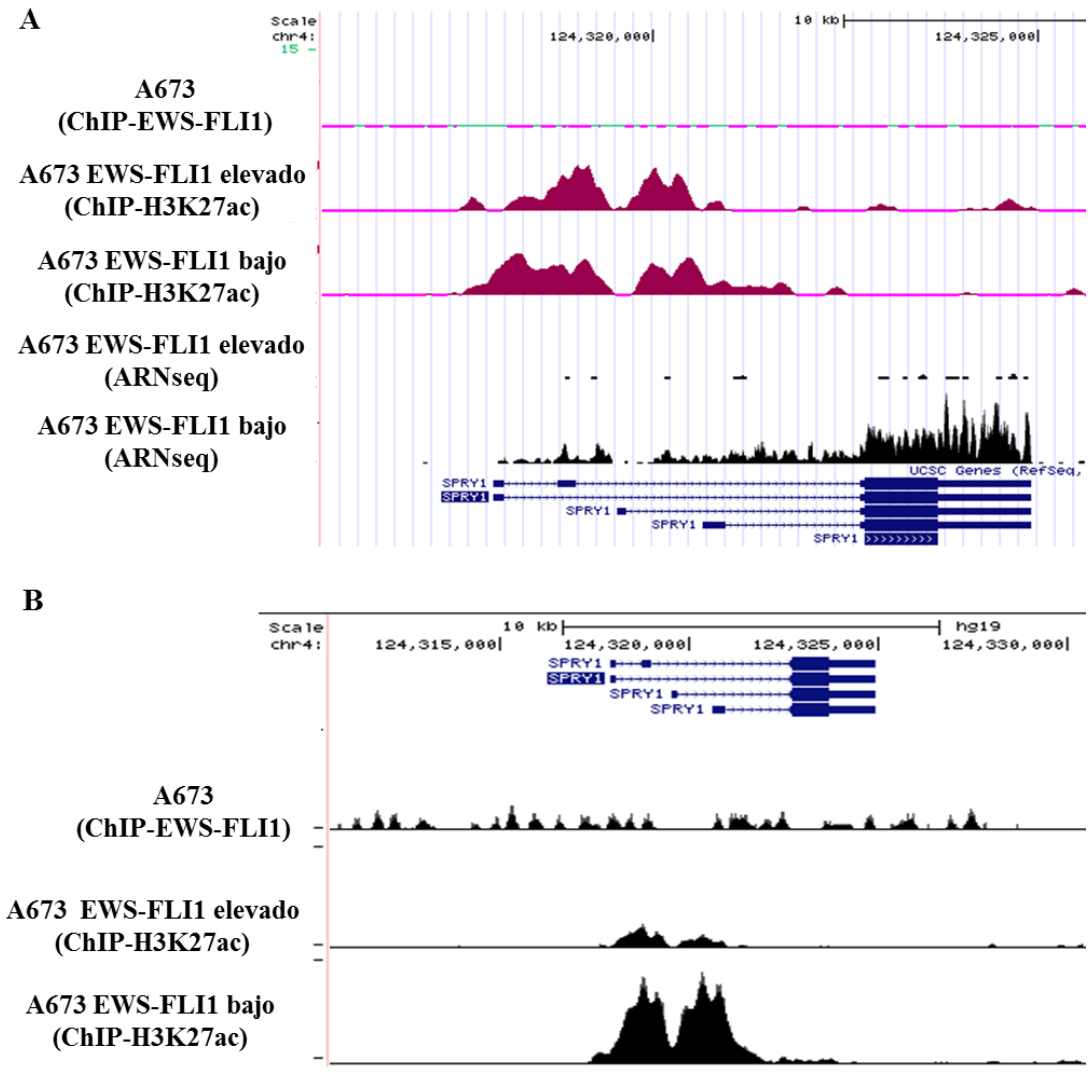

Figura 12. Los datos de ChIP-seq publicados en otros estudios sugieren que SPRY1 no es una diana directa de EWS-FLI1. Los datos que aquí se muestran derivan de estudios ya publicados donde se empleó la línea celular A673/TR/shEF con inhibición condicional de EWS-FLI1. **A.** La figura muestra las regiones genómicas cercanas al gen SPRY1 junto a un ChIP-seq para EWS-FLI1 (Bilke *et al.* 2013), un ChIP-seq-H3K27ac y un ARNseq (Tomazou *et al.* 2015). **B.** La figura muestra la región genómica cercana a SPRY1 junto a datos de ChIP-seq de Riggi *et al*. (Riggi *et al.* 2014). Se puede observar que no hay marcas específicas para EWS-FLI1 en la región promotora putativa de SPRY1, pero que al inhibir EWS-FLI1, aumenta la señal de H3K27ac, lo que sugiere que SPRY1 podría estar siendo regulado por un mecanismo epigenético.

Por otro lado, tratamos células A673 de sarcoma de Ewing con un inhibidor de la histona desacetilasa 1 (HDAC1) llamado *Suberoylanilide Hydroxamic Acid* (SAHA) o vorinostat durante 24 horas. En la **Figura 13A** observamos que a la concentración empleada (1 µM) el inhibidor SAHA era capaz de restituir la expresión del ARNm de SPRY1 2,5 veces de forma significativa en células A673. Por otro lado, estudiamos el efecto de un inhibidor de la actividad de la ADN metiltransferasa, que genera la

desmetilación del ADN (5-aza-2'-deoxicitidina, "5-aza"). En la **Figura 13B** se observa como en este caso, la inhibición de la metilación en células A673 no tiene un efecto sobre la expresión del ARNm de SPRY1.

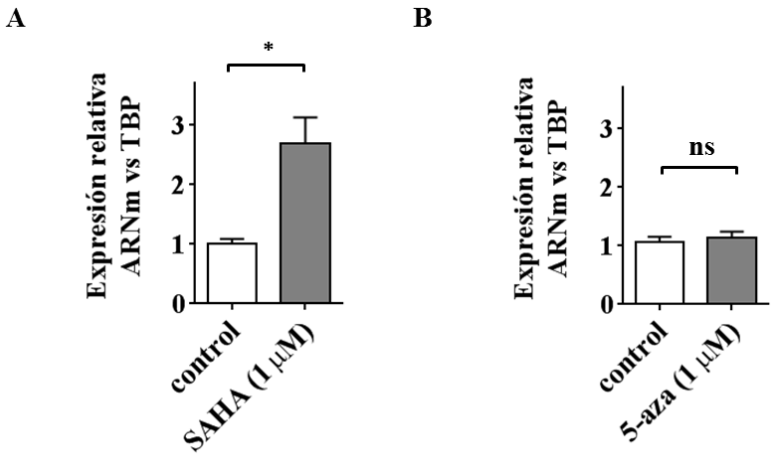

Figura 13. La inhibición de la desacetilación de histonas induce la expresión de SPRY1 en células de sarcoma de Ewing. Células A673 de sarcoma de Ewing se trataron con el inhibidor de la desacetilación de histonas SAHA (1 µM) **(A)** o el inhibidor de la ADN metiltransferasa 5-aza-2'-deoxycytidina (5-aza) (1 µM) **(B)** durante 24 o 96 horas respectivamente y posteriormente se cuantificó la expresión de ARNm de SPRY1. La figura muestra como el tratamiento con SAHA genera un incremento significativo en la expresión de SPRY1 (*P = 0,018), mientras que el tratamiento con 5-aza no genera cambios significativos. (ns: no significativo).

Por lo tanto, estos resultados concuerdan con los obtenidos en el análisis de los datos de ChIP-seq e indican que la regulación de EWS-FLI1 sobre *SPRY1* probablemente no sea directa.

En resumen, los resultados mostrados en esta sección indican que EWS-FLI1 regula negativamente la expresión de *SPRY1* en las células de sarcoma de Ewing A673 y que los niveles de expresión de *SPRY1* son muy bajos o indetectables en una serie amplia de células de sarcoma de Ewing, lo que sugiere que esta es una característica común de este tipo tumoral.

Como se ha comentado en la introducción, varios estudios sugieren que SPRY1 puede actuar como un supresor tumoral en diferentes tipos de cáncer (Kwabi-Addo *et al.* 2004, Lo *et al.* 2004, Macia *et al.* 2012, Masoumi-Moghaddam *et al.* 2014a, Liu *et al.* 2015), aunque se desconoce el mecanismo exacto.

Todo esto sugiere que SPRY1 podría actuar como un supresor tumoral también en sarcoma de Ewing. Por ello, el siguiente objetivo que abordamos en esta Tesis fue estudiar el rol de SPRY1 en la patogénesis del sarcoma de Ewing.

4.2. *SPRY1* es un gen supresor de tumores en sarcoma de Ewing

Establecimiento de modelos celulares de expresión inducible de SPRY1 en células de sarcoma de Ewing.

Con el objetivo de estudiar el rol de SPRY1 generamos un sistema inducible de re-expresión de SPRY1 dependiente de doxiciclina en células de sarcoma de Ewing. Decidimos generar tres líneas celulares diferentes (A673/TR/SPRY1, SKES/TR/SPRY1 y SKNMC/TR/SPRY1) para de esta forma poder sacar conclusiones que fueran representativas de los sarcomas de Ewing en general. Dos de estas células, A673 y SKNMC, expresan la fusión EWS-FLI1 de tipo I mientras que las células SKES expresan la fusión EWS-FLI1 de tipo II. Las células parentales fueron infectadas con el vector lentiviral pLenti6/TR para expresar de manera estable el represor de tetraciclina (A673/TR, SKES/TR y SKNMC/TR), y posteriormente con el vector pLenti4/TO/V5-DEST que incluía el ADNc de SPRY1 bajo el control de un promotor inducible por doxiciclina (**Figura 14A**). El resultado fue la generación de tres líneas celulares (A673/TR/SPRY1, SKES/TR/SPRY1 y SKNMC/TR/SPRY1) que expresaban SPRY1 tras la estimulación con doxiciclina (**Figura 14B**). Las tres líneas celulares A673/TR, SKES/TR y SKNMC/TR fueron también infectadas con el vector lentiviral pLenti4/TO/V5-DEST vacío (*Empty*) y fueron utilizadas como controles en todos los experimentos funcionales.

De cada línea celular generada se obtuvieron poblaciones policlonales, que fueron posteriormente utilizadas para la obtención de clones. Estos clones fueron analizados independientemente para verificar la inducción de SPRY1 en respuesta a doxiciclina por western blot (**Figura 14B**) y se seleccionaron aquellos clones que demostraron una expresión más elevada de SPRY1 para realizar los estudios funcionales posteriores.

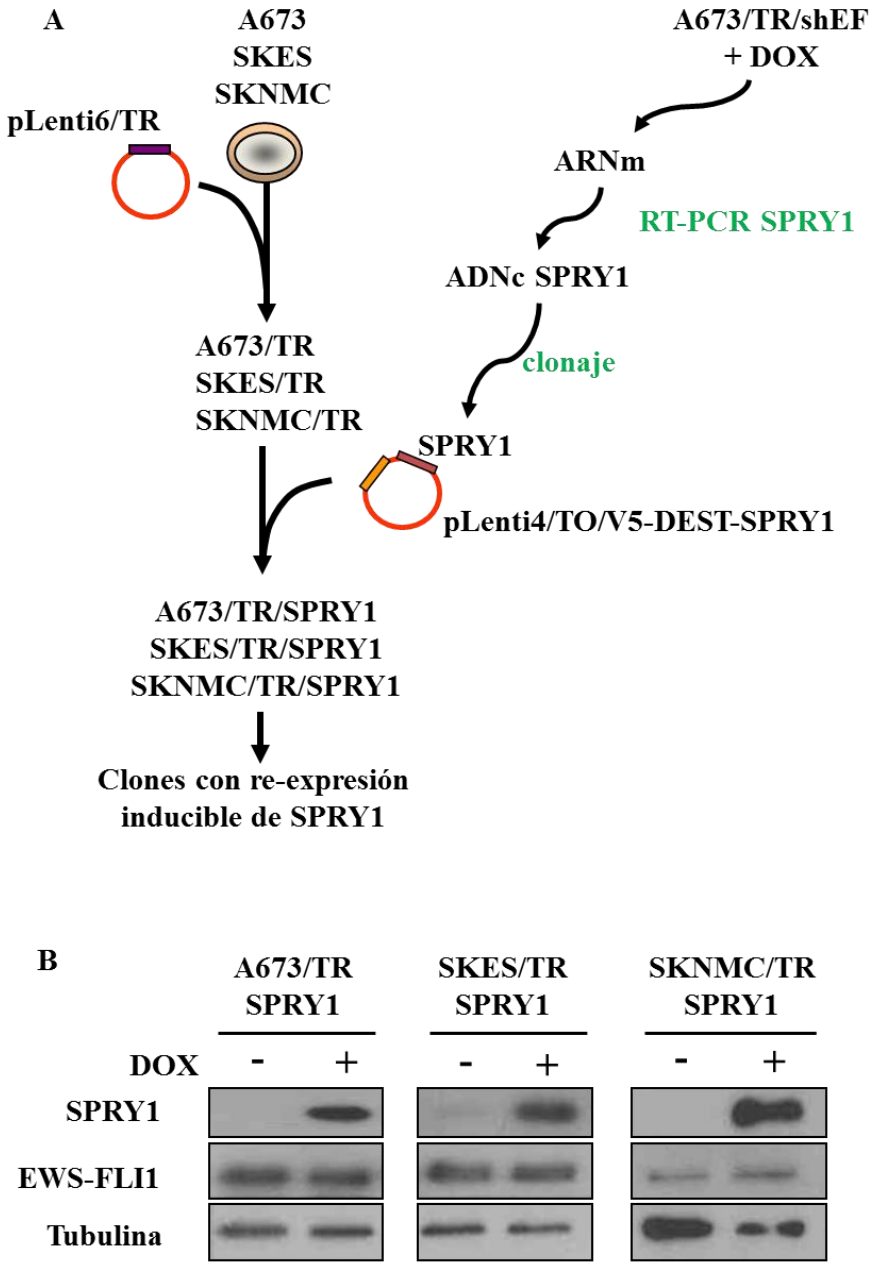

Figura 14. Establecimiento de modelos celulares de re-expresión de SPRY1 en tres líneas de sarcoma de Ewing. A. Las células A673, SKES y SKNMC de sarcoma de Ewing fueron primero infectadas con el vector pLenti6/TR para dar lugar a las células A673/TR, SKES/TR y SKNMC/TR. A continuación, estas células fueron infectadas con el vector pLenti4/TO/V5-DEST-SPRY1 para dar lugar a las células A673/TR/SPRY1, SKES/TR/SPRY1 y SKNMC/TR/SPRY1, en las que la expresión de SPRY1 se regulaba mediante la incubación con doxiciclina. **B.** La figura muestra la inducción de SPRY1 tras 72 horas de tratamiento con doxiciclina (1 µg/ml) en las células A673, SKES y SKNMC infectadas con el sistema inducible de SPRY1. A estas muestras se les extrajo proteína con la que se realizó un western blot. Las hibridaciones con anticuerpos específicos muestran como SPRY1 se induce a nivel de proteína tras el tratamiento, mientras que EWS-FLI1 se mantiene constante. Se empleó tubulina como control de carga.

Es importante destacar que en estas tres líneas celulares la expresión de EWS-FLI1 se mantiene inalterada tras la incubación con doxiciclina, como podemos observar en la **Figura 14B**. Por lo tanto, este sistema es válido para analizar las consecuencias de la re-expresión de SPRY1 en las células de sarcoma de Ewing, independientemente de EWS-FLI1.

La re-expresión de SPRY1 inhibe la proliferación y aumenta el tiempo de duplicación de las células de Ewing.

Con el objetivo de analizar el efecto de la re-expresión de SPRY1 sobre las células de sarcoma Ewing, estudiamos en primer lugar su posible influencia sobre la proliferación celular. Para ello empleamos el sistema xCELLigence, que permite monitorizar en tiempo real la proliferación celular y calcular el tiempo de duplicación.

En la **Figura 15A** podemos observar como las células tratadas con doxiciclina, y que por lo tanto re-expresaban SPRY1, proliferaron menos que las células control cultivadas en ausencia de doxiciclina (entre un 35% y un 60% menos al final del experimento). Además, el tiempo de duplicación se incrementó en todas las líneas celulares estimuladas con doxiciclina de forma significativa: de 16,3 ± 1,9 a 25,1 ± 3,4 horas para A673/TR/SPRY1 (P = 0,004), de 16,8 ± 2,06 a 24,02 ± 3,1 horas para SKES/TR/SPRY1 (P = 0,006) y de 11,7 ± 1,3 a 17,6 ± 2,4 horas para SKNMC/TR/SPRY1 (P = 0,003) (**Figura 15B**).

En la **Figura 16** se muestran fotografías representativas de las tres líneas celulares cultivadas en ausencia o presencia de doxiciclina (1 µg/ml) durante 10 días. Como se puede observar en la mencionada figura, la re-expresión de SPRY1 produce una disminución evidente del número de células.

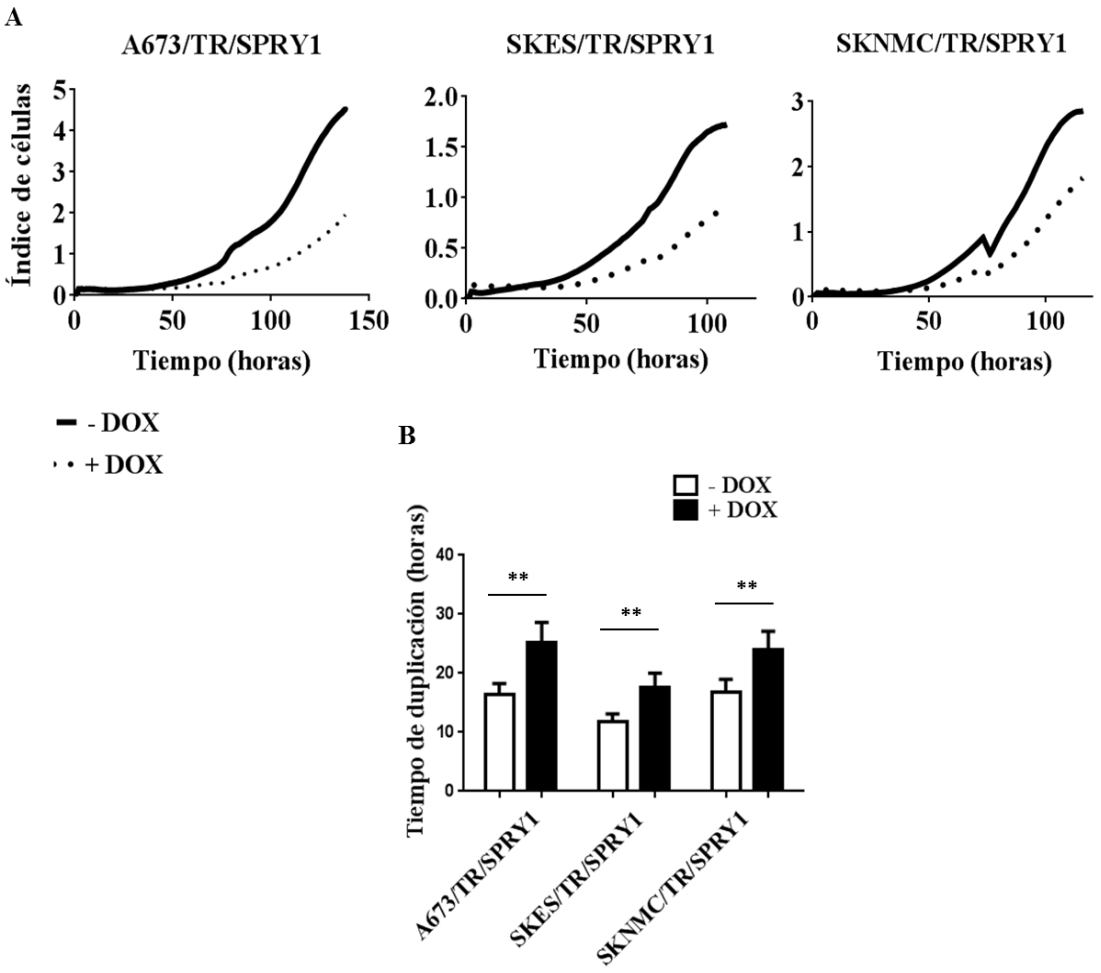

Figura 15. La re-expresión de SPRY1 inhibe la proliferación de células de sarcoma de Ewing medida en tiempo real. Se midió la proliferación celular de las células A673/TR/SPRY1, SKES/TR/SPRY1 y SKNMC/TR/SPRY1 empleando la tecnología xCELLigence en ausencia o presencia de doxiciclina (DOX, 1 µg/ml). **A.** Las gráficas muestran las curvas de crecimiento de las células cultivadas con o sin re-expresión de SPRY1 durante 120 horas donde se observa como la re-expresión de SPRY1 inhibe la proliferación de las tres líneas celulares de sarcoma de Ewing. Se muestra un experimento representativo de un total de tres realizados. Los artefactos de la gráfica que se observan a las 72 horas son consecuencia del inevitable cambio de medio realizado y el posterior reajuste de las condiciones del aparato xCELLigence. Este artefacto no afecta al resultado final. **B.** La gráfica muestra cómo la re-expresión de SPRY1 aumenta el tiempo de duplicación de las tres líneas celulares (media ± desviación estándar; ** $P < 0,01$).

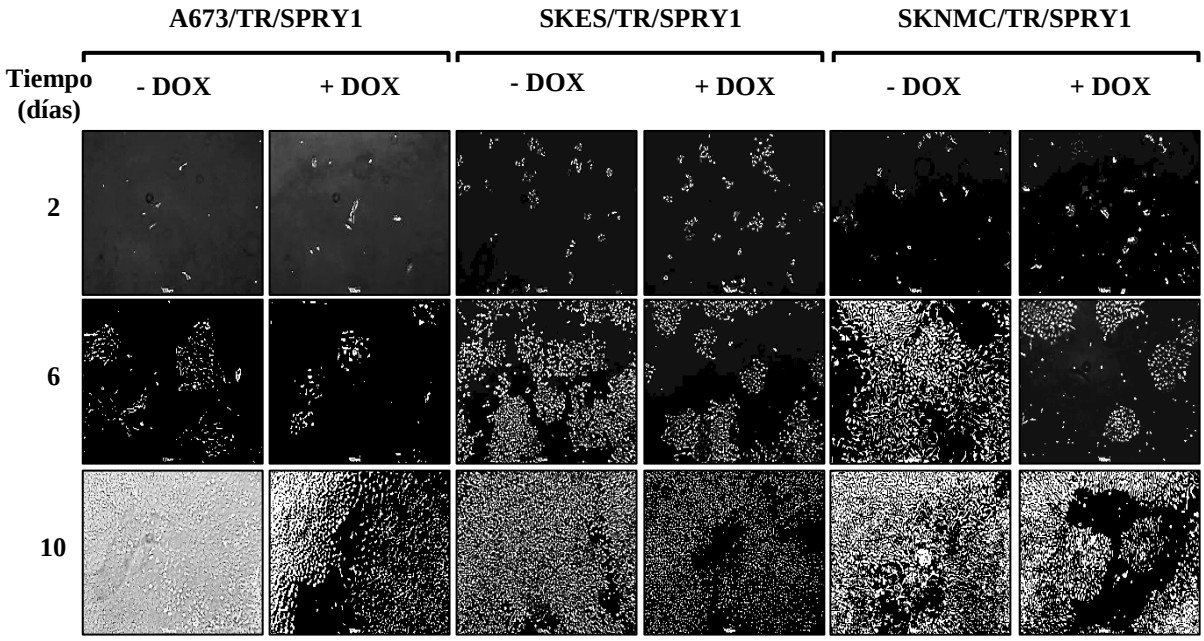

Figura 16. Proliferación a tiempos largos en líneas celulares de sarcoma de Ewing con re-expresión de SPRY1. Se sembraron células A673/TR/SPRY1, SKES/TR/SPRY1 y SKNMC/TR/SPRY1 a baja densidad y se mantuvieron en cultivo durante 10 días en ausencia o presencia de doxiciclina (DOX +/-, 1 µg/ml). Se muestran fotos representativas de la progresión de la proliferación celular en tres puntos del tiempo (días 2, 6 y final del experimento a día 10).

De forma complementaria, se realizaron estudios de síntesis de ADN mediante incorporación de bromodesoxiuridina (BrdU) para determinar el efecto de SPRY1 sobre la proliferación celular.

En condiciones estándar de cultivo (medio suplementado con 10% de SFB) la re-expresión de SPRY1 provocó una inhibición de la incorporación de BrdU entre el 30 y el 50% dependiendo del tipo celular (**Figura 17A**). Estos mismos ensayos se realizaron también en condiciones restrictivas de suero (medio suplementado con 1% de SFB) y se observó que el efecto de la re-expresión de SPRY1 fue aún más acusado, obteniéndose inhibiciones de la proliferación de entre el 50 y el 65% con respecto a las células control cultivadas en ausencia de doxiciclina (**Figura 17B**). Estos resultados sugieren que en condiciones en las que la disponibilidad de factores de crecimiento es más limitada, como podría ser el microentorno tumoral, la re-expresión de SPRY1 podría generar una inhibición más fuerte de la proliferación celular.

No se observaron diferencias en las células control infectadas con el vector lentiviral vacío cultivadas en paralelo en ausencia o en presencia de doxiciclina, indicando que los efectos observados eran específicos de la re-expresión de SPRY1 (**Figura 17C**).

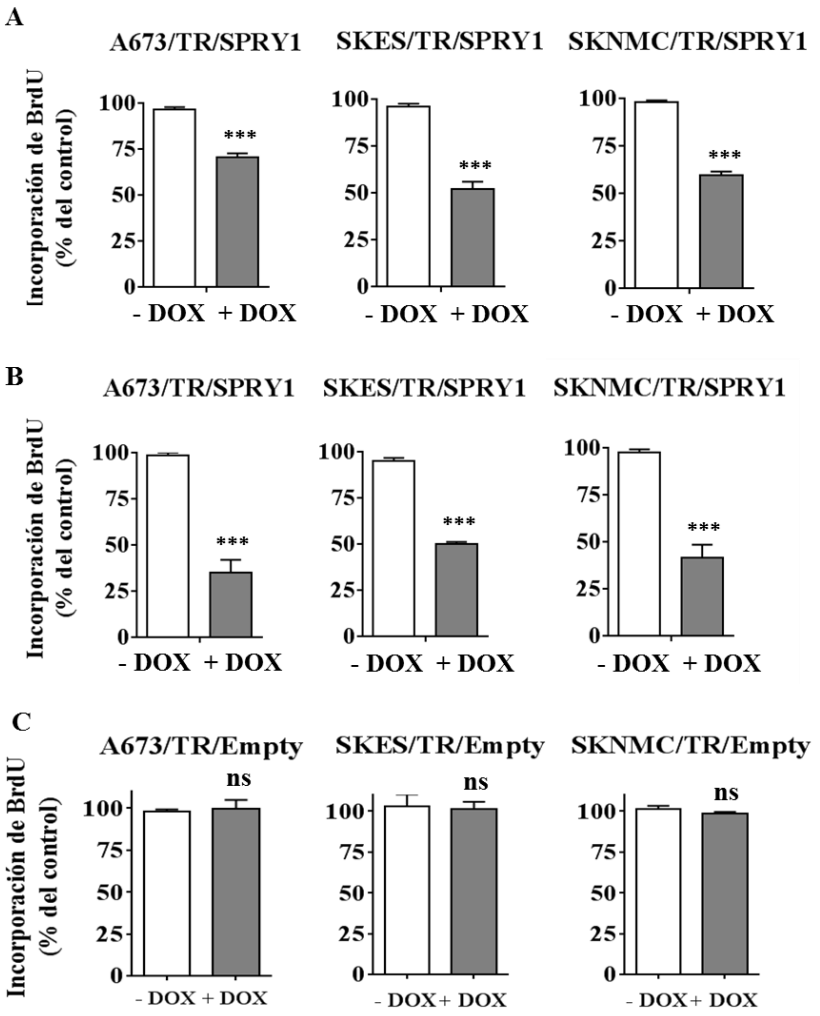

Figura 17. La re-expresión de SPRY1 inhibe la proliferación de células de sarcoma de Ewing en condiciones estándar y restrictivas de suero. A. Se sembraron células A673/TR/SPRY1, SKES/TR/SPRY1 y SKNMC/TR/SPRY1 en octuplicados y se cultivaron en ausencia o presencia de doxiciclina (DOX, 1 µg/ml) durante 72 horas en medio suplementado con 10% de suero fetal bobino (SFB) libre de tetraciclina (condiciones estándar de cultivo). Se midió la proliferación celular por incorporación de BrdU al ADN. Las gráficas muestran el porcentaje de la incorporación de BrdU en las células que re-expresan SPRY1 vs control. La figura muestra un experimento representativo (media ± desviación estándar) de tres realizados (*** $P < 0{,}005$). **B.** Las células se cultivaron como se describe en el apartado A, pero se mantuvieron al 1% de SFB (condiciones restrictivas de suero). La proliferación se midió por incorporación de BrdU y se observó una inhibición significativa en las células tratadas con doxiciclina (células con re-expresión de SPRY1) vs control. La figura muestra un experimento representativo (media ± desviación estándar) de tres experimentos independientes realizados (*** $P < 0{,}005$). **C.** Las células A673/TR/Empty, SKES/TR/Empty y SKNMC/TR/Empty (controles) se cultivaron en las mismas condiciones. Las gráficas muestran que no hay diferencias significativas entre las células tratadas en ausencia o presencia de doxiciclina (ns: no significativo).

Para estudiar si el efecto de SPRY1 sobre la inhibición de la proliferación de las células de sarcoma de Ewing era citotóxico o citoestático, se realizaron estudios de ciclo celular. Para ello, se analizaron células A673/TR/SPRY1, SKES/TR/SPRY1 y SKNMC/TR/SPRY1 no sincronizadas mediante citometría de flujo, cultivadas en ausencia o presencia de doxiciclina (1 µg/ml) durante 72 horas. Como podemos observar en la **Figura 18A**, la re-expresión de SPRY1 produjo un ligero incremento en el porcentaje de células en la fase G1 del ciclo celular que se asoció a una reducción en el porcentaje de células en la fase G2/M. Aunque las diferencias no fueron estadísticamente significativas, esta tendencia se observó en todos los experimentos realizados. Estos resultados sugieren que la inhibición de la proliferación celular en las células que re-expresan SPRY1 puede deberse, al menos parcialmente, a un efecto citoestático debido a una parada del ciclo celular en la fase G1.

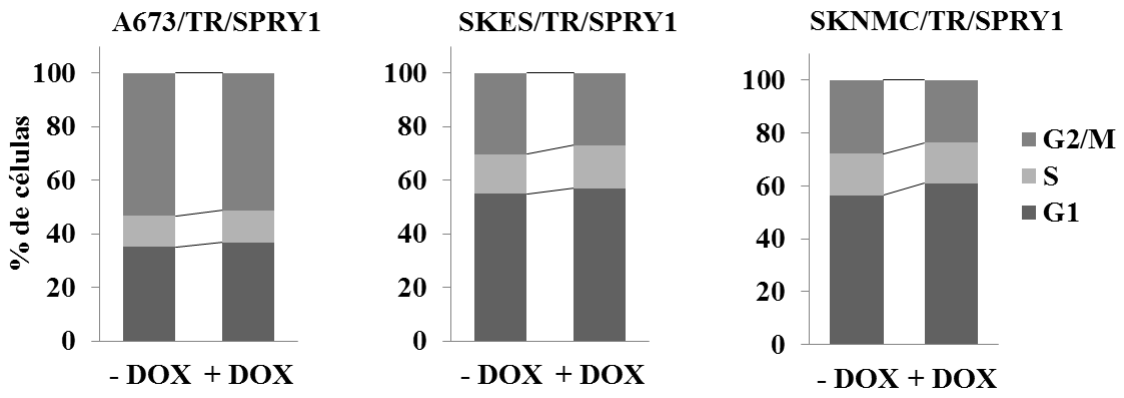

Figura 18. El efecto inhibitorio de la re-expresión de SPRY1 sobre la proliferación de células de Ewing se debe parcialmente a una parada del ciclo celular en fase G1. Se cultivaron células A673/TR/SPRY1, SKES/TR/SPRY1 y SKNMC/TR/SPRY1 en ausencia o presencia de doxiciclina (- / + DOX; 1 µg/ml) durante 72 horas y se las tiñó con yoduro de propidio para analizar el ciclo celular mediante citometría de flujo. En la figura se observa que las células presentan una tendencia no significativa a acumularse en la fase G1. Las gráficas muestran un experimento representativo de los tres realizados.

SPRY1 inhibe el crecimiento de células a baja densidad y la formación de colonias en agar blando.

A continuación analizamos el efecto de la re-expresión de SPRY1 sobre otras características de las células tumorales, como son su capacidad para formar colonias en cultivos a baja densidad y en medio semisólido. Como se puede observar en la **Figura 19A**, la re-expresión de SPRY1 inhibió significativamente el crecimiento clonogénico en las tres líneas celulares de sarcoma de Ewing (entre un 20 y un 35% de inhibición). Por el contrario, no se observó ningún efecto sobre las células control (**Figura 19B**).

Posteriormente, analizamos el efecto de SPRY1 sobre la capacidad de las células A673/TR/SPRY1, SKES/TR/SPRY1 y SKNMC/TR/SPRY1 para crecer independientemente de anclaje. Como se puede observar en la **Figura 20A**, la re-expresión de SPRY1 no generó un efecto sobre el número de colonias formadas, que resultó ser similar tanto en presencia como en ausencia de doxiciclina. Por el contrario, la re-expresión de SPRY1 provocó una disminución significativa en el tamaño de las colonias crecidas en agar blando: en la línea A673/TR/SPRY1 el tamaño medio de las colonias disminuyó un 78,4%, en SKES/TR/SPRY1 un 46,1% y en SKNMC/TR/SPRY1 un 69,7% (**Figura 20B**). Las tres líneas celulares control infectadas con el vector vacío no presentaron diferencias en la formación de colonias en medio semisólido tras el tratamiento con doxiciclina (**Figura 20C**).

Ambos resultados evidencian que la inducción de SPRY1 inhibe el crecimiento clonogénico y libre de anclaje en las tres líneas celulares de sarcoma de Ewing, ambas propiedades característica de las células transformadas, apuntando así a un posible papel onco-supresor de SPRY1.

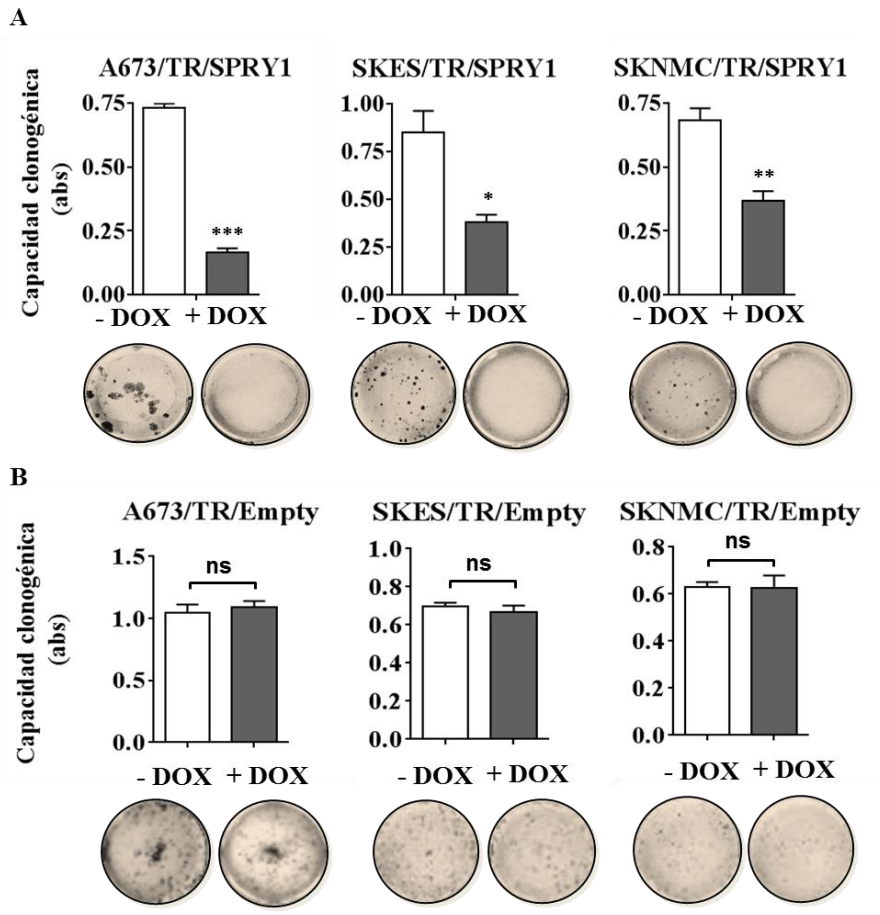

Figura 19. La re-expresión de SPRY1 inhibe el crecimiento clonogénico de las células de sarcoma de Ewing. A. Se cultivaron células A673/TR/SPRY1, SKES/TR/SPRY1 y SKNMC/TR/SPRY1 en triplicados a baja densidad y se las mantuvo en ausencia o presencia de doxiciclina (DOX, 1 µg/ml) durante 9 días. La formación de colonias se midió por tinción con cristal violeta. Las imágenes muestran pocillos representativos de los tres experimentos independientes realizados. Las gráficas muestran la cuantificación de la absorbancia medida al desteñir las células (un experimento representativo de los tres realizados, media ± desviación estándar). La re-expresión de SPRY1 inhibe significativamente el crecimiento clonogénico en las tres líneas celulares estudiadas (* $P <$ 0,05, ** $P <$ 0,01, *** $P <$ 0,005). **B.** Células A673/TR/Empty, SKES/TR/Empty y SKNMC/TR/Empty utilizadas como controles y mantenidas en las mismas condiciones que en la Figura A. Las gráficas muestran como el tratamiento con doxiciclina no genera cambios significativos en el crecimiento clonogénico de estas células (un experimento representativo de los tres realizados, media ± desviación estándar; ns: no significativo). Las imágenes muestran pocillos representativos de los tres experimentos independientes realizados.

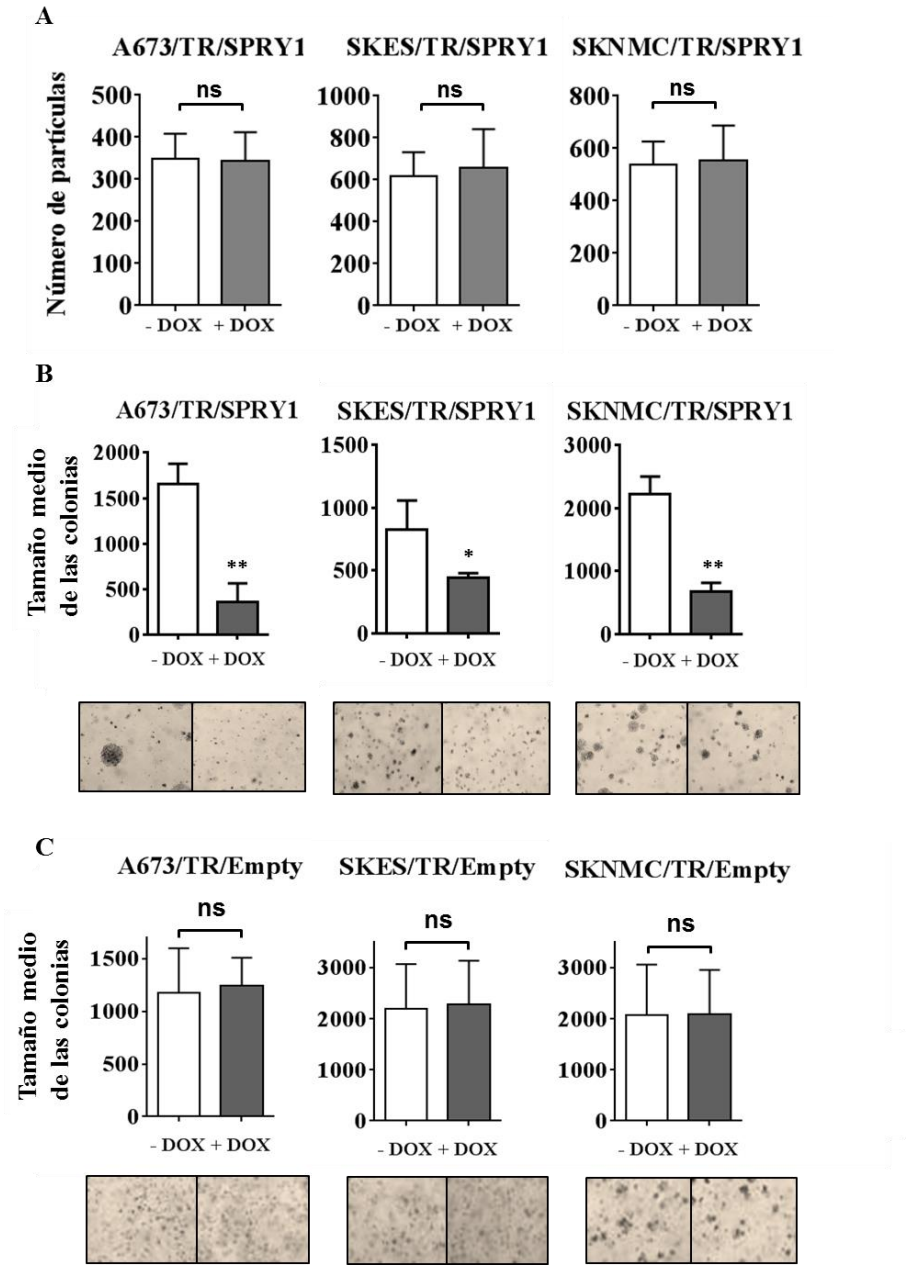

Figura 20. La re-expresión de SPRY1 inhibe el crecimiento independiente de anclaje en medio semisólidos de las células de sarcoma de Ewing. A. Las células A673/TR/SPRY1, SKES/TR/SPRY1 y SKNMC/TR/SPRY1 se sembraron en triplicados en agar blando y se cultivaron en ausencia o presencia de doxiciclina (DOX, 1 µg/ml) durante 25 días tras lo que fueron teñidas con cristal violeta. Las gráficas muestran el número de partículas (media ± desviación estándar; ns: no significativo) donde se observa que no hay diferencias significativas tras el tratamiento en ausencia o presencia de doxiciclina. **B.** Las gráficas representan el tamaño medio por colonia tras 25 días (media ± desviación estándar). La re-expresión de SPRY1 inhibe la formación de colonias en medio semisólido en las tres líneas celulares estudiadas (3 experimentos independientes; * $P < 0,05$; ** $P < 0,01$). Las fotos fueron tomadas al final del experimento y muestran imágenes representativas de la formación de colonias. **C.** Células A673/TR/Empty, SKES/TR/Empty y SKNMC/TR/Empty utilizadas como controles y mantenidas en las mismas condiciones que en la Figura A. Las gráficas muestran como el tratamiento con doxiciclina no genera cambios significativos en el crecimiento libre de anclaje en estas células (un experimento representativo de los tres realizados, media ± desviación estándar; ns: no significativo). Las imágenes muestran pocillos representativos de los tres experimentos independientes realizados.

La re-expresión de SPRY1 inhibe la migración de las células de sarcoma Ewing.

A continuación analizamos el efecto de la re-expresión de SPRY1 sobre la migración celular. Para ello primero estudiamos la capacidad de las células de sarcoma de Ewing de cerrar una herida artificial producida sobre una monocapa de células confluentes. Como se observa en la **Figura 21**, la re-expresión de SPRY1 inhibe la migración celular de las tres líneas de sarcoma de Ewing. Este efecto fue especialmente llamativo en las células SKNMC/TR/SPRY1, como se puede ver en el porcentaje de cierre de la herida: mientras que el cierre de la herida fue prácticamente total (98,6%) en las células SKNMC/TR/SPRY1 cultivadas en ausencia de doxiciclina, el porcentaje de cierre de herida fue sólo del 38,4% en presencia de doxiciclina.

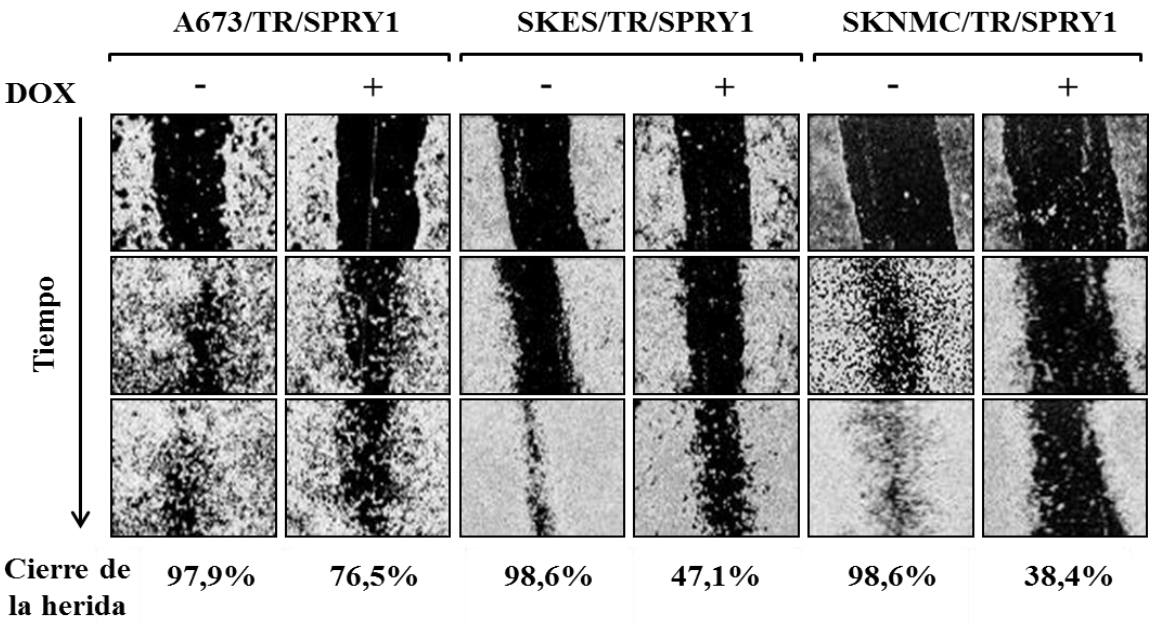

Figura 21. La re-expresión de SPRY1 inhibe la migración en monocapa de las células de sarcoma de Ewing. Se sembraron células A673/TR/SPRY1, SKES/TR/SPRY1 y SKNMC/TR/SPRY1 por triplicado y se las mantuvo en ausencia o presencia de doxiciclina (DOX, 1 µg/ml) durante 72 horas. Posteriormente se realizó una "herida" raspando la monocapa de células con la punta de una micropipeta. Las fotos muestran el cierre de la herida a lo largo del tiempo en tres puntos: al principio, a la mitad y al final del experimento. Los porcentajes muestran el cierre de la herida relativo al final del experimento con respecto al tamaño de la herida inicial. Las fotos muestran un experimento representativo de los tres realizados.

Por otro lado, también analizamos el efecto de SPRY1 sobre la migración a través de una membrana porosa inducida por suero en las tres líneas celulares. Para ello, realizamos un ensayo de transmigración a través de membranas de polietileno tereftalato con poros de 8 µm, que permiten el paso de las células a través de la

membrana en respuesta a un estímulo quimioatrayente como el suero fetal bovino (**Figura 22A**). En la **Figura 22B** se observa como la re-expresión de SPRY1 produce una disminución en la migración celular inducida por suero en las tres líneas celulares, aunque una vez más, el efecto es más pronunciado en las células SKNMC/TR/SPRY1 (aproximadamente un 60% de inhibición de la migración). No se observaron diferencias en las células control, cultivadas en presencia o ausencia de doxiciclina (**Figura 22C**).

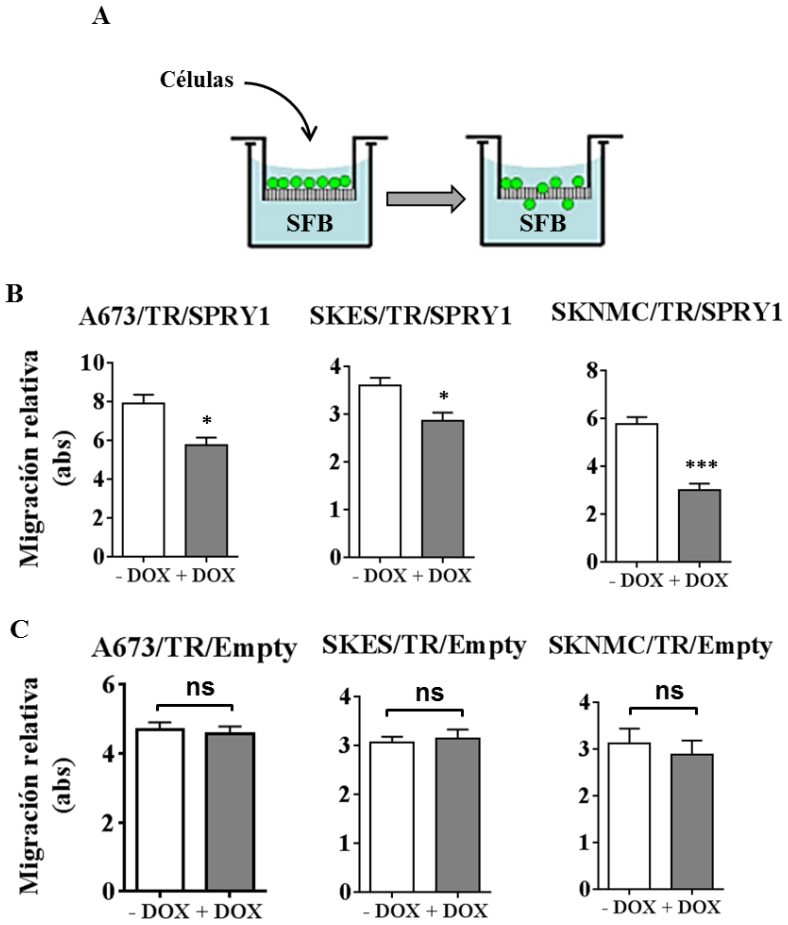

Figura 22. La re-expresión de SPRY1 inhibe la migración a través de membranas porosas en las células de sarcoma de Ewing. A. La figura muestra el esquema general del experimento, donde las células se siembran en la parte superior de la membrana porosa y migran a través de ella en respuesta a un estímulo quimioatrayente como el suero (SFB). **B.** Se incubaron células A673/TR/SPRY1, SKES/TR/SPRY1 y SKNMC/TR/SPRY1 en ausencia o presencia de doxiciclina (DOX, 1 µg/ml) durante 48 horas para inducir la re-expresión de SPRY1. Posteriormente, se las deplecionó de suero durante otras 24 horas y se las colocó en el compartimento superior de una membrana porosa. En el compartimiento inferior se añadió medio SFB al 10% y se les permitió migrar a través de la membrana porosa durante 6 horas. Las células que migraron fueron cuantificadas por tinción con cristal violeta. La figura muestra la media ± desviación estándar de dos experimentos realizados en triplicado. Las gráficas muestran datos en unidades arbitrarias de absorbancia (abs) (* $P < 0,05$; *** $P < 0,005$). **C.** Células A673/TR/Empty, SKES/TR/Empty y SKNMC/TR/Empty utilizadas como control y mantenidas en las mismas condiciones que la Figura B. Las gráficas muestran como el tratamiento con doxiciclina no tiene un efecto significativo sobre la migración de estas células control. La figura muestra la media ± desviación estándar de dos experimentos realizados en triplicado. Las gráficas muestran datos en unidades arbitrarias de absorbancia (abs) (ns: no significativo).

La re-expresión de SPRY1 produce cambios morfológicos en las células de sarcoma de Ewing.

Para analizar si el efecto de la re-expresión de SPRY1 sobre las características migratorias de las células de sarcoma de Ewing tenía su origen en un cambio de la morfología celular, realizamos un estudio del citoesqueleto empleando anticuerpos específicos: anti-vimentina, que se une a una de las proteínas fibrosas que forman los filamentos intermedios del citoesqueleto y anti-faloidina, que se une específicamente a los microfilamentos de actina.

En esta ocasión, los experimentos se llevaron a cabo en la línea celular SKNMC/TR/SPRY1 dado que, como hemos mostrado anteriormente, el efecto de la re-expresión de SPRY1 sobre sus capacidades migratorias fue más acusado en esta línea celular. Como se observa en la **Figura 23A**, las células SKNMC/TR/SPRY1 cultivadas en ausencia de doxiciclina presentaban una forma redondeada, exceptuando la zona donde los filamentos están polarizados, atendiendo a la morfología propia de células con capacidad migratoria. Sin embargo, el tratamiento con doxiciclina (1 µg/ml) cambia significativamente la morfología de las células, de tal manera que estas aparecieron menos redondeadas, con el citoplasma más extendido y con menos polarización (**Figura 23A**). Estos cambios morfológicos fueron cuantificados y, como se muestra en la **Figura 23B**, la re-expresión de SPRY1 genera una pérdida significativa de la circularidad.

En paralelo se realizó el mismo análisis con las células control (SKNMC/TR/Empty) en presencia o ausencia de doxiciclina y se comprobó que no existían diferencias significativas entre ambos tratamientos (**Figura 23A, B**), por lo que se puede concluir que los cambios morfológicos observados son consecuencia de la re-expresión de SPRY1.

Estos resultados, tomados en su conjunto, indican que la re-expresión de SPRY1 inhibe las características transformadas de las células de sarcoma de Ewing: SPRY1 inhibe la proliferación, el crecimiento clonogénico, la migración y la capacidad invasiva de las células, así como el crecimiento libre de anclaje en las líneas celulares de sarcoma de Ewing.

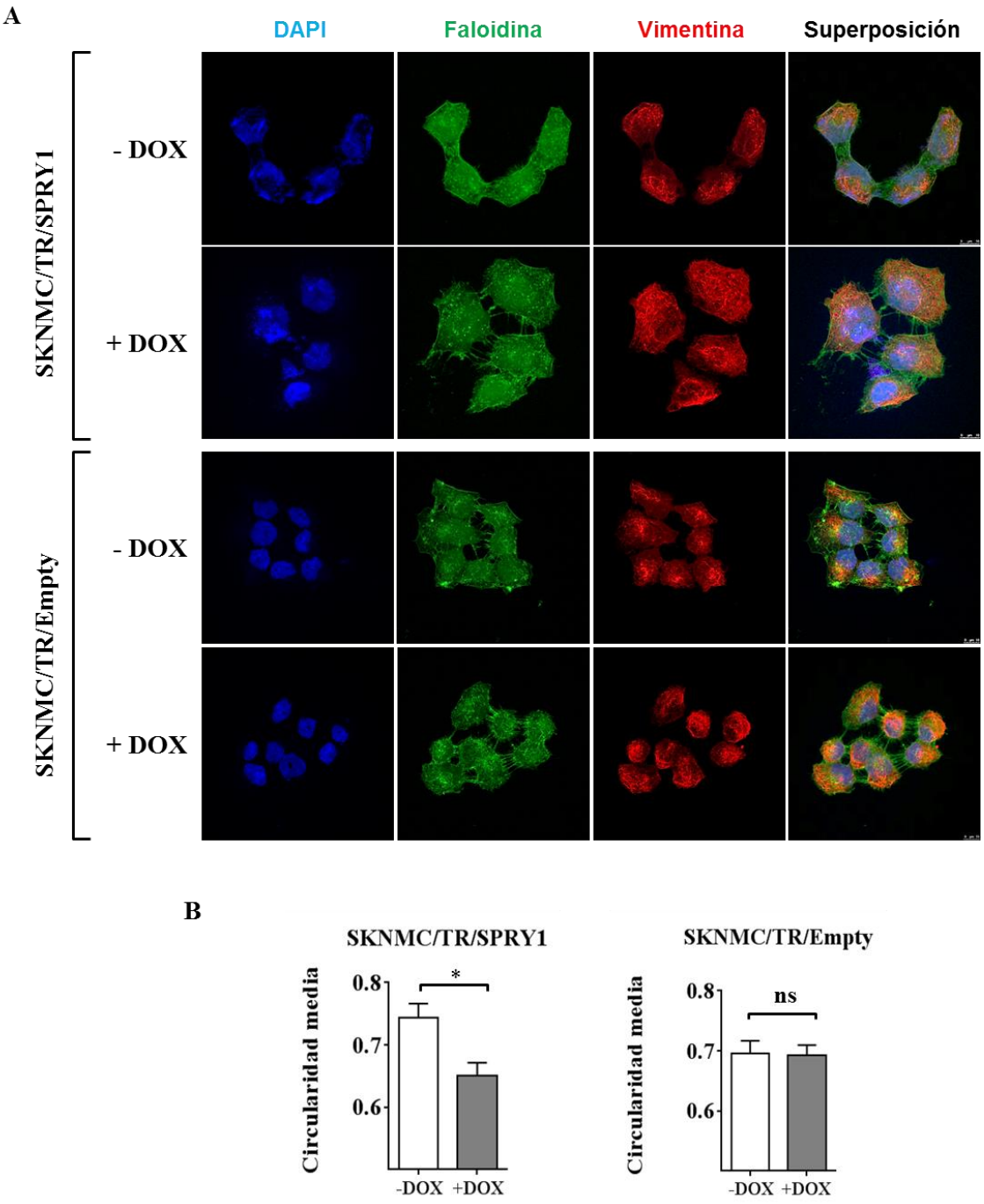

Figura 23. La re-expresión de SPRY1 genera cambios morfológicos en las células de sarcoma de Ewing. Células SKNMC/TR/SPRY1 y SKNMC/TR/Empty se trataron en ausencia o presencia de doxiciclina (1 µg/ml) durante 72 horas. Posteriormente se marcaron los componentes del citoesqueleto con anticuerpos fluorescentes para vimentina (rojo) y faloidina (verde) y los núcleos con DAPI (azul). **A.** Las imágenes muestran fotos representativas de tres experimentos independientes realizados. **B.** Las gráficas muestran la circularidad media de las células de las imágenes analizadas (media ± desviación estándar; ns: no significativo; **P* < 0,05).

4.3. Efecto de SPRY1 sobre la vía de señalización de las MAPKs

Tal y como se ha comentado en la introducción, SPRY es un regulador negativo de la vía de señalización de MAPK, una de las vías más relevantes implicadas en proliferación. En particular, SPRY1 es un inhibidor de la activación de esta ruta mediada por FGFb (Casci *et al.* 1999, Minowada *et al.* 1999, Hanafusa *et al.* 2002, Assinder *et al.* 2015). Por ello, decidimos analizar el efecto de la re-expresión de SPRY1 sobre la ruta de las MAPKs, inducida por suero o FGFb en células de sarcoma de Ewing.

La re-expresión de SPRY1 inhibe la vía de señalización Ras/MAPK/ERK en las células de sarcoma de Ewing.

En primer lugar analizamos el efecto de la re-expresión de SPRY1 sobre la activación de ERK mediada por suero. Para ello, mantuvimos las células A673/TR/SPRY1, SKES/TR/SPRY1 y SKNMC/TR/SPRY1 a baja concentración de suero (1% SFB) durante 72 horas y posteriormente estimulamos las células durante 15 minutos con medio al 10% de suero. En la **Figura 24** podemos observar que las células tratadas con doxiciclina, y que por tanto re-expresaban SPRY1, experimentaron una inhibición importante de los niveles de fosforilación de ERK: por un lado, en condiciones de niveles bajos de suero (1% SFB) se observó una inhibición de la fosforilación de ERK que variaba ente el 70% en SKNMC/TR/SPRY1 y el 45% en A673/TR/SPRY1 con respecto a las células no tratadas con doxiciclina. Tras la estimulación de las células con 10% de suero durante 15 minutos se observó una inhibición que varía entre el 50% en SKES/TR/SPRY1 y el 35% en SKNMC/TR/SPRY1 con respecto a las mismas células cultivadas en ausencia de doxiciclina.

También estudiamos el efecto de la re-expresión de SPRY1 sobre la activación de ERK mediada por FGFb, ya que FGFb es un factor de crecimiento que genera la activación de Ras y en consecuencia de ERK (Ornitz and Itoh 2015). En la **Figura 24** se puede observar como al estimular las células con FGFb, obtuvimos un aumento de los niveles de fosforilación de ERK, especialmente en las células SKES/TR/SPRY1. Además, la

re-expresión de SPRY1 generó la inhibición de la fosforilación de ERK. Este efecto es similar al descrito anteriormente con la estimulación por suero.

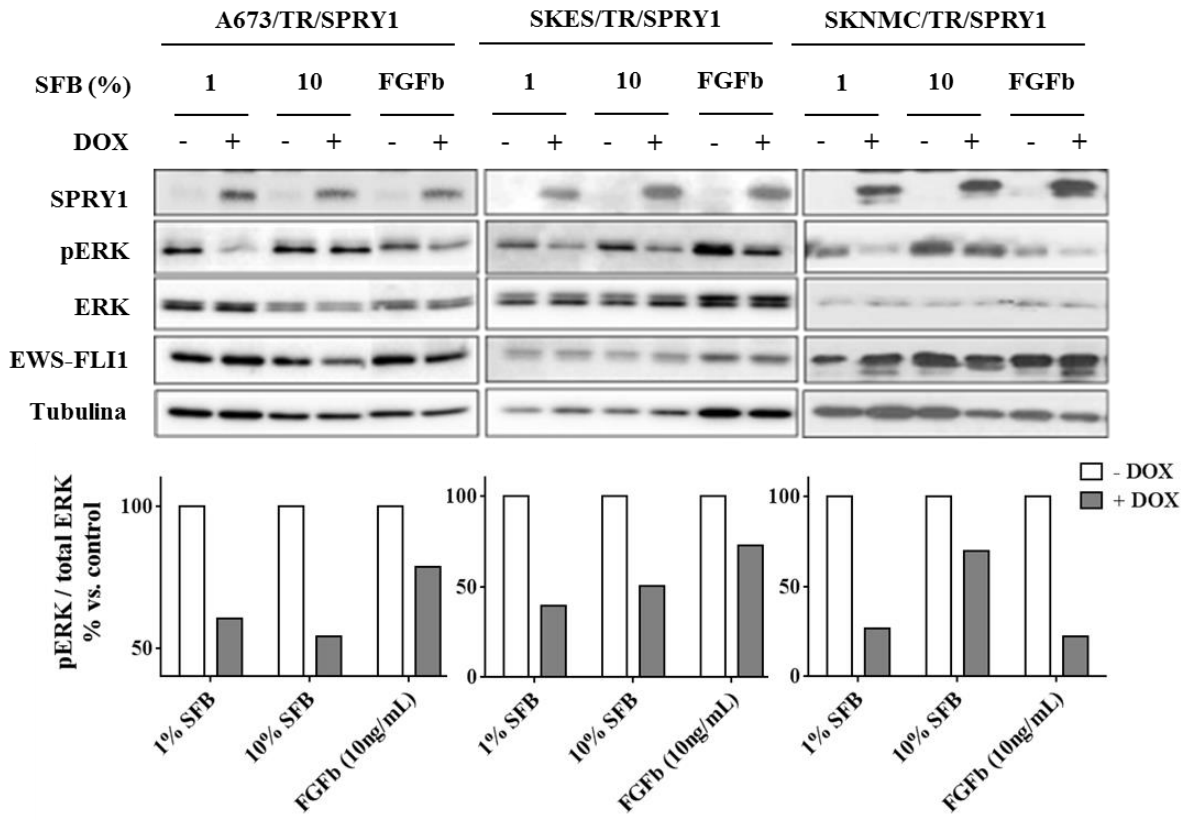

Figura 24. SPRY1 inhibe la vía de señalización de MAPK en células de sarcoma de Ewing. Las células A673/TR/SPRY1, SKES/TR/SPRY1 y SKNMC/TR/SPRY1 se incubaron en ausencia o presencia de doxiciclina (DOX, 1 µg/ml) durante 48 horas para inducir la expresión de la proteína SPRY1. Después se las deplecionó de suero durante 24 horas (1% SFB) y finalmente se las estimuló con SFB al 10% o FGFb (FGFb: factor de crecimiento fibroblástico básico) (10 ng/ml) durante 15 minutos. La presencia de las proteínas SPRY1, ERK fosforilado (pERK; Thr202/Tyr204), ERK y EWS-FLI1 se detectó con anticuerpos específicos. Se utilizó tubulina como control de carga. La re-expresión de SPRY1 inhibe la fosforilación de ERK inducida por FGFb o suero (SFB) en las tres líneas celulares. Las gráficas muestran las densitometrías correspondientes a las bandas de los western blots para la relación ERK fosforilado/ERKtotal. Las células cultivadas en ausencia de doxiciclina se emplearon como control. La figura muestra un experimento representativo de tres experimentos independientes realizados.

Estos resultados sugieren que la inhibición de SPRY1 en células de Ewing puede ser necesaria para mantener activada de forma constitutiva la ruta Ras/MAPK/ERK. Dado que la activación de la ruta de MAPK es esencial para el desarrollo del fenotipo maligno, la re-expresión de SPRY1 actuaría inhibiendo esta ruta y por tanto, limitando la transformación neoplásica de las células de sarcoma de Ewing.

El efecto de la re-expresión de SPRY1 es similar al de los inhibidores de FGFR en células de sarcoma de Ewing.

Como hemos observado anteriormente, la re-expresión de SPRY1 inhibió la fosforilación de ERK activada por FGFb. Además, se ha descrito que el FGFb induce la proliferación de varias líneas celulares de Ewing, como A673, SKNMC y POE (Grunewald *et al.* 2015). Esto nos indujo a pensar que esta ruta podía ser relevante en la patogénesis del sarcoma de Ewing y, en consecuencia, ser una nueva diana terapéutica para el tratamiento de este tumor. Por ello decidimos estudiar el efecto de inhibidores de FGFR (*Fibroblast Growth Factor Receptor*) sobre las células de sarcoma de Ewing.

Para ello testamos el efecto de 4 inhibidores de FGFR, PD173074 (PD-74), NVP-BGJ398 (BG-98), SU5402 (SU54) y PD166866 (PD-66) sobre la proliferación de 5 líneas celulares de sarcoma de Ewing (A673, SKES, SKNMC, POE y RDES) y una línea celular de fibroblastos normales que utilizamos como control (IMR90). En la **Figura 25** se observa como el empleo de estos inhibidores reduce la proliferación de todas las líneas celulares de sarcoma de Ewing, mientras que no se afecta la proliferación de los fibroblastos normales.

En la **Tabla 14** se muestran los valores de las IC50s de cada inhibidor para cada una de las líneas celulares estudiadas. De acuerdo con estos cálculos, PD-74 es uno de los inhibidores con un efecto más potente.

A continuación analizamos también el efecto de estos inhibidores de FGFR sobre el crecimiento clonogénico en tres líneas celulares de Ewing (A673, SKNMC y POE). En la **Figura 26** observamos como los 4 inhibidores de FGFR son capaces de inhibir el crecimiento a baja densidad de las tres células de sarcoma de Ewing estudiadas, y especialmente en la línea celular POE.

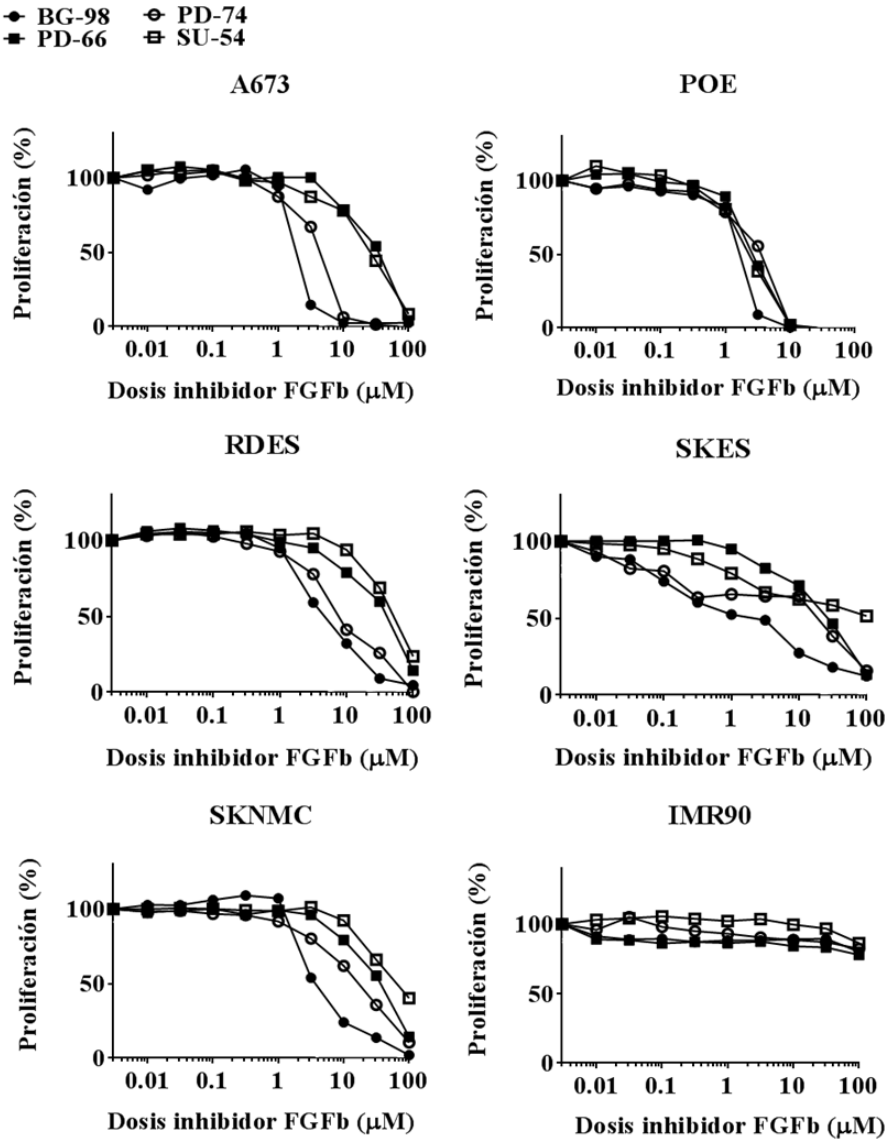

Figura 25. Los inhibidores de FGFR inhiben la proliferación celular de las líneas de sarcoma de Ewing. Cuatro inhibidores de FGFR (PD173074 [PD-74], PD166866 [PD-66], SU5402 [SU54] y NVP-BGJ398 [BG-98]) inhiben la proliferación de las células de sarcoma de Ewing A673, SKNMC, POE, RDES y SKES *in vitro* de forma dependiente de dosis. Las células normales (fibroblastos IMR90) no presentan inhibición de la proliferación con ninguno de los inhibidores utilizados. PD-74 y BG-98 son los inhibidores de FGFR más efectivos en cuatro de las 5 células de sarcoma de Ewing testadas. Las células se cultivaron en medio al 10% de SFB y la proliferación celular se midió a las 72 horas utilizando el ensayo de resazurina.

Tabla 14. Resultados de las IC50 (media ± desviación estándar) en las líneas celulares tratadas con cuatro inhibidores de FGFR diferentes: PD173074 (PD-74), PD166866 (PD-66), SU5402 (SU54), and NVP-BGJ398 (BG-98).

	IC50 (µM)			
Línea celular	**PD-74**	**PD-66**	**BG-98**	**SU54**
A673	4,03 ± 1,04	29,8 ± 1,07	2,03 ± 1,07	24,38 ± 1,04
SKNMC	15,44 ± 1,47	32,5 ± 1,04	4,38 ± 1,09	65,88 ± 1,04
POE	3,29 ± 1,11	2,33 ± 1,04	1,56 ± 1,08	1,53 ± 1,11
SKES	23,33 ± 1,03	29,09 ± 3,62	4,58 ± 1,65	91,22 ± 8,54
RDES	8,69 ± 1,07	34,95 ± 1,07	5,11 ± 1,07	50,34 ± 1,04
IMR90	-	-	-	-

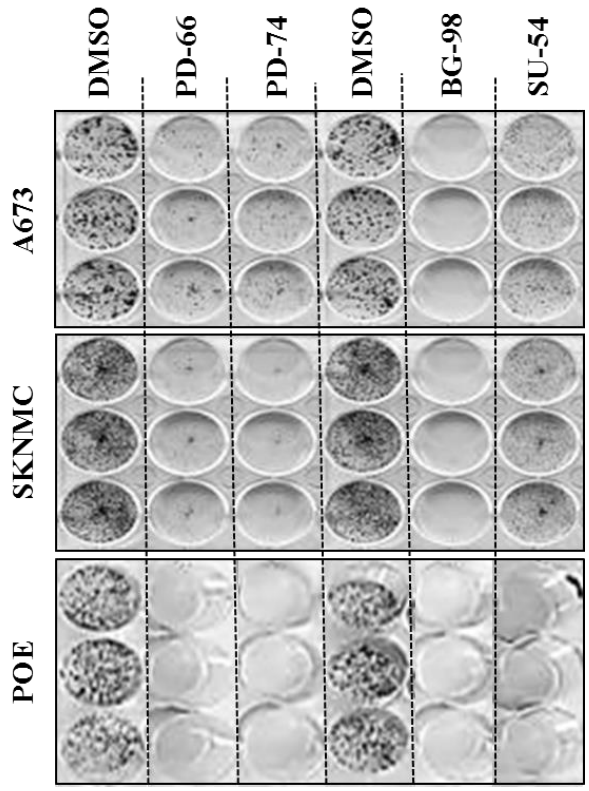

Figura 26. Los inhibidores de FGFR inhiben el crecimiento clonogénico de las líneas de sarcoma de Ewing. Los cuatro inhibidores testados, PD173074 (PD-74), PD166866 (PD-66), SU5402 (SU54) y NVP-BGJ398 (BG-98) inhiben el crecimiento clonogénico de las líneas A673, SKNMC y POE de sarcoma de Ewing *in vitro*. Las células se mantuvieron con medio al 5% de SFB durante 10-12 días en presencia de los inhibidores indicados a las concentraciones de sus IC50s y finalmente se tiñeron con cristal violeta. Las imágenes corresponden a fotografías representativas obtenidas el día final del experimento.

Análisis del efecto combinado de la re-expresión de SPRY1 y los inhibidores de FGFR sobre la proliferación celular.

Una vez analizado el efecto de los diferentes inhibidores de FGFR sobre las células de sarcoma de Ewing, decidimos estudiar el efecto de la inhibición de FGFR en combinación con la re-expresión de SPRY1 con el objetivo de determinar si ambos actuaban o no de forma sinérgica. Estos experimentos nos podrían ayudar a comprender si SPRY1 y los inhibidores de FGFR estaban actuando sobre la misma ruta.

Para ello, indujimos la re-expresión de SPRY1 en las tres líneas de sarcoma de Ewing A673/TR/SPRY1, SKES/TR/SPRY1 y SKNMC/TR/SPRY1 mediante la adición de doxiciclina (1 µg/ml) durante 72 horas y posteriormente tratamos las células con FGFb (10 ng/ml) para estimular su proliferación, el inhibidor de FGFR PD-74 (5 µM) o una combinación de ambos. Como se puede observar en la **Figura 27**, la re-expresión de SPRY1 inhibe significativamente la proliferación inducida por FGFb en las tres líneas celulares estudiadas. Estos resultados son consistentes con los descritos en la **Figura 24**, donde se observa que la re-expresión de SPRY1 inhibe significativamente la fosforilación de ERK en respuesta a FGFb. Además, esto sugiere que la inhibición de la fosforilación de ERK mediada por la re-expresión de SPRY1 contribuiría a la inhibición de la proliferación observada en las células de sarcoma de Ewing.

Por otro lado, el tratamiento con PD-74 inhibe la proliferación inducida por FGFb en las tres líneas celulares. En el caso de las células SKES/TR/SPRY1 el efecto de PD-74 sobre la proliferación celular es mayor que el de la re-expresión de SPRY1.

Al analizar el efecto conjunto de la re-expresión de SPRY1 y el tratamiento con PD-74 sobre la proliferación celular vemos como en las líneas celulares A673/TR/SPRY1 y SKES/TR/SPRY1, PD-74 no produce una mayor inhibición de la proliferación, lo que podría indicar que SPRY1 y PD-74 estuviesen actuando sobre la misma vía y por ello no se observa un efecto aditivo. Sin embargo, en la línea SKNMC/TR/SPRY1, la re-expresión de SPRY1 genera una inhibición mayor sobre la proliferación celular que el tratamiento con PD-74 sólo, lo que podría indicar que en estas células la inhibición estuviese ocurriendo por mecanismos parcialmente diferentes.

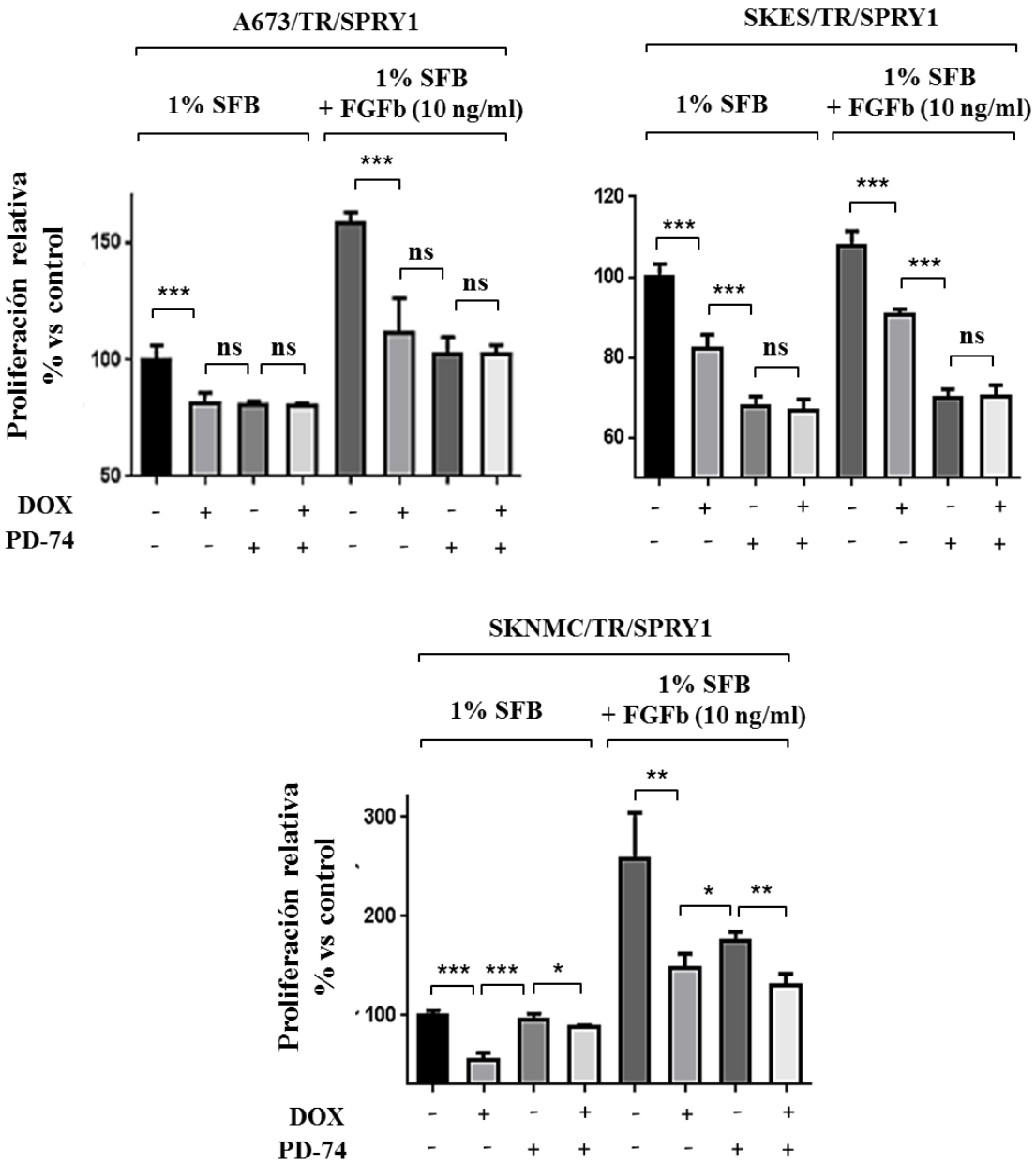

Figura 27. Análisis del efecto combinado de la re-expresión de SPRY1 y el inhibidor de FGFR PD-74 sobre la proliferación celular. Se incubaron células A673/TR/SPRY1, SKES/TR/SPRY1 y SKNMC/TR/SPRY1 en ausencia o presencia de doxiciclina (DOX, 1 µg/ml) para inducir la expresión de la proteína de SPRY1. Además, se las cultivó con SFB al 1%, FGFb (10 ng/ml), PD173074 (PD-74, 5 µM) o una combinación de FGFb y PD-74. A las 72 horas se midió la proliferación utilizando el ensayo de resazurina. Las gráficas muestran un experimento independiente (media ± desviación estándar) de los tres realizados. La re-expresión de SPRY1 y el tratamiento con PD-74 inhiben la proliferación celular inducido por FGFb (* P <0,05, ** P < 0,005, *** P < 0,001; ns = no significativo).

Con el objetivo de determinar si este efecto observado con PD-74 era común a otros inhibidores de FGFR, se analizó también el efecto de los inhibidores de FGFR BG-98, PD-66 y SU54 sobre la proliferación celular. De forma general, se puede observar en la **Figura 28** que dos de los inhibidores de FGFR (BG-98 y PD-66) inhibieron significativamente la proliferación de estas líneas celulares, más allá de la inhibición generada por la re-expresión de SPRY1 sola. En la misma **Figura 28** podemos observar también el efecto de la re-expresión de SPRY1 en combinación con la adición de los inhibidores. Los inhibidores BG-98 y PD-66 inhiben la proliferación celular en ausencia de doxiciclina más allá del efecto que ejerce la re-expresión de SPRY1 solo. Por el contrario, el efecto del inhibidor SU54 es menos potente. A pesar de que estos experimentos se habían realizado en condiciones normales de suero (10% SFB) y sin estimulación por FGFb como en los experimentos anteriores en los que se empleaba PD-74 (**Figura 27**), sí se observa una cierta concordancia en los resultados entre los diferentes inhibidores: la re-expresión de SPRY1 junto con el tratamiento con cualquiera de los inhibidores no genera una mayor inhibición de la proliferación de las células testadas, lo que podría indicar que estuviesen actuando sobre los mismos mecanismos o que se hubiese alcanzado una saturación de la inhibición de los mismos.

Es interesante mencionar que en algunos casos los resultados fueron célula e inhibidor dependientes. Por ejemplo, como hemos comentado anteriormente, el inhibidor SU54 parece no tener un efecto sobre la inhibición de la proliferación en las células SKES/TR/SPRY1, dado que la inhibición de la proliferación celular es igual al de la re-expresión de SPRY1 a diferencia de las otras dos líneas de sarcoma de Ewing testadas. En estas células (A673/TR/SPRY1 y SKNMC/TR/SPRY1), la adición de SU54 inhibe la proliferación celular más allá del efecto de la re-expresión de SPRY1 solo. Esto sugiere que algunos inhibidores como BG-98 o PD-66 podrían estar actuando de forma similar en todas las líneas celulares testadas, mientras que el inhibidor SU54 podría estar actuando mediante mecanismos diferentes dependiendo de la línea celular.

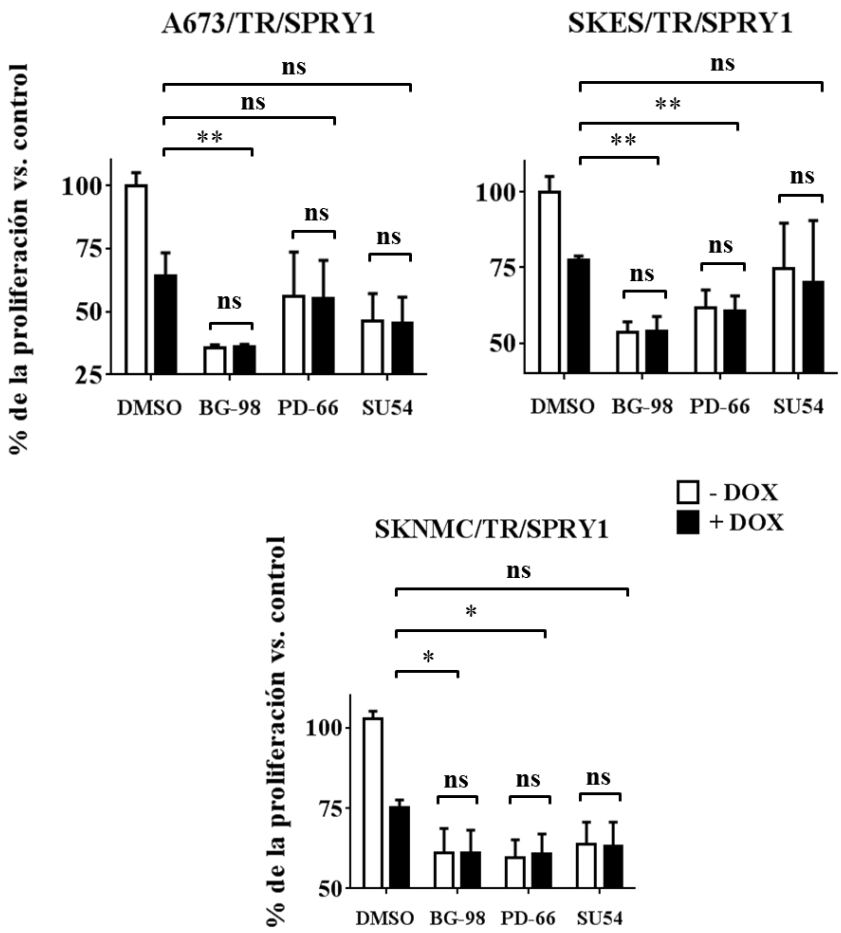

Figura 28. Análisis del efecto combinado de la re-expresión de SPRY1 y los inhibidores de FGFR BG-98, PD-66 y SU54 sobre la proliferación celular. Se trataron células A673/TR/SPRY1, SKES/TR/SPRY1 y SKNMC/TR/SPRY1 en ausencia o presencia de doxiciclina (- / + DOX; 1 µg/ml) junto con cada inhibidor (BG-98, PD-66 y SU54 a una concentración de 5 µM cada uno) en condiciones normales de suero (10% SFB). En la gráfica se observa como SPRY1 inhibe la proliferación en todos los casos. Además, BG-98 y PD-66 generan una reducción aún mayor de la proliferación en ausencia de doxiciclina, mientras que el efecto del inhibidor SU54 es menos potente. La re-expresión de SPRY1 junto con el tratamiento con cualquiera de los inhibidores no genera una mayor inhibición de la proliferación de las células testadas. Las gráficas representan la media ± desviación estándar de tres experimentos diferentes (* P <0,05, ** P < 0,005, ns = no significativo).

4.4. Potencial terapéutico de los inhibidores de FGFR en sarcoma de Ewing

A continuación, analizamos el efecto de la inhibición de FGFR sobre la formación de tumores en ratones inmunodeprimidos C.B17 SCID. Para ello se seleccionó el inhibidor

de FGFR PD-74 que, como pudimos ver en el apartado anterior, presentaba uno de los efectos más potentes en células de sarcoma de Ewing *in vitro*.

En primer lugar se empleó la línea celular POE para la formación de los xenotransplantes, dado que esta presentaba la mayor sensibilidad a este inhibidor en comparación con el resto de las líneas estudiadas (**Figura 25** y **Tabla 14**).

Los resultados de estos experimentos se muestran en la **Figura 29**. Como se puede observar en dicha figura, el tratamiento diario de los animales con una inyección intraperitoneal de 20 mg/Kg de PD-74 una vez el tumor fue detectable, inhibió significativamente el tamaño tumoral (P = 0,004).

Posteriormente se analizaron mediante inmunohistoquímica las muestras tumorales procedentes de los animales tratados con vehículo y PD-74 para determinar el efecto del inhibidor sobre la proliferación celular y la apoptosis. Como se puede observar en la **Figura 30**, los tumores procedentes de ratones que habían sido tratados con PD-74 presentaron un menor número de mitosis por campo (reducción del 50%; P = 0,001). Este resultado correlacionó con el número de células positivas para el marcador de proliferación Ki-67, que experimentó una reducción significativa en los tumores procedentes de ratones tratados con PD-74 (P < 0,01). Por otro lado, se observó un incremento significativo en el número de células apoptóticas (células *cleaved-caspasa*-3 positivas) del 40% (P = 0,001) con respecto a los ratones tratados con el vehículo (DMSO).

Finalmente y para confirmar si PD-74 tenía también un efecto antitumoral *in vivo* en otras líneas celulares de sarcoma de Ewing, se realizaron experimentos *in vivo* utilizando células SKES, que habían demostrado una menor sensibilidad a PD-74 en los experimentos previos (**Figura 25** y **Tabla 14**). En este caso también estudiamos si el efecto de PD-74 era dependiente de la dosis. Para ello se emplearon tres dosis diferentes del inhibidor de FGFR (5, 10 y 20 mg/Kg).

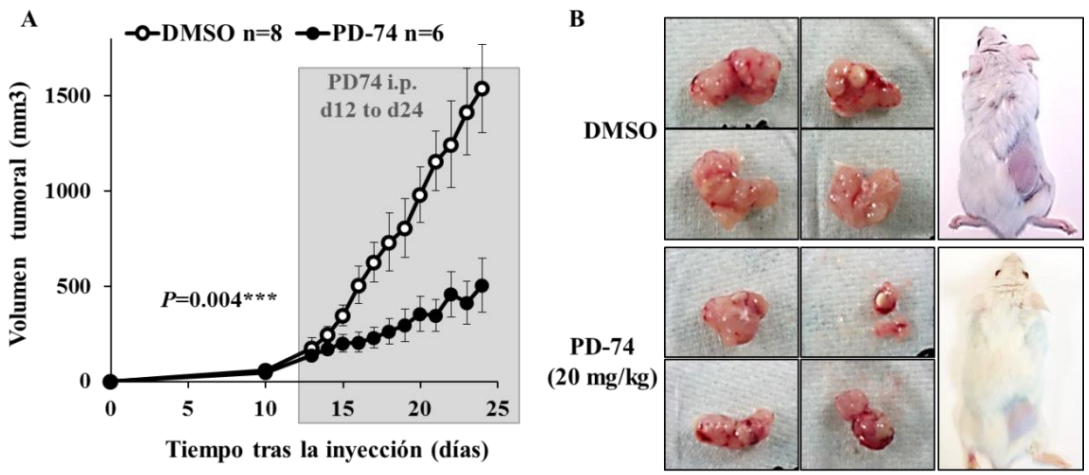

Figura 29. El inhibidor de FGFR PD-74 inhibe el crecimiento tumoral de xenotransplantes de las células POE de sarcoma de Ewing. A. Las células POE fueron inyectadas en ratones C.B17/SCID que se dividieron en 2 grupos aleatoriamente una vez el tumor había alcanzado un tamaño de 150 mm^3. A partir de este momento cada grupo fue tratado intra-peritonealmente una vez al día con PD-74 (20 mg/Kg) o el vehículo (DMSO). La gráfica muestra la evolución del volumen tumoral (media ± error estándar) de 6-8 animales por grupo a lo largo del tiempo. El recuadro gris muestra el periodo durante el que los animales fueron sometidos al tratamiento. El tratamiento con PD-74 inhibe significativamente el crecimiento del tumor (P = 0,004). **B.** Fotografías representativas de 4 tumores de cada grupo extraídos al final del experimento y un ratón representativo de cada grupo donde se puede observar la variación del tamaño de los tumores.

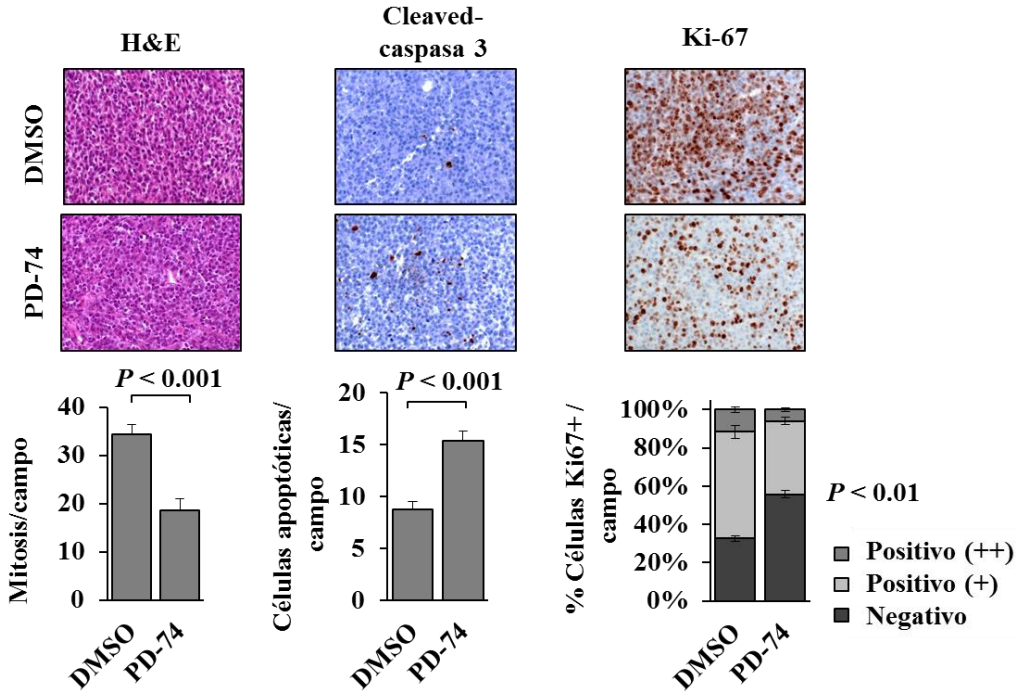

Figura 30. Estudios inmunohistoquímicos de los tumores procedentes de los experimentos *in vivo* de xenotransplantes con células POE tratadas con el inhibidor de FGFR PD-74. Las secciones de tejido se tiñeron con hematoxilina/eosina (H&E) para observar las mitosis, o se incubaron con anticuerpos anti-*cleaved*-caspasa 3 para detectar apoptosis y anti-Ki-67 para detectar proliferación. Las gráficas muestran como el tratamiento con PD-74 reduce el número de mitosis por campo (P = 0,001) e incrementa el número de células apoptóticas por campo (P = 0,001). La tinción con Ki-67 y la gráfica muestra una reducción en el porcentaje de células Ki67-positivas (++ o +) en los tumores tratados con PD-74 (P < 0,01).

Como podemos observar en la **Figura 31A y B**, PD-74 inhibió el crecimiento tumoral de las células SKES y este efecto resultó ser dependiente de la dosis: la dosis de 20 mg/Kg es capaz de inhibir de forma significativa dicho crecimiento (inhibición del 70,7% del crecimiento al final del experimento; P = 0,005).

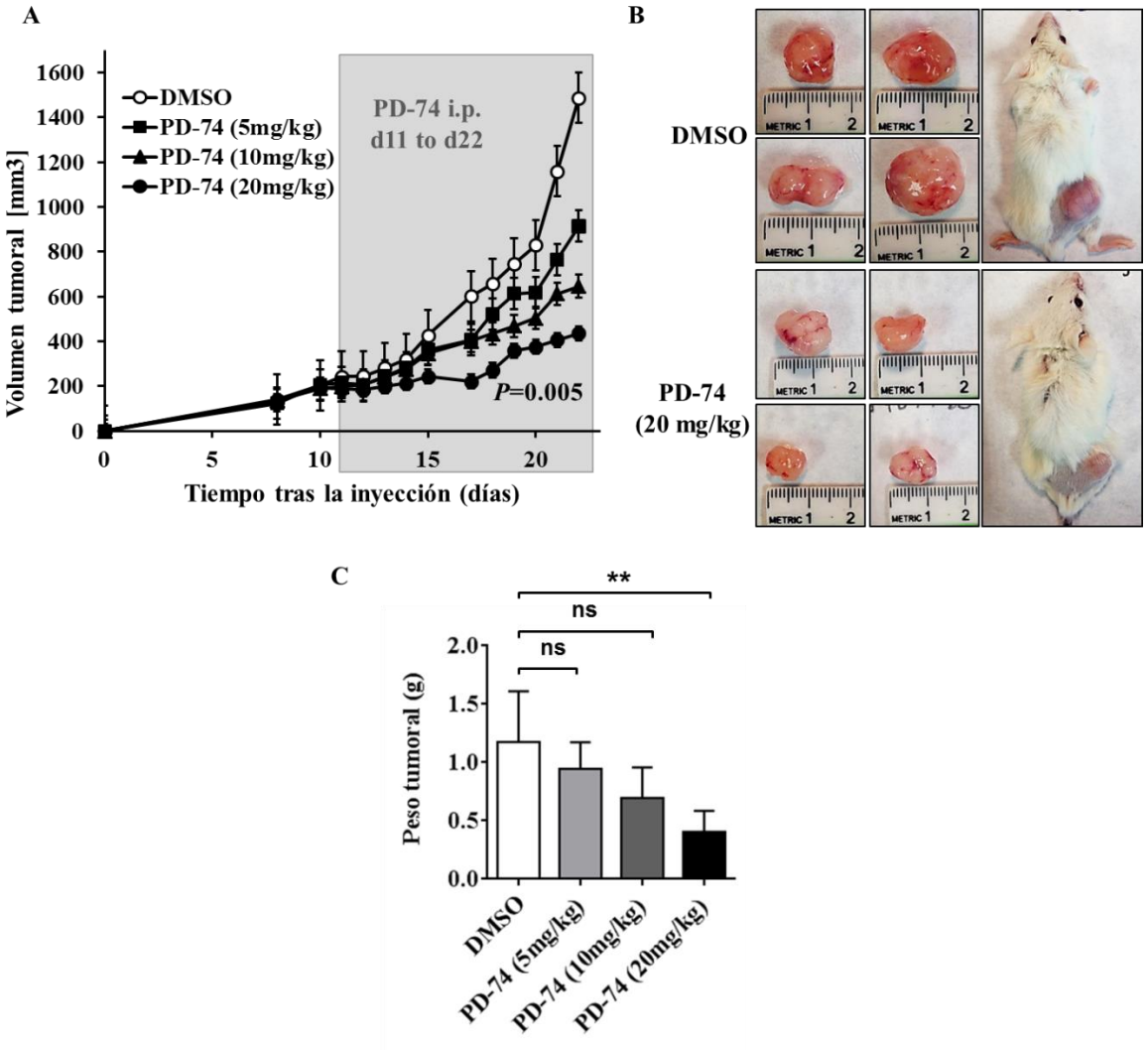

Figura 31. El inhibidor de FGFR PD-74 inhibe el crecimiento tumoral de xenotransplantes de células SKES de sarcoma de Ewing de forma dependiente de dosis. A. Las células SKES fueron inyectadas en ratones C.B17/SCID que se dividieron en 4 grupos aleatoriamente (n = 6 en cada grupo) una vez el tumor había alcanzado un tamaño de 200 mm^3. A partir de este momento cada grupo fue tratado intra-peritonealmente una vez al día con PD-74 a las dosis indicadas o el vehículo (DMSO) (recuadro gris). La gráfica muestra la evolución del volumen tumoral (media ± error estándar) de 6 animales por grupo en el tiempo. El tratamiento con PD-74 inhibe significativamente el crecimiento del tumor a la dosis de 20 mg/Kg (P = 0,005) en xenotransplantes de sarcoma de Ewing. **B.** Las imágenes muestran 4 fotos representativas de cada grupo (DMSO o PD-74 20 mg/Kg) de los tumores extraídos y un ratón representativo de cada grupo donde se puede observar el tamaño real de los tumores en centímetros. **C.** La gráfica muestra como el peso de los tumores extraídos disminuye significativamente al aumentar la dosis de tratamiento con PD-74 (**P < 0,004, media ± desviación estándar).

También se analizó el peso de los tumores extraídos tras el sacrificio del animal y se observó que, en concordancia con los resultados de progresión del tamaño tumoral, se obtuvo una disminución significativa del peso de los tumores procedentes de animales tratados con la dosis más alta de PD-74 (20 mg/Kg) al compararlo con los tumores procedentes de los animales no tratados (control, DMSO) (**Figura 31C**).

En la **Figura 32** podemos ver que los tumores de los animales tratados con PD-74 (20 mg/Kg) presentaron una reducción significativa del número de mitosis por campo (P = 0,01). Además, se detectó una disminución significativa del número de células positivas para la tinción de Ki-67 (medida de la proliferación) en los tumores tratados con PD-74 (P < 0,01) y un aumento significativo en el número de células apoptóticas por campo (P < 0,001).

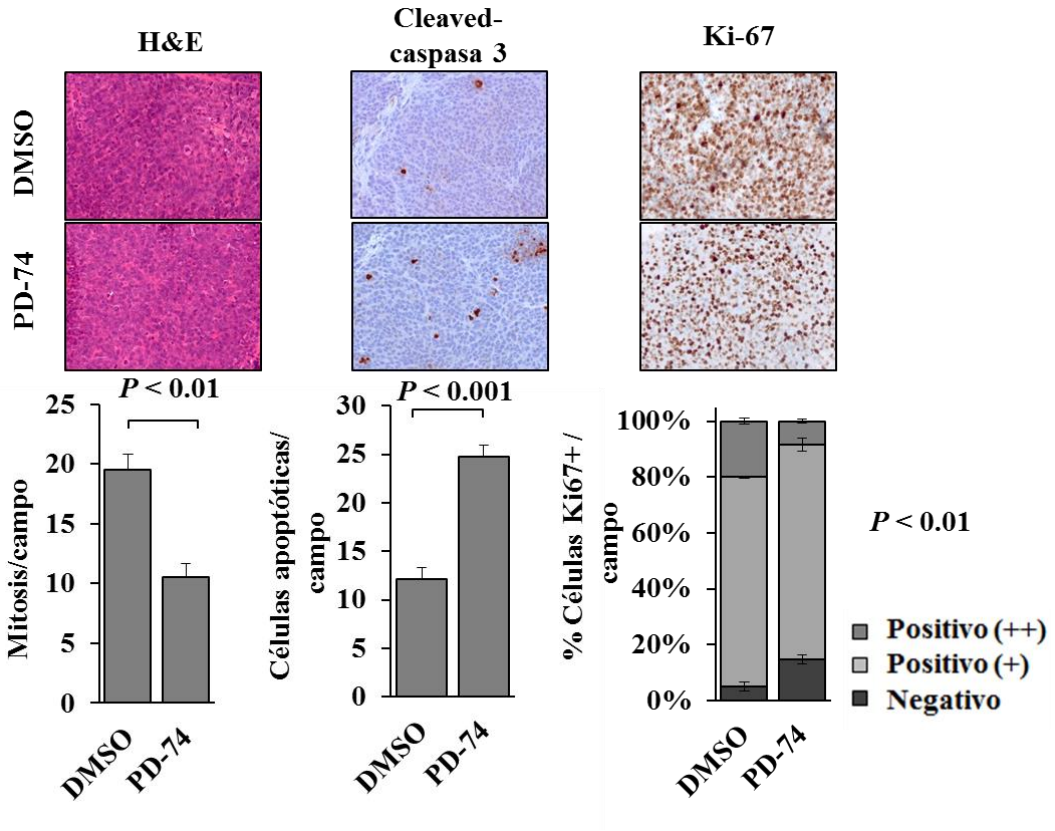

Figura 32. Estudios inmunohistoquímicos de los tumores procedentes de los experimentos *in vivo* de xenotransplantes con células SKES tratadas con el inhibidor de FGFR PD-74. Las secciones de tejido se tiñeron con hematoxilina/eosina (H&E) para observar las mitosis, o se incubaron con anticuerpos anti-*cleaved*-caspasa 3 para detectar apoptosis y anti-Ki-67 para detectar proliferación. Las gráficas muestran como el tratamiento con PD-74 a 20 mg/Kg reduce el número de mitosis por campo (P = 0,01) e incrementa el número de células apoptóticas por campo (P = 0,001). La tinción con Ki-67 y la gráfica muestra una reducción en el porcentaje de células Ki67-positivas (++ o +) en los tumores tratados con PD-74 (P < 0,01).

Durante todo el experimento se monitorizó a los animales diariamente para detectar la aparición de signos de toxicidad en el tratamiento con PD-74. Todos los animales tratados se mantuvieron en condiciones óptimas y la evolución de su peso no se vio afectada por el tratamiento, como podemos ver en la **Figura 33**.

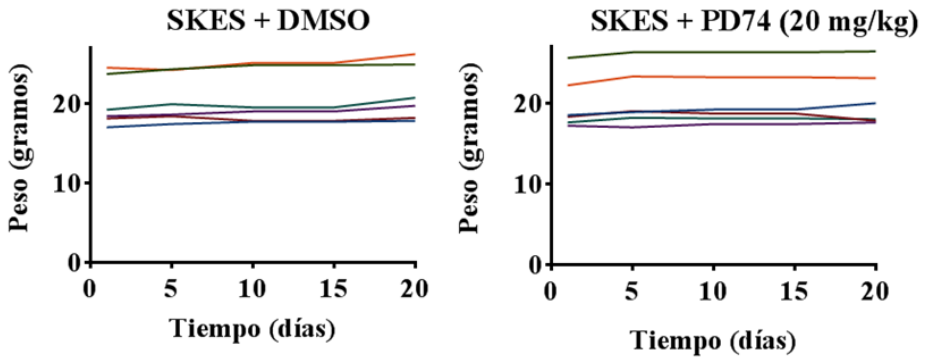

Figura 33. El tratamiento con el inhibidor PD-74 no genera toxicidad en los animales. La gráfica muestra como el peso corporal de los animales se mantuvo a lo largo del experimento en comparación con los animales tratados con vehículo. Cada línea representa a un animal.

4.5. SPRY1 podría ser un factor pronóstico en sarcoma de Ewing

Los resultados mostrados en esta Tesis sugieren que la inhibición de SPRY1 es uno de los factores que puede contribuir a mantener la vía de señalización Ras/MAPK/ERK activada constitutivamente en respuesta a estímulos externos como FGFb. En este contexto, los niveles de SPRY1 podrían correlacionar con el grado de activación de la ruta, lo que podrían tener consecuencias en la agresividad tumoral. Por ello se decidió estudiar si los niveles de expresión de SPRY1 *in situ* podían estar relacionados con el pronóstico de los pacientes de sarcoma de Ewing.

SPRY1 presenta niveles bajos de expresión, pero variables, en tumores de Ewing con respecto a otras cohortes de tumores sólidos.

Hemos mostrado previamente un análisis de los niveles de expresión de SPRY1 en una pequeña serie de tumores de Ewing primarios (**Figura 9**). Sin embargo, para poder

sacar conclusiones acerca de la utilidad pronóstica de un marcador determinado, en este caso SPRY1, es necesario analizar un número mayor de casos.

En primer lugar realizamos un análisis comparativo de los niveles de expresión de SPRY1 en una cohorte de 117 muestras de sarcoma de Ewing (Postel-Vinay *et al.* 2012) con respecto a otros 24 tipos diferentes de tumores sólidos. En la **Figura 34** se observa como las muestras de sarcoma de Ewing son unas de las que presentan los niveles más bajos de expresión de SPRY1, lo cual concuerda con los resultados que habíamos obtenido en una serie mucho más pequeña de sarcomas de Ewing (**Figura 9**). Sin embargo, en esta ocasión los niveles de expresión demostraron ser bastante variables. Dado que esta muestra es mucho mayor, concluimos que los niveles de expresión en sarcomas de Ewing, aunque bajos, presentaban también cierta variabilidad, lo cual podría tener implicaciones pronósticas.

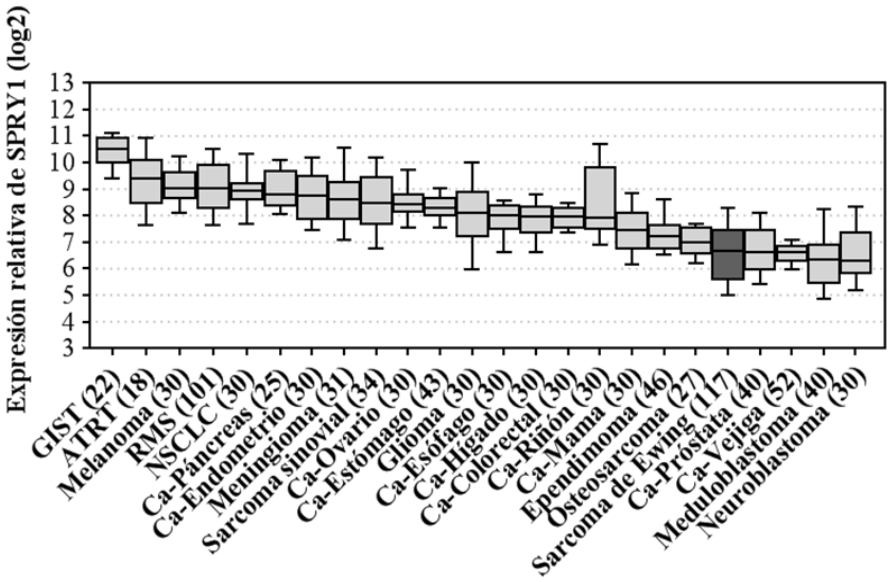

Figura 34. Niveles de expresión de ARNm de SPRY1 en 24 tipos de tumores sólidos, determinados mediante *microarrays* de ADN de Affymetrix HG-U133plus2.0. Los datos fueron obtenidos del *Gene Expression Omnibus* (GEO) o el *European bioinformatics Institute* (EBI), normalizados simultáneamente por RMA usando un *array* "*brainarray*" (v17, ENTREZG). Las líneas representan las medianas y las barras el rango intercuartil. Las líneas de desviación representan los cuartiles 10 y 90. El número de muestras analizada aparece entre paréntesis. La barra de sarcoma de Ewing aparece en gris oscuro. GIST: tumor estromal gastrointestinal, ATRT: tumor teratoideo/rabdoide atípico, RMS: rabdomiosarcoma, NSCLC: carcinoma de pulmón no microcítico, Ca-: carcinoma.

A continuación comparamos los niveles de expresión de SPRY1 en tumores y líneas celulares de sarcoma de Ewing. Para ello, analizamos los datos de expresión de la cohorte de 117 tumores primarios de sarcoma de Ewing con las 15 líneas celulares de sarcoma de Ewing incluidas en la *Cancer Cell Line Encyclopedia*. Todos estos datos se generaron usando *microarrays* de Affymetrix HG-U133Plus2.0 y por tanto son comparables una vez realizada una normalización conjunta de ambos grupos de datos.

En la **Figura 35** se muestran los niveles de expresión normalizados en líneas celulares y tumores de Ewing para los genes *SPRY1*, *LOX* (un gen reprimido por EWS-FLI1 (Agra *et al.* 2013)), *NR0B1* (un gen inducido por EWS-FLI1 (Mendiola *et al.* 2006)) y *CD99* (un gen sobre-expresado en sarcomas de Ewing utilizado como marcador en el diagnóstico inmunohistoquímico diferencial anatomopatológico (Kovar *et al.* 1990, Perlman *et al.* 1994)). Como se puede observar en dicha figura, los niveles de expresión de *LOX*, *NR0B1* y *CD99* fueron comparables entre las líneas celulares y los tumores, no apreciándose diferencias significativas. Sin embargo, los niveles de expresión de *SPRY1* fueron significativamente más altos en tumores que en las líneas celulares.

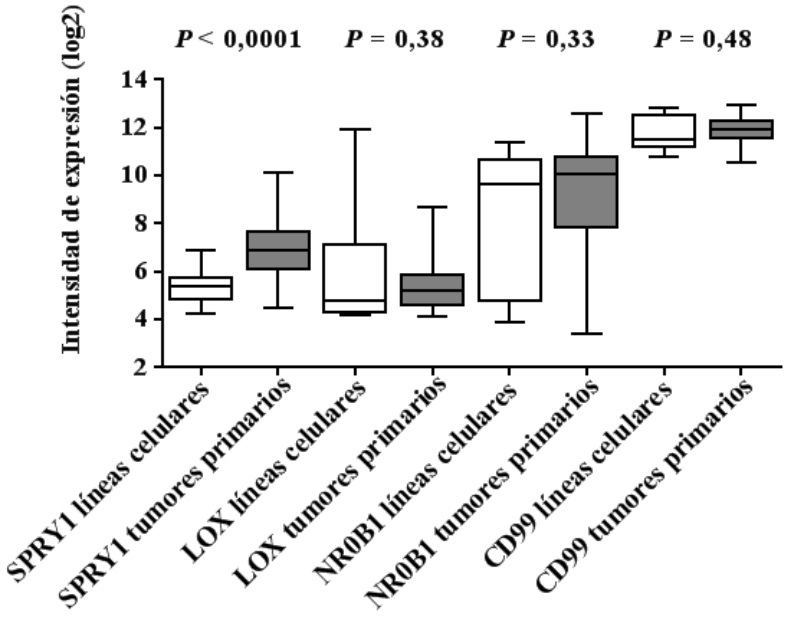

Figura 35. La expresión de SPRY1 es inferior en líneas celulares que en tumores primarios de sarcoma de Ewing. Expresión relativa de *SPRY1* comparada a otras genes diana de EWS-FLI1 (*LOX*, *NR0B1*) y CD99 en 15 líneas celulares de sarcoma de Ewing vs 117 tumores primarios de sarcoma de Ewing (todos analizados con el *microarray* Affymetrix HG-U133Plus2.0). Los datos fueron obtenidos de GEO (códigos de acceso: GSE8596, GSE36133, GSE70826, y GSE34620) y normalizados simultáneamente por RMA usando un *array* "*brainarray*" (v17, ENTREZG).

Niveles de expresión moderados de SPRY1 se asocian a un mejor pronóstico en sarcoma de Ewing.

Una vez establecido que en las muestras de tumores primarios existe una cierta variabilidad en la expresión de SPRY1, decidimos estudiar si existía una correlación entre el nivel de expresión de SPRY1 y el pronóstico de la enfermedad en los pacientes con sarcoma de Ewing.

Para ello analizamos una cohorte de 162 pacientes de sarcoma de Ewing formada por 117 casos ya publicados por Postel-Vilnay *et al.* (Postel-Vinay *et al.* 2012) y 45 casos adicionales estudiados en nuestro laboratorio mediante *arrays* de expresión. De todos los casos se dispuso de los niveles de SPRY1 y de los datos clínicos asociados como la supervivencia global, la supervivencia libre de eventos y la presencia de metástasis al diagnóstico.

En primer lugar se estableció un corte basado en el valor mediano de expresión para dividir los pacientes según el nivel de expresión de SPRY1 en "SPRY1-bajo" y "SPRY1-moderado". Como se muestra en la **Figura 36**, una expresión moderada de SPRY1 se asoció significativamente a una mayor supervivencia global (supervivencia global a 5 años de 0,70 contra 0,38, P = 0,002; test log-rank) y supervivencia libre de eventos (supervivencia libre de eventos a los 5 años de 0,72 contra 0,45, P = 0,0015; test log-rank).

Además, como se observa en la **Figura 37**, los niveles bajos de SPRY1 se asociaron a un mayor riesgo de presencia de metástasis al diagnóstico (P = 0,002, test exacto de Fisher). No se observaron diferencias entre los niveles de expresión de SPRY1 y otras variables como la edad al diagnóstico o el sexo del paciente (**Figura 38**).

En conjunto, estos resultados apuntan a la existencia de una relación entre los niveles de SPRY1 y el grado de agresividad del sarcoma de Ewing, de manera que los niveles de SPRY1 más elevados estarían asociados a un mejor pronóstico de la enfermedad.

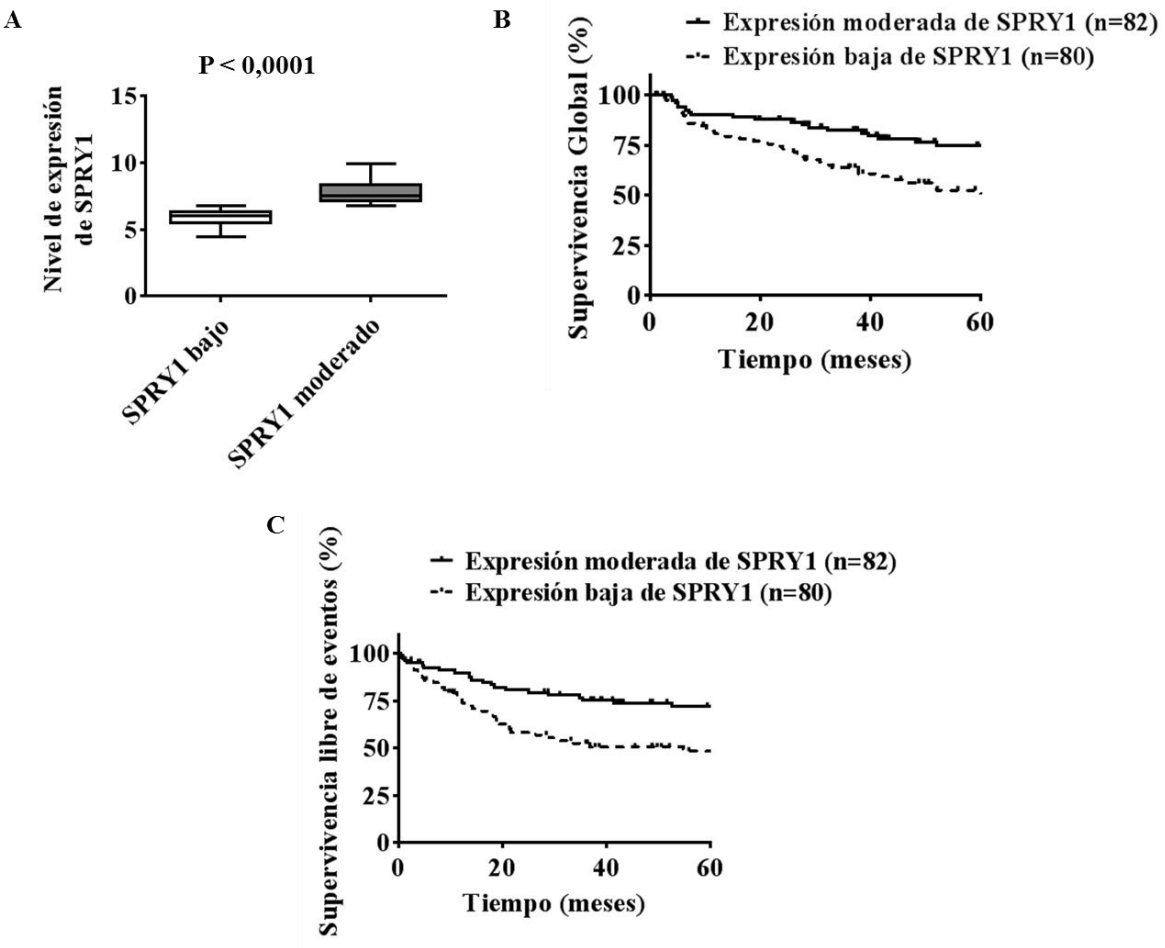

Figura 36. La expresión de SPRY1 correlaciona positivamente con un aumento de la supervivencia global de los pacientes de sarcoma de Ewing. A. La cohorte de pacientes se dividió en función de su nivel de expresión de SPRY1 en "SPRY1 bajo" y "SPRY1 moderado" utilizando como punto de corte la mediana. Ambos grupos presentan una expresión de SPRY1 significativamente diferente ($P < 0,001$). **B.** Curvas de estimación de supervivencia de Kaplan-Meier (supervivencia global) en una cohorte de pacientes de sarcoma de Ewing. Los pacientes se clasificaron según su nivel de expresión de SPRY1 en "expresión moderada" o "expresión baja" ($P = 0,002$, test log-rank). **C.** La gráfica muestra la probabilidad de supervivencia libre de eventos vs el nivel de expresión de SPRY1. La expresión moderada de SPRY1 correlaciona positivamente con una mejor supervivencia libre de eventos ($P = 0,0015$, test log rank).

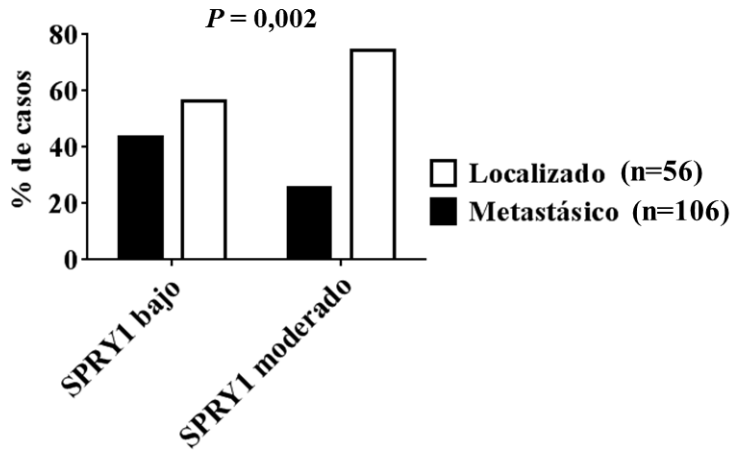

Figura 37. Los niveles de expresión moderados de SPRY1 correlacionan positivamente con un menor porcentaje de casos de metástasis al diagnóstico en los pacientes de sarcoma de Ewing. La gráfica representa el porcentaje de casos de sarcoma de Ewing con metástasis al diagnóstico vs el nivel de expresión de SPRY1 (bajo o moderado). La expresión moderada de SPRY1 correlaciona con un riesgo menor de metástasis al diagnóstico (*P* = 0,002, test exacto de Fisher).

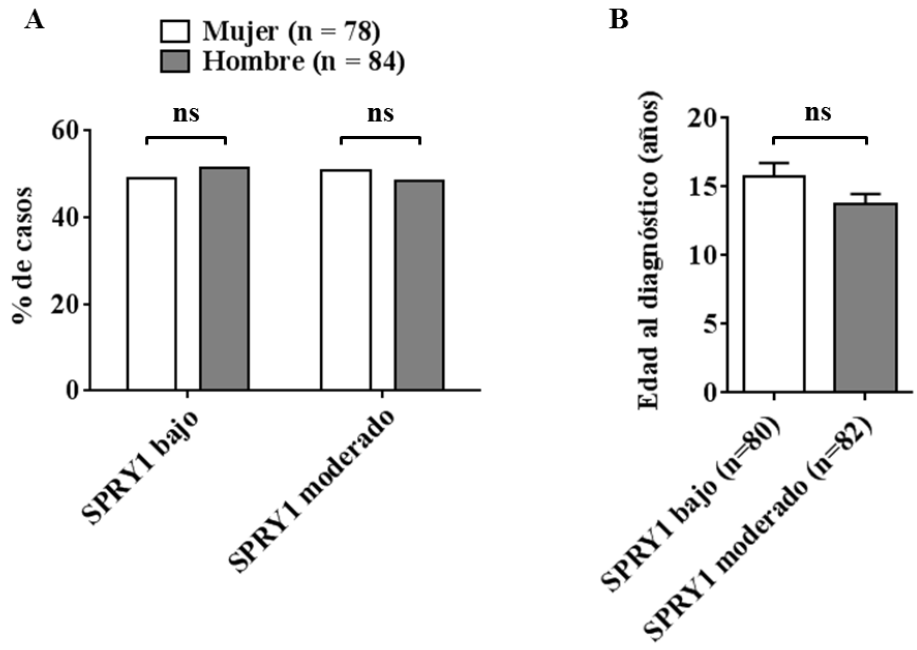

Figura 38. La expresión de SPRY1 no correlaciona con parámetros como el sexo o la edad al diagnóstico de los pacientes analizados. A. La gráfica representa el porcentaje de casos en función del sexo del paciente vs el nivel de expresión de SPRY1 y se observa como no hay diferencias significativas (ns: no significativo; Test exacto de Fisher). **B.** La gráfica muestra la edad al diagnóstico (media desviación ± estándar) vs los niveles de expresión de SPRY1 (baja o moderada). Se observa como no hay una correlación significativa entre ambos parámetros (ns: no significativo; T de *Student*).

5. Discusión

Discusión

Los sarcomas de Ewing son tumores pediátricos muy agresivos que se caracterizan, desde un punto de vista molecular, por la presencia de translocaciones cromosómicas que dan lugar a factores de transcripción quiméricos con propiedades oncogénicas. Estos factores de transcripción quiméricos, el más frecuente de los cuales es EWS-FLI1, inducen e inhiben la expresión de múltiples genes implicados en el desarrollo de estos tumores, de ahí que EWS-FLI1 juegue un papel central en la patogénesis del sarcoma de Ewing. Por ello, la identificación y la caracterización funcional de los genes diana de EWS-FLI1 son fundamentales para determinar las rutas implicadas en la patogénesis y la progresión del sarcoma de Ewing. Este conocimiento puede ser clave para establecer nuevas terapias más específicas para su tratamiento (Kovar 2014, Cidre-Aranaz and Alonso 2015).

Como se ha descrito en el apartado de la introducción, a lo largo de los últimos años se han identificado numerosas dianas de EWS-FLI1 tanto directas como indirectas, algunas de las cuáles podrían ser potenciales dianas terapéuticas. Algunos de estos genes diana han sido previamente identificados en nuestro laboratorio mediante la utilización de *arrays* de expresión y sistemas celulares de inhibición condicional de la expresión de EWS-FLI1, como por ejemplo *CCK* (Carrillo *et al.* 2007, Carrillo *et al.* 2009), *NR0B1* (Garcia-Aragoncillo *et al.* 2008), *LOX* (Agra *et al.* 2013) o *DKK1* (Navarro *et al.* 2010).

En esta Tesis hemos identificado un nuevo gen diana de EWS-FLI1, *SPRY1*, y estudiado el papel de este gen en la patogénesis del sarcoma de Ewing, con especial atención en el potencial efecto antitumoral de SPRY1 en sarcoma de Ewing. Además, se ha mostrado el rol de SPRY1 como regulador de la vía de señalización de MAPK, así como en el efecto de la inhibición de FGFR sobre la proliferación celular *in vitro* e *in vivo* en células de sarcoma de Ewing. Además se ha analizado el efecto de la utilización de diferentes inhibidores farmacológicos de FGFR sobre la proliferación de las células de sarcoma de Ewing y el posible sinergismo de estos compuestos con el efecto de SPRY1. Finalmente se ha estudiado la utilidad de emplear SPRY1 como biomarcador para determinar el pronóstico en pacientes de sarcoma de Ewing.

EWS-FLI1 regula la expresión de SPRY1 en células de sarcoma de Ewing

En esta Tesis se ha descrito que *SPRY1*, un miembro de la familia de proteínas *Sprouty*, es un gen regulado negativamente por EWS-FLI1 en la línea celular A673 derivada de sarcoma de Ewing. Este efecto resultó ser mayoritario en el caso de SPRY1, ya que la expresión del resto de miembros de la familia de proteínas *Sprouty* (SPRY2-4) fue solo parcialmente alterada, en comparación, tras la inhibición de EWS-FLI1 en nuestro sistema modelo. En concordancia con esta observación, los niveles de SPRY1 fueron indetectables o muy bajos en todas las células de sarcoma de Ewing. Estos resultados indican que EWS-FLI1 regula negativamente la expresión de SPRY1 en sarcoma de Ewing.

Actualmente se desconoce el mecanismo exacto por el que EWS-FLI1 regula negativamente la expresión de SPRY1, aunque los resultados disponibles indican que está regulación es probablemente indirecta. Por ejemplo, dos estudios independientes que emplearon ChIP-seq (Bilke *et al.* 2013, Riggi *et al.* 2014) para determinar los sitios de unión de EWS-FLI1 en el genoma de la célula tumoral A673 sugieren que EWS-FLI1 no se une directamente al promotor de *SPRY1*. Aun así es interesante destacar que en estos estudios, la inhibición de EWS-FLI1 provocó un aumento en las marcas de histonas H3K27ac localizadas en el promotor putativo de *SPRY1* que comprende el exón 1 y el intrón 1 del gen. Esto podría indicar que la regulación de *SPRY1* podría estar mediada por mecanismos epigenéticos que incluyesen modificaciones de histonas, en vez de deberse a una unión directa de EWS-FLI1 al promotor de *SPRY1*.

Otro de los posibles mecanismos epigenéticos que podrían estar implicados en la regulación negativa de *SPRY1* en sarcoma de Ewing es la metilación de su promotor, donde existe una isla CpG que ha sido descrita previamente (Fritzsche *et al.* 2006, Macia *et al.* 2012). De hecho, la hipermetilación del promotor de *SPRY1* es el mecanismo principal por el que se regula negativamente su expresión en carcinoma medular de tiroides y cáncer de próstata (Kwabi-Addo *et al.* 2009, Macia *et al.* 2012).

Sin embargo, en el caso del sarcoma de Ewing, los datos publicados indican que no hay diferencias significativas en el porcentaje de metilación de dichas islas CpG tras inhibir la expresión de EWS-FLI1 (Tomazou *et al.* 2015). Esto sugiere que el mecanismo de

regulación de *SPRY1* en sarcoma de Ewing podría ser diferente del que ocurre en otros tipos de tumores descritos anteriormente (Kwabi-Addo *et al.* 2009, Macia *et al.* 2012).

Aunque en esta Tesis no se ha realizado un estudio en profundidad de los mecanismos epigenéticos potencialmente implicados en la regulación de la expresión de SPRY1, los experimentos *in vitro* llevados a cabo con un inhibidor de la desacetilasa de histonas (SAHA) y de la metilación del ADN (5-aza-2'-deoxicitidina) indican que la inhibición de la desacetilación de histonas genera un aumento en la expresión de *SPRY1* mientras que la inhibición de la metilación no genera efectos significativos sobre los niveles de expresión de este gen. Esto concuerda con los resultados presentados por Tomazou y colaboradores, donde al tratar células de sarcoma de Ewing con inhibidores de la desacetilación de histonas como entinostat o romidepsina obtuvieron una inducción de la expresión de los transcritos que correlacionaban inversamente con la expresión de EWS-FLI1, lo que sugiere que el efecto inhibitorio de EWS-FLI1 puede ser revertido mediante el tratamiento con inhibidores de la desacetilación de histonas (Tomazou *et al.* 2015).

Todo esto refuerza la hipótesis de que la regulación de EWS-FLI1 sobre la expresión de *SPRY1* podría estar mediada por mecanismos epigenéticos que involucrasen la acetilación de histonas en su promotor.

Por otro lado, recientemente se ha descrito que EWS-FLI1 reprime de forma directa el 5% de los genes inhibidos por EWS-FLI1 y que el 95% de los genes restantes son regulados de forma indirecta mediante la inducción de represores transcripcionales (Sankar *et al.* 2013). De hecho, coincidiendo con el inicio de esta Tesis, se había publicado la caracterización de *BCL11B*, un gen inducido por EWS-FLI1, como un regulador negativo de la expresión de *SPRY1* mediante análisis de genoma completo (Wiles *et al.* 2013). De este estudio se deduce que *BCL11B* posee una cierta actividad represora sobre *SPRY1* de forma independiente de la represión generada por EWS-FLI1. Sin embargo, la represión completa de *SPRY1* requiere de una regulación más compleja que incluye posiblemente otros genes regulados por EWS-FLI1 (Wiles *et al.* 2013) y, como hemos comentado, posiblemente la participación de mecanismos de regulación epigenética.

En cualquier caso, determinar el mecanismo exacto por el que se regula la expresión de *SPRY1* en sarcoma de Ewing sería de gran interés dado que nos permitiría conocer con más profundidad las diferentes estrategias mediante las que estas células sufren la transformación neoplásica.

SPRY1 es un supresor tumoral en sarcoma de Ewing

El hecho que la expresión de *SPRY1* esté regulada negativamente por EWS-FLI1 en las células A673, que su expresión sea indetectable o muy baja en células y tumores primarios de sarcoma de Ewing y que SPRY1 sea un potente regulador negativo de la ruta de señalización Ras/MAPK/ERK (Gross *et al.* 2001), sugerían que *SPRY1* podría actuar como un gen supresor de tumores en sarcoma de Ewing. Para demostrarlo, realizamos numerosos ensayos funcionales empleando tres líneas celulares independientes de sarcoma de Ewing que fueron genéticamente manipuladas para re-expresar SPRY1 de manera condicional en respuesta a doxiciclina.

Gracias a estos modelos celulares se pudo establecer que la re-expresión de SPRY1 inhibe significativamente la proliferación, el crecimiento clonogénico y la migración de las células de sarcoma de Ewing *in vitro*, indicando que *SPRY1* actúa como un gen supresor de tumores en estas células. Los resultados obtenidos en esta Tesis sugieren que *SPRY1* es un inhibidor de la proliferación en sarcoma de Ewing, especialmente en condiciones de acceso limitado a factores de crecimiento (baja concentración de suero).

Además se comprobó cómo la re-expresión de SPRY1 inhibe el crecimiento independiente de anclaje (capacidad transformante) en las tres líneas de sarcoma de Ewing estudiadas, lo que concuerda con los resultados obtenidos en los ensayos de proliferación y migración y demuestra que SPRY1 desempeña un rol importante en la transformación maligna de estas células.

Estos resultados coinciden con los estudios llevados a cabo en otros tipos de cáncer en los que se ha descrito que la re-expresión de SPRY1 inhibe el crecimiento celular, la proliferación, la migración y la capacidad invasiva en una gran variedad de líneas celulares tumorales. Por ejemplo, la re-expresión de SPRY1 en las líneas celulares de

adenocarcinoma de pulmón A549 y carcinoma de colon HCT 116 inhibe la proliferación al favorecer la degradación lisosomal de uPAR (*urokinase plasminogen activator receptor*) (Liu *et al.* 2014). En células de cáncer de ovario SKOV-3 se ha visto que la expresión de SPRY1 correlaciona negativamente con un aumento del crecimiento, la proliferación, migración e invasión (Masoumi-Moghaddam *et al.* 2014a). Kwabi-Addo y colaboradores demostraron que la transfección de células de cáncer de próstata con SPRY1 generaba un efecto inhibitorio sobre la formación de colonias y la proliferación celular (Kwabi-Addo *et al.* 2004). Por otro lado, Macia y colaboradores han mostrado que la expresión ectópica de SPRY1 redujo la proliferación en células de carcinoma medular de tiroides (Macia *et al.* 2012). Además, en células de cáncer de mama MDA-MB-231 y de colon HCT 116 se observó una inhibición del crecimiento, de la migración y de la capacidad invasiva de líneas celulares en las que se indujo la expresión de SPRY1 (Mekkawy and Morris 2013, Mekkawy *et al.* 2014). Finalmente, también en neoplasias no epiteliales como el osteosarcoma se ha descrito que SPRY1 inhibe la capacidad invasiva de células SAOS-2 (Mekkawy and Morris 2013).

En cuanto al efecto de SPRY1 sobre la migración celular, que es una de las claves del establecimiento de metástasis (Yilmaz and Christofori 2010), se ha descrito que el *knock-down* de SPRY1 genera un aumento en la actividad de la quinasa Rho (*Ras homolog*), que es una GTPasa implicada en la estabilidad de la actina intracelular (Long *et al.* 2011). Además se ha observado que cuando las proteínas SPRED, que están estructuralmente relacionadas con las proteínas de la familia *Sprouty*, son sobre-expresadas en células de osteosarcoma metastásico LM8, se inhiben la motilidad celular, la migración y la reorganización de actina mediada por Rho (Miyoshi *et al.* 2004). Por otro lado, se ha descrito que la expresión de SPRY4 inhibe la extensión celular mediada por integrinas, necesaria para la reorganización del citoesqueleto en células musculares C2C12 (Tsumura *et al.* 2005).

De forma complementaria, los resultados expuestos en esta Tesis muestran que la re-expresión de SPRY1 en las células de sarcoma de Ewing altera la morfología generando una pérdida de la circularidad que podría ser responsable de la subsiguiente incapacidad para migrar correctamente. Aunque se ha descrito en otros sistemas que la deformación de las células cancerosas correlaciona con un mayor potencial metastásico (Pasqualato *et al.* 2013) en sarcoma de Ewing, al tratarse de células inherentemente redondas y con

poco citoplasma, se podría hipotetizar que es precisamente la pérdida de esta circularidad, ocasionada posiblemente por la presencia de un mayor número de focos de adhesión a la placa, la responsable del efecto que se observa sobre la inhibición de la migración. De hecho, Chaturvedi y colaboradores han descrito recientemente en células de sarcoma de Ewing que la inhibición de EWS-FLI1 genera un aumento en la cantidad de adhesiones focales y del tamaño de las células como consecuencia de un incremento en fibras de estrés de actina, que genera una redistribución del citoesqueleto (Chaturvedi *et al.* 2014). Esta conformación del citoesqueleto es característica de células con una menor capacidad migratoria (Smilenov *et al.* 1999, Salsmann *et al.* 2006) y coincidiría con la morfología que observamos en las células de sarcoma de Ewing cuando se re-expresa SPRY1, lo que explicaría también el efecto de SPRY1 sobre la inhibición de la migración en estas células.

En resumen, en esta Tesis se han analizado múltiples líneas celulares de sarcoma de Ewing y numerosos estudios centrados en las diferentes características de las células transformadas y se ha determinado así el efecto de SPRY1 como inhibidor de la proliferación, el crecimiento clonogénico, la migración, la capacidad invasiva y el crecimiento libre de anclaje de células de sarcoma de Ewing.

SPRY1 inhibe la ruta de las MAPK inducida por suero y FGFb en sarcoma de Ewing

Los resultados presentados en esta Tesis sugieren que la inhibición de SPRY1 favorece la proliferación mediada por FGFb y la activación de las rutas de señalización de Ras/MAPK/ERK en las células de sarcoma de Ewing. Esto se deduce de los experimentos de re-expresión de SPRY1 en las tres líneas de sarcoma de Ewing empleadas en esta Tesis donde se observa que la inducción de SPRY1 inhibe la proliferación celular y la fosforilación de ERK mediada por FGFb. Esto concordaría con los trabajos publicados previamente, que apuntan a SPRY1 como un inhibidor de las rutas reguladas por la activación de RTKs, implicadas en la activación y el mantenimiento de la proliferación celular (Shea *et al.* 2010, Liu *et al.* 2014, Masoumi-Moghaddam *et al.* 2014a, Mekkawy *et al.* 2014).

FGFb regula numerosos procesos celulares como la proliferación, migración y diferenciación en diferentes contextos, tanto fisiológicos como patológicos. Por ejemplo, FGFb está implicado en la migración de las células endoteliales durante la cicatrización en el cierre de heridas regulando la adhesión de moléculas a la superficie celular (Powers *et al.* 2000) y en la proliferación de fibroblastos de ratón (Bottcher and Niehrs 2005). En cuanto a los procesos patológicos, se ha visto que las rutas reguladas por FGFb tienen un rol preponderante en cáncer (Meier *et al.* 2003, Touat *et al.* 2015) y que en el tejido tumoral FGFb puede actuar como un factor autocrino promoviendo, por ejemplo, la angiogénesis en el tejido circundante (Powers *et al.* 2000).

Es importante destacar que, en la actualidad, las rutas de señalización activadas por FGF están emergiendo como puntos clave en la patogénesis del sarcoma de Ewing. Por ejemplo, recientemente hemos descrito que FGFb promueve la proliferación de las células de sarcoma de Ewing *in vitro* y que *EGR2*, un componente *downstream* de la ruta de FGF, es un gen diana inducido por EWS-FLI1 en estas células (Grunewald *et al.* 2015). Otros estudios han demostrado que en el microentorno óseo, FGFb regula la motilidad y la capacidad invasiva de las células de sarcoma de Ewing y que las muestras clínicas de esta neoplasia presentan expresión y activación de FGFR1 (Kamura *et al.* 2010). Por otro lado, Agelopoulos y colaboradores han demostrado recientemente que la inhibición constitutiva de *FGFR1* en células de sarcoma de Ewing impide la formación de tumores en modelos murinos de xenotransplante (Agelopoulos *et al.* 2015). Finalmente, cabe destacar que cerca del 75% de las biopsias de sarcoma de Ewing presentan niveles de fosforilación de FGFR1 moderados o altos (Kamura *et al.* 2010), aunque las mutaciones activadoras de FGFR1 son extremadamente infrecuentes en esta enfermedad (Agelopoulos *et al.* 2015).

Por otro lado se ha propuesto que el tratamiento con FGFb de células de sarcoma de Ewing, mantenidas en ausencia de suero, es capaz de restaurar la expresión de EWS-FLI1 y favorecer su proliferación; y que el tratamiento con anticuerpos neutralizadores de FGFb genera una inhibición de la expresión de EWS-FLI1 (Girnita *et al.* 2000). Más recientemente se ha descrito cómo la estimulación de células de sarcoma de Ewing por FGFb aumenta tanto su motilidad como su capacidad invasiva, efecto que es revertido mediante el uso de anticuerpos anti-FGFb (Kamura *et al.* 2010). Por lo tanto, el mantenimiento de la ruta mediada por FGF sería esencial para la patogénesis del

sarcoma de Ewing. Sin embargo, un estudio de Sturla y colaboradores describe que el tratamiento de células de sarcoma de Ewing con FGFb genera una inducción de la muerte celular y la inhibición del crecimiento de tumores en modelos *in vivo* de xenotransplante murinos (Sturla *et al.* 2000).

Todos estos resultados, sumados a los presentados en esta Tesis, indican que la ruta de señalización activada por FGF puede ser un elemento clave en la patogénesis del sarcoma de Ewing. Además sugieren que las estrategias encaminadas a bloquear esta ruta pueden ser prometedoras en el tratamiento del sarcoma de Ewing.

Los inhibidores de los receptores de FGF muestran actividad antitumoral *in vitro* e *in vivo*

A la luz de los resultados obtenidos en esta Tesis y de la importancia de la ruta de FGFR en sarcoma de Ewing descrita previamente en otros trabajos (Kamura *et al.* 2010, Grunewald *et al.* 2015), podemos especular que la activación constitutiva de los FGFRs y el mantenimiento de sus rutas de señalización *downstream* son claves en la patogénesis del sarcoma de Ewing. Además, la inhibición que EWS-FLI1 ejerce sobre *SPRY1*, que es un regulador negativo de esta ruta de señalización, constituye un mecanismo importante para mantener activas de forma constitutiva estas rutas de señalización. Esta activación sostenida de la ruta FGFR/Ras/MAPK/ERK da lugar a una transducción descontrolada de la señal inducida por FGF que puede contribuir a la progresión tumoral, tal y como ocurre en otros tumores (Meier *et al.* 2003, Touat *et al.* 2015).

Hay varios mecanismos que pueden contribuir a que la señalización por FGFR pueda aparecer activada de forma aberrante en el sarcoma de Ewing: i) como consecuencia de la inhibición de SPRY1, un regulador negativo de la ruta, lo que probablemente ocurra en la mayoría de los casos tal y como sugieren los resultados presentados en esta Tesis, ii) debido a la sobreexpresión de FGFRs como ha sido observado en un subgrupo de pacientes (Agelopoulos *et al.* 2015) y iii), debido a mutaciones somáticas de forma muy infrecuente, (Agelopoulos *et al.* 2015). Ya que muchos de los tumores presentarían alteraciones en la ruta del FGF, los pacientes de sarcoma de Ewing podrían beneficiarse

de terapias que incluyesen fármacos dirigidos a inhibir la actividad de los FGFRs o sus dianas *downstream*.

Los resultados de esta Tesis muestran cómo la inhibición de FGFR empleando 4 fármacos diferentes es capaz de inhibir la proliferación y la formación de colonias a baja densidad en varias líneas celulares de sarcoma de Ewing. Además se ha demostrado cómo la inhibición de FGFR mediante uno de estos inhibidores comerciales, es capaz de limitar significativamente el desarrollo de tumores en modelos murinos de xenotransplante de dos líneas celulares de sarcoma de Ewing. Esta inhibición se acompaña de una disminución del número de células en mitosis y un aumento de la proporción de células apoptóticas en los tumores.

La eficacia de los inhibidores de RTK depende de su capacidad para interrumpir la comunicación entre las células tumorales y su entorno (Segaliny *et al.* 2015). En el caso de los inhibidores de FGFR empleados en esta tesis, se trata fundamentalmente de inhibidores de FGFR1 que poseen diferentes IC50s (Mohammadi *et al.* 1998, Panek *et al.* 1998, Sun *et al.* 1999, Guagnano *et al.* 2011). El efecto inhibitorio de las características tumorigénicas de las células de Ewing mostrado en esta Tesis, al emplear estos compuestos, indicaría una presencia mayoritaria de este tipo de receptores de forma activa en las células de sarcoma de Ewing. De hecho, la presencia de receptores FGFR1 activados en muestras tumorales de sarcoma de Ewing ya ha sido descrita previamente por Kamura y colaboradores (Kamura *et al.* 2010).

La búsqueda de nuevos inhibidores de FGFR es un campo muy activo en el ámbito farmacéutico debido a que las vías de señalización mediadas por FGF son uno de los sistemas que se halla más comúnmente mutado en cáncer (Touat *et al.* 2015). Es importante destacar además que algunos de estos inhibidores están siendo analizados en ensayos clínicos como monoterapia para pacientes con otras neoplasias (Shaw *et al.* 2013). Por ejemplo, NVP-BGJ398, desarrollado por Novartis y que ha sido utilizado en esta Tesis, está actualmente empleándose en un ensayo clínico fase I para el tratamiento de cánceres avanzados con amplificación de FGFR1 o -2 o mutaciones en FGFR3 (tumores sólidos avanzados, cáncer de vejiga y carcinoma de célula escamosa). AZD4547, de AstraZéneca, está en estudio en un ensayo clínico fase II para el tratamiento de cánceres con amplificación de FGFR1 o -2 (cáncer gástrico, carcinoma

de célula escamosa, cáncer de esófago y cáncer de mama). Ponatinib de Ariad está en un ensayo clínico fase II para el tratamiento del carcinoma de célula escamosa avanzado y NSCLC. Por último, Dovitinib, de Novartis se ha empleado en un ensayo clínico fase II para el tratamiento de algunos tipos de cáncer con mutaciones en FGFR1, -2 o -3). Actualmente estos ensayos están aún en curso o han arrojado resultados de eficacia moderada para las patologías estudiadas.

Los resultados en sarcoma de Ewing son escasos: Agelopoulos y colaboradores describieron recientemente el caso de un paciente con sarcoma de Ewing en recaída que respondió inicialmente al tratamiento con Ponatinib (ARIAD), un inhibidor de tirosina quinasas de FGFR (Agelopoulos *et al.* 2015). Por ello es necesario continuar profundizando en el estudio de estos inhibidores de FGFR en el tratamiento de pacientes con sarcoma de Ewing.

Los niveles de expresión de SPRY1 pueden ser un nuevo factor pronóstico en sarcoma de Ewing

La importancia de SPRY1 en la regulación de la ruta activada por FGF en sarcoma de Ewing pone de relevancia la posible aplicación de los niveles de actividad de esta ruta como marcador pronóstico. Así, una medida indirecta del potencial de activación de la ruta de señalización de FGF en sarcoma de Ewing podrían ser los propios niveles de SPRY1, de manera que cuanto menor fueran los niveles de SPRY1, más probabilidades habría de tener activada la ruta del FGF. Con el objeto de valorar la utilidad pronóstica de esta hipótesis se realizó un estudio *in situ* con muestras tumorales de sarcoma de Ewing, para intentar determinar si los niveles de expresión de SPRY1 podrían ser además un marcador pronóstico de la enfermedad.

Es interesante destacar que, aunque la expresión de SPRY1 es indetectable en líneas celulares establecidas de sarcoma de Ewing, sus niveles varían en el caso de los tumores primarios. Realmente se desconocen las razones de tales diferencias entre las muestras tumorales primarias y las líneas celulares, pero se podría hipotetizar que los niveles de expresión de SPRY1 se mantienen variables en los tumores, y que son precisamente las condiciones más restrictivas propias del cultivo *in vitro* las que acaban seleccionando y

favoreciendo el crecimiento de aquellas células que presentan niveles más bajos de SPRY1. De acuerdo con esta hipótesis, se ha descrito que las líneas establecidas de sarcoma de Ewing presentan un porcentaje mucho mayor de mutaciones en *STAG2*, *TP53* y *CDKN1A* que las que aparecen en los tumores primarios (Tirode *et al.* 2014), lo que sugiere que las células que derivan de tumores más agresivos son aquellas cuya proliferación es finalmente favorecida en cultivo (Kovar *et al.* 1997, Kovar *et al.* 2003).

El sarcoma de Ewing es un tumor pediátrico muy agresivo en el que el factor de riesgo más importante es la presencia de metástasis primarias en el momento del diagnóstico. De hecho, es este factor el responsable de que normalmente la enfermedad tenga un desenlace fatal a pesar de la implementación de tratamientos quimioterapéuticos muy intensos (Gaspar *et al.* 2015). En esta Tesis se ha mostrado cómo un nivel de expresión bajo de SPRY1 en tumores, correlaciona significativamente con peores valores de supervivencia global y de supervivencia libre de eventos en una cohorte amplia (n = 162) de pacientes con sarcoma de Ewing. Además, es especialmente interesante el hecho de que los tumores primarios que mostraron niveles bajos de SPRY1 pertenecieran mayoritariamente a pacientes que presentaban metástasis en el momento del diagnóstico. Este hecho es compatible con que los tumores con niveles de expresión bajos de SPRY1 tengan un comportamiento más agresivo y concuerda también con los resultados de los experimentos *in vitro* presentados en esta Tesis. Se puede especular entonces que los tumores con expresión baja de SPRY1 podrían presentar una mayor respuesta a la estimulación por factores de crecimiento y, por tanto, tendrían un ritmo de proliferación más alto y una mayor capacidad migratoria, lo que los volvería más agresivos.

Recientemente se ha descrito que los niveles de expresión de SPRY1 podrían ser un biomarcador en cáncer de próstata con capacidad para diferenciar los carcinomas de próstata más agresivos de aquellos con menor grado de malignidad (Terada *et al.* 2014). Además, Fritzsche y colaboradores han descrito, en una cohorte de 49 pacientes con cáncer de próstata, que los niveles de SPRY1 correlacionaban inversamente con los diferentes grados de malignidad (niveles de expresión de SPRY1 cada vez más bajos a medida que se pasaban de muestras de hiperplasia de próstata a neoplasia prostática intraepitelial y a cáncer de próstata) (Fritzsche *et al.* 2006). Por otro lado, en un estudio realizado en una cohorte de 100 pacientes con cáncer de ovario, los niveles de SPRY1

resultaron ser un factor independiente a la hora de predecir la supervivencia global y la probabilidad de recurrencia del tumor (Masoumi-Moghaddam *et al.* 2015). Takahashi y colaboradores estudiaron una cohorte de 29 pacientes con carcinoma renal de células claras con diferentes pronóstico y observaron que el grupo de pacientes con mejor pronóstico presentaba niveles más elevados de SPRY1 (Takahashi *et al.* 2001). En cáncer de mama, Faratian y colaboradores estudiaron una serie de 1107 tumores primarios mediante *arrays* de expresión y observaron que los tumores que presentaban un estadio más avanzado expresaron niveles más bajos de SPRY1 (Faratian *et al.* 2011). Finalmente, los niveles de SPRY1 resultaron ser significativamente inferiores en una serie de pacientes con carcinoma ductal invasivo en comparación con tejidos normales de mama (Faratian *et al.* 2011). En resumen, numerosos estudios demuestran una relación entre los niveles de SPRY1 y el pronóstico de la enfermedad en diferentes tipos de cáncer.

En todos los casos descritos, los tumores pertenecientes a estadios más agresivos presentaron niveles más bajos de SPRY1, y viceversa, los tumores en estadios menos avanzados o los tejidos normales expresaron niveles más elevados de SPRY1. Los resultados presentados en esta Tesis indican un comportamiento similar también en sarcoma de Ewing. Hasta nuestro conocimiento, esta es la primera vez que se describe una relación entre los niveles de expresión de SPRY1 y el pronóstico de la enfermedad en sarcoma de Ewing. El análisis de este nuevo biomarcador en un estudio prospectivo podría demostrar definitivamente su utilidad a la hora de estratificar los pacientes e incluso seleccionar a los pacientes para el uso de terapias biológicas dirigidas.

SPRY1 y patogénesis en sarcoma de Ewing

Los datos presentados en esta Tesis permiten establecer que la inhibición de SPRY1 mediada por EWS-FLI1 es un mecanismo importante en la patogénesis del sarcoma de Ewing: la inhibición de SPRY1 es necesaria para la proliferación y migración de las células tumorales y el mantenimiento de la ruta de Ras/MAPK/ERK en un estado constitutivamente activo.

Además, los resultados aquí presentados sugieren que la estimulación de la proliferación mediada por FGF podría ser un factor más importante de lo que se había descrito originalmente para esta enfermedad (Kamura *et al.* 2010, Grunewald *et al.* 2015). Los resultados obtenidos con los inhibidores de los receptores de FGF así lo indican y sugieren que la utilización de inhibidores de FGFR en combinación con otros tratamientos podría constituir una nueva terapia prometedora en el tratamiento del sarcoma de Ewing.

Finalmente, se ha mostrado que una expresión más elevada de SPRY1 correlacionaba con una mejor supervivencia global y con una menor incidencia de metástasis al diagnóstico.

La **Figura 39** resume los aspectos más importantes derivados de los estudios llevados a cabo en esta Tesis y nos permite concluir que la inhibición de SPRY1 mediada por EWS-FLI1 confiere una ventaja a las células de sarcoma de Ewing. Además, el conjunto de resultados presentados en esta Tesis sugiere que la ruta FGFR/SPRY1/Ras/MAPK/ERK podría ser una nueva diana terapéutica para el tratamiento de esta devastadora enfermedad. Finalmente, proponemos que los niveles de SPRY1 constituyen un posible nuevo biomarcador de pronóstico para los pacientes de sarcoma de Ewing.

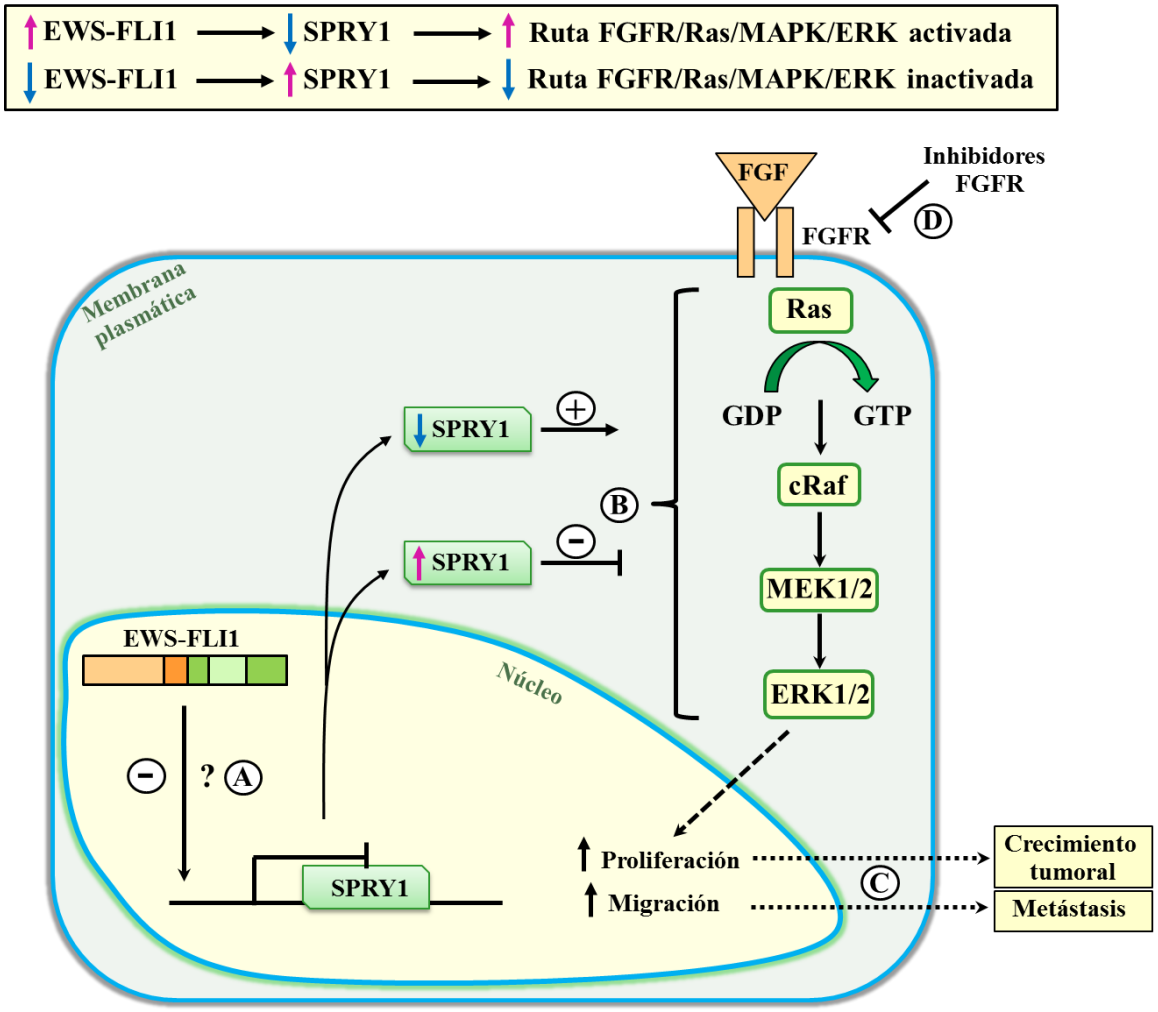

Figura 39. Resumen esquemático de los hallazgos más relevantes en esta Tesis. A. EWS-FLI1 regula negativamente la expresión de SPRY1 mediante un mecanismo todavía desconocido, pero que parece implicar mecanismos epigenéticos. **B.** La re-expresión de SPRY1 inhibe la señalización de la ruta FGFR/Ras/MAPK/ERK. **C.** Esto interfiere en la capacidad proliferativa y migratoria de las células de sarcoma de Ewing, lo que tiene un impacto en el crecimiento tumoral y potencialmente en la formación de metástasis. **D.** Los inhibidores de FGFR inhiben la proliferación de las células de sarcoma de Ewing y esta inhibición podría ocurrir a través de la misma vía de acción que SPRY1.

6. Conclusiones

Conclusiones

Las principales conclusiones que podemos extraer de los resultados obtenidos en esta Tesis son:

I. **La oncoproteína EWS-FLI1, característica del sarcoma de Ewing, inhibe la expresión de la proteína Sprouty1 (SPRY1).** Empleando células de sarcoma de Ewing A673 que expresan un ARN de interferencia inducible contra EWS-FLI1 hemos demostrado que EWS-FLI1 regula negativamente la expresión de SPRY1. Además, los resultados obtenidos mediante el análisis de datos de ChIP-seq y la inhibición de la actividad histona desacetilasas *in vitro*, sugieren que esta regulación podría ser indirecta y, al menos en parte, de tipo epigenético. Por otro lado, hemos mostrado que los niveles de expresión de SPRY1 son bajos en células y tumores primarios de sarcoma de Ewing.

II. **SPRY1 es un gen supresor de tumores en el contexto de las células de sarcoma de Ewing.** Empleando sistemas celulares de re-expresión condicional de SPRY1 desarrollados en tres líneas celulares de sarcoma de Ewing, hemos demostrado que la re-expresión de SPRY1 inhibe la proliferación celular, la migración en monocapa y a través de membrana y el crecimiento independiente de anclaje en células de sarcoma de Ewing. Todo ello indica que *SPRY1* actúa como un gen supresor de tumores en sarcoma de Ewing.

III. **SPRY1 antagoniza la activación de la ruta Ras/MAPK/ERK inducida por suero o FGFb en células de sarcoma de Ewing.** La re-expresión de SPRY1 en células de sarcoma de Ewing disminuye la fosforilación de ERK y este efecto está mediado en parte por la inhibición de la ruta controlada por los receptores de FGF.

IV. **La inhibición de FGFR reproduce el efecto de SPRY1 sobre la proliferación y el crecimiento de las células de sarcoma de Ewing.** La inhibición de SPRY1 sobre la ruta de FGFR y su efecto sobre la proliferación celular en células de sarcoma de Ewing se puede obtener mediante el uso de compuestos inhibidores de FGFR. La combinación de la re-expresión de SPRY1 con el uso de estos inhibidores no genera un efecto aditivo en la mayoría de los casos, lo que

sugiere que SPRY1 y los inhibidores de FGFR podrían actuar sobre la misma ruta.

V. **Los inhibidores de FGFR reducen el crecimiento tumoral en modelos de xenotransplantes murinos de células de sarcoma de Ewing.** La inhibición farmacológica de FGFR en modelos de xenotransplantes de ratón empleando dos líneas celulares de sarcoma de Ewing diferentes reduce significativamente su desarrollo. Los tumores procedentes de los animales tratados presentan un menor número de células mitóticas y un mayor número de células apoptóticas.

VI. **SPRY1 es un nuevo biomarcador con valor pronóstico en sarcoma de Ewing.** Empleando una cohorte amplia de pacientes de sarcoma de Ewing hemos determinado que una expresión más elevada de SPRY1 correlaciona con una mejor supervivencia global y una mayor supervivencia libre de eventos. Asimismo, niveles más bajos de expresión de SPRY1 correlacionan con mayores probabilidades de que el paciente presente metástasis en el momento del diagnóstico.

7. Bibliografía

Bibliografía

Agelopoulos, K., G. H. Richter, E. Schmidt, U. Dirksen, K. von Heyking, B. Moser, H. U. Klein, U. Kontny, M. Dugas, K. Poos, E. Korsching, T. Buch, M. Weckesser, I. Schulze, R. Besoke, A. Witten, M. Stoll, G. Kohler, W. Hartmann, E. Wardelmann, C. Rossig, D. Baumhoer, H. Jurgens, S. Burdach, W. E. Berdel and C. Muller-Tidow (2015). "Deep Sequencing in Conjunction with Expression and Functional Analyses Reveals Activation of FGFR1 in Ewing Sarcoma." Clin Cancer Res **21**(21):4935-46.

Agra, N., F. Cidre, L. Garcia-Garcia, J. de la Parra and J. Alonso (2013). "Lysyl oxidase is downregulated by the EWS/FLI1 oncoprotein and its propeptide domain displays tumor supressor activities in ewing sarcoma cells." PLoS One **8**(6): e66281.

Armengol, G., M. Tarkkanen, M. Virolainen, A. Forus, J. Valle, T. Bohling, S. Asko-Seljavaara, C. Blomqvist, I. Elomaa, E. Karaharju, A. H. Kivioja, M. A. Siimes, E. Tukiainen, M. R. Caballin, O. Myklebost and S. Knuutila (1997). "Recurrent gains of 1q, 8 and 12 in the Ewing family of tumours by comparative genomic hybridization." Br J Cancer **75**(10): 1403-1409.

Arvand, A. and C. T. Denny (2001). "Biology of EWS/ETS fusions in Ewing's family tumors." Oncogene **20**(40): 5747-5754.

Arvand, A., S. M. Welford, M. A. Teitell and C. T. Denny (2001). "The COOH-terminal domain of FLI-1 is necessary for full tumorigenesis and transcriptional modulation by EWS/FLI-1." Cancer Res **61**(13): 5311-5317.

Assinder, S. J., D. Beniamen and F. J. Lovicu (2015). "Cosuppression of Sprouty and Sprouty-related negative regulators of FGF signalling in prostate cancer: a working hypothesis." Biomed Res Int **2015**: 827462.

Bailly, R. A., R. Bosselut, J. Zucman, F. Cormier, O. Delattre, M. Roussel, G. Thomas and J. Ghysdael (1994). "DNA-binding and transcriptional activation properties of the EWS-FLI-1 fusion protein resulting from the t(11;22) translocation in Ewing sarcoma." Mol Cell Biol **14**(5): 3230-3241.

Barber-Rotenberg, J. S., S. P. Selvanathan, Y. Kong, H. V. Erkizan, T. M. Snyder, S. P. Hong, C. L. Kobs, N. L. South, S. Summer, P. J. Monroe, M. Chruszcz, V. Dobrev, P. N. Tosso, L. J. Scher, W. Minor, M. L. Brown, S. J. Metallo, A. Uren and J. A. Toretsky (2012). "Single enantiomer of YK-4-279 demonstrates specificity in targeting the oncogene EWS-FLI1." Oncotarget **3**(2): 172-182.

Barretina, J., G. Caponigro, N. Stransky, K. Venkatesan, A. A. Margolin, S. Kim, C. J. Wilson, J. Lehar, G. V. Kryukov, D. Sonkin, A. Reddy, M. Liu, L. Murray, M. F. Berger, J. E. Monahan, P. Morais, J. Meltzer, A. Korejwa, J. Jane-Valbuena, F. A. Mapa, J. Thibault, E. Bric-Furlong, P. Raman, A. Shipway, I. H. Engels, J. Cheng, G. K. Yu, J. Yu, P. Aspesi, Jr., M. de Silva, K. Jagtap, M. D. Jones, L. Wang, C. Hatton, E. Palescandolo, S. Gupta, S. Mahan, C. Sougnez, R. C. Onofrio, T. Liefeld, L. MacConaill, W. Winckler, M. Reich, N. Li, J. P. Mesirov, S. B. Gabriel, G. Getz, K. Ardlie, V. Chan, V. E. Myer, B. L. Weber, J. Porter, M. Warmuth, P. Finan, J. L. Harris, M. Meyerson, T. R. Golub, M. P. Morrissey, W. R. Sellers, R. Schlegel and L. A. Garraway (2012). "The Cancer Cell Line Encyclopedia enables predictive modelling of anticancer drug sensitivity." Nature **483**(7391): 603-607.

Baruchel, S., A. Pappo, M. Krailo, K. S. Baker, B. Wu, D. Villaluna, M. Lee-Scott, P. C. Adamson and S. M. Blaney (2012). "A phase 2 trial of trabectedin in children with recurrent rhabdomyosarcoma, Ewing sarcoma and non-rhabdomyosarcoma soft tissue sarcomas: a report from the Children's Oncology Group." Eur J Cancer **48**(4): 579-585.

Basson, M. A., S. Akbulut, J. Watson-Johnson, R. Simon, T. J. Carroll, R. Shakya, I. Gross, G. R. Martin, T. Lufkin, A. P. McMahon, P. D. Wilson, F. D. Costantini, I. J. Mason and J. D. Licht (2005). "Sprouty1 is a critical regulator of GDNF/RET-mediated kidney induction." Dev Cell **8**(2): 229-239.

Basson, M. A., J. Watson-Johnson, R. Shakya, S. Akbulut, D. Hyink, F. D. Costantini, P. D. Wilson, I. J. Mason and J. D. Licht (2006). "Branching morphogenesis of the ureteric epithelium during kidney development is coordinated by the opposing functions of GDNF and Sprouty1." Dev Biol **299**(2): 466-477.

Bastida, E., J. del Prado, L. Almirall, G. A. Jamieson and A. Ordinas (1985). "Inhibitory effects of dipyridamole on growth, nucleoside incorporation, and platelet-activating capability in the U87MG and SKNMC human tumor cell lines." Cancer Res **45**(9): 4048-4052.

Beck, R., M. J. Monument, W. S. Watkins, R. Smith, K. M. Boucher, J. D. Schiffman, L. B. Jorde, R. L. Randall and S. L. Lessnick (2012). "EWS/FLI-responsive GGAA microsatellites exhibit polymorphic differences between European and African populations." Cancer Genet **205**(6): 304-312.

Benini, S., M. C. Manara, N. Baldini, V. Cerisano, S. Massimo, M. Mercuri, P. L. Lollini, P. Nanni, P. Picci and K. Scotlandi (2001). "Inhibition of insulin-like growth factor I receptor increases the antitumor activity of doxorubicin and vincristine against Ewing's sarcoma cells." Clin Cancer Res **7**(6): 1790-1797.

Biedler, J. L., S. Roffler-Tarlov, M. Schachner and L. S. Freedman (1978). "Multiple neurotransmitter synthesis by human neuroblastoma cell lines and clones." Cancer Res **38**(11 Pt 1): 3751-3757.

Bigot, A., W. J. Duddy, Z. G. Ouandaogo, E. Negroni, V. Mariot, S. Ghimbovschi, B. Harmon, A. Wielgosik, C. Loiseau, J. Devaney, J. Dumonceaux, G. Butler-Browne, V. Mouly and S. Duguez (2015). "Age-Associated Methylation Suppresses SPRY1, Leading to a Failure of Re-quiescence and Loss of the Reserve Stem Cell Pool in Elderly Muscle." Cell Rep **13**(6): 1172-1182.

Bilke, S., R. Schwentner, F. Yang, M. Kauer, G. Jug, R. L. Walker, S. Davis, Y. J. Zhu, M. Pineda, P. S. Meltzer and H. Kovar (2013). "Oncogenic ETS fusions deregulate E2F3 target genes in Ewing sarcoma and prostate cancer." Genome Res **23**(11): 1797-1809.

Bottcher, R. T. and C. Niehrs (2005). "Fibroblast growth factor signaling during early vertebrate development." Endocr Rev **26**(1): 63-77.

Brodeur, G. M., G. Sekhon and M. N. Goldstein (1977). "Chromosomal aberrations in human neuroblastomas." Cancer **40**(5): 2256-2263.

Carrillo, J., N. Agra, N. Fernandez, A. Pestana and J. Alonso (2009). "Devazepide, a nonpeptide antagonist of CCK receptors, induces apoptosis and inhibits Ewing tumor growth." Anticancer Drugs **20**(7): 527-533.

Carrillo, J., E. Garcia-Aragoncillo, D. Azorin, N. Agra, A. Sastre, I. Gonzalez-Mediero, P. Garcia-Miguel, A. Pestana, S. Gallego, D. Segura and J. Alonso (2007). "Cholecystokinin down-regulation by RNA interference impairs Ewing tumor growth." Clin Cancer Res **13**(8): 2429-2440.

Casci, T., J. Vinos and M. Freeman (1999). "Sprouty, an intracellular inhibitor of Ras signaling." Cell **96**(5): 655-665.

Cavazzana, A. O., J. S. Miser, J. Jefferson and T. J. Triche (1987). "Experimental evidence for a neural origin of Ewing's sarcoma of bone." Am J Pathol **127**(3): 507-518.

Cidre-Aranaz, F. and J. Alonso (2015). "EWS/FLI1 Target Genes and Therapeutic Opportunities in Ewing Sarcoma." Front Oncol **5**: 162.

Cidre-Aranaz, F., T. G. Grunewald, D. Surdez, L. Garcia-Garcia, J. Carlos Lazaro, T. Kirchner, L. Gonzalez-Gonzalez, A. Sastre, P. Garcia-Miguel, S. E. Lopez-Perez, S. Monzon, O. Delattre and J. Alonso (2016). "EWS-FLI1-mediated suppression of the RAS-antagonist Sprouty 1 (SPRY1) confers aggressiveness to Ewing sarcoma." Oncogene.

Collins, S., A. Waickman, A. Basson, A. Kupfer, J. D. Licht, M. R. Horton and J. D. Powell (2012). "Regulation of CD4(+) and CD8(+) effector responses by Sprouty-1." PLoS One **7**(11): e49801.

Chambers, D. and I. Mason (2000). "Expression of sprouty2 during early development of the chick embryo is coincident with known sites of FGF signalling." Mech Dev **91**(1-2): 361-364.

Chaturvedi, A., L. M. Hoffman, C. C. Jensen, Y. C. Lin, A. H. Grossmann, R. L. Randall, S. L. Lessnick, A. L. Welm and M. C. Beckerle (2014). "Molecular dissection of the mechanism by which EWS/FLI expression compromises actin cytoskeletal integrity and cell adhesion in Ewing sarcoma." Mol Biol Cell **25**(18): 2695-2709.

Ching, S. T., G. R. Cunha, L. S. Baskin, M. A. Basson and O. D. Klein (2014). "Coordinated activity of Spry1 and Spry2 is required for normal development of the external genitalia." Dev Biol **386**(1): 1-11.

Choi, H., S. Y. Cho, R. H. Schwartz and K. Choi (2006). "Dual effects of Sprouty1 on TCR signaling depending on the differentiation state of the T cell." J Immunol **176**(10): 6034-6045.

Christofori, G. (2003). "Split personalities: the agonistic antagonist Sprouty." Nat Cell Biol **5**(5): 377-379.

Dauphinot, L., C. De Oliveira, T. Melot, N. Sevenet, V. Thomas, B. E. Weissman and O. Delattre (2001). "Analysis of the expression of cell cycle regulators in Ewing cell

lines: EWS-FLI-1 modulates p57KIP2and c-Myc expression." Oncogene **20**(25): 3258-3265.

de Maximy, A. A., Y. Nakatake, S. Moncada, N. Itoh, J. P. Thiery and S. Bellusci (1999). "Cloning and expression pattern of a mouse homologue of drosophila sprouty in the mouse embryo." Mech Dev **81**(1-2): 213-216.

Delattre, O., J. Zucman, B. Plougastel, C. Desmaze, T. Melot, M. Peter, H. Kovar, I. Joubert, P. de Jong, G. Rouleau and *et al.* (1992). "Gene fusion with an ETS DNA-binding domain caused by chromosome translocation in human tumours." Nature **359**(6391): 162-165.

Donaldson, L. W., J. M. Petersen, B. J. Graves and L. P. McIntosh (1994). "Secondary structure of the ETS domain places murine Ets-1 in the superfamily of winged helix-turn-helix DNA-binding proteins." Biochemistry **33**(46): 13509-13516.

Edwards, R. H., J. Chatten, Q. B. Xiong and F. G. Barr (1997). "Detection of gene fusions in rhabdomyosarcoma by reverse transcriptase-polymerase chain reaction assay of archival samples." Diagn Mol Pathol **6**(2): 91-97.

Erkizan, H. V., V. N. Uversky and J. A. Toretsky (2010). "Oncogenic partnerships: EWS-FLI1 protein interactions initiate key pathways of Ewing's sarcoma." Clin Cancer Res **16**(16): 4077-4083.

Esiashvili, N., M. Goodman and R. B. Marcus, Jr. (2008). "Changes in incidence and survival of Ewing sarcoma patients over the past 3 decades: Surveillance Epidemiology and End Results data." J Pediatr Hematol Oncol **30**(6): 425-430.

Faedo, A., U. Borello and J. L. Rubenstein (2010). "Repression of Fgf signaling by sprouty1-2 regulates cortical patterning in two distinct regions and times." J Neurosci **30**(11): 4015-4023.

Faratian, D., A. H. Sims, P. Mullen, C. Kay, I. Um, S. P. Langdon and D. J. Harrison (2011). "Sprouty 2 is an independent prognostic factor in breast cancer and may be useful in stratifying patients for trastuzumab therapy." PLoS One **6**(8): e23772.

Fogh, J., W. C. Wright and J. D. Loveless (1977). "Absence of HeLa cell contamination in 169 cell lines derived from human tumors." J Natl Cancer Inst **58**(2): 209-214.

Folpe, A. L., C. E. Hill, D. M. Parham, P. A. O'Shea and S. W. Weiss (2000). "Immunohistochemical detection of FLI-1 protein expression: a study of 132 round cell tumors with emphasis on CD99-positive mimics of Ewing's sarcoma/primitive neuroectodermal tumor." Am J Surg Pathol **24**(12): 1657-1662.

Fritzsche, S., M. Kenzelmann, M. J. Hoffmann, M. Muller, R. Engers, H. J. Grone and W. A. Schulz (2006). "Concomitant down-regulation of SPRY1 and SPRY2 in prostate carcinoma." Endocr Relat Cancer **13**(3): 839-849.

Frolik, C. A., P. P. Roller, J. L. Cone, L. L. Dart, D. M. Smith and M. B. Sporn (1984). "Inhibition of transforming growth factor-induced cell growth in soft agar by oxidized polyamines." Arch Biochem Biophys **230**(1): 93-102.

Gangwal, K., D. Close, C. A. Enriquez, C. P. Hill and S. L. Lessnick (2010). "Emergent Properties of EWS/FLI Regulation via GGAA Microsatellites in Ewing's Sarcoma." Genes Cancer **1**(2): 177-187.

Gangwal, K., S. Sankar, P. C. Hollenhorst, M. Kinsey, S. C. Haroldsen, A. A. Shah, K. M. Boucher, W. S. Watkins, L. B. Jorde, B. J. Graves and S. L. Lessnick (2008). "Microsatellites as EWS/FLI response elements in Ewing's sarcoma." Proc Natl Acad Sci U S A **105**(29): 10149-10154.

Garcia-Aragoncillo, E., J. Carrillo, E. Lalli, N. Agra, G. Gomez-Lopez, A. Pestana and J. Alonso (2008). "DAX1, a direct target of EWS/FLI1 oncoprotein, is a principal regulator of cell-cycle progression in Ewing's tumor cells." Oncogene **27**(46): 6034-6043.

Gartel, A. L. (2011). "Thiostrepton, proteasome inhibitors and FOXM1." Cell Cycle **10**(24): 4341-4342.

Gaspar, N., D. S. Hawkins, U. Dirksen, I. J. Lewis, S. Ferrari, M. C. Le Deley, H. Kovar, R. Grimer, J. Whelan, L. Claude, O. Delattre, M. Paulussen, P. Picci, K. Sundby Hall, H. van den Berg, R. Ladenstein, J. Michon, L. Hjorth, I. Judson, R. Luksch, M. L. Bernstein, P. Marec-Berard, B. Brennan, A. W. Craft, R. B. Womer, H. Juergens and O. Oberlin (2015). "Ewing Sarcoma: Current Management and Future Approaches Through Collaboration." J Clin Oncol **33**(27): 3036-3046.

Ginsberg, J. P., E. de Alava, M. Ladanyi, L. H. Wexler, H. Kovar, M. Paulussen, A. Zoubek, B. Dockhorn-Dworniczak, H. Juergens, J. S. Wunder, I. L. Andrulis, R. Malik, P. H. Sorensen, R. B. Womer and F. G. Barr (1999). "EWS-FLI1 and EWS-ERG gene fusions are associated with similar clinical phenotypes in Ewing's sarcoma." J Clin Oncol **17**(6): 1809-1814.

Giovanini, M. A., T. A. Eskin, S. K. Mukherji and J. P. Mickle (1994). "Granulomatous angiitis of the spinal cord: a case report." Neurosurgery **34**(3): 540-543.

Girnita, L., A. Girnita, M. Wang, J. M. Meis-Kindblom, L. G. Kindblom and O. Larsson (2000). "A link between basic fibroblast growth factor (bFGF) and EWS/FLI-1 in Ewing's sarcoma cells." Oncogene **19**(37): 4298-4301.

Grier, H. E. (1997). "The Ewing family of tumors. Ewing's sarcoma and primitive neuroectodermal tumors." Pediatr Clin North Am **44**(4): 991-1004.

Grohar, P. J., L. B. Griffin, C. Yeung, Q. R. Chen, Y. Pommier, C. Khanna, J. Khan and L. J. Helman (2011). "Ecteinascidin 743 interferes with the activity of EWS-FLI1 in Ewing sarcoma cells." Neoplasia **13**(2): 145-153.

Grohar, P. J. and L. J. Helman (2013). "Prospects and challenges for the development of new therapies for Ewing sarcoma." Pharmacol Ther **137**(2): 216-224.

Grohar, P. J., S. Kim, G. O. Rangel Rivera, N. Sen, S. Haddock, M. L. Harlow, N. K. Maloney, J. Zhu, M. O'Neill, T. L. Jones, K. Huppi, M. Grandin, K. Gehlhaus, C. A. Klumpp-Thomas, E. Buehler, L. J. Helman, S. E. Martin and N. J. Caplen (2016). "Functional Genomic Screening Reveals Splicing of the EWS-FLI1 Fusion Transcript as a Vulnerability in Ewing Sarcoma." Cell Rep **14**(3): 598-610.

Gross, I., B. Bassit, M. Benezra and J. D. Licht (2001). "Mammalian sprouty proteins inhibit cell growth and differentiation by preventing ras activation." J Biol Chem **276**(49): 46460-46468.

Gross, I., D. J. Morrison, D. P. Hyink, K. Georgas, M. A. English, M. Mericskay, S. Hosono, D. Sassoon, P. D. Wilson, M. Little and J. D. Licht (2003). "The receptor tyrosine kinase regulator Sprouty1 is a target of the tumor suppressor WT1 and important for kidney development." J Biol Chem **278**(42): 41420-41430.

Grunewald, T. G., V. Bernard, P. Gilardi-Hebenstreit, V. Raynal, D. Surdez, M. M. Aynaud, O. Mirabeau, F. Cidre-Aranaz, F. Tirode, S. Zaidi, G. Perot, A. H. Jonker, C. Lucchesi, M. C. Le Deley, O. Oberlin, P. Marec-Berard, A. S. Veron, S. Reynaud, E. Lapouble, V. Boeva, T. Rio Frio, J. Alonso, S. Bhatia, G. Pierron, G. Cancel-Tassin, O. Cussenot, D. G. Cox, L. M. Morton, M. J. Machiela, S. J. Chanock, P. Charnay and O. Delattre (2015). "Chimeric EWSR1-FLI1 regulates the Ewing sarcoma susceptibility gene EGR2 via a GGAA microsatellite." Nat Genet **47**(9): 1073-1078.

Grunewald, T. G., I. Diebold, I. Esposito, S. Plehm, K. Hauer, U. Thiel, P. da Silva-Buttkus, F. Neff, R. Unland, C. Muller-Tidow, C. Zobywalski, K. Lohrig, U. Lewandrowski, A. Sickmann, O. Prazeres da Costa, A. Gorlach, A. Cossarizza, E. Butt, G. H. Richter and S. Burdach (2012). "STEAP1 is associated with the invasive and oxidative stress phenotype of Ewing tumors." Mol Cancer Res **10**(1): 52-65.

Guagnano, V., P. Furet, C. Spanka, V. Bordas, M. Le Douget, C. Stamm, J. Brueggen, M. R. Jensen, C. Schnell, H. Schmid, M. Wartmann, J. Berghausen, P. Drueckes, A. Zimmerlin, D. Bussiere, J. Murray and D. Graus Porta (2011). "Discovery of 3-(2,6-dichloro-3,5-dimethoxy-phenyl)-1-{6-[4-(4-ethyl-piperazin-1-yl)-phenylamin o]-pyrimidin-4-yl}-1-methyl-urea (NVP-BGJ398), a potent and selective inhibitor of the fibroblast growth factor receptor family of receptor tyrosine kinase." J Med Chem **54**(20): 7066-7083.

Guillon, N., F. Tirode, V. Boeva, A. Zynovyev, E. Barillot and O. Delattre (2009). "The oncogenic EWS-FLI1 protein binds in vivo GGAA microsatellite sequences with potential transcriptional activation function." PLoS One **4**(3): e4932.

Guy, G. R., R. A. Jackson, P. Yusoff and S. Y. Chow (2009). "Sprouty proteins: modified modulators, matchmakers or missing links?" J Endocrinol **203**(2): 191-202.

Hacohen, N., S. Kramer, D. Sutherland, Y. Hiromi and M. A. Krasnow (1998). "sprouty encodes a novel antagonist of FGF signaling that patterns apical branching of the Drosophila airways." Cell **92**(2): 253-263.

Hahm, K. B., K. Cho, C. Lee, Y. H. Im, J. Chang, S. G. Choi, P. H. Sorensen, C. J. Thiele and S. J. Kim (1999). "Repression of the gene encoding the TGF-beta type II receptor is a major target of the EWS-FLI1 oncoprotein." Nat Genet **23**(2): 222-227.

Hamilton, S. N., R. Carlson, H. Hasan, S. R. Rassekh and K. Goddard (2015). "Long-term Outcomes and Complications in Pediatric Ewing Sarcoma." Am J Clin Oncol.

Hanafusa, H., S. Torii, T. Yasunaga and E. Nishida (2002). "Sprouty1 and Sprouty2 provide a control mechanism for the Ras/MAPK signalling pathway." Nat Cell Biol **4**(11): 850-858.

Hattinger, C. M., S. Rumpler, S. Strehl, I. M. Ambros, A. Zoubek, U. Potschger, H. Gadner and P. F. Ambros (1999). "Prognostic impact of deletions at 1p36 and numerical aberrations in Ewing tumors." Genes Chromosomes Cancer **24**(3): 243-254.

Herrero-Martin, D., D. Osuna, J. L. Ordonez, V. Sevillano, A. S. Martins, C. Mackintosh, M. Campos, J. Madoz-Gurpide, A. P. Otero-Motta, G. Caballero, A. T. Amaral, D. H. Wai, Y. Braun, M. Eisenacher, K. L. Schaefer, C. Poremba and E. de Alava (2009). "Stable interference of EWS-FLI1 in an Ewing sarcoma cell line impairs IGF-1/IGF-1R signalling and reveals TOPK as a new target." Br J Cancer **101**(1): 80-90.

Hibshoosh, H. and R. Lattes (1997). "Immunohistochemical and molecular genetic approaches to soft tissue tumor diagnosis: a primer." Semin Oncol **24**(5): 515-525.

Hu-Lieskovan, S., J. D. Heidel, D. W. Bartlett, M. E. Davis and T. J. Triche (2005). "Sequence-specific knockdown of EWS-FLI1 by targeted, nonviral delivery of small interfering RNA inhibits tumor growth in a murine model of metastatic Ewing's sarcoma." Cancer Res **65**(19): 8984-8992.

Hubbard, S. R. and W. T. Miller (2007). "Receptor tyrosine kinases: mechanisms of activation and signaling." Curr Opin Cell Biol **19**(2): 117-123.

Jackson, T. M., M. Bittman and L. Granowetter (2016). "Pediatric Malignant Bone Tumors: A Review and Update on Current Challenges, and Emerging Drug Targets." Curr Probl Pediatr Adolesc Health Care.

Jaishankar, S., J. Zhang, M. F. Roussel and S. J. Baker (1999). "Transforming activity of EWS/FLI is not strictly dependent upon DNA-binding activity." Oncogene **18**(40): 5592-5597.

Jeon, I. S., J. N. Davis, B. S. Braun, J. E. Sublett, M. F. Roussel, C. T. Denny and D. N. Shapiro (1995). "A variant Ewing's sarcoma translocation (7;22) fuses the EWS gene to the ETS gene ETV1." Oncogene **10**(6): 1229-1234.

Kamura, S., Y. Matsumoto, J. I. Fukushi, T. Fujiwara, K. Iida, Y. Okada and Y. Iwamoto (2010). "Basic fibroblast growth factor in the bone microenvironment enhances cell motility and invasion of Ewing's sarcoma family of tumours by activating the FGFR1-PI3K-Rac1 pathway." Br J Cancer **103**(3): 370-381.

Kaneko, Y., H. Kobayashi, M. Handa, N. Satake and N. Maseki (1997). "EWS-ERG fusion transcript produced by chromosomal insertion in a Ewing sarcoma." Genes Chromosomes Cancer **18**(3): 228-231.

Karnieli, E., H. Werner, F. J. Rauscher, 3rd, L. E. Benjamin and D. LeRoith (1996). "The IGF-I receptor gene promoter is a molecular target for the Ewing's sarcoma-Wilms' tumor 1 fusion protein." J Biol Chem **271**(32): 19304-19309.

Khoury, J. D. (2005). "Ewing sarcoma family of tumors." Adv Anat Pathol **12**(4): 212-220.

Kim, G. E., B. Beach, J. M. Gastier-Foster, J. L. Murata-Collins, J. M. Rowland, R. J. O'Donnell and R. E. Goldsby (2005). "Ewing sarcoma as a second malignant neoplasm after acute lymphoblastic leukemia." Pediatr Blood Cancer **45**(1): 57-59.

Kim, S., C. T. Denny and R. Wisdom (2006). "Cooperative DNA binding with AP-1 proteins is required for transformation by EWS-Ets fusion proteins." Mol Cell Biol **26**(7): 2467-2478.

Klein, O. D., G. Minowada, R. Peterkova, A. Kangas, B. D. Yu, H. Lesot, M. Peterka, J. Jernvall and G. R. Martin (2006). "Sprouty genes control diastema tooth development via bidirectional antagonism of epithelial-mesenchymal FGF signaling." Dev Cell **11**(2): 181-190.

Kolb, E. A., R. Gorlick, P. J. Houghton, C. L. Morton, R. Lock, H. Carol, C. P. Reynolds, J. M. Maris, S. T. Keir, C. A. Billups and M. A. Smith (2008). "Initial testing (stage 1) of a monoclonal antibody (SCH 717454) against the IGF-1 receptor by the pediatric preclinical testing program." Pediatr Blood Cancer **50**(6): 1190-1197.

Kovar, H. (2014). "Blocking the road, stopping the engine or killing the driver? Advances in targeting EWS/FLI-1 fusion in Ewing sarcoma as novel therapy." Expert Opin Ther Targets **18**(11): 1315-1328.

Kovar, H., J. Amatruda, E. Brunet, S. Burdach, F. Cidre-Aranaz, E. de Alava, U. Dirksen, W. van der Ent, P. Grohar, T. G. Grunewald, L. Helman, P. Houghton, K. Iljin, E. Korsching, M. Ladanyi, E. Lawlor, S. Lessnick, J. Ludwig, P. Meltzer, M. Metzler, J. Mora, R. Moriggl, T. Nakamura, T. Papamarkou, B. Radic Sarikas, F. Redini, G. H. Richter, C. Rossig, K. Schadler, B. W. Schafer, K. Scotlandi, N. C. Sheffield, A. Shelat, E. Snaar-Jagalska, P. Sorensen, K. Stegmaier, E. Stewart, A. Sweet-Cordero, K. Szuhai, O. M. Tirado, F. Tirode, J. Toretsky, K. Tsafou, A. Uren, A. Zinovyev and O. Delattre (2016). "The second European interdisciplinary Ewing sarcoma research summit - A joint effort to deconstructing the multiple layers of a complex disease." Oncotarget **7**(8): 8613-8624.

Kovar, H., D. N. Aryee, G. Jug, C. Henockl, M. Schemper, O. Delattre, G. Thomas and H. Gadner (1996). "EWS/FLI-1 antagonists induce growth inhibition of Ewing tumor cells in vitro." Cell Growth Differ **7**(4): 429-437.

Kovar, H., M. Dworzak, S. Strehl, E. Schnell, I. M. Ambros, P. F. Ambros and H. Gadner (1990). "Overexpression of the pseudoautosomal gene MIC2 in Ewing's sarcoma and peripheral primitive neuroectodermal tumor." Oncogene **5**(7): 1067-1070.

Kovar, H., G. Jug, D. N. Aryee, A. Zoubek, P. Ambros, B. Gruber, R. Windhager and H. Gadner (1997). "Among genes involved in the RB dependent cell cycle regulatory cascade, the p16 tumor suppressor gene is frequently lost in the Ewing family of tumors." Oncogene **15**(18): 2225-2232.

Kovar, H., S. Pospisilova, G. Jug, D. Printz and H. Gadner (2003). "Response of Ewing tumor cells to forced and activated p53 expression." Oncogene **22**(21): 3193-3204.

Kuracha, M. R., D. Burgess, E. Siefker, J. T. Cooper, J. D. Licht, M. L. Robinson and V. Govindarajan (2011). "Spry1 and Spry2 are necessary for lens vesicle separation and corneal differentiation." Invest Ophthalmol Vis Sci **52**(9): 6887-6897.

Kuracha, M. R., E. Siefker, J. D. Licht and V. Govindarajan (2013). "Spry1 and Spry2 are necessary for eyelid closure." Dev Biol **383**(2): 227-238.

Kwabi-Addo, B., C. Ren and M. Ittmann (2009). "DNA methylation and aberrant expression of Sprouty1 in human prostate cancer." Epigenetics **4**(1): 54-61.

Kwabi-Addo, B., J. Wang, H. Erdem, A. Vaid, P. Castro, G. Ayala and M. Ittmann (2004). "The expression of Sprouty1, an inhibitor of fibroblast growth factor signal transduction, is decreased in human prostate cancer." Cancer Res **64**(14): 4728-4735.

Lambert, G., J. R. Bertrand, E. Fattal, F. Subra, H. Pinto-Alphandary, C. Malvy, C. Auclair and P. Couvreur (2000). "EWS fli-1 antisense nanocapsules inhibits ewing sarcoma-related tumor in mice." Biochem Biophys Res Commun **279**(2): 401-406.

Leavey, P. J. and A. B. Collier (2008). "Ewing sarcoma: prognostic criteria, outcomes and future treatment." Expert Rev Anticancer Ther **8**(4): 617-624.

Lee, S., T. M. Bui Nguyen, D. Kovalenko, N. Adhikari, S. Grindle, S. P. Polster, R. Friesel, S. Ramakrishnan and J. L. Hall (2010). "Sprouty1 inhibits angiogenesis in association with up-regulation of p21 and p27." Mol Cell Biochem **338**(1-2): 255-261.

Lemmon, M. A. and J. Schlessinger (2010). "Cell signaling by receptor tyrosine kinases." Cell **141**(7): 1117-1134.

Lessnick, S. L., B. S. Braun, C. T. Denny and W. A. May (1995). "Multiple domains mediate transformation by the Ewing's sarcoma EWS/FLI-1 fusion gene." Oncogene **10**(3): 423-431.

Lessnick, S. L. and M. Ladanyi (2012). "Molecular pathogenesis of Ewing sarcoma: new therapeutic and transcriptional targets." Annu Rev Pathol **7**: 145-159.

Li, E. and K. Hristova (2006). "Role of receptor tyrosine kinase transmembrane domains in cell signaling and human pathologies." Biochemistry **45**(20): 6241-6251.

Li, X., V. G. Brunton, H. R. Burgar, L. M. Wheldon and J. K. Heath (2004). "FRS2-dependent SRC activation is required for fibroblast growth factor receptor-induced phosphorylation of Sprouty and suppression of ERK activity." J Cell Sci **117**(Pt 25): 6007-6017.

Lim, J., E. S. Wong, S. H. Ong, P. Yusoff, B. C. Low and G. R. Guy (2000). "Sprouty proteins are targeted to membrane ruffles upon growth factor receptor tyrosine kinase activation. Identification of a novel translocation domain." J Biol Chem **275**(42): 32837-32845.

Liu, X., Y. Lan, D. Zhang, K. Wang, Y. Wang and Z. C. Hua (2014). "SPRY1 promotes the degradation of uPAR and inhibits uPAR-mediated cell adhesion and proliferation." Am J Cancer Res **4**(6): 683-697.

Liu, Z., X. Liu, W. Cao and Z. C. Hua (2015). "Tumor-specifically hypoxia-induced therapy of SPRY1/2 displayed differential therapeutic efficacy for melanoma." Am J Cancer Res **5**(2): 792-801.

Livak KJ, Schmittgen TD (2001). "Analysis of relative gene expression data using real-time quantitative PCR and the 2(-Delta Delta C(T)) Method." Methods **25**(4):402-8.

Lo, T. L., P. Yusoff, C. W. Fong, K. Guo, B. J. McCaw, W. A. Phillips, H. Yang, E. S. Wong, H. F. Leong, Q. Zeng, T. C. Putti and G. R. Guy (2004). "The ras/mitogen-activated protein kinase pathway inhibitor and likely tumor suppressor proteins, sprouty 1 and sprouty 2 are deregulated in breast cancer." Cancer Res **64**(17): 6127-6136.

Long, J., Y. Wang, W. Wang, B. H. Chang and F. R. Danesh (2011). "MicroRNA-29c is a signature microRNA under high glucose conditions that targets Sprouty homolog 1, and its in vivo knockdown prevents progression of diabetic nephropathy." J Biol Chem **286**(13): 11837-11848.

Low, H. B. and Y. Zhang (2016). "Regulatory Roles of MAPK Phosphatases in Cancer." Immune Netw **16**(2): 85-98.

Macia, A., P. Gallel, M. Vaquero, M. Gou-Fabregas, M. Santacana, A. Maliszewska, M. Robledo, J. R. Gardiner, M. A. Basson, X. Matias-Guiu and M. Encinas (2012). "Sprouty1 is a candidate tumor-suppressor gene in medullary thyroid carcinoma." Oncogene **31**(35): 3961-3972.

Macia, A., M. Vaquero, M. Gou-Fabregas, E. Castelblanco, J. M. Valdivielso, C. Anerillas, D. Mauricio, X. Matias-Guiu, J. Ribera and M. Encinas (2014). "Sprouty1 induces a senescence-associated secretory phenotype by regulating NFkappaB activity: implications for tumorigenesis." Cell Death Differ **21**(2): 333-343.

Mackintosh, C., J. L. Ordonez, D. J. Garcia-Dominguez, V. Sevillano, A. Llombart-Bosch, K. Szuhai, K. Scotlandi, M. Alberghini, R. Sciot, F. Sinnaeve, P. C. Hogendoorn, P. Picci, S. Knuutila, U. Dirksen, M. Debiec-Rychter, K. L. Schaefer and E. de Alava (2012). "1q gain and CDT2 overexpression underlie an aggressive and highly proliferative form of Ewing sarcoma." Oncogene **31**(10): 1287-1298.

Mahoney Rogers, A. A., J. Zhang and K. Shim (2011). "Sprouty1 and Sprouty2 limit both the size of the otic placode and hindbrain Wnt8a by antagonizing FGF signaling." Dev Biol **353**(1): 94-104.

Manara, M. C., L. Landuzzi, P. Nanni, G. Nicoletti, D. Zambelli, P. L. Lollini, C. Nanni, F. Hofmann, C. Garcia-Echeverria, P. Picci and K. Scotlandi (2007). "Preclinical in vivo study of new insulin-like growth factor-I receptor--specific inhibitor in Ewing's sarcoma." Clin Cancer Res **13**(4): 1322-1330.

Mao, X., S. Miesfeldt, H. Yang, J. M. Leiden and C. B. Thompson (1994). "The FLI-1 and chimeric EWS-FLI-1 oncoproteins display similar DNA binding specificities." J Biol Chem **269**(27): 18216-18222.

Martins, A. S., C. Mackintosh, D. H. Martin, M. Campos, T. Hernandez, J. L. Ordonez and E. de Alava (2006). "Insulin-like growth factor I receptor pathway inhibition by ADW742, alone or in combination with imatinib, doxorubicin, or vincristine, is a novel therapeutic approach in Ewing tumor." Clin Cancer Res **12**(11 Pt 1): 3532-3540.

Mason, J. M., D. J. Morrison, B. Bassit, M. Dimri, H. Band, J. D. Licht and I. Gross (2004). "Tyrosine phosphorylation of Sprouty proteins regulates their ability to inhibit growth factor signaling: a dual feedback loop." Mol Biol Cell **15**(5): 2176-2188.

Masoumi-Moghaddam, S., A. Amini, A. Ehteda, A. Q. Wei and D. L. Morris (2014a). "The expression of the Sprouty 1 protein inversely correlates with growth, proliferation, migration and invasion of ovarian cancer cells." J Ovarian Res **7**: 61.

Masoumi-Moghaddam, S., A. Amini and D. L. Morris (2014b). "The developing story of Sprouty and cancer." Cancer Metastasis Rev **33**(2-3): 695-720.

Masoumi-Moghaddam, S., A. Amini, A. Q. Wei, G. Robertson and D. L. Morris (2015). "Sprouty 1 predicts prognosis in human epithelial ovarian cancer." Am J Cancer Res **5**(4): 1531-1541.

May, W. A., M. L. Gishizky, S. L. Lessnick, L. B. Lunsford, B. C. Lewis, O. Delattre, J. Zucman, G. Thomas and C. T. Denny (1993a). "Ewing sarcoma 11;22 translocation produces a chimeric transcription factor that requires the DNA-binding domain encoded by FLI1 for transformation." Proc Natl Acad Sci U S A **90**(12): 5752-5756.

May, W. A., S. L. Lessnick, B. S. Braun, M. Klemsz, B. C. Lewis, L. B. Lunsford, R. Hromas and C. T. Denny (1993b). "The Ewing's sarcoma EWS/FLI-1 fusion gene encodes a more potent transcriptional activator and is a more powerful transforming gene than FLI-1." Mol Cell Biol **13**(12): 7393-7398.

Meier, F., U. Caroli, K. Satyamoorthy, B. Schittek, J. Bauer, C. Berking, H. Moller, E. Maczey, G. Rassner, M. Herlyn and C. Garbe (2003). "Fibroblast growth factor-2 but not Mel-CAM and/or beta3 integrin promotes progression of melanocytes to melanoma." Exp Dermatol **12**(3): 296-306.

Mekkawy, A. H. and D. L. Morris (2013). "Human sprouty1 suppresses urokinase receptor-stimulated cell migration and invasion." ISRN Biochem **2013**: 598251.

Mekkawy, A. H., M. H. Pourgholami and D. L. Morris (2014). "Human Sprouty1 suppresses growth, migration, and invasion in human breast cancer cells." Tumour Biol **35**(5): 5037-5048.

Mendiola, M., J. Carrillo, E. Garcia, E. Lalli, T. Hernandez, E. de Alava, F. Tirode, O. Delattre, P. Garcia-Miguel, F. Lopez-Barea, A. Pestana and J. Alonso (2006). "The orphan nuclear receptor DAX1 is up-regulated by the EWS/FLI1 oncoprotein and is highly expressed in Ewing tumors." Int J Cancer **118**(6): 1381-1389.

Minowada, G., L. A. Jarvis, C. L. Chi, A. Neubuser, X. Sun, N. Hacohen, M. A. Krasnow and G. R. Martin (1999). "Vertebrate Sprouty genes are induced by FGF signaling and can cause chondrodysplasia when overexpressed." Development **126**(20): 4465-4475.

Mitsiades, C. S., N. Mitsiades and M. Koutsilieris (2004). "The Akt pathway: molecular targets for anti-cancer drug development." Curr Cancer Drug Targets **4**(3): 235-256.

Miyagawa, Y., H. Okita, H. Nakaijima, Y. Horiuchi, B. Sato, T. Taguchi, M. Toyoda, Y. U. Katagiri, J. Fujimoto, J. Hata, A. Umezawa and N. Kiyokawa (2008). "Inducible expression of chimeric EWS/ETS proteins confers Ewing's family tumor-like phenotypes to human mesenchymal progenitor cells." Mol Cell Biol **28**(7): 2125-2137.

Miyoshi, K., T. Wakioka, H. Nishinakamura, M. Kamio, L. Yang, M. Inoue, M. Hasegawa, Y. Yonemitsu, S. Komiya and A. Yoshimura (2004). "The Sprouty-related protein, Spred, inhibits cell motility, metastasis, and Rho-mediated actin reorganization." Oncogene **23**(33): 5567-5576.

Moghaddam, S. M., A. Amini, A. Q. Wei, M. H. Pourgholami and D. L. Morris (2012). "Initial report on differential expression of sprouty proteins 1 and 2 in human epithelial ovarian cancer cell lines." J Oncol **2012**: 373826.

Mohammadi, M., S. Froum, J. M. Hamby, M. C. Schroeder, R. L. Panek, G. H. Lu, A. V. Eliseenkova, D. Green, J. Schlessinger and S. R. Hubbard (1998). "Crystal structure of an angiogenesis inhibitor bound to the FGF receptor tyrosine kinase domain." EMBO J **17**(20): 5896-5904.

Naing, A., P. LoRusso, S. Fu, D. S. Hong, P. Anderson, R. S. Benjamin, J. Ludwig, H. X. Chen, L. A. Doyle and R. Kurzrock (2012). "Insulin growth factor-receptor (IGF-1R) antibody cixutumumab combined with the mTOR inhibitor temsirolimus in patients with refractory Ewing's sarcoma family tumors." Clin Cancer Res **18**(9): 2625-2631.

Navarro, D., N. Agra, A. Pestana, J. Alonso and J. M. Gonzalez-Sancho (2010). "The EWS/FLI1 oncogenic protein inhibits expression of the Wnt inhibitor DICKKOPF-1 gene and antagonizes beta-catenin/TCF-mediated transcription." Carcinogenesis **31**(3): 394-401.

Nichols, W. W., D. G. Murphy, V. J. Cristofalo, L. H. Toji, A. E. Greene and S. A. Dwight (1977). "Characterization of a new human diploid cell strain, IMR-90." Science **196**(4285): 60-63.

Noguera, R., T. J. Triche, S. Navarro, M. Tsokos and A. Llombart-Bosch (1992). "Dynamic model of differentiation in Ewing's sarcoma cells. Comparative analysis of morphologic, immunocytochemical, and oncogene expression parameters." Lab Invest **66**(2): 143-151.

O'Regan, S., M. F. Diebler, F. M. Meunier and S. Vyas (1995). "A Ewing's sarcoma cell line showing some, but not all, of the traits of a cholinergic neuron." J Neurochem **64**(1): 69-76.

Ohno, T., V. N. Rao and E. S. Reddy (1993). "EWS/Fli-1 chimeric protein is a transcriptional activator." Cancer Res **53**(24): 5859-5863.

Olmos, D., S. Postel-Vinay, L. R. Molife, S. H. Okuno, S. M. Schuetze, M. L. Paccagnella, G. N. Batzel, D. Yin, K. Pritchard-Jones, I. Judson, F. P. Worden, A. Gualberto, M. Scurr, J. S. de Bono and P. Haluska (2010). "Safety, pharmacokinetics, and preliminary activity of the anti-IGF-1R antibody figitumumab (CP-751,871) in patients with sarcoma and Ewing's sarcoma: a phase 1 expansion cohort study." Lancet Oncol **11**(2): 129-135.

Ordonez, J. L., A. T. Amaral, A. M. Carcaboso, D. Herrero-Martin, M. del Carmen Garcia-Macias, V. Sevillano, D. Alonso, G. Pascual-Pasto, L. San-Segundo, M. Vila-Ubach, T. Rodrigues, S. Fraile, C. Teodosio, A. Mayo-Iscar, M. Aracil, C. M. Galmarini, O. M. Tirado, J. Mora and E. de Alava (2015). "The PARP inhibitor olaparib enhances the sensitivity of Ewing sarcoma to trabectedin." Oncotarget **6**(22): 18875-18890.

Ornitz, D. M. and N. Itoh (2015). "The Fibroblast Growth Factor signaling pathway." Wiley Interdiscip Rev Dev Biol **4**(3): 215-266.

Osgood, C. L., N. Maloney, C. G. Kidd, S. M. Kitchen-Goosen, L. E. Segars, M. Gebregiorgis, G. M. Woldemichael, M. He, S. Sankar, S. L. Lessnick, M. H. Kang, M. A. Smith, L. Turner, Z. B. Madaj, M. E. Winn, L. E. Nunez, J. Gonzalez-Sabin, L. J. Helman, F. Moris and P. J. Grohar (2016). "Identification of mithramycin analogs with improved targeting of the EWS-FLI1 transcription factor." Clin Cancer Res.

Ouchida, M., T. Ohno, Y. Fujimura, V. N. Rao and E. S. Reddy (1995). "Loss of tumorigenicity of Ewing's sarcoma cells expressing antisense RNA to EWS-fusion transcripts." Oncogene **11**(6): 1049-1054.

Ozaki, K., S. Miyazaki, S. Tanimura and M. Kohno (2005). "Efficient suppression of FGF-2-induced ERK activation by the cooperative interaction among mammalian Sprouty isoforms." J Cell Sci **118**(Pt 24): 5861-5871.

Panek, R. L., G. H. Lu, T. K. Dahring, B. L. Batley, C. Connolly, J. M. Hamby and K. J. Brown (1998). "In vitro biological characterization and antiangiogenic effects of PD 166866, a selective inhibitor of the FGF-1 receptor tyrosine kinase." J Pharmacol Exp Ther **286**(1): 569-577.

Pappo, A. S., G. Vassal, J. J. Crowley, V. Bolejack, P. C. Hogendoorn, R. Chugh, M. Ladanyi, J. F. Grippo, G. Dall, A. P. Staddon, S. P. Chawla, R. G. Maki, D. M. Araujo,

B. Geoerger, K. Ganjoo, N. Marina, J. Y. Blay, S. M. Schuetze, W. A. Chow and L. J. Helman (2014). "A phase 2 trial of R1507, a monoclonal antibody to the insulin-like growth factor-1 receptor (IGF-1R), in patients with recurrent or refractory rhabdomyosarcoma, osteosarcoma, synovial sarcoma, and other soft tissue sarcomas: results of a Sarcoma Alliance for Research Through Collaboration study." Cancer **120**(16): 2448-2456.

Pasqualato, A., V. Lei, A. Cucina, S. Dinicola, F. D'Anselmi, S. Proietti, M. G. Masiello, A. Palombo and M. Bizzarri (2013). "Shape in migration: quantitative image analysis of migrating chemoresistant HCT-8 colon cancer cells." Cell Adh Migr **7**(5): 450-459.

Patel, M., J. M. Simon, M. D. Iglesia, S. B. Wu, A. W. McFadden, J. D. Lieb and I. J. Davis (2012). "Tumor-specific retargeting of an oncogenic transcription factor chimera results in dysregulation of chromatin and transcription." Genome Res **22**(2): 259-270.

Perlman, E. J., P. S. Dickman, F. B. Askin, H. E. Grier, J. S. Miser and M. P. Link (1994). "Ewing's sarcoma--routine diagnostic utilization of MIC2 analysis: a Pediatric Oncology Group/Children's Cancer Group Intergroup Study." Hum Pathol **25**(3): 304-307.

Peter, M., J. Couturier, H. Pacquement, J. Michon, G. Thomas, H. Magdelenat and O. Delattre (1997). "A new member of the ETS family fused to EWS in Ewing tumors." Oncogene **14**(10): 1159-1164.

Ponten, J. and E. Saksela (1967). "Two established in vitro cell lines from human mesenchymal tumours." Int J Cancer **2**(5): 434-447.

Postel-Vinay, S., A. S. Veron, F. Tirode, G. Pierron, S. Reynaud, H. Kovar, O. Oberlin, E. Lapouble, S. Ballet, C. Lucchesi, U. Kontny, A. Gonzalez-Neira, P. Picci, J. Alonso, A. Patino-Garcia, B. B. de Paillerets, K. Laud, C. Dina, P. Froguel, F. Clavel-Chapelon, F. Doz, J. Michon, S. J. Chanock, G. Thomas, D. G. Cox and O. Delattre (2012). "Common variants near TARDBP and EGR2 are associated with susceptibility to Ewing sarcoma." Nat Genet **44**(3): 323-327.

Potluri, V. R., F. Gilbert, C. Helsen and L. Helson (1987). "Primitive neuroectodermal tumor cell lines: chromosomal analysis of five cases." Cancer Genet Cytogenet **24**(1): 75-86.

Powers, C. J., S. W. McLeskey and A. Wellstein (2000). "Fibroblast growth factors, their receptors and signaling." Endocr Relat Cancer **7**(3): 165-197.

Prieur, A., F. Tirode, P. Cohen and O. Delattre (2004). "EWS/FLI-1 silencing and gene profiling of Ewing cells reveal downstream oncogenic pathways and a crucial role for repression of insulin-like growth factor binding protein 3." Mol Cell Biol **24**(16): 7275-7283.

Purcell, P., A. Jheon, M. P. Vivero, H. Rahimi, A. Joo and O. D. Klein (2012). "Spry1 and spry2 are essential for development of the temporomandibular joint." J Dent Res **91**(4): 387-393.

Regad, T. (2015). "Targeting RTK Signaling Pathways in Cancer." Cancers (Basel) **7**(3): 1758-1784.

Richter, G. H., S. Plehm, A. Fasan, S. Rossler, R. Unland, I. M. Bennani-Baiti, M. Hotfilder, D. Lowel, I. von Luettichau, I. Mossbrugger, L. Quintanilla-Martinez, H. Kovar, M. S. Staege, C. Muller-Tidow and S. Burdach (2009). "EZH2 is a mediator of EWS/FLI1 driven tumor growth and metastasis blocking endothelial and neuro-ectodermal differentiation." Proc Natl Acad Sci U S A **106**(13): 5324-5329.

Riggi, N., B. Knoechel, S. M. Gillespie, E. Rheinbay, G. Boulay, M. L. Suva, N. E. Rossetti, W. E. Boonseng, O. Oksuz, E. B. Cook, A. Formey, A. Patel, M. Gymrek, V. Thapar, V. Deshpande, D. T. Ting, F. J. Hornicek, G. P. Nielsen, I. Stamenkovic, M. J. Aryee, B. E. Bernstein and M. N. Rivera (2014). "EWS-FLI1 utilizes divergent chromatin remodeling mechanisms to directly activate or repress enhancer elements in Ewing sarcoma." Cancer Cell **26**(5): 668-681.

Riggi, N., M. L. Suva, C. De Vito, P. Provero, J. C. Stehle, K. Baumer, L. Cironi, M. Janiszewska, T. Petricevic, D. Suva, S. Tercier, J. M. Joseph, L. Guillou and I. Stamenkovic (2010). "EWS-FLI-1 modulates miRNA145 and SOX2 expression to initiate mesenchymal stem cell reprogramming toward Ewing sarcoma cancer stem cells." Genes Dev **24**(9): 916-932.

Riggi, N., M. L. Suva and I. Stamenkovic (2009). "Ewing's sarcoma origin: from duel to duality." Expert Rev Anticancer Ther **9**(8): 1025-1030.

Riggi, N., M. L. Suva, D. Suva, L. Cironi, P. Provero, S. Tercier, J. M. Joseph, J. C. Stehle, K. Baumer, V. Kindler and I. Stamenkovic (2008). "EWS-FLI-1 expression triggers a Ewing's sarcoma initiation program in primary human mesenchymal stem cells." Cancer Res **68**(7): 2176-2185.

Rodriguez-Galindo, C., S. L. Spunt and A. S. Pappo (2003). "Treatment of Ewing sarcoma family of tumors: current status and outlook for the future." Med Pediatr Oncol **40**(5): 276-287.

Sabatel, C., A. M. Cornet, S. P. Tabruyn, L. Malvaux, K. Castermans, J. A. Martial and I. Struman (2010). "Sprouty1, a new target of the angiostatic agent 16K prolactin, negatively regulates angiogenesis." Mol Cancer **9**: 231.

Salsmann, A., E. Schaffner-Reckinger and N. Kieffer (2006). "RGD, the Rho'd to cell spreading." Eur J Cell Biol **85**(3-4): 249-254.

Sankar, S., R. Bell, B. Stephens, R. Zhuo, S. Sharma, D. J. Bearss and S. L. Lessnick (2013). "Mechanism and relevance of EWS/FLI-mediated transcriptional repression in Ewing sarcoma." Oncogene **32**(42): 5089-5100.

Sathyanarayana, P., A. Dev, A. Pradeep, M. Ufkin, J. D. Licht and D. M. Wojchowski (2012). "Spry1 as a novel regulator of erythropoiesis, EPO/EPOR target, and suppressor of JAK2." Blood **119**(23): 5522-5531.

Scotlandi, K., S. Avnet, S. Benini, M. C. Manara, M. Serra, V. Cerisano, S. Perdichizzi, P. L. Lollini, C. De Giovanni, L. Landuzzi and P. Picci (2002a). "Expression of an IGF-I receptor dominant negative mutant induces apoptosis, inhibits tumorigenesis and enhances chemosensitivity in Ewing's sarcoma cells." Int J Cancer **101**(1): 11-16.

Scotlandi, K., S. Benini, P. Nanni, P. L. Lollini, G. Nicoletti, L. Landuzzi, M. Serra, M. C. Manara, P. Picci and N. Baldini (1998). "Blockage of insulin-like growth factor-I receptor inhibits the growth of Ewing's sarcoma in athymic mice." Cancer Res **58**(18): 4127-4131.

Scotlandi, K., C. Maini, M. C. Manara, S. Benini, M. Serra, V. Cerisano, R. Strammiello, N. Baldini, P. L. Lollini, P. Nanni, G. Nicoletti and P. Picci (2002b). "Effectiveness of insulin-like growth factor I receptor antisense strategy against Ewing's sarcoma cells." Cancer Gene Ther **9**(3): 296-307.

Schoffski, P., D. Adkins, J. Y. Blay, T. Gil, A. D. Elias, P. Rutkowski, G. K. Pennock, H. Youssoufian, H. Gelderblom, R. Willey and D. O. Grebennik (2013). "An open-label, phase 2 study evaluating the efficacy and safety of the anti-IGF-1R antibody cixutumumab in patients with previously treated advanced or metastatic soft-tissue sarcoma or Ewing family of tumours." Eur J Cancer **49**(15): 3219-3228.

Schubbert, S., K. Shannon and G. Bollag (2007). "Hyperactive Ras in developmental disorders and cancer." Nat Rev Cancer **7**(4): 295-308.

Seeger, R. C., S. A. Rayner, A. Banerjee, H. Chung, W. E. Laug, H. B. Neustein and W. F. Benedict (1977). "Morphology, growth, chromosomal pattern and fibrinolytic activity of two new human neuroblastoma cell lines." Cancer Res **37**(5): 1364-1371.

Segaliny, A. I., M. Tellez-Gabriel, M. F. Heymann and D. Heymann (2015). "Receptor tyrosine kinases: Characterisation, mechanism of action and therapeutic interests for bone cancers." J Bone Oncol **4**(1): 1-12.

Sharma, B., S. Joshi, A. Sassano, B. Majchrzak, S. Kaur, P. Aggarwal, B. Nabet, M. Bulic, B. L. Stein, B. McMahon, D. P. Baker, R. Fukunaga, J. K. Altman, J. D. Licht, E. N. Fish and L. C. Platanias (2012). "Sprouty proteins are negative regulators of interferon (IFN) signaling and IFN-inducible biological responses." J Biol Chem **287**(50): 42352-42360.

Shaw, A. T., P. P. Hsu, M. M. Awad and J. A. Engelman (2013). "Tyrosine kinase gene rearrangements in epithelial malignancies." Nat Rev Cancer **13**(11): 772-787.

Shea, K. L., W. Xiang, V. S. LaPorta, J. D. Licht, C. Keller, M. A. Basson and A. S. Brack (2010). "Sprouty1 regulates reversible quiescence of a self-renewing adult muscle stem cell pool during regeneration." Cell Stem Cell **6**(2): 117-129.

Shim, K., G. Minowada, D. E. Coling and G. R. Martin (2005). "Sprouty2, a mouse deafness gene, regulates cell fate decisions in the auditory sensory epithelium by antagonizing FGF signaling." Dev Cell **8**(4): 553-564.

Shin, E. H., M. A. Basson, M. L. Robinson, J. W. McAvoy and F. J. Lovicu (2012). "Sprouty is a negative regulator of transforming growth factor beta-induced epithelial-to-mesenchymal transition and cataract." Mol Med **18**: 861-873.

Shing, D. C., D. J. McMullan, P. Roberts, K. Smith, S. F. Chin, J. Nicholson, R. M. Tillman, P. Ramani, C. Cullinane and N. Coleman (2003). "FUS/ERG gene fusions in Ewing's tumors." Cancer Res **63**(15): 4568-4576.

Sirivatanauksorn, Y., V. Sirivatanauksorn, C. Srisawat, A. Khongmanee and C. Tongkham (2012). "Differential expression of sprouty genes in hepatocellular carcinoma." J Surg Oncol **105**(3): 273-276.

Smilenov, L. B., A. Mikhailov, R. J. Pelham, E. E. Marcantonio and G. G. Gundersen (1999). "Focal adhesion motility revealed in stationary fibroblasts." Science **286**(5442): 1172-1174.

Smith, R., L. A. Owen, D. J. Trem, J. S. Wong, J. S. Whangbo, T. R. Golub and S. L. Lessnick (2006). "Expression profiling of EWS/FLI identifies NKX2.2 as a critical target gene in Ewing's sarcoma." Cancer Cell **9**(5): 405-416.

Sorensen, P. H., S. L. Lessnick, D. Lopez-Terrada, X. F. Liu, T. J. Triche and C. T. Denny (1994). "A second Ewing's sarcoma translocation, t(21;22), fuses the EWS gene to another ETS-family transcription factor, ERG." Nat Genet **6**(2): 146-151.

Staege, M. S., C. Hutter, I. Neumann, S. Foja, U. E. Hattenhorst, G. Hansen, D. Afar and S. E. Burdach (2004). "DNA microarrays reveal relationship of Ewing family tumors to both endothelial and fetal neural crest-derived cells and define novel targets." Cancer Res **64**(22): 8213-8221.

Sturla, L. M., G. Westwood, P. J. Selby, I. J. Lewis and S. A. Burchill (2000). "Induction of cell death by basic fibroblast growth factor in Ewing's sarcoma." Cancer Res **60**(21): 6160-6170.

Sugimoto, T., E. Tatsumi, J. T. Kemshead, L. Helson, A. A. Green and J. Minowada (1984). "Determination of cell surface membrane antigens common to both human neuroblastoma and leukemia-lymphoma cell lines by a panel of 38 monoclonal antibodies." J Natl Cancer Inst **73**(1): 51-57.

Sun, L., N. Tran, C. Liang, F. Tang, A. Rice, R. Schreck, K. Waltz, L. K. Shawver, G. McMahon and C. Tang (1999). "Design, synthesis, and evaluations of substituted 3-[(3- or 4-carboxyethylpyrrol-2-yl)methylidenyl]indolin-2-ones as inhibitors of VEGF, FGF, and PDGF receptor tyrosine kinases." J Med Chem **42**(25): 5120-5130.

Surdez, D., M. Benetkiewicz, V. Perrin, Z. Y. Han, G. Pierron, S. Ballet, F. Lamoureux, F. Redini, A. V. Decouvelaere, E. Daudigeos-Dubus, B. Geoerger, G. de Pinieux, O. Delattre and F. Tirode (2012). "Targeting the EWSR1-FLI1 oncogene-induced protein kinase PKC-beta abolishes ewing sarcoma growth." Cancer Res **72**(17): 4494-4503.

Takahashi, M., D. R. Rhodes, K. A. Furge, H. Kanayama, S. Kagawa, B. B. Haab and B. T. Teh (2001). "Gene expression profiling of clear cell renal cell carcinoma: gene

identification and prognostic classification." Proc Natl Acad Sci U S A **98**(17): 9754-9759.

Tanaka, K., T. Iwakuma, K. Harimaya, H. Sato and Y. Iwamoto (1997). "EWS-Fli1 antisense oligodeoxynucleotide inhibits proliferation of human Ewing's sarcoma and primitive neuroectodermal tumor cells." J Clin Invest **99**(2): 239-247.

Taniguchi, K., T. Ayada, K. Ichiyama, R. Kohno, Y. Yonemitsu, Y. Minami, A. Kikuchi, Y. Maehara and A. Yoshimura (2007). "Sprouty2 and Sprouty4 are essential for embryonic morphogenesis and regulation of FGF signaling." Biochem Biophys Res Commun **352**(4): 896-902.

Terada, N., T. Shiraishi, Y. Zeng, K. M. Aw-Yong, S. M. Mooney, Z. Liu, S. Takahashi, J. Luo, S. E. Lupold, P. Kulkarni and R. H. Getzenberg (2014). "Correlation of Sprouty1 and Jagged1 with aggressive prostate cancer cells with different sensitivities to androgen deprivation." J Cell Biochem **115**(9): 1505-1515.

Thompson, A. D., M. A. Teitell, A. Arvand and C. T. Denny (1999). "Divergent Ewing's sarcoma EWS/ETS fusions confer a common tumorigenic phenotype on NIH3T3 cells." Oncogene **18**(40): 5506-5513.

Tirode, F., K. Laud-Duval, A. Prieur, B. Delorme, P. Charbord and O. Delattre (2007). "Mesenchymal stem cell features of Ewing tumors." Cancer Cell **11**(5): 421-429.

Tirode, F., D. Surdez, X. Ma, M. Parker, M. C. Le Deley, A. Bahrami, Z. Zhang, E. Lapouble, S. Grossetete-Lalami, M. Rusch, S. Reynaud, T. Rio-Frio, E. Hedlund, G. Wu, X. Chen, G. Pierron, O. Oberlin, S. Zaidi, G. Lemmon, P. Gupta, B. Vadodaria, J. Easton, M. Gut, L. Ding, E. R. Mardis, R. K. Wilson, S. Shurtleff, V. Laurence, J. Michon, P. Marec-Berard, I. Gut, J. Downing, M. Dyer, J. Zhang, O. Delattre, P. St. Jude Children's Research Hospital-Washington University Pediatric Cancer Genome and C. the International Cancer Genome (2014). "Genomic landscape of Ewing sarcoma defines an aggressive subtype with co-association of STAG2 and TP53 mutations." Cancer Discov **4**(11): 1342-1353.

Tomazou, E. M., N. C. Sheffield, C. Schmidl, M. Schuster, A. Schonegger, P. Datlinger, S. Kubicek, C. Bock and H. Kovar (2015). "Epigenome mapping reveals distinct modes of gene regulation and widespread enhancer reprogramming by the oncogenic fusion protein EWS-FLI1." Cell Rep **10**(7): 1082-1095.

Toretsky, J. A., Y. Connell, L. Neckers and N. K. Bhat (1997). "Inhibition of EWS-FLI-1 fusion protein with antisense oligodeoxynucleotides." J Neurooncol **31**(1-2): 9-16.

Toretsky, J. A., V. Erkizan, A. Levenson, O. D. Abaan, J. D. Parvin, T. P. Cripe, A. M. Rice, S. B. Lee and A. Uren (2006). "Oncoprotein EWS-FLI1 activity is enhanced by RNA helicase A." Cancer Res **66**(11): 5574-5581.

Touat, M., E. Ileana, S. Postel-Vinay, F. Andre and J. C. Soria (2015). "Targeting FGFR Signaling in Cancer." Clin Cancer Res **21**(12): 2684-2694.

Triche, T. J. (1988). "Diagnosis of small round cell tumors of childhood." Bull Cancer **75**(3): 297-310.

Truong, A. H. and Y. Ben-David (2000). "The role of Fli-1 in normal cell function and malignant transformation." Oncogene **19**(55): 6482-6489.

Tsumura, Y., J. Toshima, Onno C. Leeksma, K. Ohashi and K. Mizuno (2005). "Sprouty-4 negatively regulates cell spreading by inhibiting the kinase activity of testicular protein kinase." Biochemical Journal **387**(Pt 3): 627-637.

Tumilowicz, J. J., W. W. Nichols, J. J. Cholon and A. E. Greene (1970). "Definition of a continuous human cell line derived from neuroblastoma." Cancer Res **30**(8): 2110-2118.

Urano, F., A. Umezawa, H. Yabe, W. Hong, K. Yoshida, K. Fujinaga and J. Hata (1998). "Molecular analysis of Ewing's sarcoma: another fusion gene, EWS-E1AF, available for diagnosis." Jpn J Cancer Res **89**(7): 703-711.

Urs, S., T. Henderson, P. Le, C. J. Rosen and L. Liaw (2012). "Tissue-specific expression of Sprouty1 in mice protects against high-fat diet-induced fat accumulation, bone loss and metabolic dysfunction." Br J Nutr **108**(6): 1025-1033.

Urs, S., D. Venkatesh, Y. Tang, T. Henderson, X. Yang, R. E. Friesel, C. J. Rosen and L. Liaw (2010). "Sprouty1 is a critical regulatory switch of mesenchymal stem cell lineage allocation." FASEB J **24**(9): 3264-3273.

von Levetzow, C., X. Jiang, Y. Gwye, G. von Levetzow, L. Hung, A. Cooper, J. H. Hsu and E. R. Lawlor (2011). "Modeling initiation of Ewing sarcoma in human neural crest cells." PLoS One **6**(4): e19305.

Wakioka, T., A. Sasaki, R. Kato, T. Shouda, A. Matsumoto, K. Miyoshi, M. Tsuneoka, S. Komiya, R. Baron and A. Yoshimura (2001). "Spred is a Sprouty-related suppressor of Ras signalling." Nature **412**(6847): 647-651.

Whang-Peng, J., T. J. Triche, T. Knutsen, J. Miser, E. C. Douglass and M. A. Israel (1984). "Chromosome translocation in peripheral neuroepithelioma." N Engl J Med **311**(9): 584-585.

Wiles, E. T., B. Lui-Sargent, R. Bell and S. L. Lessnick (2013). "BCL11B is up-regulated by EWS/FLI and contributes to the transformed phenotype in Ewing sarcoma." PLoS One **8**(3): e59369.

Xu, H. F., Y. J. Ding, Z. X. Zhang, Z. F. Wang, C. L. Luo, B. X. Li, Y. W. Shen, L. Y. Tao and Z. Q. Zhao (2014). "MicroRNA21 regulation of the progression of viral myocarditis to dilated cardiomyopathy." Mol Med Rep **10**(1): 161-168.

Yang, X., Y. Gong, Y. Tang, H. Li, Q. He, L. Gower, L. Liaw and R. E. Friesel (2013). "Spry1 and Spry4 differentially regulate human aortic smooth muscle cell phenotype via Akt/FoxO/myocardin signaling." PLoS One **8**(3): e58746.

Yee, D., R. E. Favoni, G. S. Lebovic, F. Lombana, D. R. Powell, C. P. Reynolds and N. Rosen (1990). "Insulin-like growth factor I expression by tumors of neuroectodermal origin with the t(11;22) chromosomal translocation. A potential autocrine growth factor." J Clin Invest **86**(6): 1806-1814.

Yi, H., Y. Fujimura, M. Ouchida, D. D. Prasad, V. N. Rao and E. S. Reddy (1997). "Inhibition of apoptosis by normal and aberrant Fli-1 and erg proteins involved in human solid tumors and leukemias." Oncogene **14**(11): 1259-1268.

Yilmaz, M. and G. Christofori (2010). "Mechanisms of motility in metastasizing cells." Mol Cancer Res **8**(5): 629-642.

Zhao, Z., J. Zuber, E. Diaz-Flores, L. Lintault, S. C. Kogan, K. Shannon and S. W. Lowe (2010). "p53 loss promotes acute myeloid leukemia by enabling aberrant self-renewal." Genes Dev **24**(13): 1389-1402.

Zoubek, A., C. Pfleiderer, M. Salzer-Kuntschik, G. Amann, R. Windhager, F. M. Fink, E. Koscielniak, O. Delattre, S. Strehl, P. F. Ambros and *et al.* (1994). "Variability of EWS chimaeric transcripts in Ewing tumours: a comparison of clinical and molecular data." Br J Cancer **70**(5): 908-913.

Zucman, J., T. Melot, C. Desmaze, J. Ghysdael, B. Plougastel, M. Peter, J. M. Zucker, T. J. Triche, D. Sheer, C. Turc-Carel and *et al.* (1993). "Combinatorial generation of variable fusion proteins in the Ewing family of tumours." EMBO J **12**(12): 4481-4487.

8. Anexos

8.1 Material Suplementario

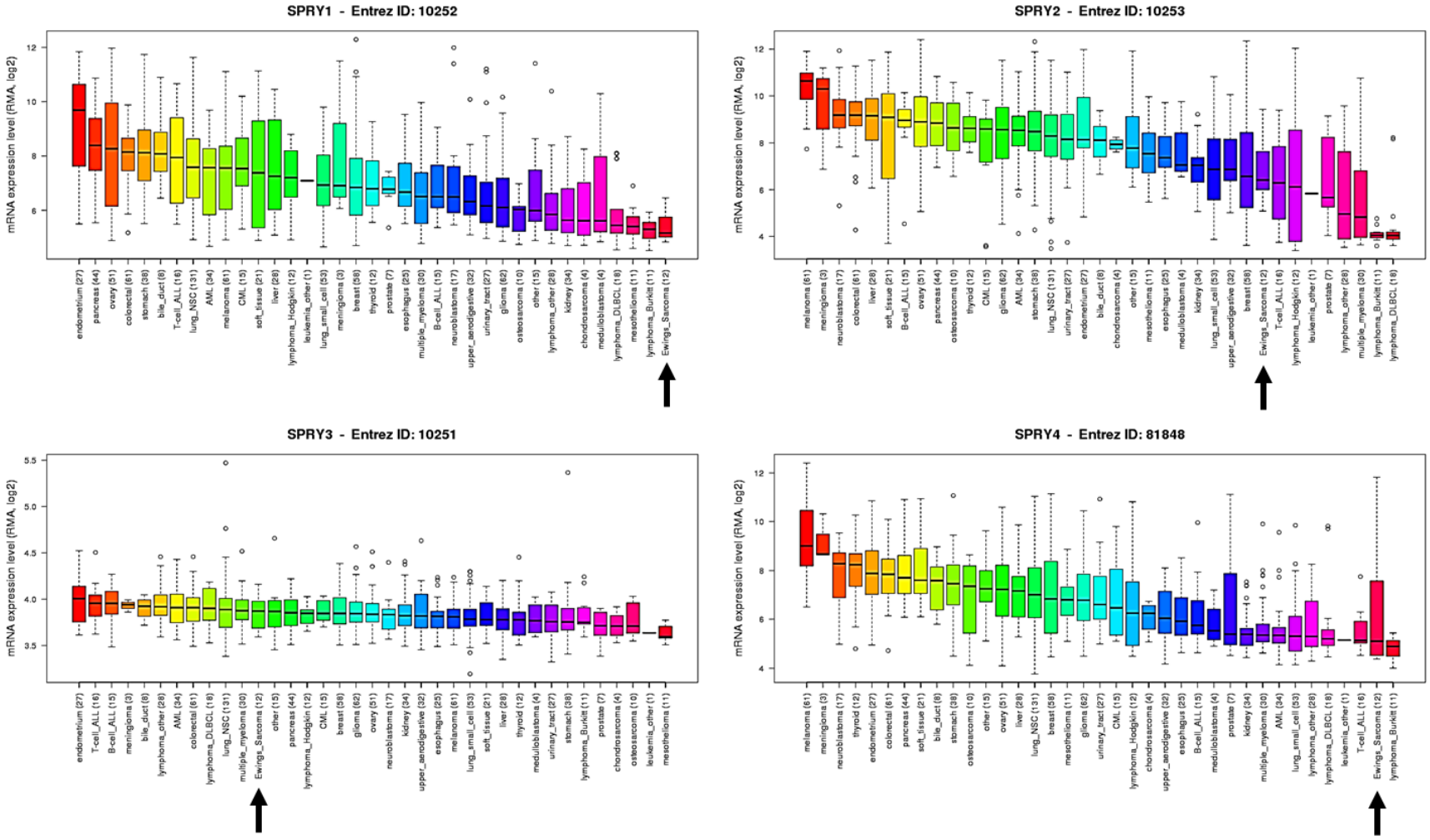

Figura Suplementaria 1. El sarcoma de Ewing presenta los niveles de expresión de SPRY1 más bajos de todos los tumores disponibles en la *Cancer Cell Line Encyclopedia* (CCLE). El análisis de los datos de expresión génica para SPRY1, -2, -3 and -4 utilizando los datos de la CCLE (datos disponibles en http://www.broadinstitute.org/ccle (Barretina *et al.* 2012)) muestra que el sarcoma de Ewing presenta los niveles de expresión de SPRY1 más bajos de todos los tumores sólidos estudiados, a diferencia de lo que se observa para SPRY2, -3 y -4.

Tabla Suplementaria 1. Niveles de expresión de las líneas celulares analizadas en la CCLE (*Cancer Cell Line Encyclopedia*). Se muestra la posición que ocupan sobre un total de 1036 líneas celulares analizadas en función del nivel de expresión de SPY1.

Posición (1036)	***Línea Celular***	***Nivel de Expresión SPRY1***
1028	U2OS	4,740753
942	SAOS-2	5,21578
829	IMR32	5,59917
488	SKNSH	7,227691
626	SHSY5Y	6,493132
2	**SKNAS**	**11,99227**
288	SJRH30	8,223732
770	A673	5,849319

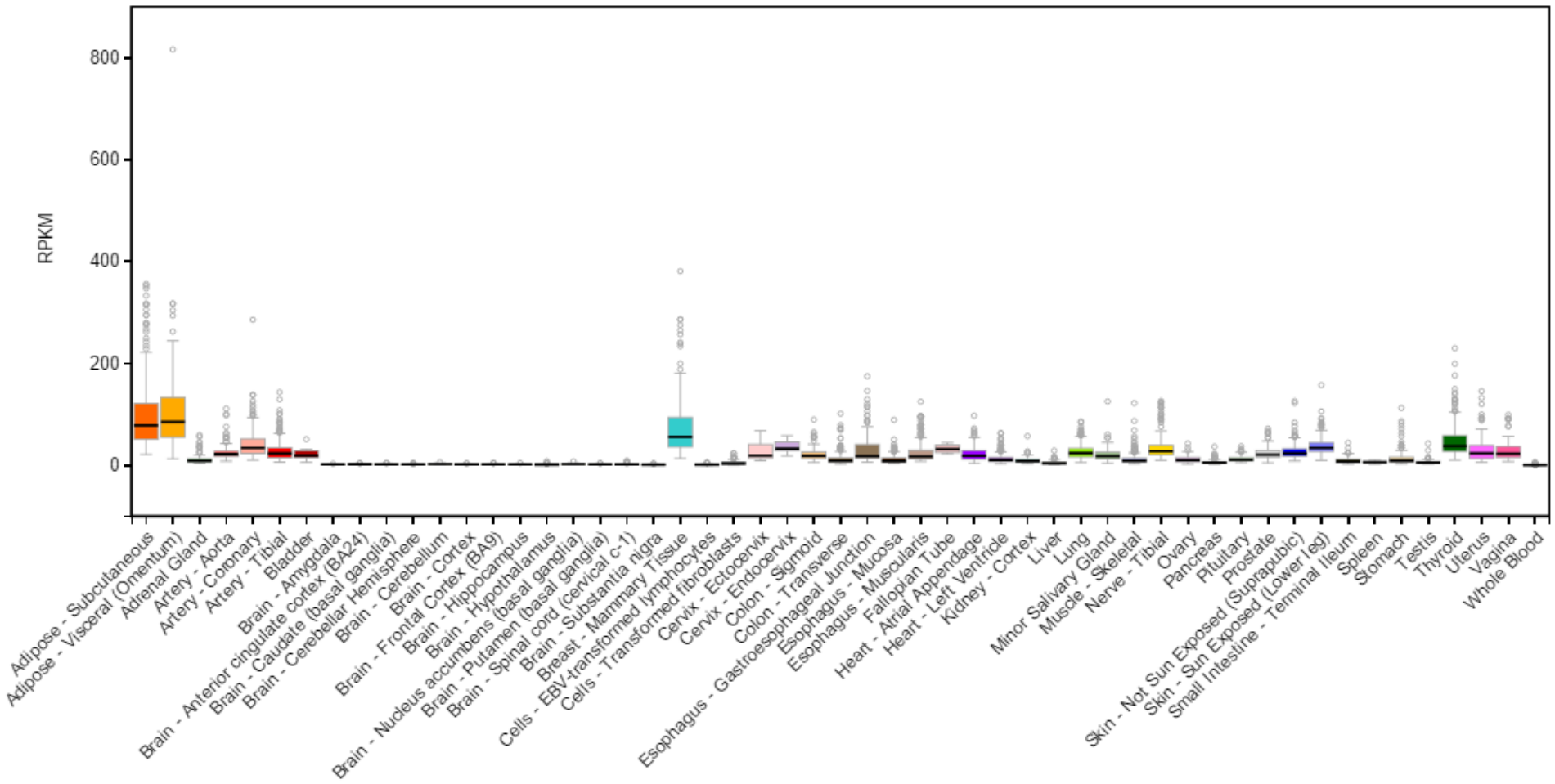

Figura Suplementaria 2. Expresión de SPRY1 en tejidos normales. La figura muestra datos del portal GTEx (http://gtexportal.org), provenientes del *GTEx Analysis Release V6* (*dbGaP Accession phs000424.v6.p1*) donde se observa que SPRY1 se expresa en mayor medida en tejido adiposo y mama. Los rectángulos muestran el valor medio de expresión y los percentiles 25 y 75. Los puntos muestran los valores atípicos.

8.2. Publicaciones

Los resultados presentados en esta Tesis han sido parcialmente publicados en el siguiente artículo:

Cidre-Aranaz F, Grünewald TGP, Surdez D, García-García L, Lázaro JC, Kirchner T, González-González L, Sastre A, García-Miguel P, López-Pérez SE, Monzón S, Delattre O, Alonso J. EWS-FLI1-mediated suppression of the RAS-antagonist Sprouty1 (SPRY1) confers aggressiveness to Ewing sarcoma. **Oncogene** 2016.

Además, durante el transcurso de la Tesis se han publicado los siguientes artículos en los que el doctorando ha participado:

Agra N*, Cidre F*, Garcia-Garcia L, de la Parra J, Alonso J. Lysyl oxidase is downregulated by the EWS/FLI1 oncoprotein and its propeptide domain displays tumor supressor activities in Ewing sarcoma cells. **PLoS One** 2013;8(6):e66281.

Cidre-Aranaz F, Alonso J. EWS/FLI1 Target Genes and Therapeutic Opportunities in Ewing Sarcoma. **Front Oncol** 2015;5:162.

Grunewald TG, Bernard V, Gilardi-Hebenstreit P, Raynal V, Surdez D, Aynaud MM, Mirabeau O, Cidre-Aranaz F, Tirode F, Zaidi S, *et al.* Chimeric EWSR1-FLI1 regulates the Ewing sarcoma susceptibility gene EGR2 via a GGAA microsatellite. **Nat Genet** 2015;47(9):1073-8.

Kovar H, Amatruda J, Brunet E, Burdach S, Cidre-Aranaz F, de Alava E, *et al.* The second European interdisciplinary Ewing sarcoma research summit - A joint effort to deconstructing the multiple layers of a complex disease. **Oncotarget** 2016;7(8):8613-24.

Rodriguez-Martin C, Cidre F, Fernandez-Teijeiro A, Gomez-Mariano G, de la Vega L, Ramos P, *et al.* Familial retinoblastoma due to intronic LINE-1 insertion causes aberrant and noncanonical mRNA splicing of the RB1 gene. **J Hum Genet** 2016.

Oncogene (2016), 1–11

www.nature.com/onc

ORIGINAL ARTICLE

EWS-FLI1-mediated suppression of the RAS-antagonist Sprouty 1 (SPRY1) confers aggressiveness to Ewing sarcoma

F Cidre-Aranaz[1], TGP Grünewald[2,3], D Surdez[2], L García-García[1], J Carlos Lázaro[1], T Kirchner[3], L González-González[1], A Sastre[4], P García-Miguel[4], SE López-Pérez[1], S Monzón[1,5], O Delattre[2] and J Alonso[1]

Ewing sarcoma is characterized by chromosomal translocations fusing the *EWS* gene with various members of the *ETS* family of transcription factors, most commonly *FLI1*. EWS-FLI1 is an aberrant transcription factor driving Ewing sarcoma tumorigenesis by either transcriptionally inducing or repressing specific target genes. Herein, we showed that *Sprouty 1* (*SPRY1*), which is a physiological negative feedback inhibitor downstream of fibroblast growth factor (FGF) receptors (FGFRs) and other RAS-activating receptors, is an EWS-FLI1 repressed gene. EWS-FLI1 knockdown specifically increased the expression of SPRY1, while other *Sprouty* family members remained unaffected. Analysis of SPRY1 expression in a panel of Ewing sarcoma cells showed that SPRY1 was not expressed in Ewing sarcoma cell lines, suggesting that it could act as a tumor suppressor gene in these cells. In agreement, induction of SPRY1 in three different Ewing sarcoma cell lines functionally impaired proliferation, clonogenic growth and migration. In addition, SPRY1 expression inhibited extracellular signal-related kinase/mitogen-activated protein kinase (MAPK) signaling induced by serum and basic FGF (bFGF). Moreover, treatment of Ewing sarcoma cells with the potent FGFR inhibitor PD-173074 reduced bFGF-induced proliferation, colony formation and *in vivo* tumor growth in a dose-dependent manner, thus mimicking SPRY1 activity in Ewing sarcoma cells. Although the expression of SPRY1 was low when compared with other tumors, SPRY1 was variably expressed in primary Ewing sarcoma tumors and higher expression levels were significantly associated with improved outcome in a large patient cohort. Taken together, our data indicate that EWS-FLI1-mediated repression of SPRY1 leads to unrestrained bFGF-induced cell proliferation, suggesting that targeting the FGFR/MAPK pathway can constitute a promising therapeutic approach for this devastating disease.

Oncogene advance online publication, 4 July 2016; doi:10.1038/onc.2016.244

INTRODUCTION

Ewing sarcomas are aggressive bone and soft-tissue sarcomas mostly affecting children and young adults.[1] Although the 5-year survival in patients with localized disease increased significantly on the addition of systemic chemotherapy to protocol treatments in the 70–80 s,[2] the prognosis and survival of patients with metastatic or recurrent disease remained generally very poor.[3] Indeed, Ewing sarcoma features high rates of early metastasis with ~20% of patients having detectable metastasis at diagnosis.[4]

The molecular hallmarks of Ewing sarcoma are nonrandom chromosomal translocations generating in-frame fusion of the *EWS* gene on chromosome 22 and the C-terminus of a member of the *ETS* family of transcription factors (that is, *FLI1*, *ERG*, *ETV1*, *FEV*, *ETV4* and *POU5F1*) including the DNA-binding domain[5] (reviewed in Mackintosh *et al.*[1]). This fusion gives rise to aberrant EWS-ETS transcription factors, EWS-FLI1 being present in 85% of cases.

EWS-FLI1 induces massive deregulation of protein expression by either transcriptionally inducing or repressing specific target genes, many of which are involved in the oncogenic process.[6] For instance, EWS-FLI1 induces the expression of *NR0B1* (*DAX1*), *EGR2*, *NKX2.2*, *CCK*, *PRKCB* or *STEAP1*,[7–11] while suppressing *IGFBP3*, *LOX*, *DKK1* or *TGFBIIR*.[12–15] All these genes have been shown to be important in Ewing sarcoma pathogenesis.

Here we report on the tumor suppressive role of another repressed EWS-FLI1-targeted gene, namely *Sprouty 1* (*SPRY1*), which is a negative feedback inhibitor of the RAS/mitogen-activated protein kinase/extracellular signal-related kinase (RAS/MAPK/ERK) pathway downstream of the fibroblast growth factor receptor (FGFR).

SPRY1 is part of the mammalian *Sprouty* gene family consisting of four members (SPRY1–4), which share important sequence similarities[16] such as a highly conserved cysteine-rich domain in the C-terminal region (which is also found in the SPRED family of proteins) and a short amino acid sequence in the N-terminus.[17] SPRY proteins differ largely in their tissue distribution, activity and interaction partners,[18] thus suggesting non-redundant functions. SPRY1 is an upstream antagonist of RAS that is activated by ERK, providing a negative feedback loop for RAS signaling. Of note, about one-third of all human cancers are thought to carry a mutated *RAS* gene that activates downstream signaling.[19] It has been suggested that SPRY1 may have a tumor suppressor function in specific tumors, as its expression is decreased in several human cancers such as breast and prostate cancer.[20–22] Indeed, several studies showed that SPRY1 overexpression in tumor cell lines inhibits cell proliferation, migration and anchorage-independent growth *in vitro*.[21,23,24]

[1]Unidad de Tumores Sólidos Infantiles, Instituto de Investigación de Enfermedades Raras, Instituto de Salud Carlos III, Majadahonda, Spain; [2]INSERM U830 'Genetics and Biology of Cancers' Institut Curie Research Center, Paris, France; [3]Laboratory for Pediatric Sarcoma Biology, Institute of Pathology, LMU Munich, Munich, Germany; [4]Unidad hemato-oncología pediátrica, Hospital Infantil Universitario La Paz, Madrid, Spain and [5]Centro de Investigación Biomédica en Red de Enfermedades Raras (CIBERER U758), Instituto de Salud Carlos III, Madrid, Spain. Correspondence: Dr J Alonso, Unidad de Tumores Sólidos Infantiles, Instituto de Investigación de Enfermedades Raras, Instituto de Salud Carlos III, Ctra. Majadahonda-Pozuelo km 2, Majadahonda Madrid 28220, Spain.
E-mail: fjalonso@isciii.es
Received 5 January 2016; revised 5 May 2016; accepted 30 May 2016

In this study, we show that SPRY1 acts as a tumor suppressor in Ewing sarcoma cells, and that SPRY1 repression is necessary for cell proliferation and migration. Interestingly, SPRY1 repression was important to ERK pathway activation. Moreover, FGFR inhibition mimicked SPRY1 effect on proliferation and growth, indicating that SPRY1 has an important role in Ewing sarcoma. Finally, elevated SPRY1 expression correlated with improved overall survival of Ewing sarcoma patients and inversely correlated with metastasis at diagnosis. Collectively, our data indicate that EWS-FLI1-mediated repression of SPRY1 confers a growth advantage to Ewing sarcoma cells, and that SPRY1 levels constitute a novel biomarker for outcome prediction of Ewing sarcoma patients. Taken together, these results suggest a rationale for targeting FGFR/SPRY1/RAS/MAPK/ERK pathway as a new therapeutic approach in this devastating disease.

RESULTS

SPRY1 expression is strongly inhibited by EWS-FLI1 in Ewing sarcoma cell lines

Analysis of a gene expression profile of A673 Ewing sarcoma cell line genetically modified to express a specific small hairpin RNA directed against EWS-FLI1 mRNA on doxycycline stimulation (A673/TR/shEF) (Gene Expression Omnibus accession code: GSE36007) indicated that *SPRY1* is strongly downregulated by EWS-FLI1. These microarray results were confirmed by reverse transcription–quantitative PCR experiments. As depicted in Figure 1a, EWS-FLI1 knockdown led to a dramatic re-expression of *SPRY1* mRNA (up to 1000-fold compared with controls), whereas the mRNA levels of the other members of the *SPRY* family (*SPRY2*, *3* and *4*) were only minimally affected. Analysis of SPRY1 protein levels in the A673/TR/shEF cell model confirmed these results. As shown in Figure 1b, SPRY1 protein was undetectable by western blotting in A673/TR/shEF grown in the absence of doxycycline. However, a strong induction of SPRY1 protein was observed on doxycycline-mediated EWS-FLI1 knockdown.

We next studied whether the inhibition of SPRY1 expression could be a common feature of Ewing sarcoma cells. We first analyzed the levels of *SPRY1* mRNA and protein in a panel of eight Ewing sarcoma cell lines harboring different EWS-FLI1 or EWS-ERG fusion proteins (Supplementary Table 1). As shown in Figures 1c and d, *SPRY1* mRNA and protein were undetectable in all Ewing sarcoma cell lines analyzed. Interestingly, the mRNA levels of the other members of the *SPRY* family were variably expressed in this panel of Ewing sarcoma cells. These data could also be confirmed assessing larger public data sets. For instance, analysis of Cancer Cell Line Encyclopedia data set[25] (http://www.broadinstitute.org/ccle/home) showed that Ewing sarcoma cell lines exhibited the lowest SPRY1 levels among all tumor cell lines analyzed (Supplementary Figure 1).

SPRY1 induction impairs cell proliferation of Ewing sarcoma cells

The strong downregulation of SPRY1 by EWS-FLI1, its absence of expression in Ewing sarcoma cell lines and the finding that it acts as a negative feedback inhibitor of the RAS/MAPK/ERK cascade suggest a potential function of SPRY1 inhibition in Ewing sarcoma. To test this hypothesis, we generated three doxycycline-inducible SPRY1 Ewing sarcoma cell lines (A673/TR/SPRY1, SKES/TR/SPRY1 and SKNMC/TR/SPRY1) and subjected them to several functional assays. As shown in Figure 2a, these genetically modified Ewing cell lines express high levels of SPRY1 protein on doxycycline stimulation, whereas the levels of the EWS-FLI1 oncoprotein remain unaffected. Thus, they constitute a suitable model to test the consequences of exclusive SPRY1 re-expression in Ewing sarcoma without affecting the levels of EWS-FLI1 oncoprotein.

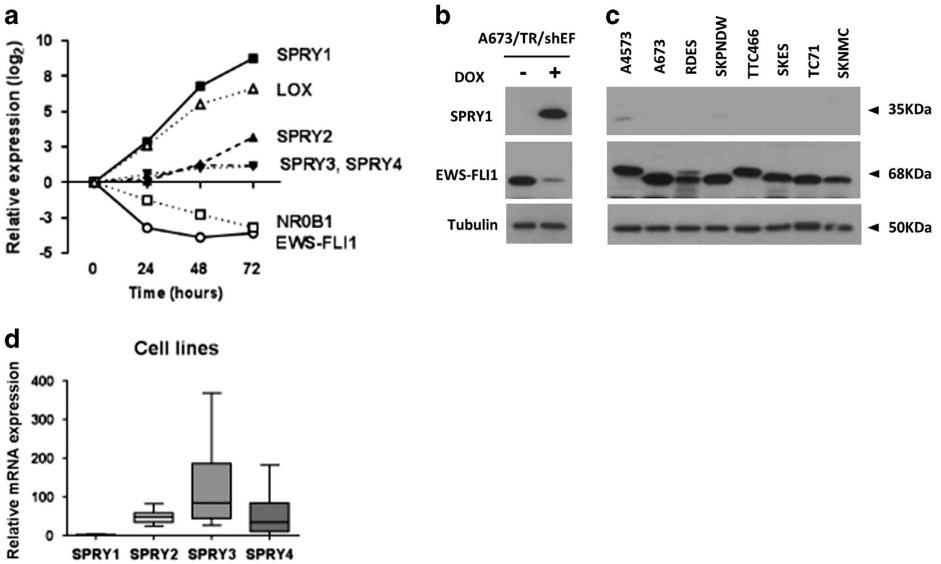

Figure 1. *SPRY1* is negatively regulated by EWS-FLI1 oncoprotein. (**a**) Time course of *SPRY1*, *2*, *3* and *4* on EWS-FLI1 doxycycline-inducible knockdown in A673/TR/shEF. EWS-FLI1 expression and two known target genes such as *LOX* and *NR0B1* were included as controls. mRNA levels were quantified by real-time reverse transcription–quantitative PCR (RT–qPCR), normalized to that of *TBP* (reference gene) and referred to unstimulated cells. Figure shows data of one out of three independent experiments done in triplicate with equivalent results. *EWS-FLI1* inhibition in A673/TR/shEF cells selectively upregulates SPRY1 more than 1000 times over the rest of the members of the *SPRY* family of genes. As expected, *LOX* appears upregulated[13] and *NR0B1* downregulated[51] on EWS-FLI1 knockdown. (**b**) SPRY1 protein is re-expressed on EWS-FLI1 knockdown in A673/TR/shEF cells. SPRY1 protein is undetectable by western blotting in A673 cells grown in the absence of doxycycline and thus expressing EWS-FLI1. Incubation of A673/TR/shEWSFLI1 cells with doxycycline (1 μg/ml, 72 h) inhibits EWS-FLI1 expression and dramatically induces re-expression of SPRY1 protein. Tubulin was used as a control for loading and transferring. (**c**) SPRY1 is undetectable at protein level by western blotting in eight Ewing sarcoma cell lines. Expression of the different EWS-ETS proteins is also shown. Tubulin was used as a control for loading and transferring. (**d**) SPRY1, 2, 3 and 4 mRNA levels in Ewing sarcoma cell lines. Box plot shows the absence of SPRY1 expression in all Ewing sarcoma cell lines tested relative to other members of the SPRY family. The figure shows the expression levels normalized to that of TBP (reference gene).

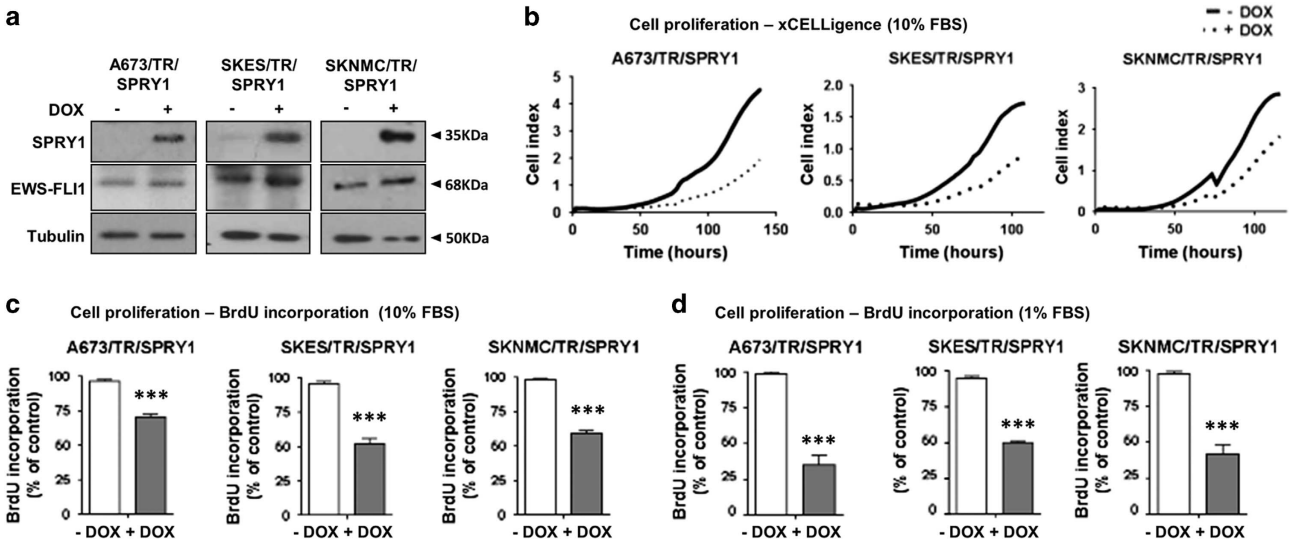

Figure 2. SPRY1 re-expression impairs proliferation in Ewing sarcoma cell lines. (**a**) A673/TR, SKES/TR and SKNMC/TR Ewing cell lines expressing constitutively the tetracycline repressor (TR) were infected with a doxycycline-inducible lentiviral vector encoding the SPRY1 cDNA. The figure shows the expression of SPRY1 protein in whole protein extracts isolated from A673/TR/SPRY1 (clone 1), SKES/TR/SPRY1 (clone 7) and SKNMC/TR/SPRY1 (clone 2) cells stimulated with doxycycline (DOX, 1 μg/ml, 72 h). High SPRY1 levels were detected in all three cell lines after doxycycline stimulation. EWS-FLI1 expression was not affected by SPRY1 ectopic expression. The same blot was stripped and incubated with anti-tubulin as a control for loading and transferring. (**b**) Cell proliferation was assayed in A673/TR/SPRY1, SKES/TR/SPRY1 and SKNMC/TR/SPRY1 cells using an xCELLigence assay with or without re-expression of SPRY1 (DOX, 1 μg/ml). Graphs depict the growth curves of the cells cultured in the absence or presence of doxycycline during 120 h and they show one representative experiment out of three independent experiments performed. Re-expression of SPRY1 produces a significant inhibition of cell proliferation. Slight artifacts in the graphs at 72 h are a consequence of media change and subsequent readjustment of the conditions in the xCELLigence device and do not affect the final result. (**c**) A673/TR/SPRY1, SKES/TR/SPRY1 and SKNMC/TR/SPRY1 cells were plated in octuplicates and cultured in the presence or absence of doxycycline (DOX, 1 μg/ml) for 72 h in 10% tetracycline-free FBS-supplemented media (standard culture conditions). Cell proliferation was assayed by bromodeoxyuridine (BrdU) incorporation into DNA. Graphs depict the percentage of cell proliferation of doxycycline-treated cells (expressing SPRY1) versus control. Figure depicts one representative experiment (mean ± s.d.) out of three independent experiments performed (***$P < 0.005$). (**d**) Cells were plated and cultured as described in **c**, but kept in 1% FBS-supplemented media (low-serum conditions). Cell proliferation is significantly inhibited in doxycycline-treated cells (expressing SPRY1) versus control. Figure depicts one representative experiment (mean ± s.d.) out of three independent experiments performed (***$P < 0.005$).

First, we studied the effect of SPRY1 induction on cell proliferation (Figures 2b–d). Induction of SPRY1 in these Ewing sarcoma cell lines on doxycycline stimulation significantly reduced their proliferation. This was observed using real-time monitoring of cell number (xCELLigence instrument, ACEA Biosciences, San Diego, CA, USA) (Figure 2b) and by bromodeoxyuridine incorporation assays (Figures 2c and d). Notably, no effect on cell proliferation was observed in cells carrying the empty vector, both in the absence and in the presence of doxycycline (data not shown). Cell proliferation inhibition was observed in standard culture media supplemented with 10% fetal bovine serum (FBS) (Figures 2b and c) and in low-serum (1% FBS) conditions as well (Figure 2d). Induction of SPRY1 in cells grown in low-serum conditions exhibited an even stronger reduction of cell proliferation (Figure 2d), probably suggesting that in conditions where there is a diminished availability of growth factors, such as in the tumor microenvironment, SPRY1 is able to markedly impair cell proliferation.

Similarly, induction of SPRY1 expression reduced clonogenic growth of the three Ewing sarcoma cell lines plated at very low density in medium supplemented with 5% FBS, whereas cells carrying the empty vector remained unaffected on doxycycline treatment (Figure 3a and Supplementary Figure 2A). When cells were tested for anchorage-independent growth in soft agar, no significant differences were observed in the number of colonies formed, whereas there was a significant difference in the size of the individual colonies (Figure 3b). No significant differences in anchorage-independent growth were observed in cells transfected with the empty vector when treated accordingly (Supplementary Figure 2B).

Finally, the three Ewing cell lines harboring the SPRY1 construct were cultured in the presence or absence of doxycycline and assayed for cell cycle in non-synchronized cells by flow cytometry. As shown in Supplementary Figure S3, the impairment in cell proliferation in SPRY1-re-expressing cells seems partially due to a cell cycle arrest in the G1 phase, although these results were not statistically significant.

Taken together, these results provide evidence that SPRY1 induction impairs cell proliferation as well as clonogenic and anchorage-independent growth of Ewing sarcoma cell lines.

SPRY1 induction impairs migration of Ewing sarcoma cells

We next analyzed the effect of SPRY1 induction in Ewing sarcoma cells on cell migration. As shown in Figure 3c, SPRY1 induction reduced the ability of A673, SKES and SKNMC Ewing sarcoma cells to close an artificial wound produced in a confluent cell monolayer (*in vitro* wound-healing assay). In addition, SPRY1 re-expression significantly impaired migration of Ewing sarcoma cells through a porous membrane (transwell assay) (Figure 3d). No differences in the migratory properties were observed in cells carrying the empty vector (data not shown).

SPRY1 repression is necessary for ERK activation and proliferation in Ewing sarcoma cells

SPRY1 has been described to inhibit MAPK/ERK pathway, which is one of the most relevant proliferative pathways in cancer. For that reason we investigated the effect of SPRY1 induction on ERK activation mediated by serum. As shown in Figure 4, SPRY1 induction reduced the levels of phospho-ERK both in low (1%) and

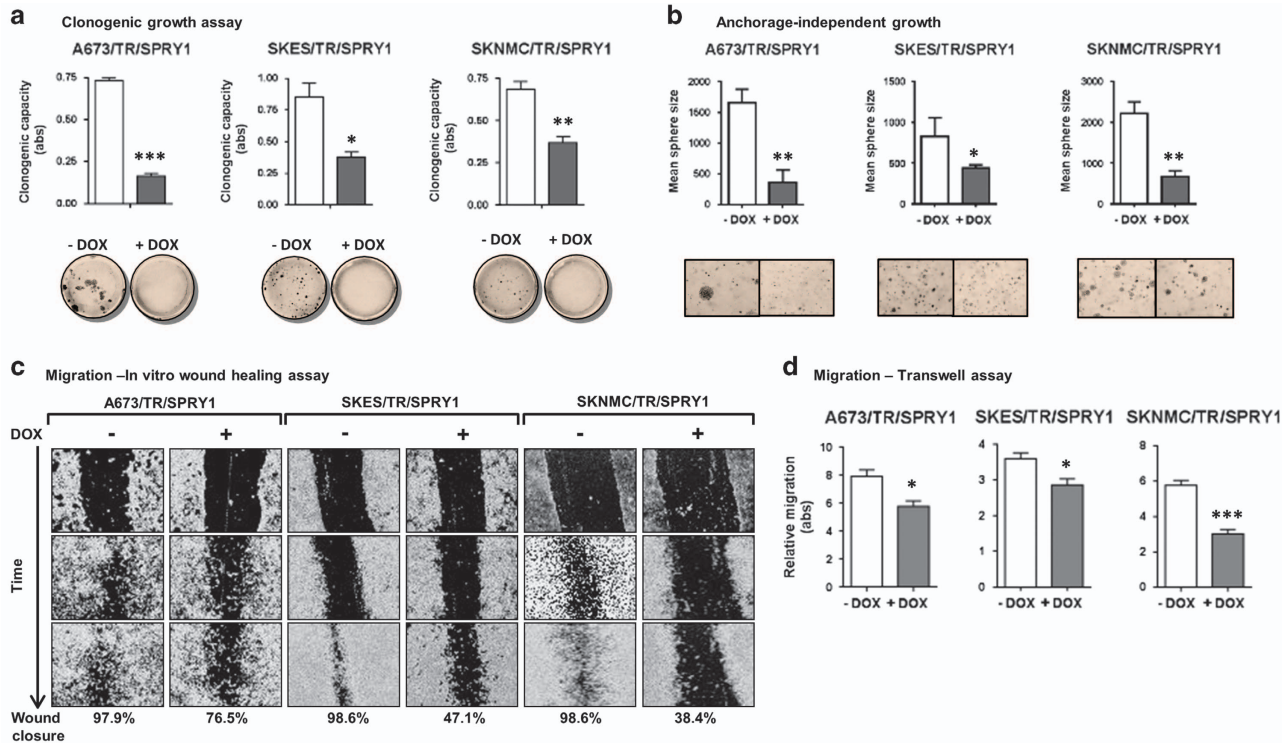

Figure 3. SPRY1 re-expression impairs Ewing sarcoma cell clonogenicity, anchorage-independent growth, migration and invasion of Ewing sarcoma cells. (**a**) A673/TR/SPRY1, SKES/TR/SPRY1 and SKNMC/TR/SPRY1 cells were platted in triplicates at low densities and treated with or without doxycycline (DOX, 1 μg/ml) for 9 days. Colony formation was measured by crystal violet staining. Pictures show representative wells of one out of three independent experiments. Graphs depict a quantification of absorbance measured after cell de-staining (one representative experiment out of three performed) (mean ± s.d.). Clonogenic growth is significantly impaired in all three cell lines on SPRY1 re-expression (*$P < 0.05$, **$P < 0.01$ and ***$P < 0.005$). (**b**) A673/TR/SPRY1, SKES/TR/SPRY1 and SKNMC/TR/SPRY1 cells were platted in triplicate in soft agar and cultured in the presence or absence of doxycycline (DOX, 1 μg/ml) during 25 days and subsequently stained with crystal violet. Pictures show representative images of sphere formation taken at the end of the experiment. Graphs depict the mean area per particle after 25 days (mean ± s.d.). SPRY1 re-expression inhibits sphere formation in all three cell lines (3 independent experiments) (*$P < 0.05$, **$P < 0.01$ and ***$P < 0.005$). (**c**) A673/TR/SPRY1, SKES/TR/SPRY1 and SKNMC/TR/SPRY1 cells were platted in triplicates and treated with or without doxycycline (DOX, 1 μg/ml) for 72 h. A 'wound gap' was created by scratching the cell monolayer using a micropipette tip. Pictures depict the healing of the gap as a consequence of cell migration at the beginning, middle and end of the experiments. Relative wound closure for each cell line at the end of the experiment is stated in percentages. Images show a representative experiment out of three performed. (**d**) A673/TR/SPRY1, SKES/TR/SPRY1 and SKNMC/TR/SPRY1 cells were incubated in the absence or presence of doxycycline (DOX, 1 μg/ml) during 48 h, to induce the expression of SPRY1 protein. Afterwards, cells were starved for another 24 h. Next, they were placed in the upper compartment of a transwell and allowed to migrate through the membrane in response to serum. Migrating cells were quantified by crystal violet staining. Figure shows mean ± s.d. of two experiments performed in triplicate. Data are shown as arbitrary units of absorbance (abs) (*$P < 0.05$ and ***$P < 0.005$).

standard (10%) serum conditions. Next, we explored the effect of SPRY1 induction on the ERK activation mediated by basic FGF (bFGF), an established and potent RAS-activating growth factor. Using bFGF stimulation we observed a similar effect on ERK activation (Figure 4) in the three Ewing cell lines.

Collectively, these results indicate that EWS-FLI1-mediated SPRY1 repression in Ewing sarcoma cells contributes to the activation of MAPK/ERK pathway and thus to the malignant features observed.

FGFR inhibitors mimic the effects of SPRY1 re-expression.

As SPRY1 proved to be capable of inhibiting ERK phosphorylation, especially when the FGF pathway was activated, we assessed the effect of four FGFR inhibitors (PD-173074 [PD-74], PD-166866 [PD-66], SU5402 [SU54] and NVP-BGJ398 [BG-98]) on Ewing sarcoma cells (A673, SKNMC, SKES, RDES and POE), in order to test whether FGFR inhibition can mimic SPRY1 effect on Ewing cell lines. Complementary to our previous finding that bFGF can induce proliferation in Ewing sarcoma cell lines (that is, A673, SKNMC and POE cells),[26] we observed that FGFR inhibition reduces proliferation of these Ewing sarcoma cells (Figure 5a), whereas it did not affect normal cells such as fibroblasts (IMR90). Consistently, FGFR inhibition through any of the four FGF inhibitors severely impairs clonogenic growth of A673, SKNMC and POE Ewing sarcoma cell lines (Figure 5b).

As POE cells exhibited high sensitivity toward this FGFR inhibiton compared with the other cells tested (Supplementary Table 2), we chose this cell line to perform *in vivo* experiments to test whether PD-74 has an antitumoral effect in a xenograft model in mice. As shown in Figure 5c, PD-74 treatment significantly inhibited tumor growth ($P = 0.004$) of Ewing sarcoma xenografts. These tumors showed an ~50% decrease in the number of mitoses ($P = 0.001$) along with a 40% increase in the number of apoptotic cells per high-power field ($P = 0.001$) when comparing vehicle versus PD-74 treatment. Moreover, Ki-67 staining for proliferation showed a significant reduction in the number of Ki67-positive cells in the tumor samples treated with PD-74 ($P < 0.01$) (Figure 5d).

To confirm whether PD-74 had an antitumoral effect in other Ewing sarcoma cell lines we performed an *in vivo* experiment using SKES cells, which presented less sensitivity to it *in vitro* (Figure 5a). As shown in Supplementary Figure S4A, PD-74 had a dose-dependent effect on SKES xenograft growth in mice, with 20 mg/kg being the most effective dose ($P = 0.005$). Again,

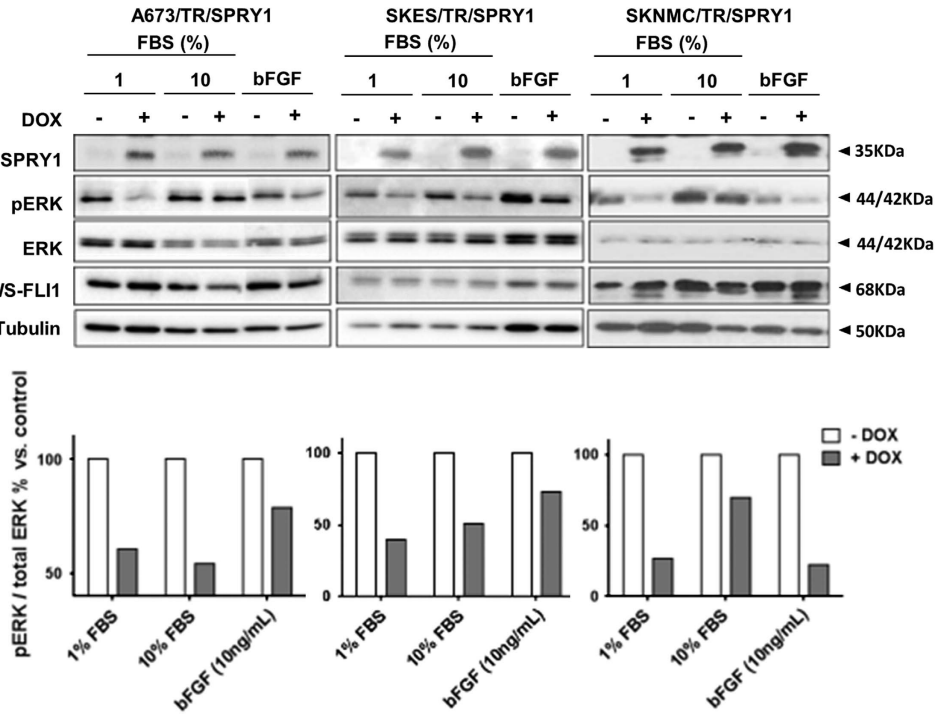

Figure 4. SPRY1 inhibits MAPK pathway in Ewing sarcoma cells by inhibiting ERK phosphorylation induced by bFGF or serum. A673/TR/SPRY1, SKES/TR/SPRY1 and SKNMC/TR/SPRY1 cells were incubated in the absence or in the presence of doxycycline (DOX, 1 μg/ml) during 48 h, to induce the expression of SPRY1 protein. Afterwards, cells were starved for an extra 24 h (1% FBS) and finally stimulated for 15 min with 10% FBS or bFGF (bFGF, basic fibroblast growth factor) (10 ng/ml) where indicated. SPRY1, phospho-ERK (pERK), ERK and EWS-FLI1 proteins were detected by specific antibodies. Anti-tubulin was used as a control for loading and transferring. SPRY1 re-expression is capable of inhibiting ERK phosphorylation induced by bFGF or serum in all three cell lines. Graphs depict densitometries corresponding to the western blotting bands showing pERK/total ERK ratios in percentage versus cells cultured in the absence of doxycycline (control). The figure shows one representative experiment out of three performed.

we observed a significant reduction of the number of mitoses ($P = 0.01$) and a significant increase in the number of apoptotic cells per high-power field ($P < 0.001$) on treatment with PD-74 (20 mg/kg) (Supplementary Figure S4B). Similarly, we detected significantly less Ki-67 positive cells on treatment of with PD-74 ($P < 0.01$) (Supplementary Figure S4B).

We next explored the combined effect of FGFR inhibition and SPRY1 re-expression. SPRY1 was re-expressed in the three Ewing sarcoma cell lines and they were concomitantly treated with either bFGF or PD-74 alone or a combination of both (Figure 6). In analogy to the results presented in Figure 2, SPRY1 significantly inhibited cell proliferation induced by bFGF in the three cell lines studied. Moreover, the effect of SPRY1 re-expression and PD-74 on cell proliferation was similar in A673 and SKNMC cells (Figure 6). Furthermore, when the three cell lines were treated with other FGF inhibitors (BG98, PD-66 and SU54), two of them (BG98 and PD-66) were able to significantly further reduce the proliferation beyond the effect of SPRY1 alone (Supplementary Figure S5). However, when SPRY1 was re-expressed concomitantly with any of the three new inhibitors tested, none of them produced a further impairment in proliferation on any of the cells tested, which is in agreement with what was previously observed with PD-74 (Supplementary Figure S5).

SPRY1 expression positively correlates with improved overall survival of Ewing sarcoma patients

Our results indicate that SPRY1 repression leads to a constitutive activation of MAPK/ERK pathway in response to external stimuli such as bFGF. Thus, we wondered whether the expression levels of SPRY1 *in situ* could be associated with clinical outcome in Ewing sarcoma patients.

First, SPRY1 mRNA levels were examined in a cohort of 117 Ewing sarcoma samples studied with gene expression microarrays and compared them with published microarray data sets comprising 24 different solid tumor types.[27] This analysis revealed that Ewing sarcoma range among the ones with the lowest SPRY1 expression (Figure 7a), although in *in situ* tumors there was more heterogeneity in the SPRY1 mRNA levels as compared with Ewing sarcoma cells in culture (Figure 7b). Moreover, there was statistically less *SPRY1* expression in Ewing sarcoma cell lines as compared with primary tumors. In fact, all cell lines except for one exhibited less *SPRY1* expression than the median sample of primary tumors. In contrast, there was no statistical difference in *LOX*, *NR0B1* and *CD99* expression in cell lines when compared with primary tumors (Figure 7b).

Next, we analyzed the correlation between SPRY1 levels in primary tumors and clinical outcome in a cohort of 162 Ewing sarcoma patients.[28] The median expression value of SPRY1 was used as a cutoff to define moderate and low SPRY1 expression levels. Using this cutoff, moderate *SPRY1* expression levels were significantly associated with a better overall survival (5-year overall survival 0.70 vs 0.38, $P = 0.002$; log-rank test) and event-free survival (5-year event-free survival 0.72 vs 0.45, $P = 0.0015$; log-rank test) (Figures 7c and d). Interestingly, low SPRY1 levels were associated with a higher risk for the presence of metastasis at diagnosis ($P = 0.002$, Fisher's exact test) (Figure 6e). Collectively, these results strongly support a relationship between the levels of SPRY1 and Ewing sarcoma aggressiveness.

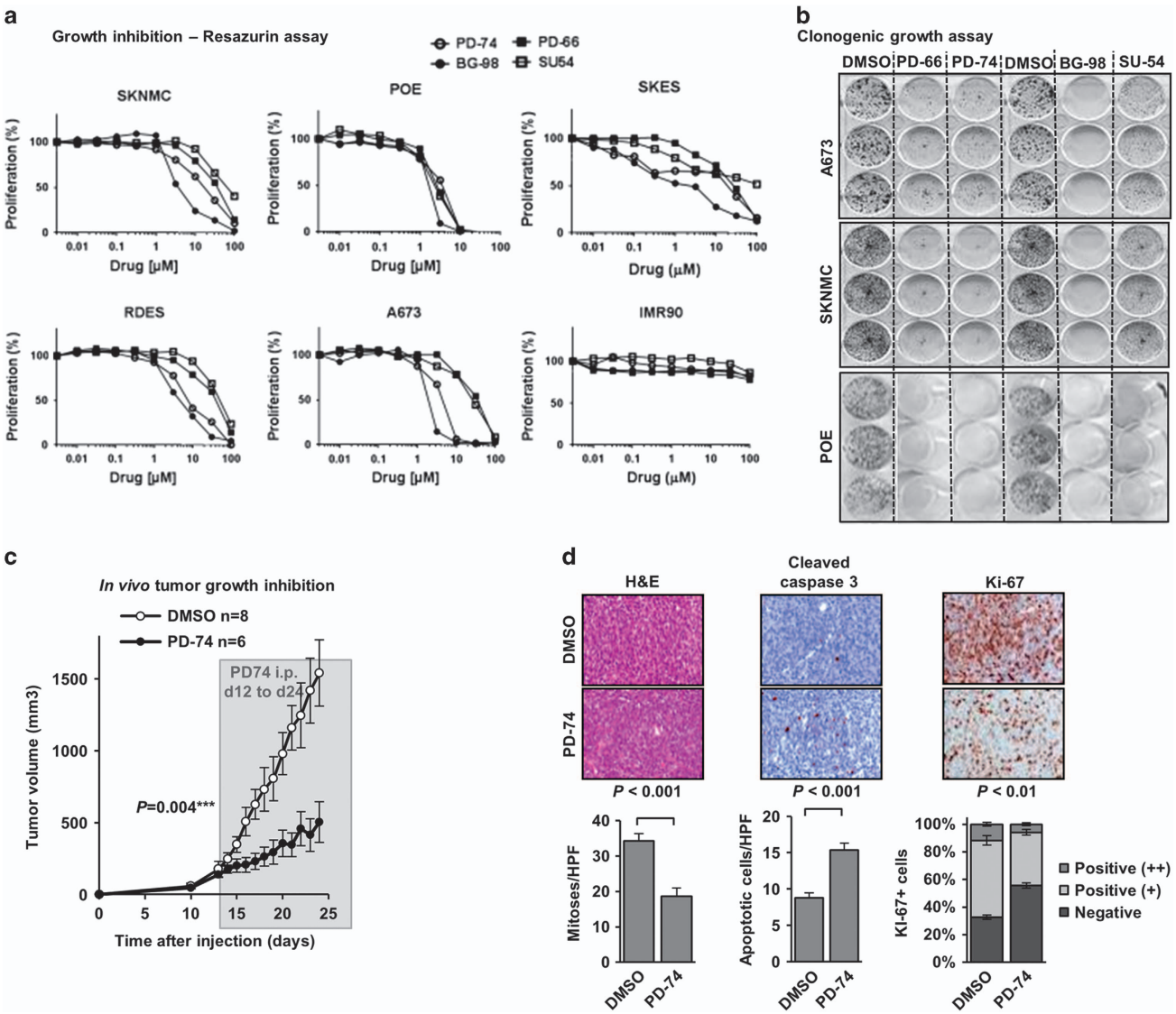

Figure 5. FGFR inhibitors block Ewing sarcoma cell line proliferation. (**a**) Four FGFR inhibitors, namely PD-173074 (PD-74), PD-166866 (PD-66), SU5402 (SU54) and NVP-BGJ398 (BG-98), inhibit A673, SKNMC, POE, RDES and SKES Ewing cell growth *in vitro* in a dose-dependent manner, whereas normal cells (IMR90 fibroblasts) remained unaffected. PD-74 proved to be most effective in four out of five Ewing sarcoma cell lines tested. Cells were grown in 10% FBS conditions and cell proliferation was measured after 72 h using a Resazurin assay. (**b**) PD-173074 (PD-74), PD-166866 (PD-66), SU5402 (SU54) and NVP-BGJ398 (BG-98) impair A673, SKNMC and POE Ewing sarcoma cells clonogenic growth *in vitro* when cells are grown at 5% FBS for 10–12 days. (**c**) C.B17/SCID mice were injected with POE cells and randomly split in groups. Each group was treated intraperitoneally once a day with PD-74 or placebo. The figure shows the evolution of tumor volume (mean ± s.e.m. of six to eight animals per group) versus time. PD-74 treatment significantly inhibits tumor growth ($P = 0.004$) of Ewing sarcoma xenografts. (**d**) Immunohistochemistry images of tumors obtained in the *in vivo* experiments. Tissue sections were stained with Ki-67 to detect proliferation and cleaved caspase 3 to detect apoptosis. The graphs show how PD-74 treatment reduces the number of mitoses ($P = 0.001$) and increases the number of apoptotic cells per field ($P = 0.001$). Ki-67 staining and graph show a reduction in the number of Ki67-positive (++ or +) cells when treated with PD-74 ($P < 0.01$).

DISCUSSION

EWS-ETS fusion proteins have a central role in the pathogenesis of Ewing sarcoma by regulating the expression of other key factors. In this sense, the identification of these regulated genes may help characterize the pathways involved in Ewing sarcoma pathogenesis and aggressiveness, and to therefore open new opportunities for targeted therapies.[29]

In this study, we showed that SPRY1, a member of the Sprouty family of proteins, is repressed by EWS-FLI1 and is not expressed in established Ewing sarcoma cell lines. The exact mechanism through which EWS-FLI1 regulates SPRY1 is still unknown. However, analysis of two independent chromatin immunoprecipitation sequencing studies[30,31] indicates that EWS-FLI1 does not bind to SPRY1 promoter directly (Supplementary Figure S6). Interestingly, on EWS-FLI1 knockdown there is an increase of H3K27ac marks located at the putative SPRY1 promoter comprising SPRY1 exon 1 and intron 1 (Supplementary Figure S6). This suggests an epigenetic mechanism of *SPRY1* regulation involving histone modifications, instead of a direct binding of EWS-FLI1 to the *SPRY1* promoter. Moreover, there were no significant differences in the percentage of SPRY1 CpG islands' methylation on modulation of EWS-FLI1 expression levels.[32] Accordingly, we propose that the actual mechanism underlying *SPRY1* regulation in Ewing sarcoma may be different from the one operating in other tumors where SPRY1 downregulation is associated with promoter methylation.[22,33,34]

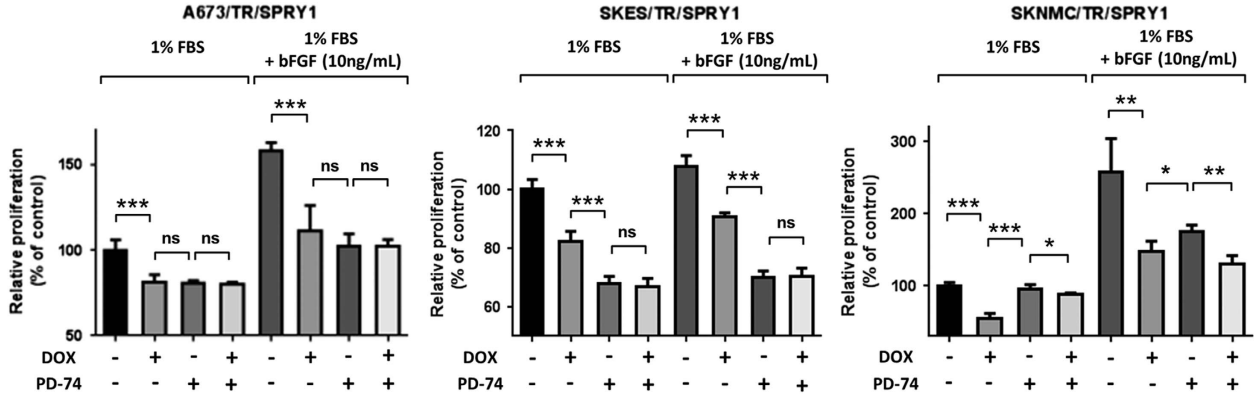

Figure 6. bFGF induces proliferation of Ewing sarcoma cells, which can be antagonized by FGFR inhibition. A673/TR/SPRY1, SKES/TR/SPRY1 and SKNMC/TR/SPRY1 cells were incubated in the absence or in the presence of doxycycline (DOX, 1 μg/ml), to induce the expression of SPRY1 protein, and were concomitantly cultured with 1% FBS, bFGF (10 ng/ml), PD-173074 (PD-74, 5 μM) or a combination of bFGF and PD-74 where indicated. Cell proliferation was measured after 72 h using the Resazurin assay. Graphs depict one independent experiment (mean ± s.d.) out of three performed. SPRY1 re-expression and PD-74 inhibit cell proliferation-induced serum or bFGF treatment (*$P < 0.05$ and **$P < 0.005$, ns, nonsignificant).

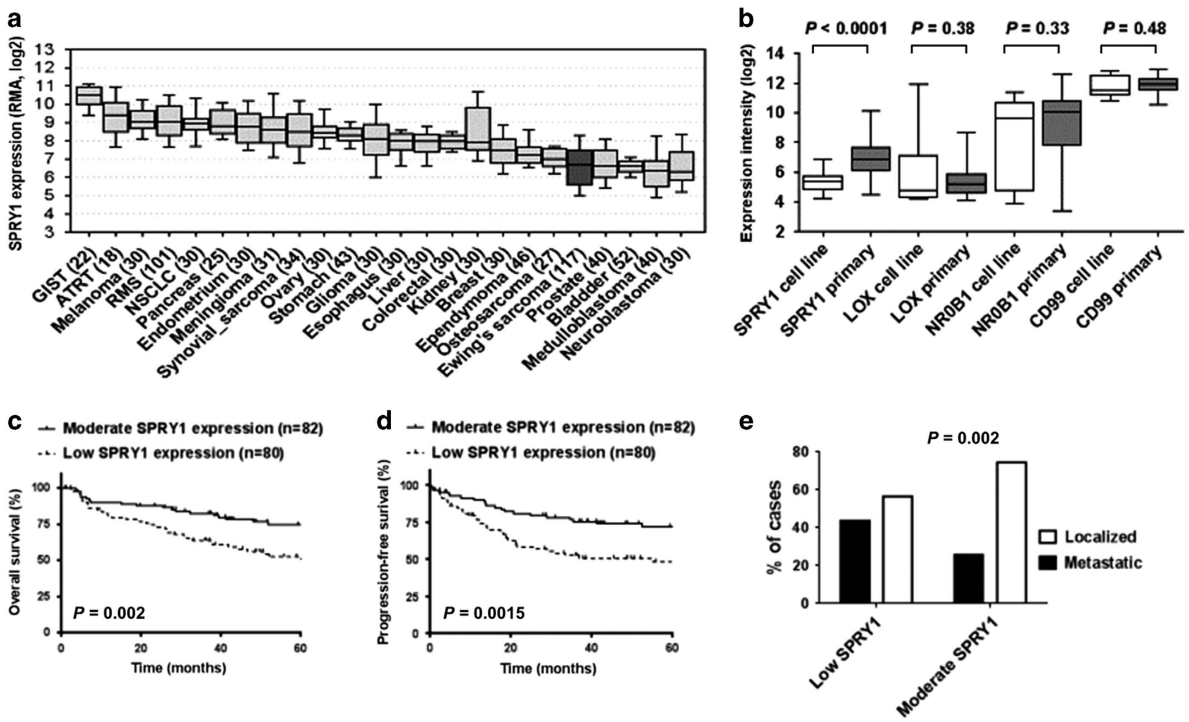

Figure 7. SPRY1 expression is positively correlated with improved overall survival of Ewing sarcoma patients. (**a**) SPRY1 mRNA expression levels in 24 different solid tumor entities as determined by Affymetrix HG-U133plus2.0 DNA microarrays. Data were retrieved from the Gene Expression Omnibus (GEO) or the European bioinformatics Institute (EBI) and simultaneously normalized by RMA using brain array CDF files (v17, ENTREZG) as previously described.[27] Data are represented as medians with boxes representing the interquartile range. Whiskers indicate the 10th and 90th percentile of the data. The number of analyzed samples is given in parentheses. Ewing sarcoma tumors are shown in gray. ATRT, atypical teratoid rhabdoid tumor; Ca-, carcinoma; GIST, gastrointestinal stromal tumor; NSCLC, non-small cell lung carcinoma; RMS, rhabdomyosarcoma. (**b**) Relative expression of *SPRY1* as compared with other EWS-FLI1 target genes (*LOX* and *NR0B1*) and CD99 in 15 individual Ewing sarcoma cell lines versus 117 primary Ewing sarcoma samples (all Affymetrix HG-U133Plus2.0 microarrays). Data were retrieved from the GEO (accession codes: GSE8596, GSE36133, GSE70826 and GSE34620) and simultaneously normalized by RMA using brainarray CDF files (v17, ENTREZG) as previously described.[27] Unpaired two-tailed Student's *T*-test. (**c**) Kaplan–Meier survival estimates (overall survival) in the Ewing sarcoma patient cohort. Patients were classified as being either SPRY1 low or moderate (cutoff: median SPRY1 expression; $P = 0.002$, log-rank test). (**d**) Graph depicts the relapse-free survival probability versus SPRY1 level of expression (low or moderate, cutoff: median SPRY1 expression). SPRY1 expression positively correlates with improved relapse-free probability ($P = 0.0015$, log rank test). (**e**) Graph shows the percentage of cases with metastasis at diagnosis versus SPRY1 level of expression (low or moderate, cutoff: median SPRY1 expression). Moderate SPRY1 expression correlates with lower risk of metastasis at diagnosis ($P = 0.002$, Fisher's exact test).

As SPRY1 has been shown to be a potent negative regulator of the RAS/MAPK/ERK signaling pathway,[35] we hypothesized that *SPRY1* may act as a tumor suppressor gene in Ewing sarcoma. In support of this notion, induction of SPRY1 in three independent Ewing sarcoma cell lines significantly impaired cell proliferation and migration. This is consistent with a tumor supressor function of SPRY1 in Ewing sarcoma and in agreement with previous reports showing that SPRY1 overexpression impairs cell growth, proliferation, migration and invasion of a variety of cancer cell lines including ovarian carcinoma, breast cancer, lung adenocarcinoma, colon carcinoma or osteosarcoma.[24,36–38]

Our results also demonstrate that SPRY1 downregulation is necessary for bFGF-mediated proliferation and activation of RAS/MAPK/ERK pathways in Ewing sarcoma cells. Thus, SPRY1 re-expression in the three Ewing sarcoma cell lines used in this study impaired cell proliferation and ERK phosphorylation induced by bFGF. bFGF is known to mediate proliferation, migration and differentiation in various cellular contexts[39–42] and FGF-regulated pathways have a preponderant role in cancer (reviewed in Touat *et al*.[43]). Notably, an important role for FGF-dependent pathways in Ewing sarcoma pathogenesis is emerging. We have recently reported that bFGF increases proliferation of Ewing sarcoma cells *in vitro*, and that *EGR2*, which is a downstream component of the FGF pathway, is an EWS-FLI1-induced target gene.[26] Other studies have demonstrated that bFGF regulates motility and invasion of Ewing sarcoma cells in the bone microenvironment.[44] In agreement, Agelopoulos *et al*.[45] recently showed that constitutive knockdown of *FGFR1* abolishes engraftment of Ewing sarcoma xenografts in mice. Interestingly, over 75% of Ewing sarcoma biopsy samples present moderate-to-high levels of FGFR1 phosphorylation,[44] although activating FGFR1 mutations are extremely rare in this disease.[45]

In light of these facts and our new results, we propose that constitutive activation of FGFRs and downstream pathways are key contributors to the pathogenesis of Ewing sarcoma, and that EWS-FLI1-mediated suppression of the negative-feedback regulator SPRY1 constitutes a major mechanism for sustained FGFR phosphorylation and thus unrestrained FGF-induced signal transduction and tumor progression. In synopsis, our results support that SPRY1 downregulation is pre-requisite for enhanced proliferation and migration of Ewing sarcoma cells induced by either EWS-FLI1 itself, external growth factor stimulation or a combination of both as part of an autocrine loop.

The importance of this pathway in Ewing sarcoma pathogenesis is additionally illustrated by FGFR-inhibition-mediated impairment of cell proliferation and clonogenic growth of Ewing sarcoma cells *in vitro*. Interestingly, the search for more efficient and specific FGFR inhibitors is an active field in the pharmaceutical industry, as FGF signaling pathways is one of the most commonly mutated systems in cancer.[43] In this regard, the Ewing sarcoma research community can take advantage of the development of these new drugs, some of which are being tested in clinical trials with promising results, particularly in tumors harboring aberrant FGFR signaling (reviewed in Touat *et al*.[43]).

FGFR signaling can be aberrantly activated in Ewing sarcoma either through downregulation of SPRY1 (as observed in most cases), through overexpression of FGFRs (as observed in subset of patients[45]), or very rarely through somatic mutations.[45] For that reason, we anticipate that Ewing sarcoma patients may benefit from targeted drugs directed against FGFRs or its downstream targets. In support of this notion, Agelopoulus *et al*.[45] reported on a single patient affected by relapsed Ewing sarcoma, who was treated with an FGFR-tyrosine kinase inhibitor (ponatinib), which led to a reduction in 18-FDG-PET activity and thus glucose uptake by the tumor.

Interestingly, although SPRY1 was undetectable in established Ewing sarcoma cell lines, its levels in primary tumors were variable. Currently, the reasons for the differences between SPRY1 levels in established cell lines and tumors *in situ* are still unknown; however, it can be hypothesized that SPRY1 levels remain variable in tumors, and that the harsh conditions of *in vitro* cell culture favor the growth of cells with lower SPRY1 levels during establishment of Ewing sarcoma cell lines. In fact, established Ewing sarcoma cell lines harbor a much higher rate of *STAG2*, *TP53* and *CDKN1A* mutations than that observed in primary tumors specimens,[46] suggesting that cells derived from more aggressive tumors are favored in culture.[47,48]

Ewing sarcoma is a very aggressive pediatric malignancy in which primary metastasis is the most unfavorable risk factor, very often leading to fatal outcome despite highly intense and toxic treatment.[49] Here we show that low *SPRY1* expression levels correlate with a significantly worse overall and event-free survival in a large cohort of Ewing sarcoma patients. More interestingly, primary tumors displaying low levels of SPRY1 were more frequently observed in patients harboring metastasis at diagnosis. This is compatible with a more aggressive behavior of SPRY1-low tumors and in agreement with the results observed in the *in vitro* experiments. We speculate that tumors expressing low levels of SPRY1 would present a higher response to external growth factor stimulation and thus exhibit higher rates of proliferation and migration, making them more aggressive. This may have a potential clinical application, as SPRY1 has been recently proposed as a possible tissue biomarker to differentiate aggressive from indolent prostate carcinomas.[50]

In summary, our data provide evidence that EWS-FLI1-mediated SPRY1 downregulation is an important mechanism in Ewing sarcoma pathogenesis. Moreover, our results strongly suggest that bFGF-mediated stimulation of cell proliferation could be more important than initially acknowledged in Ewing sarcoma, and that FGFR inhibitors may constitute promising drugs for treatment of Ewing sarcoma patients.

MATERIALS AND METHODS

Cell culture

A673/TR/shEF cells, which have been described elsewhere,[7] were cultured in Dulbecco's modified Eagle's medium supplemented with 10% tetracycline-free FBS (Clontech, Mountain View, CA, USA), 2 mM L-glutamine, 100 μg/ml zeocin and 3 μg/ml blasticidin. Induction of a small hairpin RNA against EWS-FLI1 was started by the addition of 1 μg/ml doxycycline (Sigma, St Louis, MO, USA). Ewing sarcoma cell lines A4573, TC-71, RD-ES, POE and TTC-466, and the normal fibroblast cell line IMR90 were maintained in RPMI 1640 medium, SK-PN-DW and SKNMC wild-type cells were maintained in Iscove's modified Dulbecco's medium, and wild-type A673 and SKES cells were maintained in Dulbecco's modified Eagle's medium. All media were supplemented, if not otherwise stated, with 10% FBS, 2 mM L-glutamine (Invitrogen, Paisley, UK) and 1% penicillin and streptomycin. All cells were routinely tested for mycoplasma contamination (Mycoalert mycoplasma detection kit, Lonza #LT07-318, Basel, Switzerland) and were authenticated by short tandem repeats profiling at the Genomic Facility at Biomedical Research Institute, CSIC, Madrid, Spain).

Establishment of Ewing sarcoma cell lines stably expressing doxycycline-inducible *SPRY1* cDNA

The complete coding region of *SPRY1* was reverse transcription–PCR amplified from A673/TR/shEF cells stimulated with doxycycline using primers 5′-GCGGTCGACGAGATCACTACACATGGATCC-3′ (forward) and 5′-CGGCGGCC GCTCATCATCATGATGGTTTACCCTGACC-3′ (reverse). The amplified fragments were digested with *Sal*I and *Not*I, cloned into the pENTR2B plasmid (Invitrogen) and transferred by recombination to the lentiviral doxycycline-inducible plasmid pLenti4-TO-V5-DEST (Invitrogen). Next, A673/TR, SKES/TR and SKNMC/TR Ewing sarcoma cells expressing the tetracycline repressor constitutively were infected with lentiviruses containing the SPRY1 cDNA. Control cells were infected with empty lentiviral vector. Stable clones were selected with zeocin (100 μg/ml). Induction of SPRY1 was assayed by western blottings on doxycycline (1 μg/ml) stimulation. Clones displaying the highest levels of protein expression on doxycycline stimulation were chosen for additional studies.

Reverse transcription–quantitative PCR

Reverse transcription–quantitative PCR conditions, primer and TaqMan probe sequences specific for *EWS-FLI1*, *LOX*, *NR0B1(DAX1)* and *TBP* were described elsewhere.[7,13,51] TaqMan probes for SPRY1, 2, 3 and 4 were purchased to Life Technologies (San Diego, CA, USA). Reactions were run on a RotorGene 6000 (Corbett Research, Sydney, NSW, Australia) and relative expression was calculated as previously described.[51]

Western blot analysis and antibodies

Procedure was described elsewhere.[13] Primary antibodies were purchased to the following companies: anti-FLI1 polyclonal antibody from NeoMarkers (#RB-9295-P) (Fremont, CA, USA), anti-SPRY1 monoclonal antibody from Santa Cruz Biotechnology (#100861) (Dallas, TX, USA), Tubulin monoclonal antibody from Sigma Aldrich (#T9026) (St Louis, MO, USA), and anti-Phospho-p44/42 (pERK, #9106) and anti-p44/42 ($_{total}$ERK, #9102) were from Cell Signaling (Danvers, MA, USA). Anti-mouse (#2055) and anti-rabbit IgG (#2054) horseradish peroxidase-conjugated secondary antibodies were purchased from Santa Cruz Biotechnology.

Bromodeoxyuridine proliferation assay

Cells were plated in octaplicates (1×10^3 cells per well in 96 multi-well plates) and cultured in the presence or absence of doxycycline (1 μg/ml) for 72 h in 10% or 1% tetracycline-free FBS (Clontech). Thereafter, bromodeoxyuridine chemiluminescent assay (Roche, Basel, Switzerland) was performed according to manufacturer's instructions. Chemiluminescence was measured using an Infinite M200 (Tecan, Mannerdorf, Switzerland) microplate reader.

Resazurin proliferation assay

Cells were plated in octaplicates (2.5×10^3 cells per well in 96 multi-well plates) and concomitantly cultured in the presence or absence of doxycycline (1 μg/ml) and stimuli (1% or 10% tetracycline-free FBS or 10 ng/ml bFGF) for 72 h. For bFGF-inhibitor testing, cells were grown at 10% FBS for 72 h in the presence of PD-173074 (PD-74) (Selleckchem, Houston, TX, USA), PD-166866 (PD-66) (#PZ0114, Sigma Aldrich), SU5402 (SU54) (#S7667, Selleckchem) or NVP-BGJ398 (BG-98) (#S2183, Selleckchem). Thereafter, Resazurin (#R7017, Sigma Aldrich) was added to the media at 0.15 μg/ml and incubated for 2 h at 37 °C. Fluorescence was recorded using a 560-nm excitation/590-nm emission filter set in an Infinite M200 microplate reader (Tecan).

xCELLigence proliferation assay

Cell proliferation was assayed in real time with a bioelectric xCELLigence instrument (Roche/ACEA Biosciences). In each well, $3–4 \times 10^3$ Ewing sarcoma cells were seeded in 200 μl media containing 10% tetracycline-free FBS and treated with doxycycline (1 μg/ml) or vehicle (triplicate wells/group). Cellular impedance was measured periodically and media with or without doxycycline were changed once after 72 h.

Flow cytometry analysis of cell cycle

Cells were treated with doxycycline (1 μg/ml) for 72 h to induce the expression of SPRY1 and fixed with 70% ethanol for 24 h at 4 °C. Next, they were stained with a solution of 0.005% (w/v) of propidium iodide and RNAase A as recommended by the manufacturer (BD Biosciences, San José, CA, USA) and were incubated at 37 °C for 30 min. They were then analyzed in a MACS Quant Analyzer flow cytometer (Miltenyi Biotec, Cologne, Germany).

Wound-healing assay

Cells were plated in triplicates ($2–4 \times 10^4$ cells per well in 24 multi-well plates) and were incubated with or without doxycycline (1 μg/ml) for 72 h before the assay. At the end of this period, a 'wound gap' in the cell monolayer was created using a micropipette tip. The healing of the gap by cell migrating was monitored by photographing the progress every 6–12 h until wound closure. Quantification of relative cell migration is described elsewhere.[52]

Transwell assay

Cells were pre-treated with doxycycline (1 μg/ml) for 24 h to induce the expression of SPRY1 protein. Next, they were starved (0.5% FBS) for another additional 24 h in the same doxycycline conditions. Then, 3×10^5 pretreated cells were re-suspended in 2 ml of medium containing 0.5% tetracycline-free FBS and placed in the upper chamber of transwells (8.0 μm pore size) (Corning Costar, Cambridge, MA, USA) following the procedure described elsewhere.[13]

Soft agar assays

Cells were plated by triplicate (5×10^5 cells per 60 mm dishes) in soft agar and cultured in the presence or absence of doxycycline during 25 days. Fresh culture medium was added to plates every 2–3 days. At the end of the experiment, three random fields for each plate were photographed. The number of colonies per field and its respective area were calculated using NIH ImageJ software (National Institute of Health, Bethesda, MD, USA).

Clonogenic assay

A673/TR/SPRY1, SKES/TR/SPRY1 and SKNMC/TR/SPRY1 cells were plated in triplicates at 0.5×10^3, 1×10^3 and 2×10^3 cells per well, respectively, in a 24-well plate. They were subsequently treated with or without doxycycline (1 μg/ml) and maintained for 9 days in culture media supplemented with 5% tetracycline-free FBS. Media was changed every 3–4 days and doxycycline treatment was continued. Finally, colonies were fixed, stained with crystal violet and photographed. Cells were de-stained using 50% ethanol 0.1 M sodium citrate pH 4.2. Absorbance was quantified at 560 nm using an Infinite M200 (Tecan) microplate reader.

Tumor xenografts in mice

POE and SKES cells were resuspended in PBS/matrigel (BD Biosciences, Le Pont de Claix Cedex, France) (1:1) and injected (8×10^6/200 μl) subcutaneously in the flanks of 6-week old C.B17/SCID male and female mice (Charles River Laboratories, Lyon, France). When tumor volume reached 150 mm^3 (calculated with the formula length × width × depth × 0.5432), mice were injected intraperitoneally once a day with the indicated dose of PD-173074 (5, 10 or 20 mg/kg) dissolved in 10% dimethyl sulfoxide–90% Corn Oil (Sigma) or placebo in the control group. Tumor growth was monitored with a caliper and mice were killed when tumors reached a volume of 1500 mm^3. Experiments were carried out in accordance with recommendations of the European Community (86/609/EEC), the French Competent Authority, the UKCCCR guidelines (guidelines for the welfare and use of animals in cancer research), the Ethics Committee at ISCIII (CBA #64_2015-v2) and the Spanish Competent Authority (PROEX 009/16).

Histology and immunohistochemistry

Immunohistochemistry analyses were done on formalin-fixed, paraffin-embedded xenograft tumors. All tissue samples were collected at the Institute of Pathology of the LMU Munich for immediate immunohistochemistry staining, for which 4-μm sections were cut. Antigen retrieval was carried out by microwave treatment in Dako target retrieval solution (S2369). The following primary antibodies were used: polyclonal rabbit anti-cleaved-caspase-3 (1:100 at room temperature for 60 min; #9661, Cell Signaling) or monoclonal rabbit anti-Ki67 (1:200 at room temperature for 60 min; #275R-15 clone SP6, Cell Marque, Rocklin, CA, USA). The ImmPRESS Reagent Kit anti-rabbit IgG (MP-7401, Vector Laboratories, Burlingame, CA, USA) was used for antigen detection. Sections were counterstained with hematoxylin Gill's Formula (H-3401, Vector Laboratories). The average number of positive cells was determined by analysis of 10 high-power fields (×40 magnification) for each xenograft tumor. Statistical differences between groups were calculated with an unpaired tow-tailed Student's *T*-test.

Patients

A total of 162 Ewing sarcoma patients with available clinical data and tumor samples were used in this study. This cohort consists of 117 Ewing patients for which gene expression profiles in primary tumors were analyzed with HG-U133 plus2.0 microarrays (Affymetrix, Santa Clara, CA, USA) (Gene Expression Omnibus accession number: GSE34620) and 45 patients whose gene expression profiles were studied with Uniset Human 20 K I microarrays (Codelink Amersham Bioscience, Piscataway, NJ, USA). All patients received a similar protocol treatment.

Statistical analysis

For a single comparison of two groups, two-tailed Student's *t*-test was used and a normal distribution was assumed. Variances between the groups that were compared were similar. For animal studies, the sample size was estimated to be six to eight mice considering a signal/noise ratio of 1.6–1.8, 80% power, assuming a 5% significance level and a two-sided test. No investigator blinding was done during the experiment. For *in situ* studies including overall survival and relapse-free survival probabilities, log-rank test was used. For proportions, Fisher's exact test was used. For all analyses, the level of significance was set at $P = 0.05$ and the variance was similar between groups. All statistical calculations were performed using the GraphPad Prism software version 6.0 (GraphPad Software, San Diego, CA, USA).

CONFLICT OF INTEREST

The authors declare no conflict of interest.

ACKNOWLEDGEMENTS

FC-A, LG-G, JCL, AS, PG-M, SEL-P, SM and JA are supported by Asociación Pablo Ugarte and Miguelañez SA, ASION-La Hucha de Tomás, Fundación La Sonrisa de Alex and Instituto de Salud Carlos III (PI12/00816 and Spanish Cancer Network RTICC RD12/0036/0027). TGPG is supported by a grant from 'Verein zur Förderung von Wissenschaft und Forschung an der Medizinischen Fakultät der LMU München (WiFoMed)', the Daimler and Benz Foundation in cooperation with the Reinhard Frank Foundation, by LMU Munich's Institutional Strategy LMUexcellent within the framework of the German Excellence Initiative, the 'Mehr LEBEN für krebskranke Kinder—Bettina-Bräu-Stiftung', the Walter Schulz Foundation, the Fritz Thyssen Foundation (FTH-40.15.0.030MN) and by the German Cancer Aid (DKH-111886 and DKH-70112257). The 'Genetics and Biology of Cancers' team (TGPG, DS and OD) is supported by grants from the Ligue Nationale Contre Le Cancer (Equipe labellisée). This work was also supported by the European PROVABES, ASSET and EEC FP7 grants. We also thank the following associations for their invaluable support: the Société Française des Cancers de l'Enfant, Courir pour Mathieu, Dans les pas du Géant, Olivier Chape, Les Bagouzamanon, Enfants et Santé and les Amis de Claire. We thank Dr S Navarro (University of Valencia, Valencia, Spain) and Dr TJ Triche (Children's Hospital Los Angeles, Los Angeles, USA) for providing us with Ewing sarcoma cell lines A4573 and TTC-466, respectively.

REFERENCES

1 Mackintosh C, Madoz-Gurpide J, Ordonez JL, Osuna D, Herrero-Martin D. The molecular pathogenesis of Ewing's sarcoma. *Cancer Biol Ther* 2010; **9**: 655–667.
2 Grohar PJ, Helman LJ. Prospects and challenges for the development of new therapies for Ewing sarcoma. *Pharmacol Ther* 2013; **137**: 216–224.
3 Ladenstein R, Potschger U, Le Deley MC, Whelan J, Paulussen M, Oberlin O *et al.* Primary disseminated multifocal Ewing sarcoma: results of the Euro-EWING 99 trial. *J Clin Oncol* 2010; **28**: 3284–3291.
4 Zhu L, McManus MM, Hughes DP. Understanding the biology of bone sarcoma from early initiating events through late events in metastasis and disease progression. *Front Oncol* 2013; **3**: 230.
5 Delattre O, Zucman J, Plougastel B, Desmaze C, Melot T, Peter M *et al.* Gene fusion with an ETS DNA-binding domain caused by chromosome translocation in human tumours. *Nature* 1992; **359**: 162–165.
6 Kovar H. Blocking the road, stopping the engine or killing the driver? Advances in targeting EWS/FLI-1 fusion in Ewing sarcoma as novel therapy. *Expert Opin Ther Targets* 2014; **18**: 1315–1328.
7 Carrillo J, Garcia-Aragoncillo E, Azorin D, Agra N, Sastre A, Gonzalez-Mediero I *et al.* Cholecystokinin down-regulation by RNA interference impairs Ewing tumor growth. *Clin Cancer Res* 2007; **13**: 2429–2440.
8 Garcia-Aragoncillo E, Carrillo J, Lalli E, Agra N, Gomez-Lopez G, Pestana A *et al.* DAX1, a direct target of EWS/FLI1 oncoprotein, is a principal regulator of cell-cycle progression in Ewing's tumor cells. *Oncogene* 2008; **27**: 6034–6043.
9 Smith R, Owen LA, Trem DJ, Wong JS, Whangbo JS, Golub TR *et al.* Expression profiling of EWS/FLI identifies NKX2.2 as a critical target gene in Ewing's sarcoma. *Cancer Cell* 2006; **9**: 405–416.
10 Surdez D, Benetkiewicz M, Perrin V, Han ZY, Pierron G, Ballet S *et al.* Targeting the EWSR1-FLI1 oncogene-induced protein kinase PKC-beta abolishes ewing sarcoma growth. *Cancer Res* 2012; **72**: 4494–4503.
11 Grunewald TG, Diebold I, Esposito I, Plehm S, Hauer K, Thiel U *et al.* STEAP1 is associated with the invasive and oxidative stress phenotype of Ewing tumors. *Mol Cancer Res* 2012; **10**: 52–65.
12 Prieur A, Tirode F, Cohen P, Delattre O. EWS/FLI-1 silencing and gene profiling of Ewing cells reveal downstream oncogenic pathways and a crucial role for repression of insulin-like growth factor binding protein 3. *Mol Cell Biol* 2004; **24**: 7275–7283.
13 Agra N, Cidre F, Garcia-Garcia L, de la Parra J, Alonso J. Lysyl oxidase is downregulated by the EWS/FLI1 oncoprotein and its propeptide domain displays tumor supressor activities in ewing sarcoma cells. *PLoS One* 2013; **8**: e66281.
14 Navarro D, Agra N, Pestana A, Alonso J, Gonzalez-Sancho JM. The EWS/FLI1 oncogenic protein inhibits expression of the Wnt inhibitor DICKKOPF-1 gene and antagonizes beta-catenin/TCF-mediated transcription. *Carcinogenesis* 2010; **31**: 394–401.
15 Hahm KB, Cho K, Lee C, Im YH, Chang J, Choi SG *et al.* Repression of the gene encoding the TGF-beta type II receptor is a major target of the EWS-FLI1 oncoprotein. *Nat Genet* 1999; **23**: 222–227.
16 Minowada G, Jarvis LA, Chi CL, Neubuser A, Sun X, Hacohen N *et al.* Vertebrate Sprouty genes are induced by FGF signaling and can cause chondrodysplasia when overexpressed. *Development* 1999; **126**: 4465–4475.
17 Guy GR, Wong ES, Yusoff P, Chandramouli S, Lo TL, Lim J *et al.* Sprouty: how does the branch manager work? *J Cell Sci* 2003; **116**: 3061–3068.
18 Christofori G. Split personalities: the agonistic antagonist Sprouty. *Nat Cell Biol* 2003; **5**: 377–379.
19 Zhao Z, Zuber J, Diaz-Flores E, Lintault L, Kogan SC, Shannon K *et al.* p53 loss promotes acute myeloid leukemia by enabling aberrant self-renewal. *Genes Dev* 2010; **24**: 1389–1402.
20 Fritzsche S, Kenzelmann M, Hoffmann MJ, Muller M, Engers R, Grone HJ *et al.* Concomitant down-regulation of SPRY1 and SPRY2 in prostate carcinoma. *Endocr Relat Cancer* 2006; **13**: 839–849.
21 Lo TL, Yusoff P, Fong CW, Guo K, McCaw BJ, Phillips WA *et al.* The ras/mitogen-activated protein kinase pathway inhibitor and likely tumor suppressor proteins, sprouty 1 and sprouty 2 are deregulated in breast cancer. *Cancer Res* 2004; **64**: 6127–6136.
22 Kwabi-Addo B, Ren C, Ittmann M. DNA methylation and aberrant expression of Sprouty1 in human prostate cancer. *Epigenetics* 2009; **4**: 54–61.
23 Kwabi-Addo B, Wang J, Erdem H, Vaid A, Castro P, Ayala G *et al.* The expression of Sprouty1, an inhibitor of fibroblast growth factor signal transduction, is decreased in human prostate cancer. *Cancer Res* 2004; **64**: 4728–4735.
24 Masoumi-Moghaddam S, Amini A, Ehteda A, Wei AQ, Morris DL. The expression of the Sprouty 1 protein inversely correlates with growth, proliferation, migration and invasion of ovarian cancer cells. *J Ovarian Res* 2014; **7**: 61.
25 Barretina J, Caponigro G, Stransky N, Venkatesan K, Margolin AA, Kim S *et al.* The Cancer Cell Line Encyclopedia enables predictive modelling of anticancer drug sensitivity. *Nature* 2012; **483**: 603–607.
26 Grunewald TG, Bernard V, Gilardi-Hebenstreit P, Raynal V, Surdez D, Aynaud MM *et al.* Chimeric EWSR1-FLI1 regulates the Ewing sarcoma susceptibility gene EGR2 via a GGAA microsatellite. *Nat Genet* 2015; **47**: 1073–1078.
27 Willier S, Butt E, Grunewald TG. Lysophosphatidic acid (LPA) signalling in cell migration and cancer invasion: a focussed review and analysis of LPA receptor gene expression on the basis of more than 1700 cancer microarrays. *Biol Cell* 2013; **105**: 317–333.
28 Postel-Vinay S, Veron AS, Tirode F, Pierron G, Reynaud S, Kovar H *et al.* Common variants near TARDBP and EGR2 are associated with susceptibility to Ewing sarcoma. *Nat Genet* 2012; **44**: 323–327.
29 Cidre-Aranaz F, Alonso J. EWS/FLI1 target genes and therapeutic opportunities in Ewing sarcoma. *Front Oncol* 2015; **5**: 162.
30 Bilke S, Schwentner R, Yang F, Kauer M, Jug G, Walker RL *et al.* Oncogenic ETS fusions deregulate E2F3 target genes in Ewing sarcoma and prostate cancer. *Genome Res* 2013; **23**: 1797–1809.
31 Riggi N, Knoechel B, Gillespie SM, Rheinbay E, Boulay G, Suva ML *et al.* EWS-FLI1 utilizes divergent chromatin remodeling mechanisms to directly activate or repress enhancer elements in Ewing sarcoma. *Cancer Cell* 2014; **26**: 668–681.
32 Tomazou EM, Sheffield NC, Schmidl C, Schuster M, Schonegger A, Datlinger P *et al.* Epigenome mapping reveals distinct modes of gene regulation and widespread enhancer reprogramming by the oncogenic fusion protein EWS-FLI1. *Cell Rep* 2015; **10**: 1082–1095.
33 Calvisi DF, Ladu S, Gorden A, Farina M, Lee JS, Conner EA *et al.* Mechanistic and prognostic significance of aberrant methylation in the molecular pathogenesis of human hepatocellular carcinoma. *J Clin Invest* 2007; **117**: 2713–2722.
34 Macia A, Gallel P, Vaquero M, Gou-Fabregas M, Santacana M, Maliszewska A *et al.* Sprouty1 is a candidate tumor-suppressor gene in medullary thyroid carcinoma. *Oncogene* 2012; **31**: 3961–3972.
35 Gross I, Bassit B, Benezra M, Licht JD. Mammalian sprouty proteins inhibit cell growth and differentiation by preventing ras activation. *J Biol Chem* 2001; **276**: 46460–46468.

36 Mekkawy AH, Pourgholami MH, Morris DL. Human Sprouty1 suppresses growth, migration, and invasion in human breast cancer cells. *Tumour Biol* 2014; **35**: 5037–5048.
37 Wiles ET, Lui-Sargent B, Bell R, Lessnick SL. BCL11B is up-regulated by EWS/FLI and contributes to the transformed phenotype in Ewing sarcoma. *PLoS ONE* 2013; **8**: e59369.
38 Liu X, Lan Y, Zhang D, Wang K, Wang Y, Hua ZC. SPRY1 promotes the degradation of uPAR and inhibits uPAR-mediated cell adhesion and proliferation. *Am J Cancer Res* 2014; **4**: 683–697.
39 Powers CJ, McLeskey SW, Wellstein A. Fibroblast growth factors, their receptors and signaling. *Endocr Relat Cancer* 2000; **7**: 165–197.
40 Bottcher RT, Niehrs C. Fibroblast growth factor signaling during early vertebrate development. *Endocr Rev* 2005; **26**: 63–77.
41 Chalkiadaki G, Nikitovic D, Berdiaki A, Sifaki M, Krasagakis K, Katonis P *et al.* Fibroblast growth factor-2 modulates melanoma adhesion and migration through a syndecan-4-dependent mechanism. *Int J Biochem Cell Biol* 2009; **41**: 1323–1331.
42 Yamaguchi F, Saya H, Bruner JM, Morrison RS. Differential expression of two fibroblast growth factor-receptor genes is associated with malignant progression in human astrocytomas. *Proc Natl Acad Sci USA* 1994; **91**: 484–488.
43 Touat M, Ileana E, Postel-Vinay S, Andre F, Soria JC. Targeting FGFR signaling in cancer. *Clin Cancer Res* 2015; **21**: 2684–2694.
44 Kamura S, Matsumoto Y, Fukushi JI, Fujiwara T, Iida K, Okada Y *et al.* Basic fibroblast growth factor in the bone microenvironment enhances cell motility and invasion of Ewing's sarcoma family of tumours by activating the FGFR1-PI3K-Rac1 pathway. *Br J Cancer* 2010; **103**: 370–381.
45 Agelopoulos K, Richter GH, Schmidt E, Dirksen U, von Heyking K, Moser B *et al.* Deep sequencing in conjunction with expression and functional analyses reveals activation of FGFR1 in Ewing sarcoma. *Clin Cancer Res* 2015; **21**: 4935–4946.
46 Tirode F, Surdez D, Ma X, Parker M, Le Deley MC, Bahrami A *et al.* Genomic landscape of Ewing sarcoma defines an aggressive subtype with co-association of STAG2 and TP53 mutations. *Cancer Discov* 2014; **4**: 1342–1353.
47 Kovar H, Jug G, Aryee DN, Zoubek A, Ambros P, Gruber B *et al.* Among genes involved in the RB dependent cell cycle regulatory cascade, the p16 tumor suppressor gene is frequently lost in the Ewing family of tumors. *Oncogene* 1997; **15**: 2225–2232.
48 Kovar H, Pospisilova S, Jug G, Printz D, Gadner H. Response of Ewing tumor cells to forced and activated p53 expression. *Oncogene* 2003; **22**: 3193–3204.
49 Gaspar N, Hawkins DS, Dirksen U, Lewis IJ, Ferrari S, Le Deley MC *et al.* Ewing sarcoma: current management and future approaches through collaboration. *J Clin Oncol* 2015; **33**: 3036–3046.
50 Terada N, Shiraishi T, Zeng Y, Aw-Yong KM, Liu Z, Takahashi S *et al.* Correlation of Sprouty1 and Jagged1 with aggressive prostate cancer cells with different sensitivities to androgen deprivation. *J Cell Biochem* 2014; **115**: 1505–1515.
51 Mendiola M, Carrillo J, Garcia E, Lalli E, Hernandez T, de Alava E *et al.* The orphan nuclear receptor DAX1 is up-regulated by the EWS/FLI1 oncoprotein and is highly expressed in Ewing tumors. *Int J Cancer* 2006; **118**: 1381–1389.
52 Yue PY, Leung EP, Mak NK, Wong RN. A simplified method for quantifying cell migration/wound healing in 96-well plates. *J Biomol Screen* 2010; **15**: 427–433.

Supplementary Information accompanies this paper on the Oncogene website (http://www.nature.com/onc)

OPEN ACCESS Freely available online

PLOS ONE

Lysyl Oxidase Is Downregulated by the EWS/FLI1 Oncoprotein and Its Propeptide Domain Displays Tumor Supressor Activities in Ewing Sarcoma Cells

Noelia Agra[•], **Florencia Cidre**[•], **Laura García-García, Juan de la Parra, Javier Alonso***

Unidad de Tumores Sólidos Infantiles, Área de Genética Humana, Instituto de Investigación de Enfermedades Raras, Instituto de Salud Carlos III, Majadahonda, Madrid, Spain

Abstract

Ewing sarcoma is the second most common bone malignancy in children and young adults. It is driven by oncogenic fusion proteins (i.e. EWS/FLI1) acting as aberrant transcription factors that upregulate and downregulate target genes, leading to cellular transformation. Thus, identificating these target genes and understanding their contribution to Ewing sarcoma tumorigenesis are key for the development of new therapeutic strategies. In this study we show that lysyl oxidase (LOX), an enzyme involved in maintaining structural integrity of the extracellular matrix, is downregulated by the EWS/FLI1 oncoprotein and in consequence it is not expressed in Ewing sarcoma cells and primary tumors. Using a doxycycline inducible system to restore LOX expression in an Ewing sarcoma derived cell line, we showed that LOX displays tumor suppressor activities. Interestingly, we showed that the tumor suppressor activity resides in the propeptide domain of LOX (LOX-PP), an N-terminal domain produced by proteolytic cleavage during the physiological processing of LOX. Expression of LOX-PP reduced cell proliferation, cell migration, anchorage-independent growth in soft agar and formation of tumors in immunodeficient mice. By contrast, the C-terminal domain of LOX, which contains the enzymatic activity, had the opposite effects, corroborating that the tumor suppressor activity of LOX is mediated exclusively by its propeptide domain. Finally, we showed that LOX-PP inhibits ERK/MAPK signalling pathway, and that many pathways involved in cell cycle progression were significantly deregulated by LOX-PP, providing a mechanistic explanation to the cell proliferation inhibition observed upon LOX-PP expression. In summary, our observations indicate that deregulation of the LOX gene participates in Ewing sarcoma development and identify LOX-PP as a new therapeutic target for one of the most aggressive paediatric malignancies. These findings suggest that therapeutic strategies based on the administration of LOX propeptide or functional analogues could be useful for the treatment of this devastating paediatric cancer.

Citation: Agra N, Cidre F, García-García L, de la Parra J, Alonso J (2013) Lysyl Oxidase Is Downregulated by the EWS/FLI1 Oncoprotein and Its Propeptide Domain Displays Tumor Supressor Activities in Ewing Sarcoma Cells. PLoS ONE 8(6): e66281. doi:10.1371/journal.pone.0066281

Editor: Javier S. Castresana, University of Navarra, Spain

Received June 26, 2012; **Accepted** May 9, 2013; **Published** June 4, 2013

Funding: This study was funded by grants of the Ministerio de Ciencia e Innovación (SAF2009-10158), the Fundación Científica de la Científica Española Contra el Cáncer and the Fundación María Francisca de Roviralta. N. Agra was supported by the Fundación General de la U.A.M. The funders had no role in study design, data collection and analysis, decision to publish, or preparation of the manuscript.

Competing Interests: The authors have declared that no competing interests exist.

* E-mail: fjalonso@isciii.es

• These authors contributed equally to this work.

Introduction

Ewing sarcoma is an aggressive neoplasm that mainly affects child and young adults in the first and second decade of life. It mainly occurs in bones although a small percentage of these tumors also arise in soft tissues. Even though the overall survival rates have significantly risen in the last decades, an elevated percentage of these tumors are refractory to conventional chemo- and radiotherapy, making more necessary the development of new therapeutic strategies (reviewed in [1]). The development of new therapeutic strategies will only be possible through a better knowledge of the molecular mechanisms that govern the process of malignant transformation in these tumors.

The molecular hallmark of Ewing sarcoma is the presence of chromosomal translocations that generate fusion proteins with aberrant transcriptional activities. The most common of these translocations, observed in approximately 85% of the cases, is t(11;22) that fuse the EWS gene to the FLI1 transcription factor resulting in the EWS/FLI1 fusion protein. Other fusion proteins involving the EWS gene (and less frequently other related genes) and other transcription factors of the ets family have been described in the remainder cases. During the last years, important efforts have been made to identify gene targets of the EWS/FLI1 oncoprotein in Ewing sarcoma cells (reviewed in [2–6]). Many of these target genes have been shown to regulate cell proliferation, invasiveness, metastasis or responsiveness to oxidative stress in Ewing sarcoma cells (reviews above and [7])

Cellular models engineered to silence EWS/FLI1 expression by means of RNA interference have been very useful for the identification and characterization of relevant downstream targets of EWS/FLI1 [8–19]. Particularly, inducible shRNA models have been especially advantageous, allowing us to identify some of the genes that participate in the pathogenesis of Ewing tumors, such as cholecystokinin, DKK1 and the orphan nuclear receptor DAX1/NR0B1 [8,9,20].

EWS/FLI1 induced genes are expected to work functionally like oncogenes, while EWS/FLI1 repressed genes are expected to act functionally like tumor supressor genes. It is interesting that although EWS/FLI1 was shown to act as a potent transcriptional activator [21,22], a significant proportion of EWS/FLI1 target genes are downregulated by this oncogenic protein [11,23,24]. The mechanism of this specific gene repression is only partially understood, and probably involves direct repression [11,23–25], upregulation of transcriptional repressors [26] and epigenetic mechanisms [15]. In addition, EWS/FLI1 has been also shown to regulate the expression of microRNAs that in turn are available to regulate the expression of other genes involved Ewing sarcoma tumorigenesis [27,28].

Analysis of our gene expression profile dataset in the Ewing sarcoma cell line A673 upon EWS/FLI1 knockdown showed that one of the most strongly downregulated genes by EWS/FLI1 codes for the enzyme lysyl oxidase (LOX). LOX is the major member of a family of lysyl oxidases (that include LOX and the LOX-like proteins LOXL1 to LOXL4) that share the enzyme catalytic domain (reviewed in [29–32]). LOX is synthesized as a 50-KDa inactive pre-proenzyme which is secreted into the extracellular environment and then processed by proteolytic cleavage to a functional 32-KDa LOX enzyme (LOXenz) and an 18-KDa propeptide (LOX-PP). It is well characterized that the functional mature enzyme catalyses lysine-derived covalent cross-links required for normal structural integrity of the extracellular matrix and a huge amount of information on this function, both in physiological and pathological situations, has been accumulated during several decades (reviewed in [29–32]). The role of the propeptide has been, however, much less studied, although recent reports suggest that LOX propeptide acts as a tumor suppressor in several contexts [33–35]. Currently, no data are available about the possible contribution of LOX repression to the malignant phenotype of Ewing sarcoma.

In this work, we show that EWS/FLI1 downregulates LOX expression and that, remarkably, LOX propeptide exhibits tumor suppressor activities in Ewing tumor cells. Ectopic expression of LOX propeptide in an Ewing sarcoma cell line reduced cell proliferation, cell migration, anchorage independent growth and tumor growth *in vivo*. These findings suggest that therapeutic strategies based in the administration of LOX propeptide or functional analogues could be useful for the treatment of this devastating paediatric cancer.

Results

During the last years we have used an inducible model of EWS/FLI1 knockdown in combination with whole gene expression analysis to identify and characterize EWS/FLI1 target genes relevant for Ewing sarcoma tumorigenesis ([8,9,36]). Review of these datasets (GEO accession number GSE36007) indicated that one of the genes that showed a more intense and consistent downregulation by EWS/FLI1 was the enzyme lysyl oxidase (LOX, Protein-lysine 6-oxidase EC 1.4.3.13). Consequently, we decided to study the regulation of LOX by EWS/FLI1 and the functional implications of this downregulation.

To confirm microarray data, we used A673/TR/shEF Ewing cells, which in response to doxycycline express a specific shRNA directed against EWS/FLI1 mRNA, subsequently reducing the levels of EWS/FLI1 mRNA and protein [8,9]. We isolated RNA from A673/TR/shEF cells incubated in absence or in presence of doxycycline and performed real time quantitative RT-PCR (qRT-PCR) analysis. Time-course experiments confirmed that LOX is a gene downregulated by EWS/FLI1, since LOX mRNA levels were significantly upregulated upon EWS/FLI1 knockdown in the A673 Ewing sarcoma cell line (Figure 1A). As shown in figure 1B, LOX protein was nearly undetectable in A673/TR/shEF cells in basal conditions. However, EWS/FLI1 knockdown produced a dramatic increase in LOX protein levels confirming that EWS/FLI1 downregulates LOX expression in these cells. To analyse if LOX expression downregulation is a common feature of Ewing cells, we analysed by western-blot the levels of LOX protein in a panel of Ewing derived cell lines (n = 8) harbouring different oncogenic fusion proteins. As shown in Figure 1C, LOX expression in these Ewing sarcoma cell lines was nearly undetectable, while high LOX expression was observed in IMR-90 normal fibroblasts, which were used here as a positive control of LOX expression. We then analysed the levels of LOX mRNA in Ewing primary tumors using qRT-PCR and compared them with the levels observed in the positive control IMR-90. Figure 1D shows that LOX mRNA levels are low in Ewing primary tumors compared to those observed in IMR90 cells. In addition, we searched public expression datasets in order to analyse the relative expression of LOX in Ewing sarcoma in relation to other tumor types. As shown in supplementary figure S1, LOX expression was low in Ewing sarcoma tumors, compared to other neoplasms.

Next, we analysed if epigenetic mechanisms, known to repress gene expression, could be involved in the negative regulation of LOX expression observed in Ewing sarcoma cells. We first studied the effect of Vorinostat (SAHA), a class I/II histone deacetylase inhibitor approved for clinical use in cancer patients ([37]). A673 cells were incubated in presence or absence of SAHA for 24 hours and LOX mRNA levels were quantified by qRT-PCR. As shown in Figure 2A, incubation of A673 Ewing cells with SAHA produced a 5-fold increase in LOX mRNA levels. Following, we analysed the effect of 5-aza-cytidine (5-aza), a potent inhibitor of DNA methyltransferase 1 (DNMT1) that induces demethylation and reactivation of silenced genes [38] on LOX expression. As shown in figure 2B, incubation of A673 Ewing cells with 5-aza during 72 hours produced a 10-fold increase in LOX mRNA levels. These results suggest that both histone acetylation status and DNA methylation could be involved in the negative regulation of LOX expression in A673 cells.

The fact that EWS/FLI1 downregulates LOX in the A673 Ewing sarcoma cell line and that low levels of LOX are a common feature of Ewing sarcoma cells and tumors, suggest that LOX could act as a tumor suppressor in Ewing tumors. In this case, LOX re-expression should antagonize, at least in part, the transforming properties of EWS/FLI1 in Ewing tumor cells. To confirm this hypothesis, we performed functional studies to determine the effect of LOX re-expression in the A673 Ewing cell line model.

As previously mentioned, LOX is synthesized as a 50-KDa inactive proenzyme (preLOX) which is secreted to the extracellular environment. There, it is processed by proteolytic cleavage to a functional 32-KDa LOX enzyme (LOXenz) and an 18-KDa propeptide (LOX-PP). We thus genetically modified the A673 Ewing sarcoma cell line to express LOX proenzyme (A673/TR/preLOX, aminoacides 1-415), its catalytic domain (A673/TR/LOXenz, aminoacides 166-415) and the LOX propeptide (A673/TR/LOX-PP, aminoacides 1-179) in an attempt to characterize the specific contribution of full-length LOX and of each one of the LOX-derived fragments to Ewing sarcoma tumorigenesis (Figure 3A). We have used a doxycycline-inducible system to express these proteins because, in our opinion, it has significant advantages to analyse genes that may be acting as tumor suppressors since constitutive expression of these genes is expected to produce deleterious effects on transformed cells.

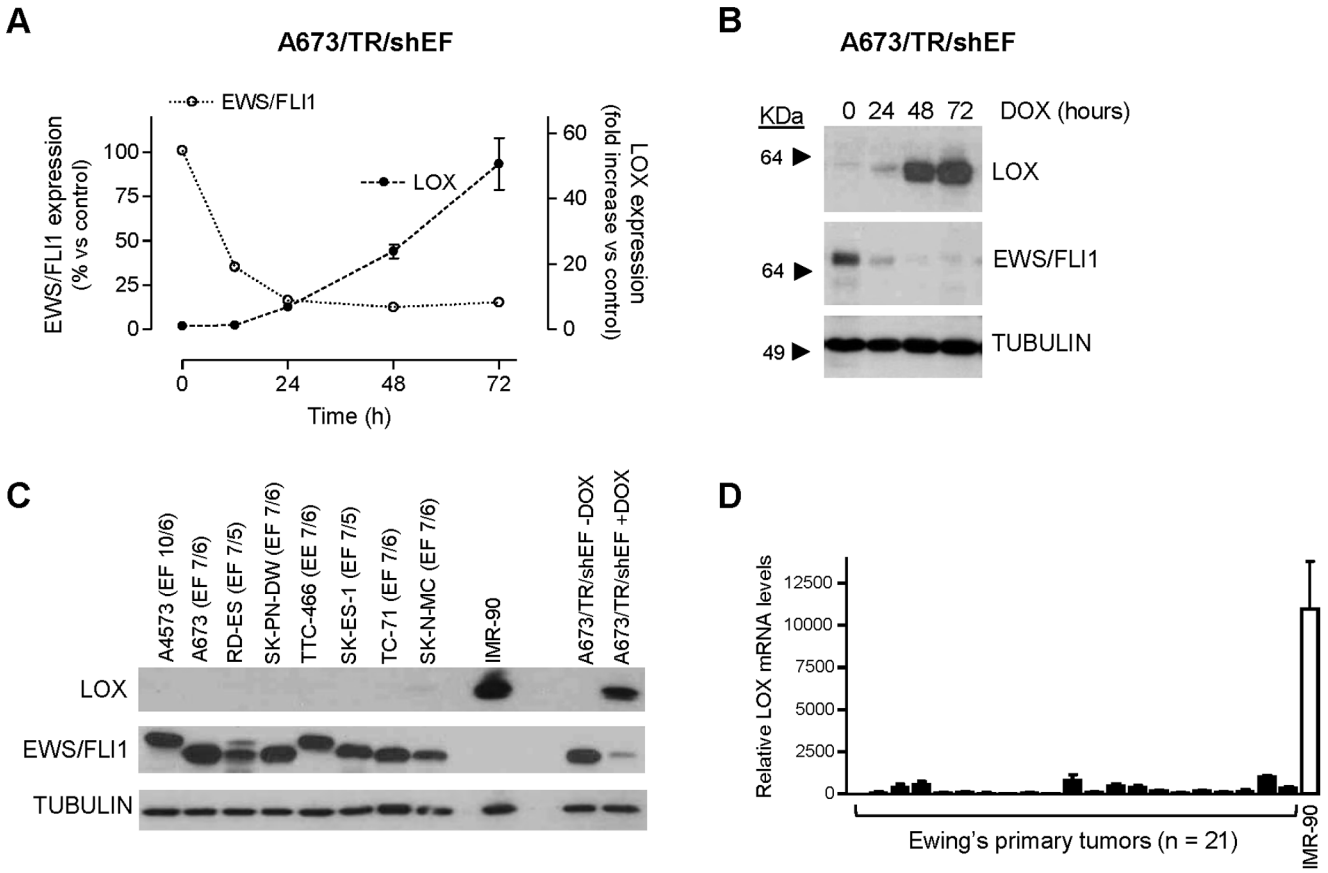

Figure 1. LOX mRNA and protein are downregulated by EWS/FLI1 in the A673 Ewing sarcoma cell line. A) A673/TR/shEF cells were stimulated by different periods of time with doxycycline (DOX, 1 μg/ml) to induce the expression of an EWS/FLI1-specific shRNA. The levels of LOX, EWS/FLI1 and TBP (reference gene) mRNA were quantified by multiplex real time qRT-PCR. For each time point, LOX and EWS/FLI1 mRNA levels were normalized to that of TBP and referred to unstimulated cells. The figure shows the data (mean±SD) of one out of two independent experiments done in triplicate with equivalent results. **B**) LOX protein levels were also determined by western-blot in the A673/TR/shEF cells stimulated with doxycycline. The same blot was stripped and successively incubated with anti-FLI1 antibody to assess the expression of EWS/FLI1 and with anti-α-tubulin as a control for loading and transferring. LOX mRNA and protein levels were strongly downregulated by EWS/FLI1. **C**) LOX protein levels were determined by western-blot in 8 Ewing derived cell lines and in normal fibroblasts IMR-90, used here as a positive control of LOX expression. A673/TR/shEF cells stimulated with doxycycline for 48 hours were also included. The type of EWS/FLI1 (EF; EWS exon/FLI1 exon) and EWS/ERG fusion (EE; EWS exon/ERG exon) present in each Ewing cell line are indicated. LOX protein expression was nearly undetectable in Ewing derived cell lines. **D**) LOX mRNA levels were quantified by qRT-PCR in a set of Ewing's primary tumors (n = 21). Normal fibroblasts IMR-90 are used as a positive control. mRNA levels were normalized to that of TBP (mean±SD). LOX mRNA levels observed in Ewing tumors were very low compared to those observed in the control fibroblast cell line IMR-90.
doi:10.1371/journal.pone.0066281.g001

As shown in Figure 3B, preLOX, LOXenz and LOX-PP mRNAs were induced upon doxycycline stimulation in the A673/TR/preLOX, A673/TR/LOXenz and A673/TR/LOX-PP Ewing cells respectively. In all cases, levels of EWS/FLI1 mRNA were not altered by doxycycline stimulation, making this an excellent model to analyse the effect of the induction of the different LOX proteins and their contribution to Ewing pathogenesis. Western-blot analyses were used to confirm the expression of the corresponding proteins: preLOX and LOXenz were detected by western-blot in whole cell extracts as proteins with molecular weights slightly larger than expected, because of the V5 N-terminal tag sequence that was fused to the proteins to facilitate their detection with an anti-V5 specific antibody (Figure 3C). In contrast, LOX-PP was not detected in whole cell extracts (Figure 3C), suggesting that it was rapidly and efficiently secreted to the culture media. To confirm this, we used immunoprecipitation to analyse the culture media of A673/TR/LOX-PP cells incubated in absence or in presence of doxycycline. As shown in figure 3D, LOX-PP was detected as a diffuse band of approximately 30 KDa in culture media of A673/TR/LOX-PP cells stimulated with doxycycline, suggesting that this protein was strongly glycosylated, as previously reported [39–41]. In order to demonstrate that this diffuse band corresponds to secreted LOX-PP highly glycosylated, we treated a fraction of the immunoprecipitated LOX-PP with the enzyme N-glycosidase (PNGase F) to remove N-linked oligosaccharides. After N-glycosidase treatment (Figure 3E), LOX-PP migrated as a single band of approximately 18 kDa, which corresponds to its predicted size according to its amino acid composition and demonstrates that LOX-PP produced by A673/TR/LOX-PP cells is processed adequately. Unglycosylated LOX-PP was also observed in untreated LOX-PP, although it was present in a very low quantity, indicating that a minimal fraction of the secreted LOX-PP was unglycosylated.

We next analyzed the effect of preLOX, LOX-PP and LOXenz on cell proliferation. As shown in Figure 4, induction of preLOX by doxycycline in A673/TR/preLOX cells resulted in a significant

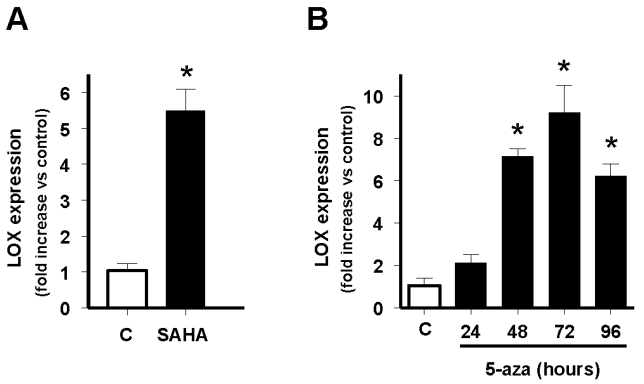

Figure 2. Effect of the histone deacetylases inhibitor SAHA and the demethylating agent 5-aza-2′-deoxycytidine on LOX mRNA levels. A) A673 cells were incubated in absence (C) or presence of SAHA 1 μM for 24 hours and the levels of LOX and TBP (reference gene) mRNAs quantified by multiplex real time qRT-PCR. LOX mRNA levels were normalized to that of TBP and referred to unstimulated control (C) cells, which were arbitrary set to 1. The figure shows the data (mean±SD) of three independent experiments done in triplicate. The figure shows the mean±SD of one out of two independent experiments done in duplicate (*$P<0.01$ vs control). B) A673 cells were incubated in the absence (C) or presence of 5-aza-2′-deoxycytidine 1 μM for 24, 48, 72 or 96 hours and the levels of LOX and TBP (reference gene) mRNAs quantified by qRT-PCR and analysed as above. The figure shows the mean±SD of two independent experiments done in duplicate (*$P<0.01$ vs control). Both SAHA and 5-aza-2′-deoxycytidine produce a significant increase in the levels of LOX mRNA in A673 cells.
doi:10.1371/journal.pone.0066281.g002

reduction (30%) in the number of population doubling accumulated during 25 days. This inhibitory effect on cell proliferation was clearly more pronounced (45%) when LOX-PP was induced in A673/TR/LOX-PP cells. Interestingly, the effect of LOXenz on cell proliferation was the opposite, with an increase in the number of population doubling upon LOXenz induction. No effect on cell proliferation was observed in A673 cells carrying the empty vector, both in absence and in presence of doxycycline. To confirm these effects on cell proliferation, we performed additional experiments using an available commercial kit designed to quantify viable cells (Cell-titer fluor cell viability assay). As shown in Figure 4B, induction of preLOX in two independent clones of A673/TR/preLOX cells produced a reduction (about 20%) in the number of viable cells. This inhibitory effect on cell number became again more pronounced (about 50%) when LOX-PP was induced in A673/TR/LOX-PP cells. By contrast, the induction of LOXenz resulted in an increase in the number of viable cells. Taken together, these results demonstrate that preLOX inhibits cell proliferation in Ewing cell lines and more interestingly, that this inhibitory effect on cell proliferation resides in the LOX propeptide. To additionally characterize these findings, we used the irreversible antagonist of lysyl oxidase activity β-aminopropionitrile (β-APN) [33]. As shown in Figure 4C, treatment with β-APN increased the inhibitory effect of preLOX on cell proliferation. Since preLOX expression results in the production of both the propeptide domain LOX-PP and the catalytic domain LOXenz, this result indicates that lysyl oxidase activity (which resides in LOXenz) is partially counteracting the cell proliferation inhibition mediated by LOX-PP. Furthermore, β-APN totally blocked the stimulatory effect of LOXenz on cell proliferation, demonstrating that this effect is entirely dependent on the lysyl oxidase catalytic activity. In concordance with this, β-APN had no effect on the cell proliferation inhibition observed upon LOX-PP induction. These results confirm that the inhibitory effect of LOX on cell proliferation resides in the LOX propeptide. Subsequently, we analyzed the effect of an exogenous source of LOX-PP on cell proliferation. For this purpose, we incubated A673 cells with LOX-PP rich media, obtained from conditioned media of A673/TR/LOX-PP cells stimulated with doxycycline during 72 hours. Control media, without LOX-PP, was obtained in parallel from the same cells incubated in absence of doxycycline for 72 hours. As shown in figure 4D, LOX-PP enriched media, reduced by 50% the cell number in A673 Ewing cells.

Following, we analysed the effect of preLOX, LOX-PP and LOXenz on cell migration and the ability to grow in an anchorage-independent manner. In Figure 5A are shown the effects of preLOX, LOX-PP and LOXenz on cell migration through porous membranes in response to serum. Induction of preLOX with doxycycline in the A673/TR/preLOX cells did not produce a significant difference in the number of cells migrating through the membrane. However, the induction of LOX-PP in A673/TR/LOX-PP cells decreased cell migration through the porous membranes by 35%, indicating that LOX-PP is also active in inhibiting cell migration. In this case, LOXenz also showed the opposite effect when compared to LOX-PP. Thus, LOXenz increased the migration of A673 cells by 25%. Afterwards, we analysed the effect of preLOX, LOX-PP and LOXenz on the ability of A673 cells to grow in soft agar. As shown in Figure 5B, preLOX and LOX-PP induction decreased the number of colonies grown in soft agar by approximately 25% and 30%, respectively. By contrast, LOXenz increased the number of colonies by about 50%.

Subsequently, we performed xenograft experiments to analyse the effect of LOX-PP on tumor growth *in vivo* (Figure 5C). Mice were injected subcutaneously with A673/TR/empty or A673/TR/LOX-PP and each group of animals was split into two groups of treatment, one of which was given doxycycline in the drinking water to induce the expression of the corresponding protein. As expected, animals injected with A673/TR/empty cells produced tumors both in the absence and in the presence of doxycycline in the drinking water. Animals injected with A673/TR/LOX-PP cells but not treated with doxycycline also developed tumors at the same rate as the animals injected with the A673/TR/empty control cells. However, we did not detect visible tumors in the animals injected with A673/TR/LOX-PP cells and treated with doxycycline, and thus expressing LOX-PP. Taken all together these results indicate that LOX-PP is a suppressor of Ewing sarcoma tumorigenesis.

Following, in an attempt to identify the pathways involved in the antiproliferative effect of LOX-PP we analysed by western-blot the status of the PI3K/AKT and ERK/MAPK pathways. As shown in Figure 6, induction of LOX-PP with doxycycline had no effect on the levels of activated Akt (P-Ser 473). By contrast, LOX-PP produced a marked inhibition of the levels of activated Erk (P-Tyr 204).

Finally, we performed a gene expression microarray experiment to identify genes and pathways specifically regulated by LOX-PP in A673 cells (GEO accession number GSE46407). Thus, we stimulated A673/TR/LOX-PP cells with doxycycline for 72 hours and compared its gene expression profile to that of the control cells A673/TR/empty. In order to identify pathways specifically affected by LOX-PP in A673 cells, we analysed the expression data sets with GSEA (Gene Set Enrichment Analysis) [42]. As shown in supplementary table S1, GSEA analysis identified many gene sets/pathways from the REACTOME curated database (www.reactome.org) that were significantly regulated by LOX-PP (FDR<0.005). Among the 19 gene sets

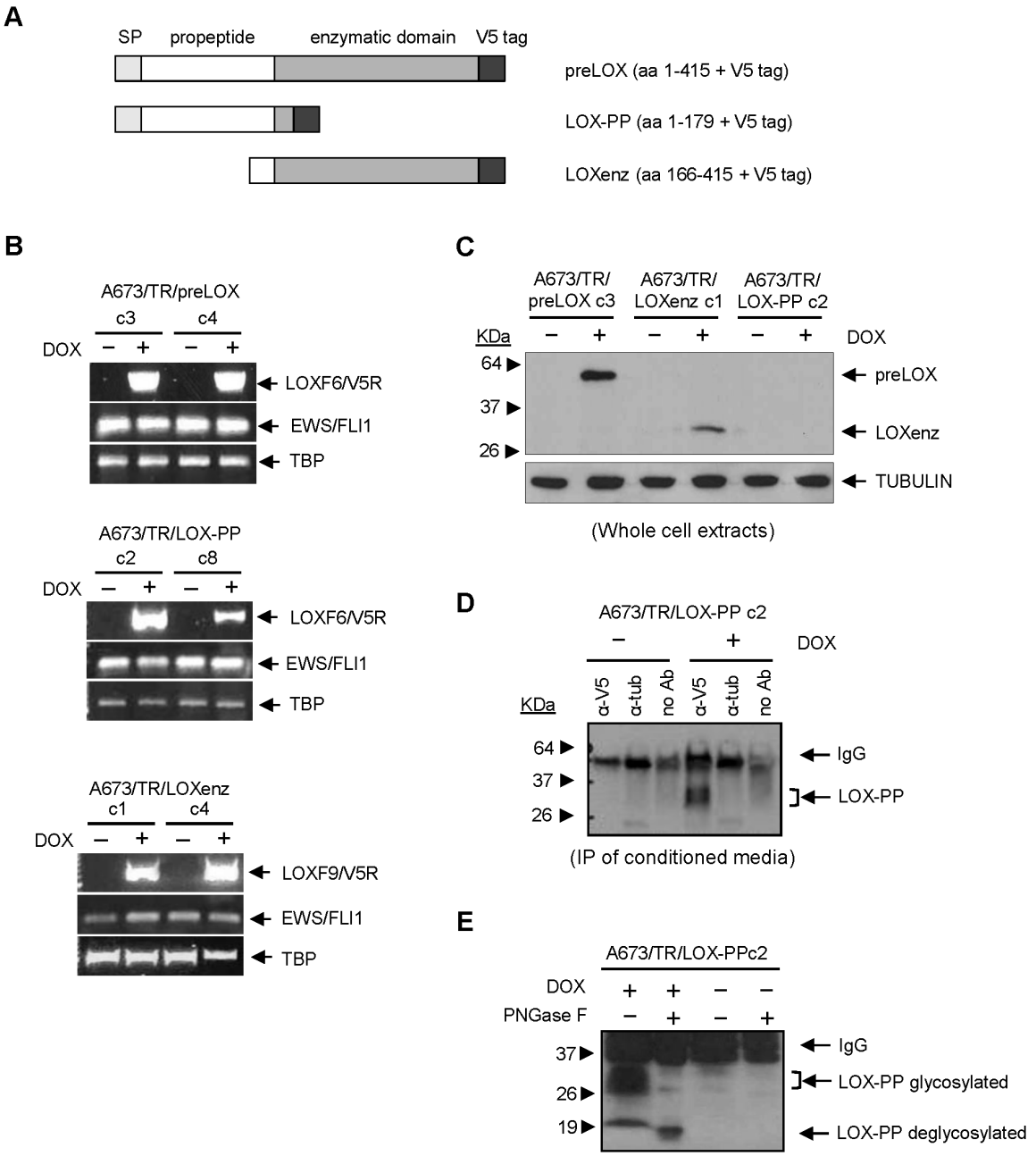

Figure 3. Establishment of Ewing sarcoma cell lines expressing doxycycline-inducible preLOX, LOX-PP and LOXenz proteins. A) Schematic representation of preLOX, LOX-PP and LOXenz cDNAs cloned in the doxycycline-inducible lentiviral vector pLenti-TO-V5-DEST. SP: signal peptide. **B**) A673/TR Ewing cell line expressing high levels of the tetracycline repressor (TR) was infected with the doxycycline-inducible lentiviral vector encoding the different LOX cDNAs and stable clones were selected. The figure shows two independent clones for each construction stimulated with doxycycline (DOX, 1 μg/ml, 48 hours) to induce the expression of the corresponding mRNAs. preLOX, LOX-PP and LOXenz mRNAs were detected by RT-PCR using LOX-specific (LOXF6 or LOXF9) and V5 tag-specific primers (V5R). EWS/FLI1 fusion mRNA remained unchanged upon LOX induction. TBP (TATA-binding protein) was used as an internal housekeeping control. **C**) Whole protein extracts were isolated from A673/TR/ preLOX (clone 3), A673/TR/LOXenz (clone 1) and A673/TR/LOX-PP (clon 2) cells stimulated with doxycycline (DOX, 1 μg/ml, 48 hours) and analysed by western-blot to detect the expression of preLOX, LOXenz and LOX-PP proteins, respectively, using an anti-V5 antibody. The same blot was stripped and incubated with anti-α-tubulin as a control for loading and transferring. preLOX and LOXenz, but not LOX-PP, were detected in whole cell extracts. **D**) Conditioned media derived from A673/TR/LOX-PP (clone 2) incubated with doxycycline (DOX, 1 μg/ml, 48 hours) was concentrated and immunoprecipitated with an anti-V5 antibody to confirm the secretion of LOX-PP in the culture media. An anti-α-tubulin or no antibody were used as negative controls. LOX-PP was detected in the culture media derived from A673/TR/LOX-PP stimulated with doxycycline indicating that LOX-PP was efficiently processed and secreted. **E**) Conditioned media derived from A673/TR/LOX-PP cells stimulated with doxycycline was immunoprecipitated and untreated or treated with the enzyme peptide-N-glycosidase (PNGase F). Glycosylated LOX-PP was observed as a diffused band of approximately 30 KDa in the untreated sample, that became a defined band of 18 KDa upon deglycosylation treatment. A673/TR/LOX-PP cells without doxycycline were used as a negative control of LOX-PP production.
doi:10.1371/journal.pone.0066281.g003

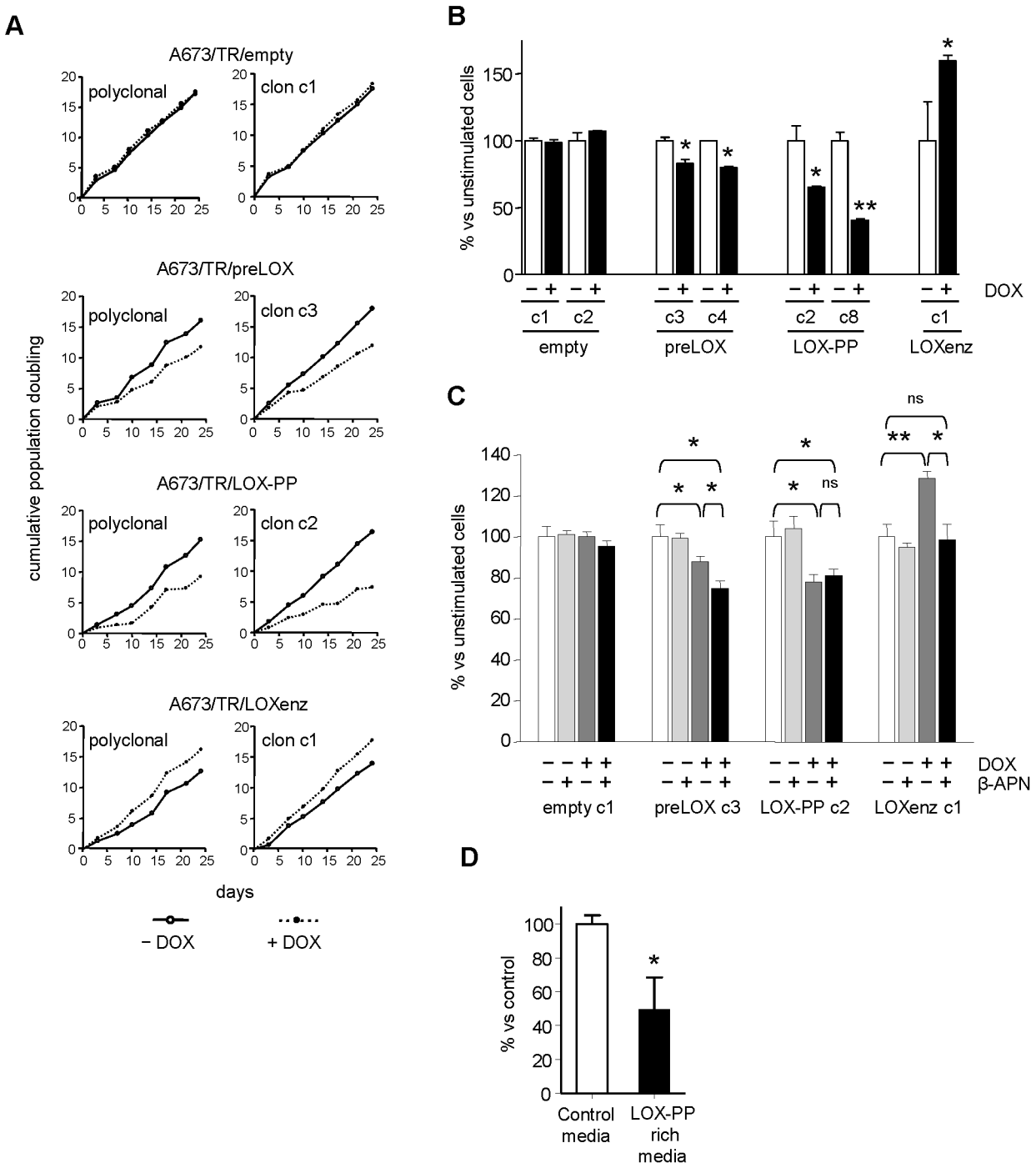

Figure 4. Induction of preLOX and LOX-PP inhibits cell proliferation in A673 Ewing sarcoma cells. A) A polyclonal population and a representative clone of A673/TR/empty (control cells), A673/TR/preLOX, A673/TR/LOX-PP and A673/TR/LOXenz cells were maintained during 25 days in standard culture medium or in culture medium containing doxycycline (DOX, 1 μg/ml) to induce the expression of the corresponding proteins. Cumulative number of population doubling were determined by counting cells at different periods of time and plotted versus time. **B**) Representative clones of A673/TR/empty, A673/TR/preLOX, A673/TR/LOX-PP and A673/TR/LOXenz cells were incubated in the absence or in the presence of doxycycline (DOX, 1 μg/ml) for 5 days to induce the corresponding proteins and cell growth quantified by CellTiter-Fluor assay. The figure shows the mean±SD of one out of three independent experiments done in triplicate with similar results. Data are shown as percentage versus unstimulated cells, which were arbitrarily set to 100 (*$P<0.05$, **$P<0.005$ versus unstimulated cells). **C**) A673/TR/empty, A673/TR/preLOX, A673/TR/LOX-PP and A673/TR/LOXenz cells were incubated in the absence or in the presence of doxycycline (DOX, 1 μg/ml) and in the absence or in the presence of the irreversible antagonist of lysyl oxidase activity β-aminopropionitrile (β-APN, 500 μM). The figure shows the mean±SD of one out of two independent experiments done in triplicate with equivalent results. Data are shown as percentage versus unstimulated cells, which were arbitrarily set to 100 (*$P<0.05$, **$P<0.005$, ns: not significant). **D**) A673 cells were incubated during 72 hours with conditioned media derived from A673/TR/LOX-PP cells cultured in absence of doxycycline (control) or conditioned media derived from the same cells cultured in presence of doxycycline to induce the expression of LOX-PP (LOX-PP rich media). The figure shows the mean±SD of two independent experiments done in triplicate. Data are shown as percentage versus cells incubated with control media, which were arbitrarily set to 100 (*$P<0.05$). LOX-PP rich media significantly reduced cell proliferation of A673 cells.
doi:10.1371/journal.pone.0066281.g004

displaying a FDR<0.005, 14 were related to DNA synthesis and replication and cell cycle regulation (Supplementary table S1 and figure S2), indicating that LOX-PP was clearly affecting cell proliferation. LOX-PP induction also affected other pathways related to cell metabolism (3 gene sets) and extracellular matrix organization (2 gene sets). Taken together, these data suggest that LOX-PP is affecting cell proliferation, first, by producing a significant inhibition of the ERK/MAPK pathway, and subsequently, by affecting pathways involved in cell cycle progression.

Discussion

Ewing sarcoma is a highly aggressive paediatric cancer that in an elevated percentage of cases is refractory to standard treatments (reviewed in [1]). Therefore, studies designed to identify new therapeutic targets in Ewing tumors are eagerly needed. Ewing sarcoma is characterized by chromosomal translocations that lead to the expression of chimeric transcription factors (the most frequent of which is the fusion protein EWS/FLI1), which are thought to be the responsible for tumor initiation [3–5]. Because EWS/FLI1 (and the related fusion proteins) deregulates a large set of target genes, identification of these genes is not only important to increase our understanding about Ewing tumorigenesis, but more importantly to identify new targets that could be pharmacologically modulated.

Whole genome expression analysis has been especially useful to identify EWS/FLI1 target genes and to provide a relevant amount of information about genes and pathways involved in Ewing tumorigenesis [43]. However, in order to identify new valuable therapeutic targets, functional analysis should be performed "gene to gene" to establish the individual contribution of each gene to the malignant phenotype. With this in mind, in this work we analysed the contribution of lysyl oxidase (LOX), a EWS/FLI1 downregulated gene target, to Ewing tumorigenesis.

Microarray studies and real time quantitative RT-PCR demonstrated that LOX mRNA was downregulated by the EWS/FLI1 oncoprotein in the A673 Ewing sarcoma cell line.

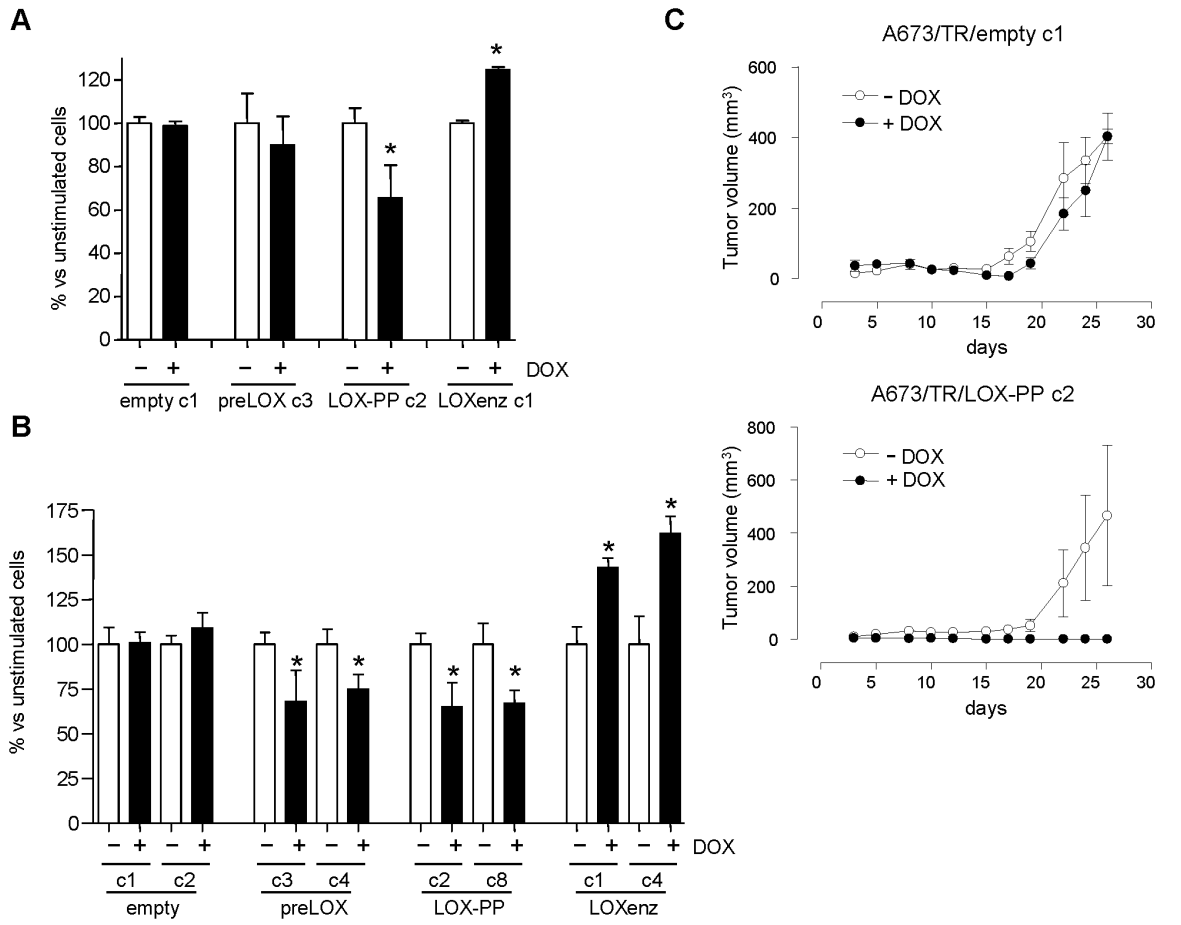

Figure 5. LOX-PP induction inhibits growth in soft agar, cell migration and tumor growth *in vivo*. **A**) A673/TR/empty, A673/TR/preLOX, A673/TR/LOX-PP and A673/TR/LOXenz cells were grown in soft agar in the absence or in the presence of doxycycline (DOX, 1 μg/ml)) for 25 days. Culture dishes were then photographed and colony number was calculated. The figure shows the mean±SEM of three independent experiments done in triplicate. Data are shown as percentage versus unstimulated cells, which were arbitrarily set to 100 (*$P<0.05$, versus unstimulated cells). **B**) Two representative clones of A673/TR/empty, A673/TR/preLOX, A673/TR/LOX-PP and A673/TR/LOXenz cells were incubated in the absence or in the presence of doxycycline (DOX, 1 μg/ml) during 48 hours to induce the expression of the corresponding proteins. Afterwards, cells were placed in the upper compartment of a transwell and allowed to migrate through the membrane in response to serum. Migrating cells were quantified by crystal violet staining. The figure shows the mean±SEM of one experiment done in triplicate. Data are shown as percentage versus unstimulated cells, which were arbitrarily set to 100 (*$P<0.05$, versus unstimulated cells). **C**) Nude mice were injected with A673/TR/empty clone 1 (n = 7) or A673/TR/LOX-PP clone 2 (n = 8) cells and split in two groups, one of which was given doxycycline (DOX, 1 mg/ml) in the drinking water to induce the expression of the corresponding protein. The figure shows the evolution of tumor volume (mean±SEM of 3–4 animals per group) versus time.
doi:10.1371/journal.pone.0066281.g005

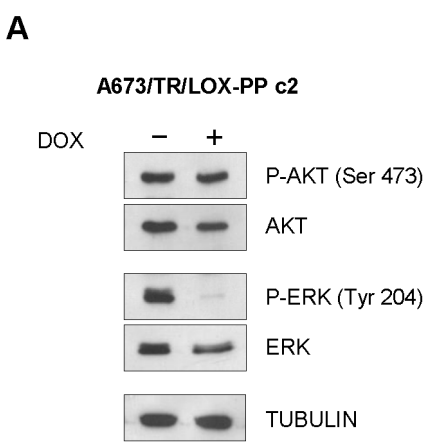

Figure 6. LOX-PP interferes with ERK signalling. A673/TR/LOX-PP cells (clone 2) were incubated in the absence or in the presence of doxycycline (DOX, 1 μg/ml, 48 hours) and the levels of activates P-AKT (Ser 473) and P-ERK (Tyr 204) determined by western-blot. The same blot was stripped and successively incubated with anti-AKT, anti-ERK and anti-α-tubulin as controls for loading and transferring.
doi:10.1371/journal.pone.0066281.g006

Our results are consistent with other previously reported data, in which EWS/FLI1 was also shown to downregulate LOX expression in A673 and other Ewing cell lines (i.e. EWS502 and TC-71) [11,17,18,44]. In agreement with this, we observed no expression (or nearly undetectable) of LOX protein in eight different Ewing cell lines. In addition, LOX mRNA levels were also low in a series of Ewing primary tumors, which was also confirmed searching public available datasets. Loss of LOX expression has been reported in a variety of human cancers. More than two decades ago, Kuivaniemi et al. [45] observed deficient LOX production in a variety of malignant transformed cells, such as HT-1080 (fibrosarcoma), A-204 (rhabdomyosarcoma) or G-361 (melanoma). More recently, reduced LOX expression has been reported to occur in lung and pancreatic cancer [46,47] and during malignant progression of prostate and colorectal cancers [48,49]. Therefore, at least in some types of tumors, LOX expression correlates negatively with malignant transformation.

Our results suggest that epigenetic mechanisms could be involved in the downregulation of LOX mRNA in A673 Ewing cells. In this sense, both the histone deacetylase inhibitor SAHA and the demethylating agent 5-aza-citidine restored, at least partially, LOX expression in A673 cells. It is difficult to assess the quantitative contribution of these mechanisms to LOX repression, because of the elevated toxicity of these agents, in particular SAHA, but our results indicate that both could be involved. While we were doing this work, Lessnick's lab described that EWS/FLI1 oncoprotein was directly involved in the repression of LOX promoter [25]. Interestingly, the repression of LOX promoter was dependent on the interaction of EWS/FLI1 with the NuRD repressor complex. In concordance with this, Sankar et al, showed that LOX mRNA levels increased upon incubation of A673 cells with SAHA, in agreement with our results. In addition, we also showed that DNA methylation can be involved in the repression of LOX gene in A673 cells, although we did not demonstrate if this was an indirect or a direct mechanism.

One of the most interesting findings of our work is the demonstration that lysyl oxidase and particularly, the lysyl oxidase propeptide (LOX-PP) is a suppressor of Ewing sarcoma tumorigenesis. Expression of LOX propeptide decreased cell proliferation, migration, colony formation in soft agar and growth of tumors *in vivo*. In addition, conditioned media containing high levels of LOX-PP impaired cell proliferation in A673 Ewing cells. By contrast, expression of the LOX domain containing the lysyl oxidase activity (namely here LOXenz) showed the opposite effects. Interestingly, when full-length LOX protein (preLOX) was expressed in Ewing tumor cells, the inhibitory effect of LOX-PP on cell proliferation was dominant on the stimulatory effect mediated by LOXenz. Thus, preLOX expression produced a net inhibitory effect on cell proliferation, which could explain why LOX downregulation is advantageous for Ewing tumor cells. Taken together, our results demonstrate that LOX propeptide is a suppressor of Ewing tumorigenesis. Although we have performed the experiments with the prototype Ewing cell line A673, we anticipate that LOX-PP will also affect the growth and transforming properties of other Ewing cell lines. In this sense, Sankar et al have shown in their recently published article that LOX (preLOX) overexpression reduced the ability of three Ewing cell lines (A673, TC71, TC32) to form colonies in soft agar [25]. Although in that study it was not analysed the effect of LOX propeptide itself, these results, taken together with ours, suggest that LOX-PP could act as an antitumor agent for the majority of Ewing sarcoma cells.

The first evidence about the tumor suppressor activity of LOX came from studies addressed to identify the genes involved in the IFN-γ mediated-reversion of ras-transformed malignant cells. In these studies, a gene called ras recision gene (rrg) was isolated and shown to be responsible for malignant reversion [50]. In agreement with this, increased LOX expression was also found in spontaneous revertants of H-ras transformed rat fibroblasts [51] while reduced LOX expression was observed in ras-transformed cells [52]. In addition, Giampuzzi et al. reported that normal rat kidney fibroblasts (NRK-49F) in which LOX mRNA was knocked down by antisense lysyl oxidase showed loose attachment to the plate and anchorage-independent growth and were highly tumorigenic in nude mice [53]. These findings evidence a role of LOX as a tumor suppressor, highlighting its particular role in controlling Ras activation and growth factor dependence.

Palamakumbura et al, described for the first time that the lysyl oxidase propeptide, but not the lysyl oxidase enzyme, was responsible for the inhibition of ras-dependent transformation of NIH3T3 cells as determined by effects on cell proliferation assays, growth in soft agar and Akt-dependent induction of NF-kappaB activity [33]. Subsequently, LOX-PP was shown to act as a tumor suppressor in several cancer cells. For example, LOX-PP reverts the invasive phenotype of breast cancer cells [34], inhibits the transformed phenotype of lung and pancreatic cancer cells [35], interferes with FAK activation in breast cancer cells [54] and inhibits prostate cancer cell growth by targeting FGF-2 cell binding and signalling [55].

The mechanism through LOX-PP act as a tumor suppressor begins now to be only partially understood. LOX-PP has been shown to impair both PI3K/Akt and ERK signalling pathways. Thus, ectopic pre-LOX and LOX-PP expression in H1299 lung cancer and PANC-1 pancreatic cancer cells inhibited growth in soft agar and migration and reduced activation of ERK and Akt, with LOX-PP showing substantially higher activity [35]. In MIA PaCa-2 (a pancreatic cancer cell), LOX-PP attenuated the ERK and Akt activities and decreased the levels of the NF-Kβ p65 and RelB subunits and cyclin D1, which are activated by RAS signalling [56]. Palamakumbura et al. [55] showed that recombinant LOX-PP protein inhibits serum-stimulated DNA synthesis and ERK and PI3K/Akt pathways in DU 145 and PC-3 androgen-independent cell lines. Our data indicate that the inhibition of proliferation observed upon LOX-PP expression in

A673 Ewing cells could be mainly mediated by inhibition of the ERK pathway, while the PI3K/Akt pathway does not seem to be involved. Therefore, specific downstream targets of LOX-PP can depend on the cellular context. Studies carried out with gene expression microarrays shown as well that LOX-PP modified the expression of genes involved in specific pathways related to DNA synthesis and replication and cell cycle regulation, indicating that LOX-PP was clearly affecting cell proliferation. These results suggest that LOX-PP is affecting cell proliferation, first, by producing a significant inhibition of the ERK/MAPK pathway, and subsequently, by affecting pathways involved in cell cycle progression.

In summary, in this work we shown that LOX is a gene repressed by the EWS/FLI1 oncoprotein and that its ectopic re-expression in an Ewing cell line inhibits cell proliferation. We also shown that this function is attributed to the LOX propeptide, an N-terminal fragment of the LOX protein released during processing, which in turn is able to decrease cell proliferation and migration and to inhibit the formation of colonies in soft agar and the growth of tumors *in vivo*. Our data indicates that LOX propeptide is a tumor suppressor gene in Ewing's tumors, providing the bases for a rational use of LOX propeptide, derived peptides or synthetic peptidomimetics in Ewing's therapy. Recently, it has been shown that LOX-PP sensitizes pancreatic and breast cancer cells to doxorubicin-induced apoptosis, providing a rationale for LOX-PP usage in adjuvant chemotherapy [56]. Thus, in light of the broad inhibitory activities of LOX-PP shown in this work, it will be interesting to further explore the use of LOX-PP as a potential treatment for Ewing tumors in combination with standard chemotherapy agents.

Materials and Methods

Ethics statement

Experiments with mice were all carried out in accordance with Institutional and European Union guidelines for the care and use of laboratory animals. Procedures were approved by the Comité de Ética de la Investigación y Bienestar Animal (CEIyBA) of the Instituto de Salud Carlos III (Certificate number: PA-24_2012). Animals were sacrificed using an overdose of sodium pentobarbital and all efforts were made to minimize suffering.

Tumors used in this study were provided by the Departments of Pathology and Oncology Units of several Spanish Children's Hospitals. A written informed consent was obtained from each patient's guardian. This study was approved by the Comité de Ética de la Investigación y Bienestar Animal (CEIyBA) of the Instituto de Salud Carlos III (Certificate number: PI- 14_2012).

Cell lines

The Ewing sarcoma cell lines A673 (CRL-1598), SK-ES-1 (HTB-86), RD-ES (HTB-166), SK-N-MC (HTB-10), and SKPN-DW (CRL-2139) were purchased from the American Type Culture Collection (Manassas, VA, USA). Ewing sarcoma cell lines A4573 [57] and TTC-466 [58] were generous gifts from Dr. S. Navarro (University of Valencia, Valencia, Spain) and Dr. T.J. Triche (Children's Hospital Los Angeles, Los Angeles, CA), respectively.

Materials

Stock solution of doxycycline (Invitrogen, Grand Island, NY, USA) were made in PBS 1x. Vorinostat (SAHA) (Sigma-Aldrich, St. Louis, MD, USA) was dissolved in DMSO to generate a stock solution and stored at −20°C until use. This solution was then dissolved in sterile PBS 1X to obtain the desired concentrations. 5-Aza-2′-deoxycytidine (Sigma-Aldrich) was dissolved in DMSO and stored at −80°C in small aliquots until use.

Establishment of Ewing̀s cell lines stably expressing doxycycline-inducible cDNA of LOX, LOX-PP and LOXenz

The complete sequence of LOX (LOX), the propeptide region of LOX (LOX-PP) and the mature form of LOX containing the enzymatic activity (LOXenz) were PCR-amplified from the LOX cDNA cloned into the vector pCMV6-XL5 (Origene, Rockville, USA). LOX cDNA (aminoacids 1-415) was amplified using primers LOX-F3 (5′-GGGGGATCCCAATC TGGCAAAAG-GAGTGATGC-3′) and LOX-R3 (5′-GGGCTCGAG-GAAATTGTGCAGCC TGAGGCATA-3′); LOX-PP cDNA (aminoacids 1–179) was amplified using primers LOX-F3 and LOX-R7 (5′-GGGCTCGAGGTCAGAGTACTTG-TAGGGGTTGTA-3′); LOXenz cDNA (aminoacids 166–415) was amplified using primers LOX-F7 (5′-GGGGGATCCA-GAAGTTCCTGCGCTCAGTAA-3′) and LOX-R3. The amplified fragments were digested with BamHI and XhoI, cloned into the pENTR2B plasmid (Invitrogen) and transferred by recombination to the lentiviral doxycycline-inducible plasmid pLenti4-TO-V5-DEST (Invitrogen). Then, A673/TR Ewing sarcoma cells expressing the tetracycline repressor [8,9] were infected with lentiviruses containing the corresponding cDNAs. Control cells were infected with empty lentiviral vector. Stable clones were selected with zeocin (100 μg/ml). Induction of LOX, LOX-PP and LOXenz were assayed by quantitative RT–PCR and/or western-blots upon doxycycline (1 μg/ml) stimulation. Clones displaying the highest levels of mRNA and/or protein expression upon doxycycline stimulation were chosen for additional studies.

Multiplex real-time quantitative RT-PCR

Real-time PCR was performed to quantify steady state mRNA levels as described elsewhere [13]. Sequences of the primers and TaqMan probes used were as following: for EWS/FLI1, EWS/FLI1-F, 5′-AGCCAAGCTCCAAGTCAATATAG-3′, EWS/FLI1-R, 5′ –TCCTCTTCTGACTGAGTCATAAG-3′; and EWS/FLI1 TaqMan probe, 5′-TET-AACAGAGCAGCAGC-TACGGGCAGCA-TAMRA-3′; For LOX, we used a commercially available TaqMan probe mix (Hs00942480_m1, Applied Biosystems, Foster City, CA); for TATA-binding protein (TBP; used as a reference gene), TBP-F, 5′-GAACATCATGGATCA-GAACAACAG-3′, TBP-R, 5′ ATTGGTGTTCTGAA-TAGGCTGTG 3′; and TBP TaqMan probe 5′ FAM-CTGCCACCTTACGCTCAGGGCTTGG-TAMRA 3′.

Western Blot analysis

Whole cell extracts were obtained directly from cell layers lysed in RIPA buffer (1× PBS, 0,1% SDS, 1% NP-40, 0,5% sodium deoxycholate) supplemented with a protease and phosphatase inhibitor cocktail (Roche). For immunoprecipitation of LOX-PP, conditioned media was collected and concentrated 10× using a 10,000 molecular weight cut-off Amicon Ultra centrifugal filter units (Millipore, Billerica, MA, USA). Then, 1.5 ml of concentrated media were cleared with 25 μl of protein A Sepharose (GE Healthcare, Uppsala, Sweden) and supernatant incubated with 1 μl of anti-V5 overnight at 4°C with rocking. Next, 25 μl of protein A Sepharose were added, incubated 1–4 hours at 4°C with rocking and antigen-antibody complex precipitated by centrifugation. The pelleted precipitates containing LOX bound proteins were washed 3 times in PBS containing 0,5% Triton X-100 and 1 mM PMSF and directed resuspended in Laemli buffer. To perform LOX-PP deglycosylation, immunoprecipitated LOX-PP

was subjected to Peptide-N-Glycosidase F (PNGase F) treatment according to manufacturer instructions (New England BioLabs, Ipswich, MA). Treated and untreated samples were then resuspended in Laemli buffer prior to gel electrophoresis.

Proteins were subjected to electrophoresis on 10 or 12% SDS-polyacrylamide gel, blotted onto PVDF membranes (Pall, Port Washington, NY, USA) and incubated with the corresponding primary antibodies. After incubation with the secondary HRP-conjugated antibody, membranes were subjected to enhanced chemiluminescence (ECL, GE Healthcare) detection analysis. To ensure equal loading of samples in each lane, membranes were stripped and reprobed with an anti-tubulin monoclonal antibody.

Anti-FLI1 antibody (# 554267) was purchased from BD Pharmingen (San Diego, CA, USA), anti-LOX (# L4794) and anti-tubulin (# T9026) from Sigma-Aldrich, anti-V5 (# R960-25) from Invitrogen, anti-P-Erk (P-Tyr 204, # sc-7383) from Santa Cruz Biotechnology (Santa Cruz, CA, USA), anti-Akt (# 9272), anti-P-Akt (P-Ser 473, # 9271) and anti-Erk (# 9102) from Cell Signalling (Boston, MA, USA). Horseradish peroxidase-conjugated secondary antibodies were purchased from Santa Cruz Biotechonology.

Cell proliferation assays

Cumulative population doubling was determined in cells grown during 25 days in the absence or in the presence of doxycycline (1 μg/ml) in 100 mm dishes. Before reached confluence, the cells were trypsinized and counted to determine the number of cell duplications. Cell proliferation was also quantified with the CellTiter-Fluor assay (Promega, Madison, WI, USA). Briefly, 3.000 cells were seeded into 96-well plate and allowed to attach for 48 h. Then, cells were incubated in presence of stimulus for 5 days. Culture medium was replaced every 2–3 days with medium containing the corresponding stimulus. At the end of the experiment, CellTiter-Fluor reagent was added to each well and incubated for 1 h at 37°C. Fluorescence was measured using an Infinite M200 (Tecan, Männerdorf, Switzerland) microplate reader. To analyse the effect of an exogenous source of LOX-PP on cell proliferation, we used a standard MTT assay to quantify viable cells (Promega). In these assays, A673 cells were plated at a density of 5.000 cells/well in 96-well plates, incubated during 72 hours with conditioned culture media and then treated with MTT solution according to manufacturer's instructions. Conditioned culture media were obtained and prepared from A673/TR/LOX-PP cells incubated in presence (LOX-PP rich media) or in absence (control media) of doxycycline as described in the previous section.

Colony formation assay

Cells were plated by triplicate (50,000 cells per 60 mm dishes) in soft agar and cultured in presence or absence of doxycycline during 25 days. Fresh culture medium was added to plates every 2–3 days. At the end of the experiment, three random fields for each plate were photographed. The number of colonies for field and its respective area were calculated using the image analysis software ImageJ [59] (National Institute of Health, Bethesda, MD, USA)

Cell migration assay

Cells were pre-treated with doxycycline for 24 hours to induce the expression of the corresponding LOX proteins. Next, 300.000 pre-treated cells were suspended in 2 ml of medium containing 0.5% fetal bovine serum and placed in the upper compartment of Transwells (8.0 μm pore size) (Corning Costar, Cambridge, MA, USA). The lower compartment was filled with 3 ml of medium containing 10% fetal bovine serum as chemoattractant. After 6 h of incubation to allow cells to migrate through the membrane, the cells remaining on the upper face of the membrane were removed using a cotton wool swab, while the cells on the lower side of the membrane were fixed with methanol and stained with crystal violet. After washing with PBS, crystal violet was dissolved in PBS with 2% SDS and absorbance quantified at 560 nm using an Infinite M200 (Tecan) microplate reader.

Tumor formation assay in nude mice

Athymic 6-week-old female BALB/c nu/nu mice (Harlan Ibérica, Barcelona, Spain) were used in these experiments, which were all carried out in accordance with Institutional and European Union guidelines. Cells were washed twice in PBS and resuspended in Matrigel (BD Biosciences) diluted 1/10 in DMEM at a density of 5×10^7 cells/ml. Animals were subcutaneously injected with the cell solution (0.1 ml) into the left flanks of the mice. Animals were then kept under pathogen free conditions and observed daily for any visible signs of tumors at the injection sites. The tumor volume was measured every 2 or 3 days and calculated using the formula $L\times W^2\times\pi/6$, where L is the length and W is the width of the tumor. When indicated, doxycycline was given by oral route in natural mineral water at a concentration of 1 mg/mL Control animals received water alone. When tumor volume reached 0,5 cm^3, mice were sacrificed and tumors were removed.

Gene expression profiles and functional genomic analyses

To identify genes and pathways regulated by LOX-PP in A673 cells, we used Agilent SurePrint G3 60K v2 microarrays. We analysed the RNA isolated from three separate experiments performed with A673/TR/empty (control cells) and A673/TR/LOX-PP cells stimulated with doxycycline for 72 h to induce the expression of LOX-PP. Labelling, hybridization and scanning were performed at NIMGenetics (Madrid, Spain). Functional genomic analysis was carried out using Gene Set Enrichment Analyses (GSEA) (http://www.broadinstitute.org/gsea/index.jsp, [42]. GSEA is a computational method that determines whether an a priori defined set of genes (made for example by genes that belong to a defined pathway or by genes that share a cis-regulatory motif) is overrepresented at the top or bottom of a ranked list of genes (in our case the list of genes differentially regulated by LOX-PP, ranked using the Student's t-test metric). Gene set permutation was carried out to compute NES (Normalized Enrichment Score) that reflects the degree to which a gene set is overrepresented at the top or bottom of a ranked list of genes. We considered that a gene set/pathway is significantly altered by LOX-PP if that gene set reached a False Discovery Rate (FDR) bellow 0.5% (FDR$<$0.005), which represent a very stringent FDR cut-off. The FDR estimates the probability that a gene set with a given NES represents a false positive finding.

Statistical analysis

For a single comparison of two groups, two tailed Student's t test was used. For all analyses, the level of significance was set at $P<0.05$. All statistical calculations were made using the GraphPad Prism statistical software version 4.0 (GraphPad Software, San Diego, CA).

Supporting Information

Figure S1 Relative expression of LOX in human tumors.
(TIFF)

Figure S2 Functional analysis of gene expression profiles deregulated by LOX-PP (GSEA analysis).
(TIFF)

Table S1 Summary report of gene sets derived from the Reactome pathway database enrichment in A673 cells upon LOX-PP expression.
(PDF)

Acknowledgments

We thank to Dr. E. Lalli for support in proofreading the manuscript and helpful comments.

Author Contributions

Conceived and designed the experiments: NA FC JA. Performed the experiments: NA FC LGG JP. Analyzed the data: NA FC LGG JP JA. Wrote the paper: NA FC JA.

References

1. Potratz J, Dirksen U, Jurgens H, Craft A (2012) Ewing Sarcoma: Clinical State-of-the-Art. Pediatr Hematol Oncol 29: 1–11.
2. Ordonez JL, Osuna D, Herrero D, de Alava E, Madoz-Gurpide J (2009) Advances in Ewing's sarcoma research: where are we now and what lies ahead? Cancer Res 69: 7140–7150.
3. Toomey EC, Schiffman JD, Lessnick SL (2010) Recent advances in the molecular pathogenesis of Ewing's sarcoma. Oncogene 29: 4504–4516.
4. Mackintosh C, Madoz-Gurpide J, Ordonez JL, Osuna D, Herrero-Martin D (2010) The molecular pathogenesis of Ewing's sarcoma. Cancer Biol Ther 9: 655–667.
5. Kovar H (2010) Downstream EWS/FLI1 - upstream Ewing's sarcoma. Genome Med 2: 8.
6. Lessnick SL, Ladanyi M (2011) Molecular Pathogenesis of Ewing Sarcoma: New Therapeutic and Transcriptional Targets. Annu Rev Pathol.
7. Grunewald TG, Diebold I, Esposito I, Plehm S, Hauer K, et al. (2012) STEAP1 Is Associated with the Invasive and Oxidative Stress Phenotype of Ewing Tumors. Mol Cancer Res 10: 52–65.
8. Carrillo J, Garcia-Aragoncillo E, Azorin D, Agra N, Sastre A, et al. (2007) Cholecystokinin down-regulation by RNA interference impairs Ewing tumor growth. Clin Cancer Res 13: 2429–2440.
9. Garcia-Aragoncillo E, Carrillo J, Lalli E, Agra N, Gomez-Lopez G, et al. (2008) DAX1, a direct target of EWS/FLI1 oncoprotein, is a principal regulator of cell-cycle progression in Ewing's tumor cells. Oncogene 27: 6034–6043.
10. Herrero-Martin D, Osuna D, Ordonez JL, Sevillano V, Martins AS, et al. (2009) Stable interference of EWS-FLI1 in an Ewing sarcoma cell line impairs IGF-1/IGF-1R signalling and reveals TOPK as a new target. Br J Cancer 101: 80–90.
11. Prieur A, Tirode F, Cohen P, Delattre O (2004) EWS/FLI-1 silencing and gene profiling of Ewing cells reveal downstream oncogenic pathways and a crucial role for repression of insulin-like growth factor binding protein 3. Mol Cell Biol 24: 7275–7283.
12. Tirado OM, Mateo-Lozano S, Villar J, Dettin LE, Llort A, et al. (2006) Caveolin-1 (CAV1) is a target of EWS/FLI-1 and a key determinant of the oncogenic phenotype and tumorigenicity of Ewing's sarcoma cells. Cancer Res 66: 9937–9947.
13. Mendiola M, Carrillo J, Garcia E, Lalli E, Hernandez T, et al. (2006) The orphan nuclear receptor DAX1 is up-regulated by the EWS/FLI1 oncoprotein and is highly expressed in Ewing tumors. Int J Cancer 118: 1381–1389.
14. Ban J, Jug G, Mestdagh P, Schwentner R, Kauer M, et al. (2011) Hsa-mir-145 is the top EWS-FLI1-repressed microRNA involved in a positive feedback loop in Ewing's sarcoma. Oncogene 30: 2173–2180.
15. Richter GH, Plehm S, Fasan A, Rossler S, Unland R, et al. (2009) EZH2 is a mediator of EWS/FLI1 driven tumor growth and metastasis blocking endothelial and neuro-ectodermal differentiation. Proc Natl Acad Sci U S A 106: 5324–5329.
16. Ban J, Bennani-Baiti IM, Kauer M, Schaefer KL, Poremba C, et al. (2008) EWS-FLI1 suppresses NOTCH-activated p53 in Ewing's sarcoma. Cancer Res 68: 7100–7109.
17. Smith R, Owen LA, Trem DJ, Wong JS, Whangbo JS, et al. (2006) Expression profiling of EWS/FLI identifies NKX2.2 as a critical target gene in Ewing's sarcoma. Cancer Cell 9: 405–416.
18. Kinsey M, Smith R, Lessnick SL (2006) NR0B1 is required for the oncogenic phenotype mediated by EWS/FLI in Ewing's sarcoma. Mol Cancer Res 4: 851–859.
19. Luo W, Gangwal K, Sankar S, Boucher KM, Thomas D, et al. (2009) GSTM4 is a microsatellite-containing EWS/FLI target involved in Ewing's sarcoma oncogenesis and therapeutic resistance. Oncogene 28: 4126–4132.
20. Navarro D, Agra N, Pestana A, Alonso J, Gonzalez-Sancho JM (2010) The EWS/FLI1 oncogenic protein inhibits expression of the Wnt inhibitor DICKKOPF-1 gene and antagonizes beta-catenin/TCF-mediated transcription. Carcinogenesis 31: 394–401.
21. May WA, Lessnick SL, Braun BS, Klemsz M, Lewis BC, et al. (1993) The Ewing's sarcoma EWS/FLI-1 fusion gene encodes a more potent transcriptional activator and is a more powerful transforming gene than FLI-1. Mol Cell Biol 13: 7393–7398.
22. Bailly RA, Bosselut R, Zucman J, Cormier F, Delattre O, et al. (1994) DNA-binding and transcriptional activation properties of the EWS-FLI-1 fusion protein resulting from the t(11;22) translocation in Ewing sarcoma. Mol Cell Biol 14: 3230–3241.
23. Nakatani F, Tanaka K, Sakimura R, Matsumoto Y, Matsunobu T, et al. (2003) Identification of p21WAF1/CIP1 as a direct target of EWS-Fli1 oncogenic fusion protein. J Biol Chem 278: 15105–15115.
24. Hahm KB, Cho K, Lee C, Im YH, Chang J, et al. (1999) Repression of the gene encoding the TGF-beta type II receptor is a major target of the EWS-FLI1 oncoprotein. Nat Genet 23: 222–227.
25. Sankar S, Bell R, Stephens B, Zhuo R, Sharma S, et al. (2012) Mechanism and relevance of EWS/FLI-mediated transcriptional repression in Ewing sarcoma. Oncogene.
26. Owen LA, Kowalewski AA, Lessnick SL (2008) EWS/FLI mediates transcriptional repression via NKX2.2 during oncogenic transformation in Ewing's sarcoma. PLoS One 3: e1965.
27. De Vito C, Riggi N, Suva ML, Janiszewska M, Horlbeck J, et al. (2011) Let-7a is a direct EWS-FLI-1 target implicated in Ewing's sarcoma development. PLoS One 6: e23592.
28. Nakatani F, Ferracin M, Manara MC, Ventura S, Del Monaco V, et al. (2012) miR-34a predicts survival of Ewing's sarcoma patients and directly influences cell chemo-sensitivity and malignancy. J Pathol 226: 796–805.
29. Lucero HA, Kagan HM (2006) Lysyl oxidase: an oxidative enzyme and effector of cell function. Cell Mol Life Sci 63: 2304–2316.
30. Molnar J, Fong KS, He QP, Hayashi K, Kim Y, et al. (2003) Structural and functional diversity of lysyl oxidase and the LOX-like proteins. Biochim Biophys Acta 1647: 220–224.
31. Kagan HM, Li W (2003) Lysyl oxidase: properties, specificity, and biological roles inside and outside of the cell. J Cell Biochem 88: 660–672.
32. Smith-Mungo LI, Kagan HM (1998) Lysyl oxidase: properties, regulation and multiple functions in biology. Matrix Biol 16: 387–398.
33. Palamakumbura AH, Jeay S, Guo Y, Pischon N, Sommer P, et al. (2004) The propeptide domain of lysyl oxidase induces phenotypic reversion of ras-transformed cells. J Biol Chem 279: 40593–40600.
34. Min C, Kirsch KH, Zhao Y, Jeay S, Palamakumbura AH, et al. (2007) The tumor suppressor activity of the lysyl oxidase propeptide reverses the invasive phenotype of Her-2/neu-driven breast cancer. Cancer Res 67: 1105–1112.
35. Wu M, Min C, Wang X, Yu Z, Kirsch KH, et al. (2007) Repression of BCL2 by the tumor suppressor activity of the lysyl oxidase propeptide inhibits transformed phenotype of lung and pancreatic cancer cells. Cancer Res 67: 6278–6285.
36. Navarro D, Agra N, Pestana A, Alonso J, Gonzalez-Sancho JM (2010) The EWS/FLI1 oncogenic protein inhibits expression of the Wnt inhibitor DICKKOPF-1 gene and antagonizes beta-catenin/TCF-mediated transcription. Carcinogenesis 31: 394–401.
37. Duvic M, Vu J (2007) Vorinostat: a new oral histone deacetylase inhibitor approved for cutaneous T-cell lymphoma. Expert Opin Investig Drugs 16: 1111–1120.
38. Robert MF, Morin S, Beaulieu N, Gauthier F, Chute IC, et al. (2003) DNMT1 is required to maintain CpG methylation and aberrant gene silencing in human cancer cells. Nat Genet 33: 61–65.
39. Hurtado PA, Vora S, Sume SS, Yang D, St Hilaire C, et al. (2008) Lysyl oxidase propeptide inhibits smooth muscle cell signaling and proliferation. Biochem Biophys Res Commun 366: 156–161.
40. Vora SR, Guo Y, Stephens DN, Salih E, Vu ED, et al. (2010) Characterization of recombinant lysyl oxidase propeptide. Biochemistry 49: 2962–2972.
41. Guo Y, Pischon N, Palamakumbura AH, Trackman PC (2007) Intracellular distribution of the lysyl oxidase propeptide in osteoblastic cells. Am J Physiol Cell Physiol 292: C2095–2102.
42. Subramanian A, Tamayo P, Mootha VK, Mukherjee S, Ebert BL, et al. (2005) Gene set enrichment analysis: a knowledge-based approach for interpreting genome-wide expression profiles. Proc Natl Acad Sci U S A 102: 15545–15550.
43. Kauer M, Ban J, Kofler R, Walker B, Davis S, et al. (2009) A molecular function map of Ewing's sarcoma. PLoS One 4: e5415.
44. Hancock JD, Lessnick SL (2008) A transcriptional profiling meta-analysis reveals a core EWS-FLI gene expression signature. Cell Cycle 7: 250–256.
45. Kuivaniemi H, Korhonen RM, Vaheri A, Kivirikko KI (1986) Deficient production of lysyl oxidase in cultures of malignantly transformed human cells. FEBS Lett 195: 261–264.
46. Bouez C, Reynaud C, Noblesse E, Thepot A, Gleyzal C, et al. (2006) The lysyl oxidase LOX is absent in basal and squamous cell carcinomas and its knockdown induces an invading phenotype in a skin equivalent model. Clin Cancer Res 12: 1463–1469.

47. Hamalainen ER, Kemppainen R, Kuivaniemi H, Tromp G, Vaheri A, et al. (1995) Quantitative polymerase chain reaction of lysyl oxidase mRNA in malignantly transformed human cell lines demonstrates that their low lysyl oxidase activity is due to low quantities of its mRNA and low levels of transcription of the respective gene. J Biol Chem 270: 21590–21593.
48. Csiszar K, Fong SF, Ujfalusi A, Krawetz SA, Salvati EP, et al. (2002) Somatic mutations of the lysyl oxidase gene on chromosome 5q23.1 in colorectal tumors. Int J Cancer 97: 636–642.
49. Ren C, Yang G, Timme TL, Wheeler TM, Thompson TC (1998) Reduced lysyl oxidase messenger RNA levels in experimental and human prostate cancer. Cancer Res 58: 1285–1290.
50. Kenyon K, Contente S, Trackman PC, Tang J, Kagan HM, et al. (1991) Lysyl oxidase and rrg messenger RNA. Science 253: 802.
51. Hajnal A, Klemenz R, Schafer R (1993) Up-regulation of lysyl oxidase in spontaneous revertants of H-ras-transformed rat fibroblasts. Cancer Res 53: 4670–4675.
52. Jeay S, Pianetti S, Kagan HM, Sonenshein GE (2003) Lysyl oxidase inhibits ras-mediated transformation by preventing activation of NF-kappa B. Mol Cell Biol 23: 2251–2263.
53. Giampuzzi M, Botti G, Cilli M, Gusmano R, Borel A, et al. (2001) Down-regulation of lysyl oxidase-induced tumorigenic transformation in NRK-49F cells characterized by constitutive activation of ras proto-oncogene. J Biol Chem 276: 29226–29232.
54. Zhao Y, Min C, Vora SR, Trackman PC, Sonenshein GE, et al. (2009) The lysyl oxidase pro-peptide attenuates fibronectin-mediated activation of focal adhesion kinase and p130Cas in breast cancer cells. J Biol Chem 284: 1385–1393.
55. Palamakumbura AH, Vora SR, Nugent MA, Kirsch KH, Sonenshein GE, et al. (2009) Lysyl oxidase propeptide inhibits prostate cancer cell growth by mechanisms that target FGF-2-cell binding and signaling. Oncogene 28: 3390–3400.
56. Min C, Zhao Y, Romagnoli M, Trackman PC, Sonenshein GE, et al. (2010) Lysyl oxidase propeptide sensitizes pancreatic and breast cancer cells to doxorubicin-induced apoptosis. J Cell Biochem 111: 1160–1168.
57. Navarro S, Gonzalez-Devesa M, Ferrandez-Izquierdo A, Triche TJ, Llombart-Bosch A (1990) Scanning electron microscopic evidence for neural differentiation in Ewing's sarcoma cell lines. Virchows Arch A Pathol Anat Histopathol 416: 383–391.
58. Sorensen PH, Lessnick SL, Lopez-Terrada D, Liu XF, Triche TJ, et al. (1994) A second Ewing's sarcoma translocation, t(21;22), fuses the EWS gene to another ETS-family transcription factor, ERG. Nat Genet 6: 146–151.
59. Abramoff MD, Magalhaes PJ, Ram SJ (2004) Image processing with ImageJ. Biophotonics International 11: 36–42.

frontiers in Oncology

REVIEW
published: 20 July 2015
doi: 10.3389/fonc.2015.00162

EWS/FLI1 target genes and therapeutic opportunities in Ewing sarcoma

Florencia Cidre-Aranaz and Javier Alonso *

Unidad de Tumores Sólidos Infantiles, Área de Genética Humana, Instituto de Investigación de Enfermedades Raras, Instituto de Salud Carlos III, Madrid, Spain

Ewing sarcoma is an aggressive bone malignancy that affect children and young adults. Ewing sarcoma is the second most common primary bone malignancy in pediatric patients. Although significant progress has been made in the treatment of Ewing sarcoma since it was first described in the 1920s, in the last decade survival rates have remained unacceptably invariable, thus pointing to the need for new approaches centered in the molecular basis of the disease. Ewing sarcoma driving mutation, *EWS–FLI1*, which results from a chromosomal translocation, encodes an aberrant transcription factor. Since its first characterization in 1990s, many molecular targets have been described to be regulated by this chimeric transcription factor. Their contribution to orchestrate Ewing sarcoma phenotype has been reported over the last decades. In this work, we will focus on the description of a selection of EWS/FLI1 targets, their functional role, and their potential clinical relevance. We will also discuss their role in other types of cancer as well as the need for further studies to be performed in order to achieve a broader understanding of their particular contribution to Ewing sarcoma development.

Keywords: Ewing sarcoma, EWS/FLI1, DAX-1, GLI1, FOXO1, FOXM1, CCK, LOX

OPEN ACCESS

Edited by:
Thomas Grunewald, Ludwig Maximilian University of Munich, Germany

Reviewed by:
Elizabeth R. Lawlor, University of Michigan, USA
Eleni Tomazou, Children's Cancer Research Institute, Austria

***Correspondence:**
Javier Alonso, Unidad de Tumores Sólidos Infantiles, Área de Genética Humana, Instituto de Investigación de Enfermedades Raras, Instituto de Salud Carlos III, Ctra. Pozuelo-Majadahonda, km 2, 28220 Majadahonda, Madrid, Spain
fjalonso@isciii.es

Specialty section:
This article was submitted to Pediatric Oncology, a section of the journal Frontiers in Oncology

Received: *29 April 2015*
Accepted: *06 July 2015*
Published: *20 July 2015*

Citation:
Cidre-Aranaz F and Alonso J (2015) EWS/FLI1 target genes and therapeutic opportunities in Ewing sarcoma. Front. Oncol. 5:162. doi: 10.3389/fonc.2015.00162

Introduction

Ewing sarcoma is a rare tumor that arises mainly in the bones of children and adolescents. Despite the improvements in treatment achieved during the last decades, survival rates have remained unacceptably low, even in patients with localized disease, since a great proportion of Ewing sarcoma tumors are refractory to conventional treatment and relapses are frequent (1). In addition, approximately 25% of cases present disseminated disease at diagnosis, which have a very poor prognosis (2). Thus, there is an urgent need for new targeted therapies that may offer a higher efficiency and less adverse effects than the conventional chemo/radiotherapies that are used nowadays.

In this sense, understanding the molecular basis of Ewing sarcoma pathogenesis provides key information that may help to design new targeted biological therapies. Ewing sarcomas are characterized by chromosomal translocations that fuse the *EWSR1* gene to some members of the ETS family of transcription factors (3), being FLI1 the most frequently implicated [t(11;22)(q24;q12)] (4). The EWS/FLI1 fusion protein is an aberrant transcription factor that is essential for Ewing tumor development, since it regulates the expression of multiple target genes and governs the oncogenic processes that lead to malignant transformation of a yet undefined cancer precursor cell. Provided that the oncogenic properties of EWS/FLI1 rely on its capability to induce or repress specific target genes, these target genes can likewise offer interesting opportunities to identify new targeted therapies.

In the past years, an important effort to identify EWS/FLI1 genes functionally relevant for Ewing sarcoma pathogenesis has been carried out. As a consequence, many genes that play an important role in Ewing sarcoma have been identified (5–17). This has revealed some key molecular pathways involved in Ewing pathogenesis, and more importantly it has provided new molecular targets.

A comprehensive discussion of all EWS/FLI1 target genes identified to date and their implications in targeted therapy is beyond the scope of this review. Thus, here we have focused on a selection of six EWS/FLI1 target genes that, in our opinion, can represent attractive opportunities for future studies that may lead to discovering new therapeutic approaches. This selection takes into account the presence of significant data – in Ewing or in other systems – regarding potential therapeutic applications. Four genes encode for transcriptional regulators while the other two encode for secreted proteins.

Transcriptional Regulators

DAX-1 (NR0B1)

DAX-1 is a gene that belongs to the super family of nuclear receptors (official name *NR0B1*, standing for Nuclear Receptor Subfamily 0, Group B, Member 1). Nuclear receptors are transcription factors that undergo activation upon binding of small ligands such as retinoic acid or steroids. However, there is no known ligand for DAX-1, and thus we refer to it as an orphan nuclear receptor. Germline mutations in this gene are the cause of dosage-sensitive sex reversal (DSS) in XY individuals and adrenal hypoplasia congenital (AHC), which is characterized by adrenal insufficiency, and hypogonadotropic hypogonadism in males. DAX-1 is a master regulator of steroidogenesis that negatively regulates the steroidogenic factor 1 (SF1), an important transcriptional activator of genes involved in steroid hormone production (18, 19). In addition, DAX-1 plays an important role in several biological processes such as osteoblast differentiation (20), ion homeostasis and transport, lipid transport, or skeletal development (21) among others. More recently, DAX-1 has been involved in the maintenance of mouse embryonic stem cell pluripotency through regulation of stem cell genes like *Oct-3/4* (22–24).

Given that DAX-1 function is mainly linked to steroidogenesis, it was surprising to find this gene associated to Ewing sarcoma, a tumor with no known relationship with steroidogenic tissues. Gene expression profiles performed in two heterologous cell models ectopically expressing EWS/FLI1 (HEK293 and HeLa cells) demonstrated that DAX-1 was specifically induced by EWS/FLI1, but not by wildtype FLI1 (25). In addition, it was shown that DAX-1 was highly expressed in Ewing sarcoma cell lines and tumors, while it was not expressed in other pediatric tumors such as rhabdomyosarcoma or neuroblastoma. Finally, DAX-1 expression was demonstrated to depend on EWS/FLI1 expression in the A673 Ewing sarcoma cell line upon EWS/FLI1 knockdown. An independent study showed similar findings, confirming that DAX-1 is a target of the EWS/FLI1 oncoprotein (26).

Several functional studies have demonstrated that DAX-1 plays a critical role in Ewing sarcoma pathogenesis: DAX-1 knockdown impairs Ewing sarcoma cell proliferation, G1 cell arrest induction, inhibits anchorage independent growth of colonies in soft agar, and drastically inhibits growth of xenotransplanted tumor cells in immunodeficient mice (9, 25, 26). These results are highly consistent since they were obtained in independent laboratories, using several Ewing sarcoma cell lines (TC71, EWS502, and A673) and different gene knockdown technologies (i.e., transient retrovirus infection or inducible expression of EWS/FLI1 shRNAs). Interestingly, characterization of the gene expression profile regulated by DAX-1 in Ewing sarcoma cell lines has also provided interesting findings regarding the function of DAX-1 in Ewing sarcoma. These studies showed that a significant percentage of the genes regulated by EWS/FLI1 in Ewing sarcoma cells are also under the control of DAX-1, reinforcing the importance of DAX-1 in Ewing sarcoma pathogenesis. In fact, two independent works demonstrated that EWS/FLI1 and DAX-1 transcriptional profiles share a significant number of genes, suggesting that DAX-1 not only contributes to the EWS/FLI1 transcriptional signature but also that there is a hierarchy controlled by EWS/FLI1 and in which some genes, such as *DAX-1*, can play a more prominent role (9, 27). The study of the mechanism through which EWS/FLI1 upregulates DAX-1 expression in Ewing sarcoma cells revealed an unexpected finding: EWS/FLI1 directly interacts with *DAX-1* promoter through binding to a GGAA-rich sequence (9, 28). This motif resulted to be a polymorphic microsatellite located in the *DAX-1* promoter. It has been demonstrated that EWS/FLI1 binds similar sequences located in the promoters of other EWS/FLI1 target genes, indicating that this mechanism of gene transcriptional activation is frequently used by EWS/FLI1 to regulate the expression of some oncogenic genes (28) [i.e., *Caveolin-1* (*CAV1*) (7), *glutathione S-transferase M4* (*GSTM4*) (29), *FCGRT* (*Fc fragment of IgG, receptor, transporter, alpha*), *FVT1/KDSR* (*3-ketodihydrosphingosine reductase*)or *ABHD6* (*Abhydrolase Domain-Containing Protein*) (30)]. The fact that *DAX-1* expression is regulated through a polymorphic repeat of the GGAA motif raised the question if the number of repeats could be somehow linked to the level of *DAX-1* expression and, as a consequence, to the malignant phenotype of Ewing sarcoma. Several biochemical studies demonstrated a relationship between the number of GGAA repeats and the degree of promoter activation, indicating that it was necessary a minimum of nine repeats to obtain a response to EWS/FLI1 (30). However, the attempts to establish a relationship between the length of the microsatellite located in *DAX-1* promoter and the clinical prognosis have raised contradictory results. For instance, GGAA microsatellites were longer in African populations, which are known to have a lower incidence of Ewing sarcoma but a worse overall survival when compared to European populations (31, 32). Conversely, in another study based on 112 patients, the length of the DAX-1 microsatellite showed no influence on clinical outcomes (33).

Taking into account all these results, *DAX-1* can be considered as one of the most relevant EWS/FLI1 gene targets. The fact that DAX-1 expression results essential for EWS/FLI1-mediated oncogenesis opens the possibility, at least in theory, to consider *DAX-1* targeting as an attractive therapeutic approach in Ewing sarcoma. As a consequence, a more profound understanding of the functions that DAX-1 exerts in Ewing sarcoma and the

molecular mechanism involved in them can provide new clues on how to interfere with its expression or function in this cancer (34).

DAX-1 is located in the nucleus of Ewing sarcoma cells, where it presumably interacts with other transcription factors and cofactors to regulate downstream target genes that are important for oncogenesis. Interestingly, a combination of biochemical and gene expression profile experiments leads to the observation that EWS/FLI1 and DAX-1 interact physically. Specifically, it was found that both the amino- and carboxyl-termini of DAX-1 interacted with EWS/FLI1 (27). This result opens the attractive possibility that interfering EWS/FLI1-DAX-1 interaction could lead to new therapeutic opportunities. To go forward in this line of work, it would be necessary to finely map the regions involved in this interaction in order to design small molecules with the ability to block it. Since DAX-1 and EWS/FLI1 interaction could be necessary for full EWS/FLI1-mediated oncogenesis, disturbing it could be therapeutically valuable.

DAX-1 has been shown to interact in different cellular contexts with a variety of transcriptional regulators, mainly corepressors. For example, DAX-1 interacts with Alien corepressor through its silencing domain and this interaction has been shown to be important for AHC pathogenesis (35). DAX-1 has also been shown to interact directly with the androgen receptor, NR3C4, inhibiting its activation (36) and other partners such as NR5A1 (37) and ESRRγ (38). To date, a systematic analysis of the protein–protein interactions in which DAX-1 is involved in Ewing sarcoma cells and the role that these interactions can play in Ewing sarcoma pathogenesis has not been carried out. Experiments focused on identifying and characterizing these interactions could provide clues for designing synthetic drugs to target them. On the other hand, it has been shown that DAX-1 C-terminal domain contains a potent transcriptional repressor domain that, when altered by mutations in AHC patients, impairs its nuclear localization, and therefore its transcriptional activity (39), suggesting that there is a potential field for developing drugs to modulate DAX-1 subcellular localization and consequently its function.

As with any new drug, the possible side effects of a new therapeutic approach must be also taken into consideration. For instance, prolonged DAX-1 blockage may lead to disequilibrium in steroid hormones production, which could lead to Cushing-like syndrome (40). These hypothetical complications, compared with the severity of Ewing sarcoma itself, would be perfectly assumable. One theoretical advantage of using therapeutic approaches targeting *DAX-1* is that this gene is only expressed in a limited number of tissues, mainly in adrenal gland and testis, and probably DAX-1 targeting will only affect these organs. In summary, although there are currently no drugs able to target DAX-1 and block its function, studies intended to understand its structure, its mechanism of interaction with other transcriptional (co)factors, and the identification of other protein–protein interactions in the Ewing sarcoma context could provide new insights to design new therapeutic molecules (**Figure 1**).

GLI1

GLI1 (*Glioma-Associated Oncogene Homolog 1)* is a transcription factor belonging to the Kruper family of zinc finger proteins. GLI1 is a component of the canonical Hedgehog pathway: extracellular Sonic Hedgehog (Shh) binds to the PTCH receptor causing the liberation of Smooth (SMO) from the PTCH-SMO complex. Subsequently, activated SMO releases GLI1 from the complex that it forms with Suppressor of Fused (SUFU), which permits GLI1 nuclear translocation where it regulates gene transcription of genes involved in normal cell growth and differentiation such as the embryonic pattern formation (41). Although this pathway is mainly active during embryogenesis, it remains active in some adult tissues, where it is involved in homeostasis and stem-cell maintenance (42, 43).

Zwerner et al. described an association between EWS/FLI1 and GLI1 in Ewing sarcoma cells. They showed that NIH3T3 cells expressing *EWS/FLI1* presented the expected malignant phenotype concomitantly with augmented levels of GLI1 (44). Moreover, when GLI1 expression was knocked-down by RNA interference, the transformed phenotype was reduced (demonstrated by a decrease in the anchorage independent growth) indicating that GLI1 plays an important role in the maintenance of the malignant phenotype induced by EWS/FLI1. Interestingly, SUFU overexpression, which is expected to inhibit GLI1, also produced similar effects in NIH3T3 cells. In TC32 Ewing sarcoma cells, EWS/FLI1 knocking down using RNA interference produced a reduction in *GLI1* expression levels. Also, ChIP studies demonstrated that GLI1 is a direct target of EWS/FLI1 (45). Moreover, when a shRNA against GLI1 was used in the Ewing sarcoma cell line TC32, the transformed phenotype was inhibited (measured by reduction in anchorage independent growth) (44). Interestingly, and in contrast with what it is usually observed in other types of cancer, GLI1 deregulation in Ewing sarcoma is independent of Shh since its activation did not produce phenotypic changes nor did a pharmacological blockage of SMO using cyclopamine (an inhibitor of Shh signaling by direct binding to SMO) (45).

Subsequently Joo et al. (46) showed that Ewing primary tumors expressed high levels of GLI1. These authors also confirmed using RNAi that the expression of GLI1 in Ewing sarcoma cells (TC71) is dependent on EWS/FLI1 and that GLI1 expression was relevant for the maintenance of the transformed phenotype. Strikingly, re-analysis of gene expression profiles showed that genes that were traditionally thought to be transcriptionally modulated by EWS/FLI1, such as *NKX2.2*, *Patched (PTCH)* or *GAS1*, were indeed dependent on GLI1 expression, meaning that the gene expression network regulated by EWS/FLI1 holds a hierarchy in which GLI1 has a prominent role.

Deregulation of the Shh–GLI1 pathway has been showed to lead to tumorigenesis and aggressive phenotypes (progression, metastasis and therapeutic resistance) of numerous cancer types such as basal cell carcinomas (47), colorectal carcinoma (48), breast cancer (49), and bone and soft tissue sarcomas (50).

Given the importance of Shh–GLI1 pathway in cancer, some therapeutic approaches, focused on the blocking of this pathway, have been developed over the years. One of these strategies consisted in searching for small molecule inhibitors of the pathway. Thus, Shh–GLI1 pathway inhibitors, such as cyclopamine, have been successfully tested in some cancer types such as medulloblastoma (51), pancreatic adenocarcinoma (52), small-cell lung cancer (SCLC) (53), gastric adenocarcinomas (54), and esophageal cancer (55).

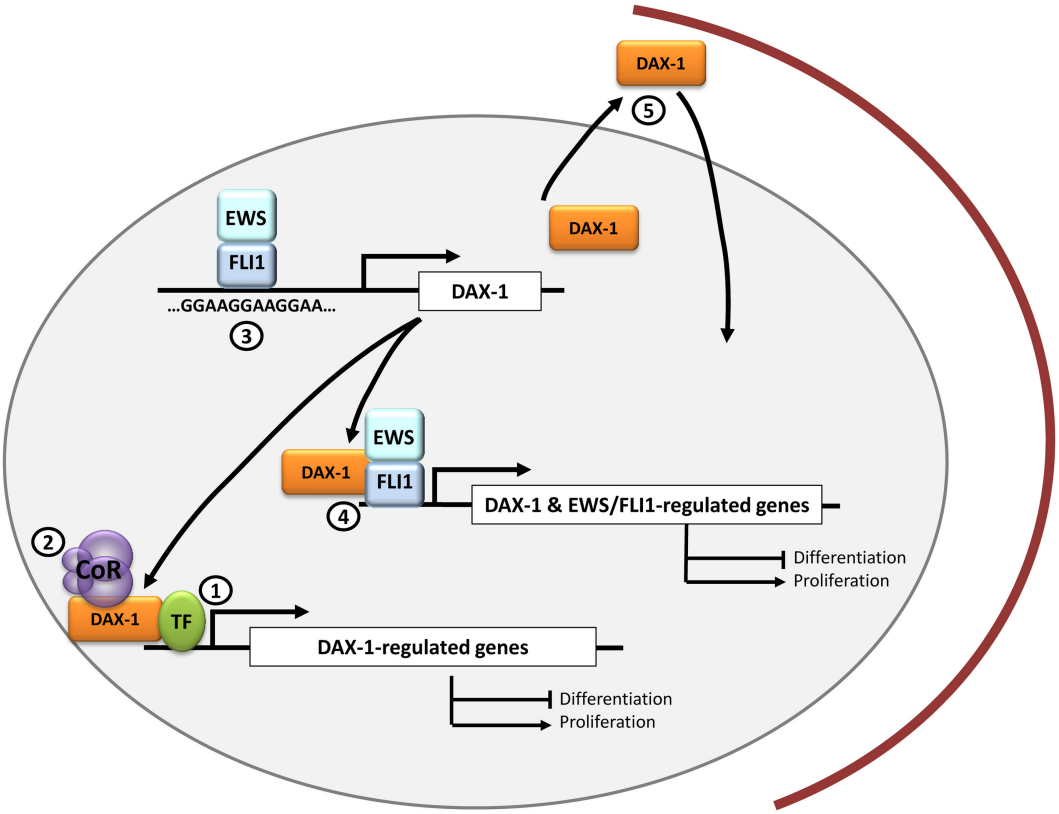

FIGURE 1 | DAX-1 and therapeutic opportunities in Ewing sarcoma. DAX-1 expression is upregulated by EWS/FLI1 in Ewing sarcoma cells through a direct interaction with a polymorphic GGAA microsatellite located in the *DAX-1* promoter. Since DAX-1 expression is essential for EWS/FLI1-mediated oncogenesis, it is still necessary to ascertain if it interacts with other transcription factors (1) and/or co-repressors (2) in the nucleus of Ewing sarcoma cells. This could open new therapeutic approaches for designing molecules to target these interactions. Potential therapeutic targets may be molecules that prevent EWS/FLI1 binding to the GGAA-rich motifs in *DAX-1* promoter (3) or drugs directed toward the EWS/FLI1-DAX-1 interaction, whose concurrence could be necessary to regulate the expression of certain genes (4). Finally, DAX-1 C-terminal domain can impair DAX-1 nuclear localization when altered so it could be potentially targeted to modulate its subcellular localization and thus its function (5).

The fact that GLI1 expression is constitutively induced by EWS/FLI1 in Ewing sarcoma suggests that drugs acting upstream GLI1 will be ineffective in blocking this pathway in this cancer. In agreement with this, cyclopamine treatment of Ewing sarcoma cells would have no effect on the malignant characteristics of Ewing sarcoma cells. For this reason, efforts should be directed toward developing and studying drugs targeting GLI1 expression or function directly. In this sense, arsenic trioxide (ATO), an old drug recently reintroduced in the repertoire of anticancer drugs, has been found to inhibit cell growth by targeting GLI proteins (56). In the specific case of Ewing sarcoma, ATO presented cytotoxicity in cell lines with upregulated GLI1 expression (TC-71, SKES and A4573), and curbed xenograft growth performed with TC-71 cells (57). ATO was also found to inhibit Ewing cells (RDES and A673) migration and invasiveness, thus implying that it could also have a therapeutic effect on metastasis (58). Of note, ATO has already been tested in combination with other chemotherapeutic drugs (etoposide and paclitaxel) in a preliminary study that included Ewing sarcoma and metastatic osteosarcoma patients where tumor growth was controlled in 75% of cases (59). However, since Ewing sarcoma is mainly a pediatric cancer, it is necessary to further investigate its effects and to be prudent when designing clinical studies given the roles of the Shh–GLI1 pathway in development.

Finally, it has been described a correlation between GLI1 expression levels and/or prognosis and recurrence in some cancer types. For instance, in a study comprising 25 clinical samples of colorectal carcinoma, Shh expression was found upregulated and, interestingly, when GLI1 expression was analyzed by *in situ* hybridization, it was mainly found in the malignant crypts of adenocarcinomas (48). Also, it has been described a positive correlation between GLI1 expression and tumor grade and/or lymph node status, pointing to a role of GLI1 in metastasis. Some examples are breast cancer, where high GLI1 expression measured in a TMA containing 204 tumor samples was associated with poor prognosis and progressive stages of disease (49) or bone and soft tissue sarcomas, where higher GLI1 expression correlated with more aggressive outcomes (50). In the specific case of Ewing sarcoma, these studies remain to be performed, especially considering that a deeper knowledge on this field could lead to a more efficient patient stratification that could help improve treatment.

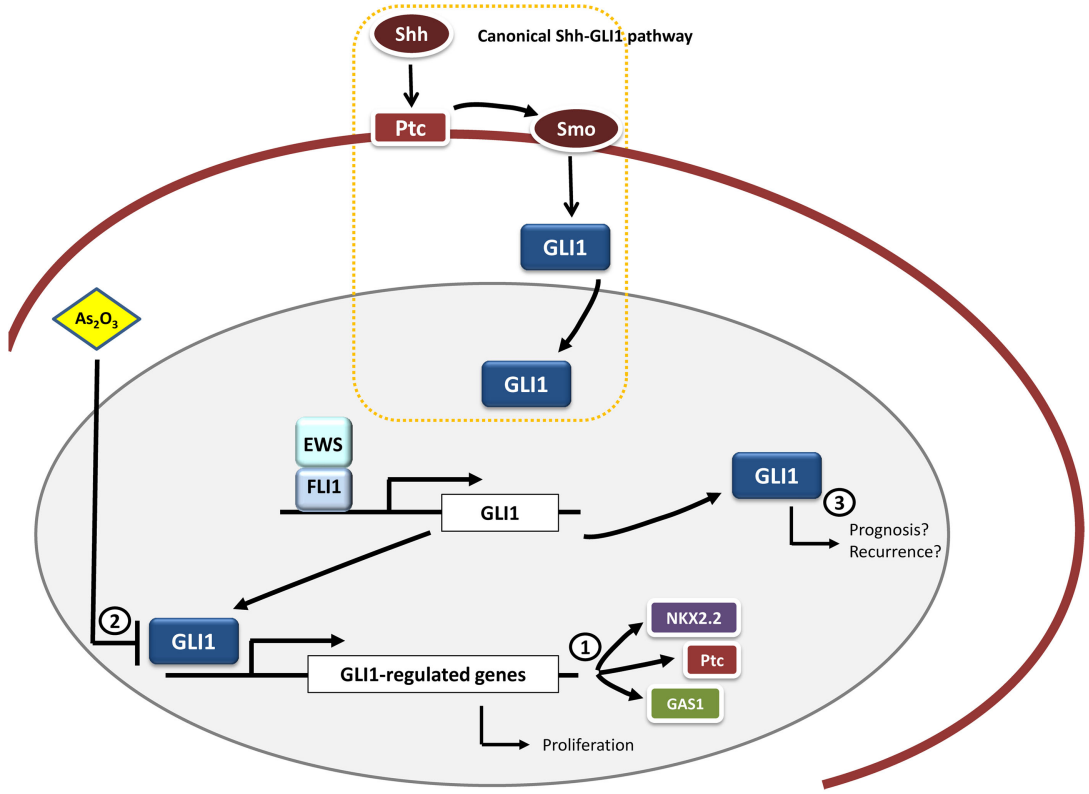

FIGURE 2 | GLI1 and therapeutic opportunities in Ewing sarcoma. *GLI1* is an upregulated direct target gene of EWS/FLI1 in Ewing sarcoma cells. Functional studies have demonstrated that GLI1 expression is relevant for the maintenance of the transformed phenotype in this system. Moreover, some genes transcriptionally modulated by EWS/FLI1 depend on GLI1 expression, including *NKX2.2, PATCH*, and *GAS1* (1). Therapeutic opportunities may include the use of molecules capable of inhibiting GLI1-mediated transcription, such as arsenic trioxide (As_2O_3) (2). Also it may be interesting to ascertain the possible link between GLI1 expression pattern and prognosis in Ewing sarcoma given that this correlation between GLI1 expression and bad prognosis exists in other tumor types (breast cancer and bone and soft tissue sarcomas) (3).

There is still an urgent need for further functional studies that can ascertain the exact role of this pathway in Ewing sarcoma development and progression. These studies could help to synthesize new compounds or small molecules that could target GLI1 with better efficacies either alone or in combination with normal chemotherapeutic treatments (**Figure 2**).

Forkhead Box (FOX) of Transcription Factors

Forkhead box proteins are an extensive family of transcriptional regulators that share a common DNA binding domain (the forkhead domain). There are 19 subgroups (FOXA to FOXS) organized on the basis of sequence homology inside and outside the forkhead domain. FOX proteins regulate gene networks that are involved in cell cycle progression, proliferation, differentiation, metabolism, senescence, survival, or apoptosis (60). Thus, it is not strange that these transcription factors have been shown to have roles in cancer. Interestingly, some members of this family have been shown to act as tumor suppressor genes, while others have been shown to be pro-oncogenic. Examples of both of these opposed functions have been identified in Ewing sarcoma.

The FOXO subgroup (consisting of FOXO1, FOXO3A, FOXO4, and FOXO6) are key negative regulators of cell proliferation and survival. They induce cell cycle arrest at G1 (61) and apoptosis and DNA repair (62). They are thus considered bona fide tumor suppressors. For example, in prostate cancer, *FOXO1* is found transcriptionally downregulated and the induction of its expression in prostate cancer cells inhibits cell proliferation and survival (63). In addition, FOXO1 has been also shown to regulate other hallmarks of cancer such as angiogenesis. Thus, FOXO1 loss of function increases blood vessel formation and promotes endothelial cell proliferation and migration (64, 65).

FOXOs transcriptional activity is regulated by changes in their cellular localization, which is mediated by protein kinases such as the serum/glucocorticoid kinase (SGK) and the protein kinase B (AKT) [reviewed in Ref. (66)]. These transcription factors can also undergo different post-translational modifications that regulate their activity including deacetylation mediated by Sirt1 and ubiquitination mediated by Skp2 and Mdm2 (67).

EWS/FLI1 binds to the FOXO1 promoter and represses its expression in Ewing sarcoma cells (68). In accordance with this, FOXO1 is expressed at lower levels in primary Ewing sarcoma as compared to other tissues (16). Induction of FOXO1 in two Ewing sarcoma cells (A673 and SKNMC) resulted in impaired cell proliferation and reduced soft agar colony formation capability, confirming that FOXO1 is a tumor suppressor in Ewing

sarcoma and that its inhibition is important for Ewing sarcoma growth. Interestingly, EWS/FLI1 also indirectly regulates the subcellular localization of FOXO1 and thus controls its transcriptional activity. CDK2- (which is upregulated by EWS/FLI1 and acts as a negative regulator of FOXO1 transcriptional activity) and AKT-mediated phosphorylation of FOXO1 cooperate to block its transport to the nucleus thus inhibiting its transcriptional activity. These findings demonstrate that EWS/FLI1 blocks FOXO1 activity at several different levels in Ewing sarcoma cells.

Since FOXO1 acts as a tumor suppressor in Ewing sarcoma, a valuable therapeutic approach can consist in the reactivation of FOXO1 activity. In this regard, methylseleninic acid (MSA), a chemical compound previously shown to reactivate FOXO1 in prostate cancer, was tested in Ewing sarcoma cells (69). Treatment of Ewing sarcoma cells with MSA induced FOXO1 expression in a concentration-dependent manner, which correlated with apoptotic-mediated cell death. This effect was mediated at least in part by FOXO1, since the knockdown of endogenously induced FOXO1 significantly reduced the apoptotic effect of MSA. Notably, administration of MSA in an orthotopic mouse xenotransplantation model significantly reduced tumor growth, suggesting that MSA could be a potential therapeutic approach in Ewing sarcoma. However, it should be taken into account that high concentrations of selenium are usually associated with intoxication, which can make this approach problematic. This means that any potential application of MSA should use effective, low doses, which in combination with conventional chemotherapeutic drugs can reach the desired anti-tumoral effects. Particularly, MSA has already been proved to synergize well with some chemotherapeutic drugs that are frequently used in Ewing sarcoma, such as etoposide or doxorubicin (70) (**Figure 3**). Since reactivation of FOXO1 in Ewing sarcoma cells has shown to be effective both *in vitro* and *in vivo*, more studies are necessary to understand the mechanism involved in the regulation of FOXO1 expression and its transcriptional activity in order to identify new therapeutic targets.

FOXM1 is another member of the FOX family of transcription factors that contrary to FOXO displays a pro-oncogenic role in cancer. In fact, FOXM1 is one of the most commonly overexpressed genes in solid tumors (71). Initially, FOXM1 was described as a proliferation-specific mammalian transcription factor, expressed in proliferating cells but not in quiescent or terminally differentiated cells. In addition to this, and over the years, FOXM1 has also been implicated in cell migration, invasion, angiogenesis, metastasis, or oxidative stress (72).

Christensen et al. showed that EWS/FLI1 upregulated the levels of FOXM1 in four Ewing sarcoma cell lines, although the mechanism appeared to be indirect (17). In agreement with this, FOXM1 is expressed at high levels in Ewing sarcoma cell lines and primary tumors. In order to characterize the relevance of FOXM1 in Ewing sarcoma pathogenesis, the authors performed FOXM1

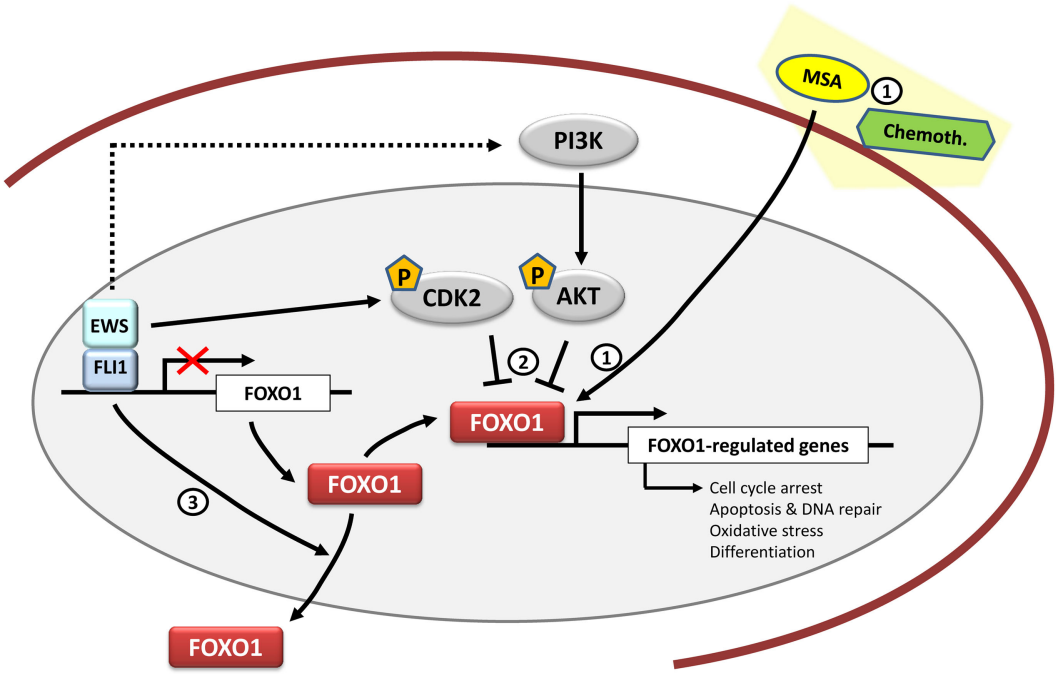

FIGURE 3 | FOXO1 and therapeutic opportunities in Ewing sarcoma. *FOXO1* is a direct target gene of EWS/FLI1 and its expression is repressed by EWS/FLI1 in Ewing sarcoma cells. Functional studies have shown that *FOXO1* acts as a tumor suppressor in the Ewing sarcoma cell context. Therapeutically, Methane Sulfonic Acid (MSA) may be used as a potential treatment in synergy with other chemotherapeutic agents such as doxorubicin or etoposide. However, its mechanism of action in Ewing sarcoma is still unknown (1). Also there is still a need to clarify the FOXO1 activities mediated by kinases such as CDK2 and AKT (2) together with the regulation of its subcellular localization (3), and to determine if they may be mediated by EWS/FLI1.

knockdown experiments demonstrating that FOXM1 downregulation correlates with a significant reduction in anchorage independent growth.

Interestingly, pharmacological approaches addressed to reduce FOXM1 levels have also been tested in Ewing sarcoma cells with notable results. Thiostrepton, a thiazole antibiotic, has been shown to act as a proteosomal inhibitor (73) and also to physically interact with FOXM1 consequently inhibiting FOXM1 binding to target promoters (74). FOXM1 expression was inhibited by treatment with thiostrepton, which paralleled with an increase in apoptosis in a variety of Ewing sarcoma cell lines (17). Thiostrepton was also shown to inhibit tumor growth in mouse xenograft models (75). Strikingly, in this work, thiostrepton was able to concomitantly inhibit the expression of EWS/FLI1 both at mRNA and protein levels in three Ewing cell lines and in tumors derived from thiostrepton-treated mouse xenograft models (75). Although the mechanism by which thiostrepton promotes EWS/FLI1 downregulation was not characterized, these results suggest that this drug may show greater efficacy in Ewing sarcoma tumors in comparison to other tumors.

As stated above, FOXM1 is frequently overexpressed in cancer and takes part in each hallmark of cancer. Consequently it has been argued that targeting FOXM1 could provide an opportunity to treat cancer. It has also been proposed that FOXM1 could be the "Achilles heel" of cancer (76). Taken together, these findings suggest that targeting FOXM1 may be also an opportunity for Ewing sarcoma treatment (**Figure 4**).

Secreted Proteins

Cholecystokinin

Cholecystokinin (CCK) is a neuropeptide that displays a diversity of functions in the organism. It was originally discovered in the gastrointestinal tract, where it mainly regulates pancreatic secretion of digestive enzymes. In addition, CCK is one of the most abundant and widely distributed neuropeptides in the brain, where it modulates intrinsic neuronal excitability and synaptic transmission. CCK is secreted as a prohormone (proCCK) that subsequently undergoes post-translational processing (tyrosine sulfatation, endoproteolytic cleavage, basic residue removal, and C-terminal amidation), resulting in the production of CCK biologically active forms, mainly CCK8 (77).

More than two decades ago, CCK was found to be specifically expressed in a group of human cancer cell lines that included Ewing sarcoma, neuroepithelioma and leiomyosarcomas, as opposed to other tumor cell lines derived from osteogenic sarcomas, rhabdomyosarcoma, melanoma, and SCLC (78). Subsequent studies carried out in tumor specimens confirmed that CCK expression was high in the majority of Ewing sarcomas, whereas in other tumors, CCK-positive cases ranged from 50% in leiomyosarcomas to 0% in medulloblastomas, central primitive neuroectodermal tumors (PNET), neuroblastomas, and rhabdomyosarcomas (79). In agreement with this, a later study demonstrated the presence of proCCK in the supernatant of Ewing sarcoma cell lines in culture, indicating that CCK is actively

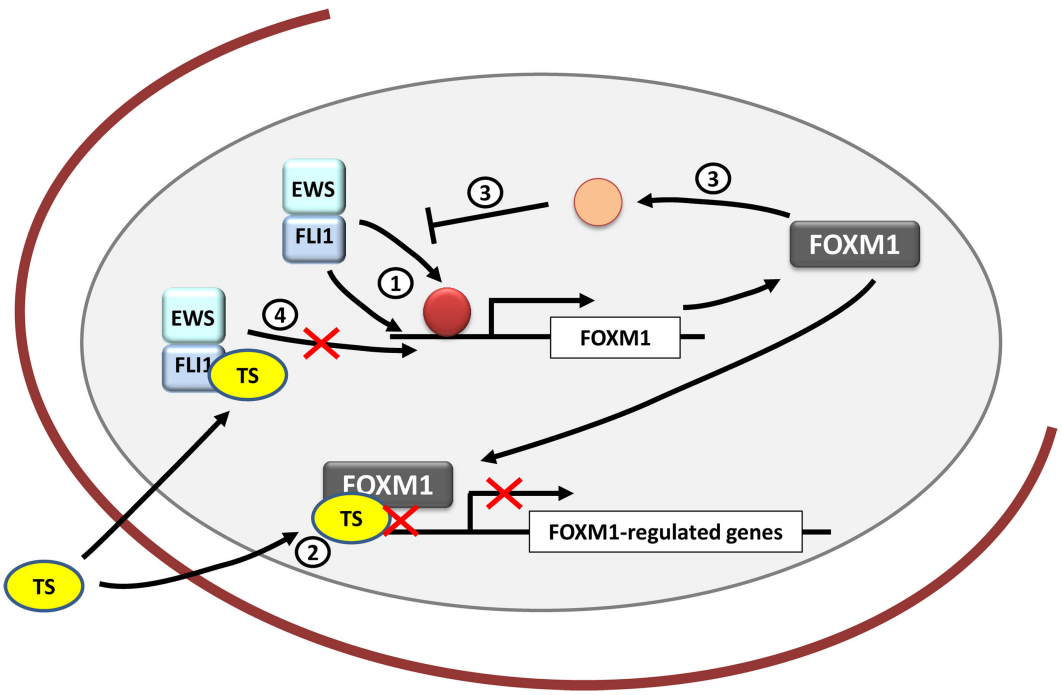

FIGURE 4 | FOXM1 and therapeutic opportunities in Ewing sarcoma. *FOXM1* is upregulated by EWS/FLI1 in Ewing sarcoma cells, although it is unknown whether its regulation is direct or indirect (1). Thiostrepton (TS) blocks FOXM1 in Ewing sarcoma cells decreasing their neoplastic features (2). However, the exact mechanism underlying these effects remains unexplained. In addition, FOXM1 has been shown to be capable of inhibiting EWS/FLI1 probably by an indirect mechanism that still needs to be clarified (3). Also TS has been proved to inhibit EWS/FLI1 expression in Ewing cells, although the exact mechanism is still unknown (4).

secreted by Ewing sarcoma cells (80). Interestingly, these authors found high concentrations of proCCK in the plasma of Ewing sarcoma patients but not in patients with other pediatric tumors such as osteosarcoma, neuroblastoma, nephroblastoma, rhabdomyosarcoma or synovial sarcoma. Interestingly, the levels of proCCK in plasma correlated with tumor size and recurrence. In addition, proCCK levels in plasma decreased after chemotherapeutic treatment, concurrently with a reduction in tumor size and in one patient, proCCK levels increased again correlating with tumor recurrence. All together, these results consistently demonstrate that CCK is expressed and secreted at high levels in Ewing sarcoma.

The first data demonstrating a relationship between *CCK* expression and EWS/FLI1 came from studies performed in heterologous systems: ectopic expression of EWS/FLI1 in the RD rhabdomyosarcoma cell line and in HeLa cells (81) upregulated *CCK* mRNA levels. This relationship between EWS/FLI1 and CCK was confirmed in Ewing sarcoma cells. Thus, EWS/FLI1 knockdown in A673 and SK-PN-DW Ewing sarcoma cell lines downregulated CCK mRNA levels, demonstrating that *CCK* expression is dependent on EWS/FLI1. Whether *CCK* is a direct or indirect target of EWS/FLI1 is a question that yet remains to be determined (8). Regarding the functional relevance of CCK in Ewing sarcoma, it was shown that downregulation of *CCK* using a shRNA inducible system, inhibited cell proliferation *in vitro* and tumor growth *in vivo*. In addition, CCK-rich culture media or exogenous CCK-8 was able to stimulate Ewing sarcoma cell proliferation *in vitro,* suggesting that CCK is an autocrine growth factor in Ewing sarcoma cells (8, 82). Unfortunately, to date no studies have been carried out to decipher the mechanisms that underlie this effect in Ewing sarcoma.

The fact that *CCK* is highly expressed in Ewing sarcoma and the observation that it can act as an autocrine growth factor *in vivo* suggest that blocking this autocrine loop, for example, using CCK receptor antagonists, could be of therapeutic interest. CCK and gastrin (a closely related hormone) share two G-protein coupled receptors, named CCKAR and CCKBR that trigger numerous pathways that transmit the mitogenic signal to the nucleus to promote cell proliferation. Whereas CCKA receptors are specific for CCK, CCKB receptors can bind CCK and gastrin with high affinity. Expression of CCK receptors in Ewing sarcoma has been scantly studied with contradictory results. Schaer and Reubi reported a lack of CCK receptors expression in a collection of 11 Ewing sarcoma tumors using autoradiography and ^{32}P-labeled CCK-8 as a probe (79). However, more recently it was demonstrated the existence of both CCKA and B receptors mRNA in two Ewing sarcoma cell lines (A673 and SK-PN-DW) and a cohort of ten primary tumors (8).

Treatment of Ewing sarcoma cell lines with devazepide, a specific CCKAR antagonist derived from the benzodiazepine family, induced apoptosis *in vitro* and significantly reduced the tumor growth in a mouse xenograft model (83). However, these effects were observed with IC_{50} values 10,000-fold higher that those necessary to efficiently block the binding of CCK to its CCKA receptor. In addition, one specific antagonist of the CCKB receptor (L365 260) had no effect on Ewing sarcoma cell proliferation or viability (83). These results suggest that in Ewing sarcoma cells there could be an alternative mechanism of action that could involve CCK receptors other than the standard ones, and open the possibility that cell proliferation induced by CCK in Ewing sarcoma cell lines could also be mediated through a yet unknown mechanism.

Regardless of the possibility to block CCK-induced proliferation with specific antagonists, the expression of CCK receptors in tumors can itself be therapeutically useful. In this sense, a model of metastatic medullary thyroid cancer has been successfully used to evaluate the diagnostic and therapeutic potential of radiolabeled gastrin directed to target CCKB receptor-expressing tumors *in vivo* (84). Using this approach, a collection of radiolabeled peptides derived from gastrin and cholecystokinin families showed anti-tumoral activity in xenograft models of medullary thyroid cancer (85) [also extensively reviewed in Ref. (86)]. This means that radiolabeled CCK or other compounds with high affinity for CCK receptors could be useful for diagnosis (i.e., imaging) and perhaps also for the treatment of Ewing sarcoma.

In summary, although high levels of CCK in Ewing sarcoma tumors were described more than two decades ago, research in this field has been scattered during the last years, and many questions remain unresolved. For example, it is not clear enough what type of CCK receptors are expressed in Ewing sarcoma tumors or the mechanism and intracellular signaling pathways involved in CCK-mediated cell proliferation. Any progress in this regard would help to develop molecules capable of interfering with this autocrine loop (**Figure 5**).

LOX

Lysyl oxidase (LOX) (protein lysine-6-oxidase; EC 1.4.3.13) is a member of a family of lysyl oxidases that share the enzyme catalytic domain. This family includes LOX and the LOX-like proteins LOXL1 to 4. These enzymes catalyze lysine-derived covalent crosslinking of collagen and elastin and therefore their function is key for maintaining the structural integrity of the extracellular matrix [extensively reviewed in (87–90)]. LOX is synthesized as a 50-KDa inactive proenzyme (preLOX), which is secreted to the extracellular environment where it is proteolytically processed into a functional 32-KDa LOX enzyme and an 18-KDa propeptide (LOX-PP). Together with the critical role that LOX plays in maintaining the properties of the connective tissues, it has been also shown to play important roles in cancer.

The first evidence of a relationship between LOX and cancer comes from experiments designed to identify genes involved in Ras-mediated transformation of NIH-3T3 mouse fibroblasts (91). Several functional experiments demonstrated that *LOX* had properties that are characteristic of a suppressor gene. Thus, *LOX* antisense cDNA was able to retransform *H-ras*-transformed revertants (92) and confer tumorigenic features to normal rat kidney fibroblasts (NRK-49F) (93).

Since LOX is proteolytically processed into a fragment containing the lysyl oxidase enzymatic activity and an N-terminal propeptide (LOX-PP), experiments were conducted to determine in which of these fragments resided the tumor suppressor activity. Thus, Palamakumbura et al. described for the first time that recombinant LOX-PP was able to inhibit neoplastic transformation features in Ras-transformed mouse fibroblasts such as

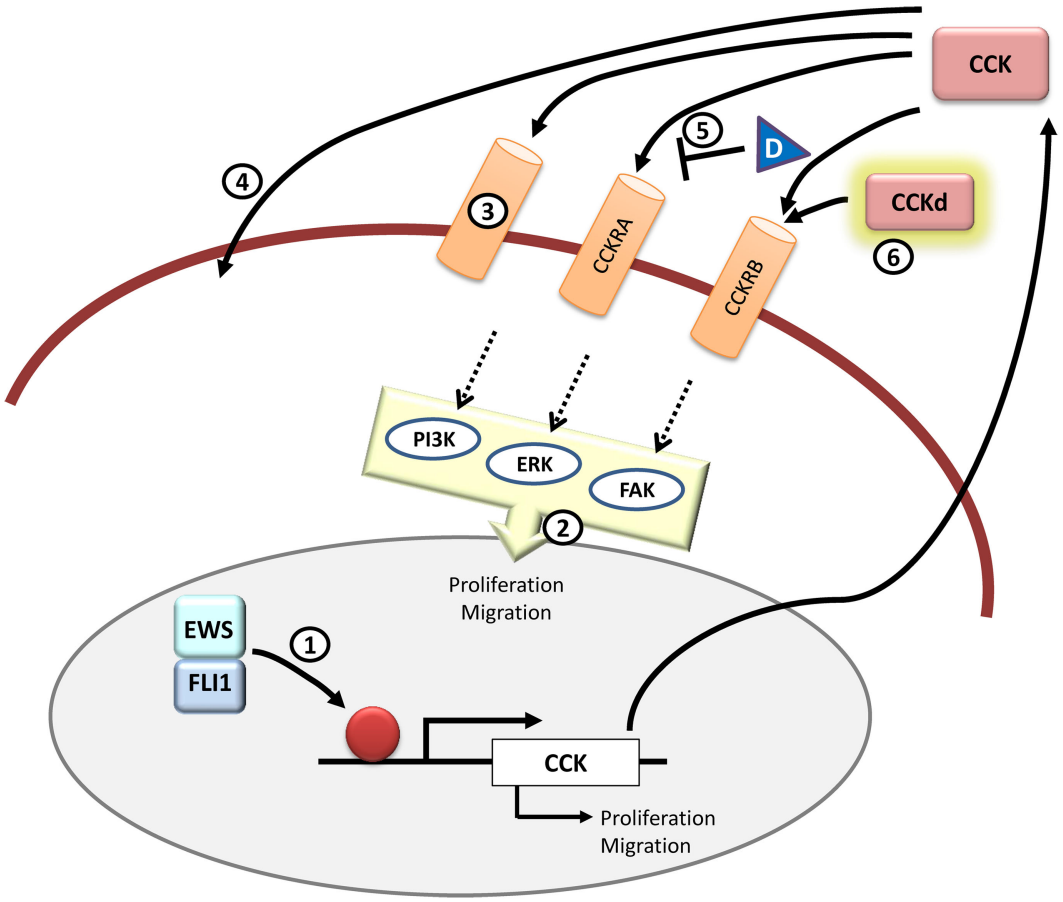

FIGURE 5 | CCK and therapeutic opportunities in Ewing sarcoma. *CCK* is an EWS/FLI1 target gene and its expression is elevated in Ewing sarcoma cells. Functionally, inhibition of CCK expression impairs growth and migration in Ewing sarcoma cells. It still remains to be addressed if *CCK* is a direct EWS/FLI1 target or not (1) and which is the exact signaling pathway that takes place once CCK binds to its receptors in the cells (2). Also it is still unknown whether CCK binds exclusively to its canonical CCKRs or if there are other receptors (3) or even if it can enter directly into the cell through some yet unknown mechanism (4). Therapeutically, it may be interesting to further test receptor antagonists other than devazepide (D) that could interfere with CCK binding to its receptors in Ewing sarcoma cells (5). Also, from a diagnosis point of view, it could be useful to test radiolabeled CCK derivatives (CCKd) to be used in imaging technologies (6). All in all, more studies are needed to define the principal components and pathways that are involved in the CCK-autocrine loop.

growth in anchorage independent conditions and Ras-dependent induction of *NFκB* (94). Currently, numerous studies support that the tumor suppressor activity of LOX resides in the 18-kDa propeptide fragment LOX-PP and not in the lysyl oxidase enzyme.

In agreement with its tumor suppressor activity, LOX expression has been reported to be downregulated in many different types of human cancer, such as fibrosarcoma, rhabdomyosarcoma, and melanoma cells (95), lung (96), pancreatic cancer (97), prostate (98), and colorectal cancers (99), which means that LOX expression levels negatively correlate with malignant transformations. By contrast, LOX expression has been also reported to be increased in a number of human cancers [i.e., breast and colon carcinomas (100, 101)] particularly in the metastatic and more aggressive forms of the disease. Interestingly, in these cases, metastatic and invasive properties have been related to the lysyl oxidase activity of LOX, rather than to LOX-PP (100, 101).

The anti-tumor activity of LOX-PP has been demonstrated in various types of tumor cells although the mechanism underlying the tumor suppressor activity of LOX-PP still needs to be clarified. Data obtained until now indicate that LOX-PP can act at different levels, and that the pathways and functions affected can depend of the cancer or cell model studied. For example, in Her-2/neu-transformed NF639 breast cancer cells, ectopic expression of LOX-PP interferes with fibronectin-stimulated tyrosine phosphorylation of cellular proteins involved in integrin signaling, inactivating the focal adhesion kinase (FAK), and consequently diminishes the migratory response (102). In other breast cancer cells driven by Her-2/neu (ERBB2), LOX-PP expression suppressed AKT, ERK, and NFκB activation, as well as cell migration, growth in soft agar and tumor formation in nude mice (103). Moreover, in cells derived from prostate cancer (DU145 and PC-3), LOX-PP blocks FGF-2 binding to the cell, inhibiting MAPK/ERK and PI3K/Akt pathways and blocking serum-stimulated DNA synthesis and cell proliferation (104). On the other hand, LOX-PP decreased the levels of NF-κB and cyclin D1 in Her-2/neu-transformed NF639 breast cancer cells and MIA PaCa-2 pancreatic cancer cells, together with a reduction in migration and growth in soft agar (105). Finally, in PANC-1

pancreatic cancer cells, LOX-PP also impaired AKT and ERK activity and growth in soft agar and cell migration (97).

Recently, a connection between LOX and Ewing sarcoma pathogenesis has been also demonstrated. Thus, EWS/FLI1 knockdown in Ewing sarcoma cells induces the expression of *LOX* indicating that this gene is strongly repressed by EWS/FLI1 in these cells (15). An independent study showed that *LOX* is a direct target of EWS/FLI1 by using ChIP assays (106). In agreement with this, LOX expression was found to be low or undetectable in a group of Ewing sarcoma cell lines and primary tumors (15). Since these data suggested that LOX could act as a tumor suppressor in Ewing sarcoma, functional studies were carried out. Thus, ectopic expression of LOX-PP in the A673 Ewing sarcoma cell line reduced cell proliferation, cell migration, anchorage independent growth, and impaired tumor growth *in vivo*, indicating that it had tumor suppressor activities in this cell, in line with what was observed in other tumors. By contrast, the mature LOX enzyme displayed the opposite effects. Interestingly, when full-length LOX, including LOX enzyme and LOX-PP activities was expressed in A673 cells, the anti-tumor effects prevailed (15). Altogether, these studies indicate that LOX plays an important role in Ewing pathogenesis by acting as a tumor suppressor gene.

The mechanisms involved in LOX-PP-mediated suppression in Ewing sarcoma have only been partially studied. In one study, ectopic expression of LOX-PP showed to impair ERK signaling pathway, whereas the PI3K/AKT pathway remained unaffected (15). Interestingly, in this work, an analysis of the gene expression profile induced by LOX-PP expression in the A673 Ewing cell line showed that a significant proportion of the genes affected belonged to pathways involved in cell proliferation and cell cycle control. Given the impact that LOX-PP expression has on tumorigenesis, it is necessary to extend these studies in order to characterize in more detail the pathways that may be affected by the exposition of Ewing sarcoma cells to LOX-PP, and particularly to determine which specific growth factor pathways could be affected by LOX-PP.

Other interesting aspect that remains to be determined is the identification of the proteins that interact with LOX-PP in Ewing sarcoma cells. In other cell types, LOX-PP has been shown to interact with a number of proteins such as Hsp70, c-Raf or CIN85 (107), so it would be interesting to identify and characterize LOX-PP partners in the specific Ewing sarcoma cell context and to elucidate their role in LOX-PP mediated tumor suppression.

The fact that LOX-PP acts as a tumor suppressor gene in cancer, and specifically in Ewing sarcoma, invites to assess the therapeutic value of LOX-PP. The easiest strategy is to evaluate the effect of the administration of LOX-PP on tumor cells. Thus, recombinant LOX-PP has been used to ascertain its therapeutic potential in several cancer types both *in vitro* and *in vivo* (94, 97, 102–105, 108, 109). In all cases, exogenous LOX-PP reduced tumor cells growth, supporting the therapeutic usefulness of this strategy. Interestingly, in one study, the combination of LOX-PP with the chemotherapeutic agent doxorubicin in breast and pancreatic cancer cells *in vitro* showed an enhanced cytotoxic effect of doxorubicin when the cells were first sensitize by incubation with LOX-PP (105). These results mean that even if LOX-PP is not capable of inducing complete cell death by itself, it could potentially sensitize cancer cells to standard therapies thus allowing to lower the doses and adverse side effects associated to conventional chemotherapy and radiotherapy. At the moment, there are no data about the effect of exogenous administration of LOX-PP, alone or in combination with chemotherapeutic drugs, on Ewing sarcoma cells. These preclinical studies are therefore needed to test if this strategy can represent a promising line of research in order to find new therapeutic approaches to treat Ewing sarcoma patients.

Since *LOX* expression, and thus LOX-PP, is downregulated in Ewing sarcoma cells by EWS/FLI1 (15, 106), other therapeutic approach could be the induction of LOX expression, and thus LOX-PP, in these cells. In this line, it has been proposed that EWS/FLI1 binds to *LOX* promoter and downregulates *LOX* expression by recruiting the NuRD transcriptional repressor complex containing the HDACs and LSD1 associated proteins. Interestingly, the use of HDACs inhibitors (vorinostat/SAHA) or LSD1 inhibitors (HCI-2509) induced an increase in the levels of LOX mRNA in A673 Ewing sarcoma cells, which suggest that the anti-tumor effect of these drugs could be mediated, at least in part, by the upregulation of *LOX* (106). However, induction of *LOX* expression to achieve an increased production of anti-tumorigenic LOX-PP in Ewing sarcoma cells may not be as beneficial as expected: while induction of *LOX* expression would cause an increase in LOX-PP, it also would produce an increase in the production of the LOX mature enzyme, which has been showed to be pro-oncogenic in Ewing sarcoma cells and other tumors (15, 100, 101).

Other opportunities for therapeutic interventions could be derived from the identification and characterization of LOX-PP interactions with other proteins, mainly intracellular proteins involved in cell signaling and regulation of tumorigenic processes. Biochemical studies have shown that LOX-PP is an intrinsically disordered protein (110). These proteins are expected to participate in signaling processes due to their capability to adopt interconverting structures and to interact with their partners, and have been proposed to be potential drug targets (111). Thus, characterization of the exact motifs that are involved in LOX-PP interactions can open the door to the identification of targetable proteins and the design of small molecules capable to reproduce the effect of LOX-PP.

In summary, LOX, and more specifically LOX-PP, has been showed to have anti-tumorigenic properties, which could be exploited to treat cancer cells. Regarding Ewing sarcoma, it is yet more than necessary to characterize the pathways involved in LOX-PP mediated tumor-suppression, in particular the identification of the protein interactions that mediate this response, in order to identify key factors that could provide new therapeutic targets (**Figure 6**).

Conclusion

Ewing sarcoma is driven by EWS/FLI1, which is a protein generated by a tumor-specific aberrant translocation. Although it may seem like a perfect target for therapeutic applications, directed therapies toward it have failed to reach the clinic (112). For this reason, the identification of EWS–FLI target genes and their role in tumor signaling networks have been addressed in the last years, and some excellent reviews have assessed this topic (4, 113, 114).

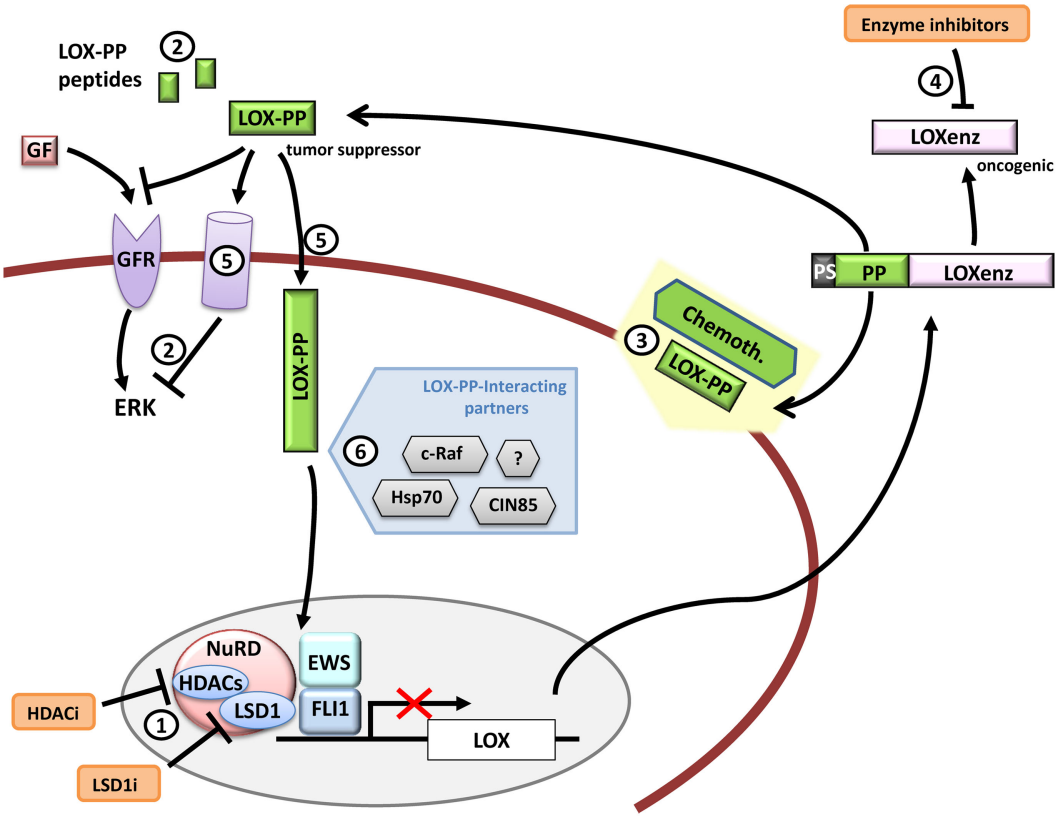

FIGURE 6 | LOX and therapeutic opportunities in Ewing sarcoma. *LOX* expression is repressed by EWS/FLI1 in Ewing sarcoma cells. Functional studies have demonstrated that LOX acts as a tumor suppressor gene in Ewing sarcoma and that its activity resides in its propeptide domain (LOX-PP). Therapeutic opportunities could include for example (1) *LOX* de-repression by targeting repression complexes that interact with EWS/FLI1 at the *LOX* promoter, (2) administration of LOX-PP or LOX-PP active derived peptides to block ERK signaling alone or in combination with traditional chemotherapy (3) or blocking the LOXenz fraction activity (4). The mechanisms through which LOX-PP exerts its anti-tumor activity are largely unknown, especially in Ewing sarcoma. For instance, it is currently unknown if LOX-PP specific receptors (5) (intracellular or transmembrane) are necessary to produce its anti-tumor activities or if the different LOX-PP-interacting proteins may interfere with its activity in Ewing sarcoma (6). Any advance in these aspects could provide new clues to design new therapeutic tools.

This review is focused on the EWS/FLI1 downstream regulatory network, particularly on EWS/FLI1 up- and down-regulated target genes on which the study of potential targeted therapies could be of clinical interest. Also, we stated some current questions regarding pathways and unknown mechanisms underlying the functional effects of these genes in Ewing sarcoma that still remain unresolved and could help find key clues for the future studies of this disease. There are plenty of mechanisms regarding EWS/FLI1 target genes that are still unknown and a deeper knowledge on them could potentially lead to the development of more specific and less toxic therapies in Ewing sarcoma.

Author Contributions

FC-A and JA wrote the manuscript and designed the figures. JA corrected and supervised the manuscript.

Acknowledgments

FC-A and JA are supported by Asociación Pablo Ugarte, Miguelañez S.A, ASION-La Hucha de Tomás, Instituto de Salud Carlos III PI12/00816 and Instituto de Salud Carlos III RTICC RD12/0036/0027.

References

1. Potratz J, Dirksen U, Jurgens H, Craft A. Ewing sarcoma: clinical state-of-the-art. *Pediatr Hematol Oncol* (2012) **29**(1):1–11. doi:10.3109/08880018.2011.622034
2. Esiashvili N, Goodman M, Marcus RB Jr. Changes in incidence and survival of Ewing sarcoma patients over the past 3 decades: surveillance epidemiology and end results data. *J Pediatr Hematol Oncol* (2008) **30**(6):425–30. doi:10.1097/MPH.0b013e31816e22f3
3. Delattre O, Zucman J, Plougastel B, Desmaze C, Melot T, Peter M, et al. Gene fusion with an ETS DNA-binding domain caused by chromosome translocation in human tumours. *Nature* (1992) **359**(6391):162–5. doi:10.1038/359162a0
4. Kovar H. Blocking the road, stopping the engine or killing the driver? Advances in targeting EWS/FLI-1 fusion in Ewing sarcoma as novel therapy. *Expert Opin Ther Targets* (2014) **18**(11):1315–28. doi:10.1517/14728222.2014.947963
5. Je EM, An CH, Yoo NJ, Lee SH. Mutational analysis of PIK3CA, JAK2, BRAF, FOXL2, IDH1, AKT1 and EZH2 oncogenes in sarcomas. *APMIS* (2012) **120**(8):635–9. doi:10.1111/j.1600-0463.2012.02878.x
6. Grunewald TG, Ranft A, Esposito I, da Silva-Buttkus P, Aichler M, Baumhoer D, et al. High STEAP1 expression is associated with improved outcome

of Ewing's sarcoma patients. *Ann Oncol* (2012) **23**(8):2185–90. doi:10.1093/annonc/mdr605
7. Tirado OM, Mateo-Lozano S, Villar J, Dettin LE, Llort A, Gallego S, et al. Caveolin-1 (CAV1) is a target of EWS/FLI-1 and a key determinant of the oncogenic phenotype and tumorigenicity of Ewing's sarcoma cells. *Cancer Res* (2006) **66**(20):9937–47. doi:10.1158/0008-5472.CAN-06-0927
8. Carrillo J, Garcia-Aragoncillo E, Azorin D, Agra N, Sastre A, Gonzalez-Mediero I, et al. Cholecystokinin down-regulation by RNA interference impairs Ewing tumor growth. *Clin Cancer Res* (2007) **13**(8):2429–40. doi:10.1158/1078-0432.CCR-06-1762
9. Garcia-Aragoncillo E, Carrillo J, Lalli E, Agra N, Gomez-Lopez G, Pestana A, et al. DAX1, a direct target of EWS/FLI1 oncoprotein, is a principal regulator of cell-cycle progression in Ewing's tumor cells. *Oncogene* (2008) **27**(46):6034–43. doi:10.1038/onc.2008.203
10. Smith R, Owen LA, Trem DJ, Wong JS, Whangbo JS, Golub TR, et al. Expression profiling of EWS/FLI identifies NKX2.2 as a critical target gene in Ewing's sarcoma. *Cancer Cell* (2006) **9**(5):405–16. doi:10.1016/j.ccr.2006.04.004
11. Hahm KB, Cho K, Lee C, Im YH, Chang J, Choi SG, et al. Repression of the gene encoding the TGF-beta type II receptor is a major target of the EWS-FLI1 oncoprotein. *Nat Genet* (1999) **23**(2):222–7. doi:10.1038/13854
12. Mosakhani N, Guled M, Leen G, Calabuig-Farinas S, Niini T, Machado I, et al. An integrated analysis of miRNA and gene copy numbers in xenografts of Ewing's sarcoma. *J Exp Clin Cancer Res* (2012) **31**:24. doi:10.1186/1756-9966-31-24
13. Navarro D, Agra N, Pestana A, Alonso J, Gonzalez-Sancho JM. The EWS/FLI1 oncogenic protein inhibits expression of the Wnt inhibitor DICKKOPF-1 gene and antagonizes beta-catenin/TCF-mediated transcription. *Carcinogenesis* (2010) **31**(3):394–401. doi:10.1093/carcin/bgp317
14. Prieur A, Tirode F, Cohen P, Delattre O. EWS/FLI-1 silencing and gene profiling of Ewing cells reveal downstream oncogenic pathways and a crucial role for repression of insulin-like growth factor binding protein 3. *Mol Cell Biol* (2004) **24**(16):7275–83. doi:10.1128/MCB.24.16.7275-7283.2004
15. Agra N, Cidre F, Garcia-Garcia L, de la Parra J, Alonso J. Lysyl oxidase is downregulated by the EWS/FLI1 oncoprotein and its propeptide domain displays tumor supressor activities in Ewing sarcoma cells. *PLoS One* (2013) **8**(6):e66281. doi:10.1371/journal.pone.0066281
16. Niedan S, Kauer M, Aryee DN, Kofler R, Schwentner R, Meier A, et al. Suppression of FOXO1 is responsible for a growth regulatory repressive transcriptional sub-signature of EWS-FLI1 in Ewing sarcoma. *Oncogene* (2013) **33**(30):3927–38. doi:10.1038/onc.2013.361
17. Christensen L, Joo J, Lee S, Wai D, Triche TJ, May WA. FOXM1 is an oncogenic mediator in Ewing sarcoma. *PLoS One* (2013) **8**(1):e54556. doi:10.1371/journal.pone.0054556
18. Zanaria E, Muscatelli F, Bardoni B, Strom TM, Guioli S, Guo W, et al. An unusual member of the nuclear hormone receptor superfamily responsible for X-linked adrenal hypoplasia congenita. *Nature* (1994) **372**(6507):635–41. doi:10.1038/372635a0
19. Lalli E, Sassone-Corsi P. DAX-1, an unusual orphan receptor at the crossroads of steroidogenic function and sexual differentiation. *Mol Endocrinol* (2003) **17**(8):1445–53. doi:10.1210/me.2003-0159
20. Billiard J, Moran RA, Whitley MZ, Chatterjee-Kishore M, Gillis K, Brown EL, et al. Transcriptional profiling of human osteoblast differentiation. *J Cell Biochem* (2003) **89**(2):389–400. doi:10.1002/jcb.10514
21. Martins RS, Power DM, Fuentes J, Deloffre LA, Canario AV. DAX1 regulatory networks unveil conserved and potentially new functions. *Gene* (2013) **530**(1):66–74. doi:10.1016/j.gene.2013.07.052
22. van den Berg DL, Snoek T, Mullin NP, Yates A, Bezstarosti K, Demmers J, et al. An Oct4-centered protein interaction network in embryonic stem cells. *Cell Stem Cell* (2010) **6**(4):369–81. doi:10.1016/j.stem.2010.02.014
23. Kelly VR, Xu B, Kuick R, Koenig RJ, Hammer GD. Dax1 up-regulates Oct4 expression in mouse embryonic stem cells via LRH-1 and SRA. *Mol Endocrinol* (2010) **24**(12):2281–91. doi:10.1210/me.2010-0133
24. Zhang J, Liu G, Ruan Y, Wang J, Zhao K, Wan Y, et al. Dax1 and Nanog act in parallel to stabilize mouse embryonic stem cells and induced pluripotency. *Nat Commun* (2014) **5**:5042. doi:10.1038/ncomms6042
25. Mendiola M, Carrillo J, Garcia E, Lalli E, Hernandez T, de Alava E, et al. The orphan nuclear receptor DAX1 is up-regulated by the EWS/FLI1 oncoprotein and is highly expressed in Ewing tumors. *Int J Cancer* (2006) **118**(6):1381–9. doi:10.1002/ijc.21578
26. Kinsey M, Smith R, Lessnick SL. NR0B1 is required for the oncogenic phenotype mediated by EWS/FLI in Ewing's sarcoma. *Mol Cancer Res* (2006) **4**(11):851–9. doi:10.1158/1541-7786.MCR-06-0090
27. Kinsey M, Smith R, Iyer AK, McCabe ER, Lessnick SL. EWS/FLI and its downstream target NR0B1 interact directly to modulate transcription and oncogenesis in Ewing's sarcoma. *Cancer Res* (2009) **69**(23):9047–55. doi:10.1158/0008-5472.CAN-09-1540
28. Gangwal K, Sankar S, Hollenhorst PC, Kinsey M, Haroldsen SC, Shah AA, et al. Microsatellites as EWS/FLI response elements in Ewing's sarcoma. *Proc Natl Acad Sci U S A* (2008) **105**(29):10149–54. doi:10.1073/pnas.0801073105
29. Luo W, Gangwal K, Sankar S, Boucher KM, Thomas D, Lessnick SL. GSTM4 is a microsatellite-containing EWS/FLI target involved in Ewing's sarcoma oncogenesis and therapeutic resistance. *Oncogene* (2009) **28**(46):4126–32. doi:10.1038/onc.2009.262
30. Guillon N, Tirode F, Boeva V, Zynovyev A, Barillot E, Delattre O. The oncogenic EWS-FLI1 protein binds in vivo GGAA microsatellite sequences with potential transcriptional activation function. *PLoS One* (2009) **4**(3):e4932. doi:10.1371/journal.pone.0004932
31. Beck R, Monument MJ, Watkins WS, Smith R, Boucher KM, Schiffman JD, et al. EWS/FLI-responsive GGAA microsatellites exhibit polymorphic differences between European and African populations. *Cancer Genet* (2012) **205**(6):304–12. doi:10.1016/j.cancergen.2012.04.004
32. Worch J, Matthay KK, Neuhaus J, Goldsby R, DuBois SG. Ethnic and racial differences in patients with Ewing sarcoma. *Cancer* (2010) **116**(4):983–8. doi:10.1002/cncr.24865
33. Monument MJ, Johnson KM, McIlvaine E, Abegglen L, Watkins WS, Jorde LB, et al. Clinical and biochemical function of polymorphic NR0B1 GGAA-microsatellites in Ewing sarcoma: a report from the Children's Oncology Group. *PLoS One* (2014) **9**(8):e104378. doi:10.1371/journal.pone.0104378
34. Lalli E, Alonso J. Targeting DAX-1 in embryonic stem cells and cancer. *Expert Opin Ther Targets* (2010) **14**(2):169–77. doi:10.1517/14728220903531454
35. Altincicek B, Tenbaum SP, Dressel U, Thormeyer D, Renkawitz R, Baniahmad A. Interaction of the corepressor Alien with DAX-1 is abrogated by mutations of DAX-1 involved in adrenal hypoplasia congenita. *J Biol Chem* (2000) **275**(11):7662–7. doi:10.1074/jbc.275.11.7662
36. Holter E, Kotaja N, Makela S, Strauss L, Kietz S, Janne OA, et al. Inhibition of androgen receptor (AR) function by the reproductive orphan nuclear receptor DAX-1. *Mol Endocrinol* (2002) **16**(3):515–28. doi:10.1210/mend.16.3.0804
37. Lopez D, Shea-Eaton W, Sanchez MD, McLean MP. DAX-1 represses the high-density lipoprotein receptor through interaction with positive regulators sterol regulatory element-binding protein-1a and steroidogenic factor-1. *Endocrinology* (2001) **142**(12):5097–106. doi:10.1210/endo.142.12.8523
38. Albers M, Kranz H, Kober I, Kaiser C, Klink M, Suckow J, et al. Automated yeast two-hybrid screening for nuclear receptor-interacting proteins. *Mol Cell Proteomics* (2005) **4**(2):205–13. doi:10.1074/mcp.M400169-MCP200
39. Lehmann SG, Wurtz JM, Renaud JP, Sassone-Corsi P, Lalli E. Structure-function analysis reveals the molecular determinants of the impaired biological function of DAX-1 mutants in AHC patients. *Hum Mol Genet* (2003) **12**(9):1063–72. doi:10.1093/hmg/ddg108
40. Shibata H, Ikeda Y, Mukai T, Morohashi K, Kurihara I, Ando T, et al. Expression profiles of COUP-TF, DAX-1, and SF-1 in the human adrenal gland and adrenocortical tumors: possible implications in steroidogenesis. *Mol Genet Metab* (2001) **74**(1–2):206–16. doi:10.1006/mgme.2001.3231
41. Jessell TM. Neuronal specification in the spinal cord: inductive signals and transcriptional codes. *Nat Rev Genet* (2000) **1**(1):20–9. doi:10.1038/35049541
42. Reya T, Morrison SJ, Clarke MF, Weissman IL. Stem cells, cancer, and cancer stem cells. *Nature* (2001) **414**(6859):105–11. doi:10.1038/35102167
43. Machold R, Hayashi S, Rutlin M, Muzumdar MD, Nery S, Corbin JG, et al. Sonic Hedgehog is required for progenitor cell maintenance in telencephalic stem cell niches. *Neuron* (2003) **39**(6):937–50. doi:10.1016/S0896-6273(03)00561-0
44. Zwerner JP, Joo J, Warner KL, Christensen L, Hu-Lieskovan S, Triche TJ, et al. The EWS/FLI1 oncogenic transcription factor deregulates GLI1. *Oncogene* (2008) **27**(23):3282–91. doi:10.1038/sj.onc.1210991
45. Beauchamp E, Bulut G, Abaan O, Chen K, Merchant A, Matsui W, et al. GLI1 is a direct transcriptional target of EWS-FLI1 oncoprotein. *J Biol Chem* (2009) **284**(14):9074–82. doi:10.1074/jbc.M806233200

46. Joo J, Christensen L, Warner K, States L, Kang H-G, Vo K, et al. GLI1 Is a central mediator of EWS/FLI1 signaling in Ewing tumors. *PLoS One* (2009) **4**(10):e7608. doi:10.1371/journal.pone.0007608
47. Oro AE, Higgins KM, Hu Z, Bonifas JM, Epstein EH Jr, Scott MP. Basal cell carcinomas in mice overexpressing sonic Hedgehog. *Science* (1997) **276**(5313):817–21. doi:10.1126/science.276.5313.817
48. Bian Y-H, Huang S-H, Yang L, Ma X-L, Xie J-W, Zhang H-W. Sonic Hedgehog-Gli1 pathway in colorectal adenocarcinomas. *World J Gastroenterol* (2007) **13**(11):1659–65. doi:10.3748/wjg.v13.i11.1659
49. ten Haaf A, Bektas N, von Serenyi S, Losen I, Arweiler EC, Hartmann A, et al. Expression of the glioma-associated oncogene homolog (GLI) 1 in human breast cancer is associated with unfavourable overall survival. *BMC Cancer* (2009) **9**:298. doi:10.1186/1471-2407-9-298
50. Stein U, Eder C, Karsten U, Haensch W, Walther W, Schlag PM. GLI gene expression in bone and soft tissue sarcomas of adult patients correlates with tumor grade. *Cancer Res* (1999) **59**(8):1890–5.
51. Berman DM, Karhadkar SS, Hallahan AR, Pritchard JI, Eberhart CG, Watkins DN, et al. Medulloblastoma growth inhibition by Hedgehog pathway blockade. *Science* (2002) **297**(5586):1559–61. doi:10.1126/science.1073733
52. Thayer SP, Pasca di Magliano M, Heiser PW, Nielsen CM, Roberts DJ, Lauwers GY, et al. Hedgehog is an early and late mediator of pancreatic cancer tumorigenesis. *Nature* (2003) **425**(6960):851–6. doi:10.1038/nature02009
53. Watkins DN, Berman DM, Burkholder SG, Wang B, Beachy PA, Baylin SB. Hedgehog signalling within airway epithelial progenitors and in small-cell lung cancer. *Nature* (2003) **422**(6929):313–7. doi:10.1038/nature01493
54. Ma X, Chen K, Huang S, Zhang X, Adegboyega PA, Evers BM, et al. Frequent activation of the Hedgehog pathway in advanced gastric adenocarcinomas. *Carcinogenesis* (2005) **26**(10):1698–705. doi:10.1093/carcin/bgi130
55. Ma X, Sheng T, Zhang Y, Zhang X, He J, Huang S, et al. Hedgehog signaling is activated in subsets of esophageal cancers. *Int J Cancer* (2006) **118**(1):139–48. doi:10.1002/ijc.21295
56. Raju GP. Arsenic: a potentially useful poison for Hedgehog-driven cancers. *J Clin Invest* (2011) **121**(1):14–6. doi:10.1172/JCI45692
57. Beauchamp EM, Ringer L, Bulut G, Sajwan KP, Hall MD, Lee YC, et al. Arsenic trioxide inhibits human cancer cell growth and tumor development in mice by blocking Hedgehog/GLI pathway. *J Clin Invest* (2011) **121**(1):148–60. doi:10.1172/JCI42874
58. Zhang S, Guo W, Ren TT, Lu XC, Tang GQ, Zhao FL. Arsenic trioxide inhibits Ewing's sarcoma cell invasiveness by targeting p38(MAPK) and c-Jun N-terminal kinase. *Anticancer Drugs* (2012) **23**(1):108–18. doi:10.1097/CAD.0b013e32834bfd68
59. Guo W, Tang XD, Tang S, Yang Y. [Preliminary report of combination chemotherapy including Arsenic trioxide for stage III osteosarcoma and Ewing sarcoma]. *Zhonghua Wai Ke Za Zhi* (2006) **44**(12):805–8.
60. Lam EW, Brosens JJ, Gomes AR, Koo CY. Forkhead box proteins: tuning forks for transcriptional harmony. *Nat Rev Cancer* (2013) **13**(7):482–95. doi:10.1038/nrc3539
61. Nakamura N, Ramaswamy S, Vazquez F, Signoretti S, Loda M, Sellers WR. Forkhead transcription factors are critical effectors of cell death and cell cycle arrest downstream of PTEN. *Mol Cell Biol* (2000) **20**(23):8969–82. doi:10.1128/MCB.20.23.8969-8982.2000
62. Brunet A, Bonni A, Zigmond MJ, Lin MZ, Juo P, Hu LS, et al. Akt promotes cell survival by phosphorylating and inhibiting a Forkhead transcription factor. *Cell* (1999) **96**(6):857–68. doi:10.1016/S0092-8674(00)80595-4
63. Dong XY, Chen C, Sun X, Guo P, Vessella RL, Wang RX, et al. FOXO1A is a candidate for the 13q14 tumor suppressor gene inhibiting androgen receptor signaling in prostate cancer. *Cancer Res* (2006) **66**(14):6998–7006. doi:10.1158/0008-5472.CAN-06-0411
64. Potente M, Urbich C, Sasaki K-I, Hofmann WK, Heeschen C, Aicher A, et al. Involvement of Foxo transcription factors in angiogenesis and postnatal neovascularization. *J Clin Invest* (2005) **115**(9):2382–92. doi:10.1172/JCI23126
65. Fosbrink M, Niculescu F, Rus V, Shin ML, Rus H. C5b-9-induced endothelial cell proliferation and migration are dependent on Akt inactivation of forkhead transcription factor FOXO1. *J Biol Chem* (2006) **281**(28):19009–18. doi:10.1074/jbc.M602055200
66. Wang Y, Zhou Y, Graves DT. FOXO transcription factors: their clinical significance and regulation. *Biomed Res Int* (2014) **2014**:925350. doi:10.1155/2014/925350
67. Yang Y, Hou H, Haller EM, Nicosia SV, Bai W. Suppression of FOXO1 activity by FHL2 through SIRT1-mediated deacetylation. *EMBO J* (2005) **24**(5):1021–32. doi:10.1038/sj.emboj.7600570
68. Yang L, Hu H-M, Zielinska-Kwiatkowska A, Chansky HA. FOXO1 is a direct target of EWS-Fli1 oncogenic fusion protein in Ewing's sarcoma cells. *Biochem Biophys Res Commun* (2010) **402**(1):129–34. doi:10.1016/j.bbrc.2010.09.129
69. Zhang H, Fang J, Yao D, Wu Y, Ip C, Dong Y. Activation of FOXO1 is critical for the anticancer effect of methylseleninic acid in prostate cancer cells. *Prostate* (2010) **70**(12):1265–73. doi:10.1002/pros.21162
70. Gonzalez-Moreno O, Segura V, Serrano D, Nguewa P, de las Rivas J, Calvo A. Methylseleninic acid enhances the effect of etoposide to inhibit prostate cancer growth in vivo. *Int J Cancer* (2007) **121**(6):1197–204. doi:10.1002/ijc.22764
71. Halasi M, Gartel AL. Targeting FOXM1 in cancer. *Biochem Pharmacol* (2013) **85**(5):644–52. doi:10.1016/j.bcp.2012.10.013
72. Kalin TV, Ustiyan V, Kalinichenko VV. Multiple faces of FoxM1 transcription factor: lessons from transgenic mouse models. *Cell Cycle* (2011) **10**(3):396–405. doi:10.4161/cc.10.3.14709
73. Gartel AL. Thiostrepton, proteasome inhibitors and FOXM1. *Cell Cycle* (2011) **10**(24):4341–2. doi:10.4161/cc.10.24.18544
74. Hegde NS, Sanders DA, Rodriguez R, Balasubramanian S. The transcription factor FOXM1 is a cellular target of the natural product thiostrepton. *Nat Chem* (2011) **3**(9):725–31. doi:10.1038/nchem.1114
75. Sengupta A, Rahman M, Mateo-Lozano S, Tirado OM, Notario V. The dual inhibitory effect of thiostrepton on FoxM1 and EWS/FLI1 provides a novel therapeutic option for Ewing's sarcoma. *Int J Oncol* (2013) **43**(3):803–12. doi:10.3892/ijo.2013.2016
76. Radhakrishnan SK, Gartel AL. FOXM1: the Achilles' heel of cancer? *Nat Rev Cancer* (2008) **8**(3):c1. doi:10.1038/nrc2223-c1
77. Beinfeld MC. Biosynthesis and processing of pro CCK: recent progress and future challenges. *Life Sci* (2003) **72**(7):747–57. doi:10.1016/S0024-3205(02)02330-5
78. Friedman JM, Vitale M, Maimon J, Israel MA, Horowitz ME, Schneider BS. Expression of the cholecystokinin gene in pediatric tumors. *Proc Natl Acad Sci U S A* (1992) **89**(13):5819–23. doi:10.1073/pnas.89.13.5819
79. Schaer JC, Reubi JC. High gastrin and cholecystokinin (CCK) gene expression in human neuronal, renal, and myogenic stem cell tumors: comparison with CCK-A and CCK-B receptor contents. *J Clin Endocrinol Metab* (1999) **84**(1):233–9. doi:10.1210/jcem.84.1.5400
80. Reubi JC, Koefoed P, Hansen T, Stauffer E, Rauch D, Nielsen FC, et al. Procholecystokinin as marker of human Ewing sarcomas. *Clin Cancer Res* (2004) **10**(16):5523–30. doi:10.1158/1078-0432.CCR-1015-03
81. Hu-Lieskovan S, Zhang J, Wu L, Shimada H, Schofield DE, Triche TJ. EWS-FLI1 fusion protein up-regulates critical genes in neural crest development and is responsible for the observed phenotype of Ewing's family of tumors. *Cancer Res* (2005) **65**(11):4633–44. doi:10.1158/0008-5472.CAN-04-2857
82. Deng C, Hsueh AJ. Evolution of a potential hormone antagonist following gene splicing during primate evolution. *PLoS One* (2013) **8**(5):e64610. doi:10.1371/journal.pone.0064610
83. Carrillo J, Agra N, Fernandez N, Pestana A, Alonso J. Devazepide, a non-peptide antagonist of CCK receptors, induces apoptosis and inhibits Ewing tumor growth. *Anticancer Drugs* (2009) **20**(7):527–33. doi:10.1097/CAD.0b013e32832c3a4f
84. Behr TM, Jenner N, Radetzky S, Behe M, Gratz S, Yucekent S, et al. Targeting of cholecystokinin-B/gastrin receptors in vivo: preclinical and initial clinical evaluation of the diagnostic and therapeutic potential of radiolabelled gastrin. *Eur J Nucl Med* (1998) **25**(4):424–30. doi:10.1007/s002590050241
85. Behr TM, Behe M, Angerstein C, Gratz S, Mach R, Hagemann L, et al. Cholecystokinin-B/gastrin receptor binding peptides: preclinical development and evaluation of their diagnostic and therapeutic potential. *Clin Cancer Res* (1999) **5**(10 Suppl):3124s–38s.
86. Roosenburg S, Laverman P, van Delft FL, Boerman OC. Radiolabeled CCK/gastrin peptides for imaging and therapy of CCK2 receptor-expressing tumors. *Amino Acids* (2011) **41**(5):1049–58. doi:10.1007/s00726-010-0501-y
87. Lucero HA, Kagan HM. Lysyl oxidase: an oxidative enzyme and effector of cell function. *Cell Mol Life Sci* (2006) **63**(19–20):2304–16. doi:10.1007/s00018-006-6149-9
88. Molnar J, Fong KS, He QP, Hayashi K, Kim Y, Fong SF, et al. Structural and functional diversity of lysyl oxidase and the LOX-like proteins. *Biochim Biophys Acta* (2003) **1647**(1–2):220–4. doi:10.1016/S1570-9639(03)00053-0

89. Kagan HM, Li W. Lysyl oxidase: properties, specificity, and biological roles inside and outside of the cell. *J Cell Biochem* (2003) **88**(4):660–72. doi:10.1002/jcb.10413
90. Smith-Mungo LI, Kagan HM. Lysyl oxidase: properties, regulation and multiple functions in biology. *Matrix Biol* (1998) **16**(7):387–98. doi:10.1016/S0945-053X(98)90012-9
91. Kenyon K, Contente S, Trackman PC, Tang J, Kagan HM, Friedman RM. Lysyl oxidase and rrg messenger RNA. *Science* (1991) **253**(5021):802. doi:10.1126/science.1678898
92. Contente S, Kenyon K, Rimoldi D, Friedman RM. Expression of gene rrg is associated with reversion of NIH 3T3 transformed by LTR-c-H-ras. *Science* (1990) **249**(4970):796–8. doi:10.1126/science.1697103
93. Giampuzzi M, Botti G, Cilli M, Gusmano R, Borel A, Sommer P, et al. Down-regulation of lysyl oxidase-induced tumorigenic transformation in NRK-49F cells characterized by constitutive activation of ras proto-oncogene. *J Biol Chem* (2001) **276**(31):29226–32. doi:10.1074/jbc.M101695200
94. Palamakumbura AH, Jeay S, Guo Y, Pischon N, Sommer P, Sonenshein GE, et al. The propeptide domain of lysyl oxidase induces phenotypic reversion of ras-transformed cells. *J Biol Chem* (2004) **279**(39):40593–600. doi:10.1074/jbc.M406639200
95. Kuivaniemi H, Korhonen RM, Vaheri A, Kivirikko KI. Deficient production of lysyl oxidase in cultures of malignantly transformed human cells. *FEBS Lett* (1986) **195**(1–2):261–4. doi:10.1016/0014-5793(86)80172-7
96. Hamalainen ER, Kemppainen R, Kuivaniemi H, Tromp G, Vaheri A, Pihlajaniemi T, et al. Quantitative polymerase chain reaction of lysyl oxidase mRNA in malignantly transformed human cell lines demonstrates that their low lysyl oxidase activity is due to low quantities of its mRNA and low levels of transcription of the respective gene. *J Biol Chem* (1995) **270**(37):21590–3. doi:10.1074/jbc.270.37.21590
97. Wu M, Min C, Wang X, Yu Z, Kirsch KH, Trackman PC, et al. Repression of BCL2 by the tumor suppressor activity of the lysyl oxidase propeptide inhibits transformed phenotype of lung and pancreatic cancer cells. *Cancer Res* (2007) **67**(13):6278–85. doi:10.1158/0008-5472.CAN-07-0776
98. Ren C, Yang G, Timme TL, Wheeler TM, Thompson TC. Reduced lysyl oxidase messenger RNA levels in experimental and human prostate cancer. *Cancer Res* (1998) **58**(6):1285–90.
99. Csiszar K, Fong SF, Ujfalusi A, Krawetz SA, Salvati EP, Mackenzie JW, et al. Somatic mutations of the lysyl oxidase gene on chromosome 5q23.1 in colorectal tumors. *Int J Cancer* (2002) **97**(5):636–42. doi:10.1002/ijc.10035
100. Kirschmann DA, Seftor EA, Fong SF, Nieva DR, Sullivan CM, Edwards EM, et al. A molecular role for lysyl oxidase in breast cancer invasion. *Cancer Res* (2002) **62**(15):4478–83.
101. Baker AM, Cox TR, Bird D, Lang G, Murray GI, Sun XF, et al. The role of lysyl oxidase in SRC-dependent proliferation and metastasis of colorectal cancer. *J Natl Cancer Inst* (2011) **103**(5):407–24. doi:10.1093/jnci/djq569
102. Zhao Y, Min C, Vora SR, Trackman PC, Sonenshein GE, Kirsch KH. The lysyl oxidase pro-peptide attenuates fibronectin-mediated activation of focal adhesion kinase and p130Cas in breast cancer cells. *J Biol Chem* (2009) **284**(3):1385–93. doi:10.1074/jbc.M802612200
103. Min C, Kirsch KH, Zhao Y, Jeay S, Palamakumbura AH, Trackman PC, et al. The tumor suppressor activity of the lysyl oxidase propeptide reverses the invasive phenotype of Her-2/neu-driven breast cancer. *Cancer Res* (2007) **67**(3):1105–12. doi:10.1158/0008-5472.CAN-06-3867
104. Palamakumbura AH, Vora SR, Nugent MA, Kirsch KH, Sonenshein GE, Trackman PC. Lysyl oxidase propeptide inhibits prostate cancer cell growth by mechanisms that target FGF-2-cell binding and signaling. *Oncogene* (2009) **28**(38):3390–400. doi:10.1038/onc.2009.203
105. Min C, Zhao Y, Romagnoli M, Trackman PC, Sonenshein GE, Kirsch KH. Lysyl oxidase propeptide sensitizes pancreatic and breast cancer cells to doxorubicin-induced apoptosis. *J Cell Biochem* (2010) **111**(5):1160–8. doi:10.1002/jcb.22828
106. Sankar S, Bell R, Stephens B, Zhuo R, Sharma S, Bearss DJ, et al. Mechanism and relevance of EWS/FLI-mediated transcriptional repression in Ewing sarcoma. *Oncogene* (2013) **32**(42):5089–100. doi:10.1038/onc.2012.525
107. Sato S, Trackman PC, Maki JM, Myllyharju J, Kirsch KH, Sonenshein GE. The Ras signaling inhibitor LOX-PP interacts with Hsp70 and c-Raf to reduce Erk activation and transformed phenotype of breast cancer cells. *Mol Cell Biol* (2011) **31**(13):2683–95. doi:10.1128/MCB.01148-10
108. Bais MV, Nugent MA, Stephens DN, Sume SS, Kirsch KH, Sonenshein GE, et al. Recombinant lysyl oxidase propeptide protein inhibits growth and promotes apoptosis of pre-existing murine breast cancer xenografts. *PLoS One* (2012) **7**(2):e31188. doi:10.1371/journal.pone.0031188
109. Bais MV, Ozdener GB, Sonenshein GE, Trackman PC. Effects of tumor-suppressor lysyl oxidase propeptide on prostate cancer xenograft growth and its direct interactions with DNA repair pathways. *Oncogene* (2015) **34**(15):1928–37. doi:10.1038/onc.2014.147
110. Vora SR, Guo Y, Stephens DN, Salih E, Vu ED, Kirsch KH, et al. Characterization of recombinant lysyl oxidase propeptide. *Biochemistry* (2010) **49**(13):2962–72. doi:10.1021/bi902218p
111. Metallo SJ. Intrinsically disordered proteins are potential drug targets. *Curr Opin Chem Biol* (2010) **14**(4):481–8. doi:10.1016/j.cbpa.2010.06.169
112. Uren A, Toretsky JA. Ewing's sarcoma oncoprotein EWS-FLI1: the perfect target without a therapeutic agent. *Future Oncol* (2005) **1**(4):521–8. doi:10.2217/14796694.1.4.521
113. Lessnick SL, Ladanyi M. Molecular pathogenesis of Ewing sarcoma: new therapeutic and transcriptional targets. *Annu Rev Pathol* (2012) **7**:145–59. doi:10.1146/annurev-pathol-011110-130237
114. McAllister NR, Lessnick SL. The potential for molecular therapeutic targets in Ewing's sarcoma. *Curr Treat Options Oncol* (2005) **6**(6):461–71. doi:10.1007/s11864-005-0025-y

Conflict of Interest Statement: The authors declare that the research was conducted in the absence of any commercial or financial relationships that could be construed as a potential conflict of interest.

nature genetics

Chimeric EWSR1-FLI1 regulates the Ewing sarcoma susceptibility gene *EGR2* via a GGAA microsatellite

Thomas G P Grünewald[1,2,17], Virginie Bernard[3], Pascale Gilardi-Hebenstreit[4], Virginie Raynal[1–3], Didier Surdez[1,2], Marie-Ming Aynaud[1,2], Olivier Mirabeau[1,2], Florencia Cidre-Aranaz[5], Franck Tirode[1,2], Sakina Zaidi[1,2], Gaëlle Perot[6], Anneliene H Jonker[1,2], Carlo Lucchesi[1,2], Marie-Cécile Le Deley[7], Odile Oberlin[8], Perrine Marec-Bérard[9], Amélie S Véron[10], Stephanie Reynaud[11], Eve Lapouble[11], Valentina Boeva[12,13], Thomas Rio Frio[3], Javier Alonso[5], Smita Bhatia[14], Gaëlle Pierron[11], Geraldine Cancel-Tassin[15], Olivier Cussenot[15], David G Cox[10], Lindsay M Morton[16], Mitchell J Machiela[16], Stephen J Chanock[16], Patrick Charnay[4] & Olivier Delattre[1–3,11]

Deciphering the ways in which somatic mutations and germline susceptibility variants cooperate to promote cancer is challenging. Ewing sarcoma is characterized by fusions between *EWSR1* and members of the ETS gene family, usually *EWSR1-FLI1*, leading to the generation of oncogenic transcription factors that bind DNA at GGAA motifs[1–3]. A recent genome-wide association study[4] identified susceptibility variants near *EGR2*. Here we found that *EGR2* knockdown inhibited proliferation, clonogenicity and spheroidal growth *in vitro* and induced regression of Ewing sarcoma xenografts. Targeted germline deep sequencing of the *EGR2* locus in affected subjects and controls identified 291 Ewing-associated SNPs. At rs79965208, the A risk allele connected adjacent GGAA repeats by converting an interspaced GGAT motif into a GGAA motif, thereby increasing the number of consecutive GGAA motifs and thus the EWSR1-FLI1–dependent enhancer activity of this sequence, with epigenetic characteristics of an active regulatory element. EWSR1-FLI1 preferentially bound to the A risk allele, which increased global and allele-specific *EGR2* expression. Collectively, our findings establish cooperation between a dominant oncogene and a susceptibility variant that regulates a major driver of Ewing sarcomagenesis.

Ewing sarcoma is an aggressive pediatric malignancy that likely arises from neural crest– or mesoderm-derived mesenchymal stem cells (MSCs)[5,6]. It is driven by oncogenic fusions between *EWSR1* and genes in the ETS family (mostly *FLI1*)[1,7]. EWSR1-FLI1 binds DNA either at ETS-like consensus sites containing a GGAA core motif or, more specifically with respect to other ETS family members, at GGAA microsatellites, where the enhancer activity increases with the number of consecutive GGAA motifs[2,3]. Notably, ~40% of EWSR1-FLI1 binding occupancy maps to GGAA microsatellites[8]. Aside from *EWSR1-FLI1*, Ewing sarcoma is known for its paucity of recurrent somatic abnormalities[9–11].

Epidemiological studies have documented striking disparities in the incidence of Ewing sarcoma across human populations[12], implying a strong contribution of germline variation to Ewing sarcoma tumorigenesis. Our recent genome-wide association study (GWAS) identified three significant susceptibility loci with higher odds ratios (ORs) than commonly observed in adult cancers (OR > 1.5, compared with OR < 1.3 for adult cancers)[4,13]. However, the potential oncogenic cooperation between the major *EWSR1-FLI1* somatic alteration and these Ewing sarcoma susceptibility loci remains to be elucidated. Here we focused on the chr10q21.3 susceptibility locus, which harbors two plausible candidate genes, *ADO* (2-aminoethanethiol dioxygenase), encoding a non-heme iron enzyme that converts cysteamine into taurine[14], and *EGR2* (early growth response 2; also known as *KROX20*), encoding a conserved zinc-finger transcription factor that promotes proliferation, differentiation and/or survival in different cell types, including neural crest–derived Schwann cells and mesoderm-derived osteoprogenitors[15,16]. Previous data showed that *ADO* and *EGR2* are overexpressed in Ewing sarcoma compared with other solid tumors

[1]Genetics and Biology of Cancers Unit, Institut Curie, PSL Research University, Paris, France. [2]INSERM U830, Institut Curie Research Center, Paris, France. [3]Institut Curie Genomics of Excellence (ICGex) Platform, Institut Curie Research Center, Paris, France. [4]École Normale Supérieure (ENS), Institut de Biologie de l'ENS (IBENS), INSERM U1024, CNRS UMR8197, Paris, France. [5]Instituto de Investigación de Enfermedades Raras, Instituto de Salud Carlos III, Madrid, Spain. [6]INSERM U916 Biology of Sarcomas, Institut Bergonié, Bordeaux, France. [7]Département d'Epidémiologie et de Biostatistiques, Institut Gustave Roussy, Villejuif, France. [8]Département de Pédiatrie, Institut Gustave Roussy, Villejuif, France. [9]Institute for Pediatric Hematology and Oncology, Leon-Bérard Cancer Center, University of Lyon, Lyon, France. [10]INSERM U1052, Léon-Bérard Cancer Centre, Cancer Research Center of Lyon, Lyon, France. [11]Unité Génétique Somatique (UGS), Institut Curie Centre Hospitalier, Paris, France. [12]INSERM U900, Bioinformatics, Biostatistics, Epidemiology and Computational Systems Biology of Cancer, Institut Curie Research Center, Paris, France. [13]Mines ParisTech, Fontainebleau, France. [14]Institute for Cancer Outcomes and Survivorship, School of Medicine, University of Alabama, Birmingham, Alabama, USA. [15]Centre de Recherche sur les Pathologies Prostatiques (CeRePP)–Laboratory for Urology, Research Team 2, UPMC, Hôpital Tenon, Paris, France. [16]Division of Cancer Epidemiology and Genetics (DCEG), National Cancer Institute (NCI), Bethesda, Maryland, USA. [17]Present address: Laboratory for Pediatric Sarcoma Biology, Institute of Pathology, LMU Munich, Munich, Germany. Correspondence should be addressed to O.D. (olivier.delattre@curie.fr).

Received 27 April; accepted 30 June; published online 27 July 2015; doi:10.1038/ng.3363

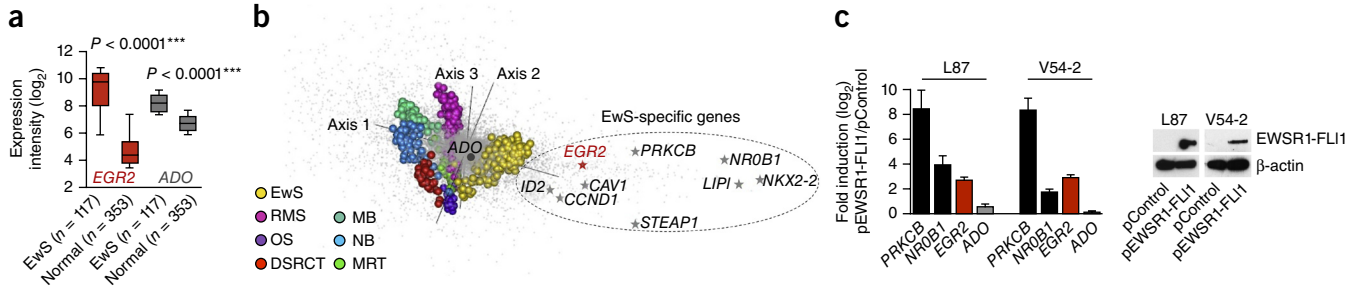

Figure 1 *EGR2* overexpression is mediated by EWSR1-FLI1. (**a**) *EGR2* and *ADO* expression levels in Ewing sarcoma (EwS, GSE34620) and normal tissue (GSE3526). The normal-body atlas consisted of 353 microarrays representing 63 individual tissue types (**Supplementary Fig. 1**). Data are shown as medians (horizontal bars) with ranges for the 25th–75th percentile (box) and 10th–90th percentile (whiskers). *P* values determined via two-tailed unpaired Student's *t*-test with Welch's correction. (**b**) Between-group analysis. Genes (gray dots) and tumor samples (colored spheres) are separated along three axes. EwS, Ewing sarcoma ($n = 279$); RMS, rhabdomyosarcoma ($n = 121$); OS, osteosarcoma ($n = 25$); DSRCT, desmoplastic small-round-cell tumor ($n = 32$); MB, medulloblastoma ($n = 52$); NB, neuroblastoma ($n = 64$); MRT, malignant rhabdoid tumor ($n = 35$). The main genes specifically overexpressed in Ewing sarcoma are indicated. (**c**) Quantitative real-time PCR analysis of *EGR2* and *ADO* expression in human MSC lines L87 and V54-2 after ectopic EWSR1-FLI1 expression (pEWSR1-FLI1) as compared with empty vector (pControl). Data are shown as the mean and s.e.m.; $n \geq 9$ independent experiments. The EWSR1-FLI1 targets *NR0B1* and *PRKCB* served as positive controls[17,35]. EWSR1-FLI1 expression was confirmed by immunoblot (loading control: β-actin).

and that their elevated expression is associated with risk alleles[4]. *EGR2* and, to a lesser extent, *ADO* are also strongly overexpressed in Ewing sarcoma relative to their expression in normal tissues (**Fig. 1a** and **Supplementary Fig. 1**). Comparative analysis of microarray data from seven pediatric soft tissue and brain tumor types showed that *EGR2*, but not *ADO*, clusters with established EWSR1-FLI1 target genes[17] (**Fig. 1b**). To further explore the expression quantitative trait locus (eQTL) properties of the Ewing sarcoma chr10 susceptibility locus, we evaluated available genotype and matched expression data sets from Ewing sarcoma and other small-round-cell tumors, as well as from normal tissues[4,18–23]. Interestingly, the Ewing sarcoma risk-associated rs1848797, which was genotyped in all data sets, was associated with higher *EGR2* and *ADO* expression only in Ewing sarcoma, and not in *EWSR1-FLI1*–negative tissues (**Table 1**, **Supplementary Data** and **Supplementary Fig. 2**). Moreover, ectopic *EWSR1-FLI1* expression in human MSCs specifically induced *EGR2* expression (**Fig. 1c**), whereas *EWSR1-FLI1* knockdown by specific small interfering RNA (siRNA) consistently reduced *EGR2* expression in four different Ewing sarcoma cell lines (**Supplementary Fig. 3**). Such regulation by *EWSR1-FLI1* was not observed for *ADO*. These data strongly suggest that *EGR2* and *ADO* are specifically regulated by eQTLs in Ewing sarcoma, but that only *EGR2* is *EWSR1-FLI1* dependent.

Knockdown experiments showed that inhibition of *EGR2*, but not of *ADO*, impaired the proliferation and clonogenicity of four different Ewing sarcoma cell lines, reduced cell cycle progression through S-phase and reduced cell viability (**Fig. 2a**,**b** and **Supplementary Fig. 4**). To confirm the contribution of *EGR2* to Ewing sarcoma growth, we generated Ewing sarcoma cell lines with a doxycycline-inducible anti-*EGR2* small-hairpin RNA (shRNA) expression system. Long-term *EGR2* knockdown not only dramatically reduced anchorage-independent spheroidal growth *in vitro* but, even more strikingly, also induced the regression of Ewing sarcoma xenografts *in vivo* (**Fig. 2c**,**d**). Consistent with the hypothesis that *EGR2* acts downstream of *EWSR1-FLI1*, transcriptome profiling of Ewing sarcoma cells after knockdown of either gene showed highly significantly overlapping transcriptional signatures (**Fig. 2e** and **Supplementary Data**). Collectively, these data suggest that *EGR2* is an EWSR1-FLI1–induced target gene critical for Ewing sarcoma tumorigenicity.

As several reports have shown that *EGR2* acts downstream of the epidermal growth factor (EGF) and fibroblast growth factor (FGF) pathway[15,24,25], we explored a potential contribution of these pathways to Ewing sarcoma growth and *EGR2* regulation. Whereas EGF receptors (EGFRs) are minimally expressed in Ewing sarcoma, some FGF receptors (FGFRs), particularly FGFR1, are highly expressed (**Supplementary Fig. 5a**). Consistently, bFGF, but not EGF, strongly induced both proliferation of and *EGR2* expression in Ewing sarcoma cells (**Supplementary Fig. 5b**,**c**). These data indicate that EWSR1-FLI1 and FGF signaling converge to upregulate the expression of *EGR2*.

To fine-map the chr10 susceptibility locus and to identify variants that potentially contribute to *EGR2* overexpression, we performed targeted deep sequencing across the chr10 susceptibility locus, including the flanking haplotype blocks, in the germline DNA of 343 individuals with Ewing sarcoma and 251 genetically matched controls (median target-region coverage ≥ 10×, 91.35%; median nucleotide coverage, 217×). Genetic matching was based on principal-component analysis[4] of SNP array data (**Supplementary Fig. 6**). After quality control metrics had been applied to the sequencing data (for example, ≥10× coverage per position, genotype call rate of ≥90% and compliance with Hardy-Weinberg equilibrium), 290 common SNPs (minor allele frequency > 0.05) were identified that were significantly associated with Ewing sarcoma ($P < 0.05$; **Fig. 3a**, **Supplementary Data** and **Supplementary Fig. 7**). These included all 14 sentinel SNPs reported in our previous GWAS[4]. Haplotype and linkage disequilibrium (LD) analysis showed that this locus consists of discrete subhaploblocks (**Fig. 3a** and **Supplementary Data**).

Table 1 Overexpression of *EGR2* and *ADO* is mediated by Ewing sarcoma–specific eQTLs

			P value correlation with rs1848797	
	Tissue type	*n*	*EGR2*	*ADO*
Malignant	Ewing sarcoma	117	0.0077	0.0023
	Medulloblastoma	283	ns	ns
	Neuroblastoma	74	ns	ns
	AML	106	ns	ns
Normal	LCL	329	ns	ns
	Airway epithelium	114	ns	ns
	Broad GTEx	1,421	ns	ns

eQTL analyses across tissue types identified Ewing sarcoma–specific correlations of *EGR2* and *ADO* expression with the risk allele at rs1848797. The Broad GTEx database comprised 13 normal tissue types (≥60 samples per tissue type). ns, not significant; AML, acute myeloid leukemia; LCL, lymphoblastoid cell lines.

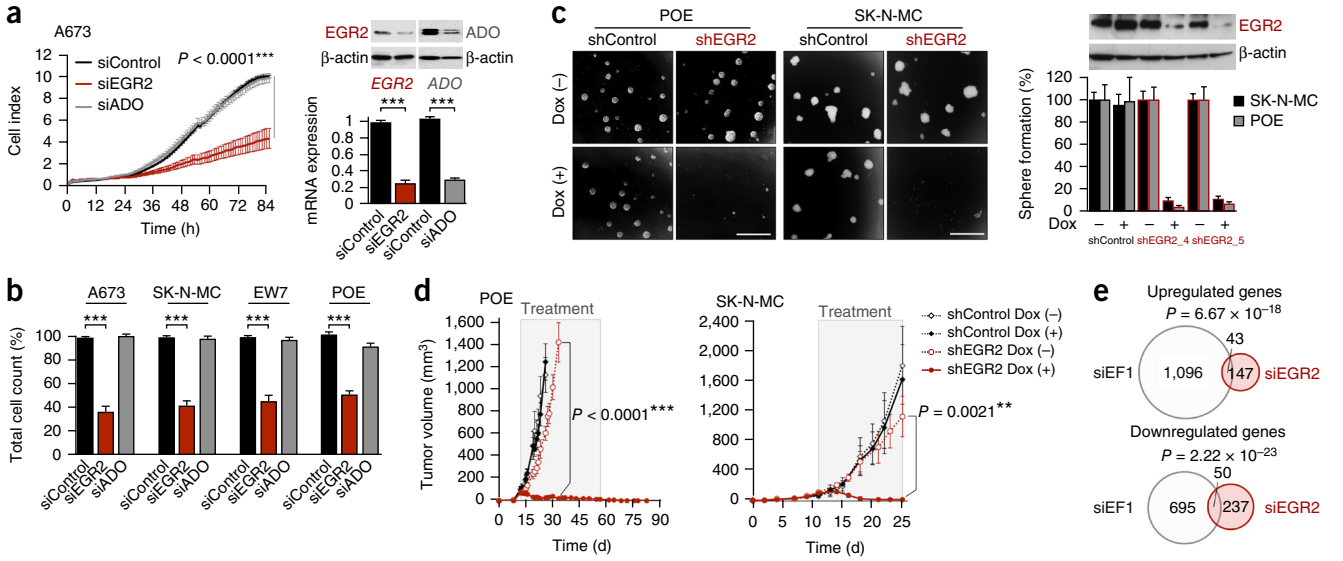

Figure 2 EGR2 is critical for the growth and tumorigenicity of Ewing sarcoma. (**a**) xCELLigence proliferation kinetics of A673 cells. Data shown are the mean ± s.e.m. of results obtained with two different siRNAs against *EGR2* and three different siRNAs against *ADO*; $n \geq 6$ technical replicates. EGR2 or ADO knockdown was confirmed at 48 h by quantitative real-time PCR (mean ± s.e.m., $n \geq 4$ independent experiments) and immunoblot (loading control: β-actin). (**b**) Validation of xCELLigence results by cell counting (including supernatant) 96 h after transfection of A673, SK-N-MC, EW7 and POE cells. Data are mean and s.e.m. of results obtained with two different siRNAs against *EGR2* and three different siRNAs against *ADO*; $n \geq 3$ independent experiments. (**c**) Left, phase-contrast images of sphere-formation assays (scale bars, 1 mm). Right, mean and s.e.m. of $n \geq 3$ independent experiments performed with SK-N-MC and POE containing a doxycycline-inducible shRNA against *EGR2* (shEGR2_4 or shEGR2_5). Also shown is a representative EGR2 immunoblot for POE cells (96-h doxycycline treatment; loading control, β-actin). (**d**) Growth curves for subcutaneously xenografted POE or SK-N-MC cells in mice (shControl and shEGR2_4). When tumors reached a volume of 75–100 mm^3, doxycycline and sucrose (Dox +) or sucrose alone (Dox –) was added to the drinking water (treatment). Mean ± s.e.m.; $n \geq 6$ mice per group. *P* values determined via two-tailed unpaired Student's *t*-test. (**e**) Size-proportional Venn diagrams of up- and downregulated genes 48 h after knockdown of *EWSR1-FLI1* (siEF1) or *EGR2* (siEGR2) in A673 and SK-N-MC cells (minimum $\log_2$ fold change ± 0.5, Benjamini-Hochberg–corrected $P < 0.05$). Fisher's exact test.

To prioritize SNPs for functional assessment, we crossed our sequencing data with published chromatin immunoprecipitation (ChIP)-Seq, DNase-Seq and ENCODE data, with particular focus on Ewing sarcoma cell lines[8,26,27], as recent studies have suggested that most causal SNPs cluster in epigenetically active and cell-type-specific regulatory elements[28,29] (**Fig. 3a**). We also included data on conserved *EGR2* regulatory elements previously mapped in animal models[30] (**Fig. 3a** and **Supplementary Fig. 8**). We observed activating chromatin marks, signals for formaldehyde-assisted isolation of regulatory elements (FAIRE) and/or DNaseI hypersensitivity at five main loci: two loci corresponding to known *EGR2* regulatory elements (MSE (myelinating Schwann cell enhancer)[30] and BoneE (bone enhancer) (unpublished data); **Supplementary Fig. 8**), one to the *ADO* promoter, and two to GGAA microsatellites (mSat1 and mSat2) that overlapped with EWSR1-FLI1 ChIP-Seq signals (**Fig. 3a**). Because the *ADO* promoter does not contain Ewing sarcoma–associated SNPs, it was not further investigated. Luciferase reporter assays indicated that BoneE and MSE had no and weak activity in Ewing sarcoma, respectively (**Fig. 3b**,**c**). In contrast, both GGAA microsatellites exhibited strong EWSR1-FLI1–dependent enhancer-like activity (**Fig. 3b**,**c**). This activity corresponded to EWSR1-FLI1–dependent activating chromatin marks H3K4me1 and H3K27ac (**Fig. 3a**) and was consistent with recent evidence suggesting that EWSR1-FLI1 can act as a pioneer transcription factor to create *de novo* enhancers at GGAA microsatellites[27].

Because of its observed higher enhancer activity, relatively simpler structure compared with that of mSat1, and localization in the sub-haploblock containing some of the most significant Ewing sarcoma–associated SNPs (**Figs. 3a** and **4a** and **Supplementary Fig. 9**), we focused on mSat2 and carried out PCR-based targeted long-read (300/300 nt) deep resequencing of all samples to analyze its genetic architecture. This yielded 1,158 analyzable mSat2 sequences, which revealed another SNP, rs79965208, in strong LD ($D' = 0.97$) with the nearby rs6479860, one of the strongest sentinel SNPs from our GWAS[4] (**Fig. 4a** and **Supplementary Data**). The significant association of the A allele of rs79965208 with Ewing sarcoma ($P = 0.022$, logistic regression) was replicated in two independent cohorts, the first based on direct sequencing of this SNP in 156 additional Ewing sarcoma subjects and 184 controls of European descent ($P = 6.15 \times 10^{-3}$, logistic regression), and the second on imputation from the 1000 Genomes Project Phase 3 reference panel[31] of 162 individuals with first primary Ewing sarcoma from the Childhood Cancer Survivor Study[32] genotyped on Illumina HumanOmni5Exome arrays and 435 cancer-free controls from the Division of Cancer Epidemiology and Genetics ($P = 9.33 \times 10^{-6}$, logistic regression) (**Supplementary Data**).

Interestingly, rs79965208 converts a GGAT motif into a GGAA motif, thereby connecting two adjacent GGAA repeats (**Fig. 4a**). The first GGAA repeat is polymorphic and contains a median number of 11 GGAA motifs, whereas the second is not polymorphic and is composed of four GGAA motifs. The A allele at rs79965208 therefore increases the median number of consecutive GGAA motifs from 11 to 16.

The previously described threshold for exponentially increasing EWSR1-FLI1–dependent enhancer activity is >12 consecutive GGAA motifs[3]. In the current study, a significantly larger proportion of Ewing sarcoma mSat2 sequences contained >12 GGAA motifs than did controls (65.88% versus 54.99%, $P = 2.10 \times 10^{-6}$, two-tailed Fisher's exact test). We subsequently examined the enhancer properties of mSat2 corresponding to the reference sequence (hg19) containing either the T or the A allele at rs79965208 in a luciferase assay. Relative to the T allele, the A allele increased the EWSR1-FLI1–induced enhancer

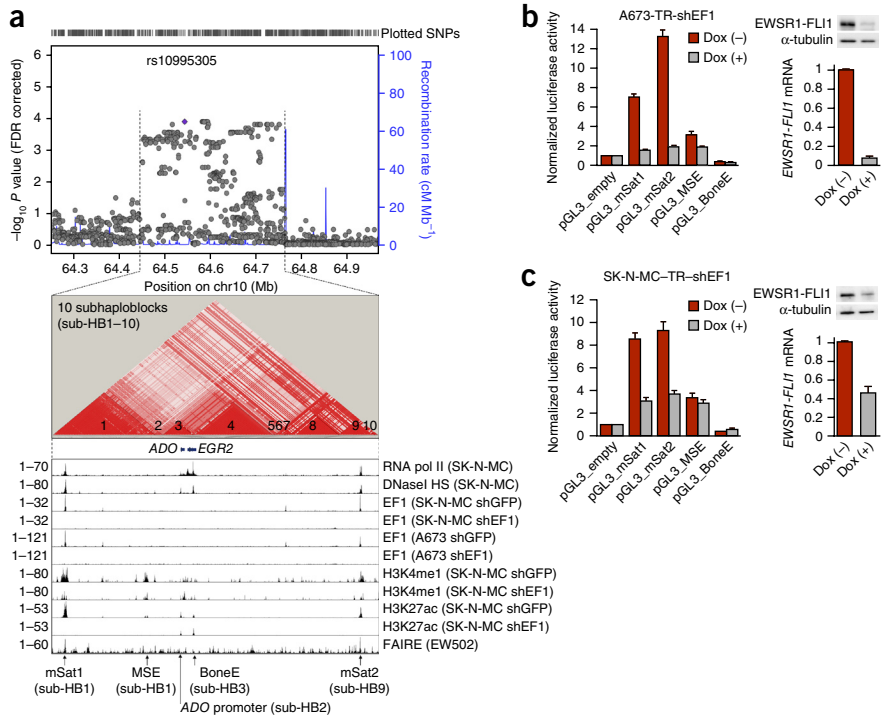

Figure 3 Fine-mapping and epigenetic profiling revealed candidate *EGR2* regulatory elements. (**a**) Top, Manhattan plot of 1,440 SNPs identified by targeted deep sequencing within the chr10 susceptibility locus and flanking haplotype blocks. rs10995305 was the SNP most significantly associated with Ewing sarcoma at this locus (false discovery rate (FDR)-corrected $P = 1.27 \times 10^{-4}$). The blue lines indicate the recombination-rate estimates from the HapMap project[36]. Middle, LD plot of the chr10 susceptibility locus hotspot (chr10:64,449,549–64,756,872) based on the analysis of 290 significant Ewing sarcoma–associated SNPs in 343 affected subjects (a subset of the original GWAS cohort[4]) and 251 controls. Bottom, epigenetic profile of the chr10 susceptibility locus hotspot in the Ewing sarcoma cell lines SK-N-MC, A673 and EW502. Displayed are signals from published ChIP-Seq or DNase-Seq data for RNA polymerase II (pol II), DNaseI hypersensitivity (HS), EWSR1-FLI1 (EF1), H3K4me1 and H3K27ac in Ewing sarcoma cells transfected with either a control shRNA (shGFP) or a specific shRNA against *EWSR1-FLI1* (shEF1), and FAIRE[8,26,27]. The read count is given on the left. mSat1 and mSat2 are GGAA microsatellites (**Supplementary Fig. 8**). (**b**,**c**) Normalized luciferase reporter signals in A673-TR-shEF1 and SK-N-MC–TR–shEF1 cells containing a doxycycline-inducible shRNA against *EWSR1-FLI1*. EWSR1-FLI1 knockdown was confirmed by quantitative real-time PCR and immunoblot (loading control: α-tubulin). Data are shown as means and s.e.m.; $n \geq 5$ independent experiments.

activity of mSat2 (**Fig. 4b**). This transcription-activation property was observed in two Ewing sarcoma cell lines and was strictly dependent on EWSR1-FLI1, as its doxycycline-induced knockdown abrogated luciferase activity (**Fig. 4b**).

In accordance with the reporter assays, the A allele was associated with significantly higher *EGR2* expression in Ewing sarcoma tumors (**Fig. 4c**). Consistently, ChIP experiments in the A/T Ewing sarcoma cell line MHH-ES1 using a specific antibody to FLI1 followed by

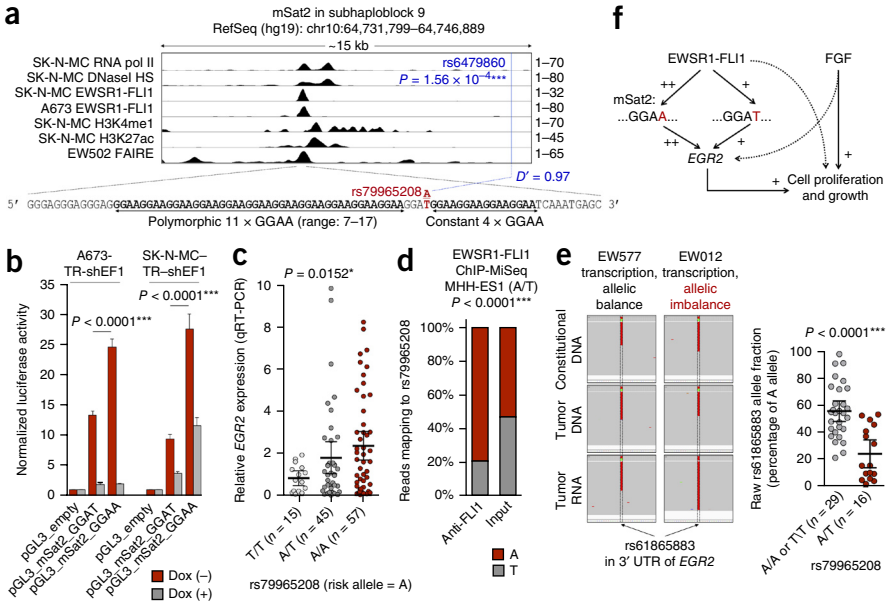

Figure 4 Germline variation at mSat2 modulates *EWSR1-FLI1*–dependent *EGR2* expression. (**a**) Coordinates, epigenetic profile and sequence of the mSat2 locus. Consistent with previous studies, H3K4me1 and H3K27ac signals peaked adjacent to the repetitive GGAA mSat[8,27]. The *P* value reported for rs6479860 reflects the significance of its association with Ewing sarcoma. (**b**) Luciferase reporter signals of mSat2 with the T or A allele at rs79965208. Data are mean and s.e.m.; $n \geq 6$ independent experiments. *P* values determined via two-tailed unpaired Student's *t*-test. (**c**) *EGR2* expression measured by quantitative real-time PCR in 117 Ewing samples (103 primary tumors and 14 cell lines). *EGR2* expression was normalized to that of *RPLP0* and is displayed as expression relative to that of the median sample (set as 1). Horizontal bars represent means, and whiskers represent the 95% confidence interval boundaries. *P* value determined via linear regression. (**d**) Allele fraction of reads mapping to rs79965208 generated in a ChIP-MiSeq experiment in the A/T Ewing cell line MHH-ES1 (**Supplementary Fig. 10** and **Supplementary Data**). (**e**) Left, representative Integrative Genomics Viewer[37] pile-up of reads covering the *EGR2* 3′ UTR rs61865883 in matched constitutional or tumor DNA and tumor-derived RNA. The sample EW012 exhibited transcriptional allelic imbalance of *EGR2*, whereas EW577 did not. Right, raw rs61865883 allele fractions of targeted RNA deep sequencing in 45 Ewing sarcomas heterozygous (A/T) for the transcribed *EGR2* 3′ UTR allelic marker rs61865883. Horizontal bars represent means, and whiskers show the 95% confidence interval boundaries. *P* values determined via parametric two-tailed Student's *t*-test. (**f**) Regulatory model of EWSR1-FLI1 and mSat2 controlling *EGR2* expression and proliferation of Ewing sarcoma cells in convergence with the FGF pathway.

targeted deep sequencing of mSat2 identified significant enrichment of reads containing the A allele (**Fig. 4d** and **Supplementary Fig. 10**), indicating that EWSR1-FLI1 preferentially bound to the A allele of rs79965208. Moreover, taking advantage of a transcribed SNP in the 3′ UTR of *EGR2* (rs61865883), we assessed allele-specific *EGR2* expression via targeted RNA deep sequencing. Across 45 individuals with heterozygosity for rs61865883, the transcriptional allelic imbalance was significantly higher in 16 tumors heterozygous for rs79965208 (A/T) than in 29 tumors homozygous (A/A or T/T) for this locus (**Fig. 4e**). Collectively, our results show that *EGR2* is a Ewing sarcoma susceptibility gene whose overexpression in tumors is mediated by EWSR1-FLI1 through a risk-conferring enhancer-like polymorphic GGAA microsatellite (**Fig. 4f**).

Importantly, we noted that the chr10 signal was strongly reduced when we performed association testing conditionally on rs79965208, which indicated that this SNP is a major functional variant at this locus. However, some association signal was still observed, so it remains plausible that other SNPs could also have a regulatory effect on *EGR2* expression through other mechanisms (**Supplementary Fig. 11**). The relatively low *EGR2* expression observed in some Ewing sarcoma cases, particularly in cases with the T/T genotype, suggests that *EGR2* might not always be absolutely necessary for Ewing sarcoma growth, and that growth may thus rely on alternative 'transformation-facilitating genes', possibly linked to other Ewing sarcoma susceptibility loci. However, we could not test whether Ewing sarcoma cells with a T/T genotype at rs79965208 have decreased sensitivity to *EGR2* knockdown, as the T/T genotype was not observed across 21 different Ewing sarcoma cell lines (**Supplementary Data**).

As the incidence of Ewing sarcoma is higher in Europeans than in Africans[12], we investigated the frequency of the A allele at rs79965208 across human populations, as determined by the 1000 Genomes Project[31] (**Supplementary Data**). Strikingly, the A risk allele is highly significantly more frequent in non-African human populations (mean, 0.64; range, 0.57–0.70; $n = 1{,}886$) than in Africans (0.25; $n = 691$) ($P = 2.20 \times 10^{-16}$, Fisher's exact test), which suggests that rs79965208 underwent a recent expansion in non-Africans and that it might contribute to the variable susceptibility to Ewing sarcoma across populations.

To our knowledge, this constitutes one of the first reports of how a germline variant highly correlated with the reported GWAS signal can inform our understanding of a cancer-specific acquired genetic abnormality[22]. Furthermore, our findings are in line with predictions that causal variants are not necessarily among the most significant variations leading to the identification of the susceptibility loci, but rather are in strong LD with them[33,34]. Moreover, they illustrate the contribution of a common germline variant that alters one or more key biological pathways in Ewing sarcoma through the modification of transcription regulatory elements that mediate the effects of a dominant oncogene[13].

URLs. https://www.addgene.org/21915/; http://www.gtexportal.org/home/; http://www.r-project.org/; https://github.com/jstjohn/SeqPrep; http://broadinstitute.github.io/picard/; http://www.clustal.org/omega/.

METHODS

Methods and any associated references are available in the online version of the paper.

Accession codes. Primary microarray data are compliant with the MIAME guidelines and were deposited at the Gene Expression Omnibus (GEO) under accession GSE62090.

Note: Any Supplementary Information and Source Data files are available in the online version of the paper.

ACKNOWLEDGMENTS

T.G.P.G. is supported by a grant from the German Research Foundation (DFG GR3728/2-1), by the Daimler and Benz Foundation in cooperation with the Reinhard Frank Foundation, by LMU Munich's Institutional Strategy LMUexcellent within the framework of the German Excellence Initiative and by the Mehr LEBEN für krebskranke Kinder–Bettina-Bräu-Stiftung. D.S. is supported by the Institut Curie–SIRIC (Site de Recherche Intégrée en Cancérologie) program. F.C.-A. is supported by a grant from the Asociación Pablo Ugarte and Instituto de Salud Carlos III RTICC RD12/0036/0027. D.G.C. is supported by a grant from the InfoSarcomes Association. The Childhood Cancer Survivor Study is supported by the National Cancer Institute (CA55727, G.T. Armstrong), with funding for genotyping from the Intramural Research Program of the National Institutes of Health, National Cancer Institute. This work was supported by grants from the Institut Curie; INSERM; the Agence Nationale de la Recherche (Investissements d'Avenir) (ANR-10-EQPX-03); the Cancéropôle Ile-de-France (ANR10-INBS-09-08); the Ligue Nationale Contre le Cancer (Equipe labellisée); the Institut National du Cancer (PLBIO14-237); the European PROVABES (ERA-649 NET TRANSCAN JTC-2011), ASSET (FP7-HEALTH-2010-259348) and EEC (HEALTH-F2-2013-602856) projects; and the Société Française des Cancers de l'Enfant. The following associations supported this work: Courir pour Mathieu, Dans les pas du Géant, Olivier Chape, Les Bagouzamanon, Enfants et Santé, and les Amis de Claire. The Charnay laboratory was financed by INSERM, the CNRS, the Ministère de la Recherche et Technologie, and the Fondation pour la Recherche Médicale. It has received support under the program "Investissements d'Avenir" launched by the French Government and implemented by the ANR, with the references ANR-10-LABX-54 MEMOLIFE and ANR-11-IDEX-0001-02 PSL* Research University. We thank J. Maris for providing genotype information for the neuroblastoma data set, and we thank L. Liang and W. Cookson for providing access to genotype data on the LCL data set. We thank H. Kovar (Children's Cancer Research Institute Vienna, Vienna, Austria) for providing cell lines STA-ET-1, STA-ET-3 and STA-ET-8, and F. Redini (University of Nantes, Nantes, France) for providing cell line TC-32. Human MSC lines L87 and V54-2 were kindly provided by P. Nelson (University Hospital LMU, Munich, Germany). We also thank the following clinicians and pathologists for providing samples used in this work: I. Aerts, P. Anract, C. Bergeron, L. Boccon-Gibod, F. Boman, F. Bourdeaut, C. Bouvier, R. Bouvier, L. Brugiéres, E. Cassagnau, J. Champigneulle, C. Cordonnier, J. M. Coindre, N. Corradini, A. Coulomb-Lhermine, A. De Muret, G. De Pinieux, A.S. Defachelles, A. Deville, F. Dijoud, F. Doz, C. Dufour, K. Fernandez, N. Gaspard, L. Galmiche-Rolland, C. Glorion, A. Gomez-Brouchet, J.M. Guinebretiere, H. Jouan, C. Jeanne-Pasquier, B. Kantelip, F. Labrousse, V. Laithier, F. Larousserie, G. Leverger, C. Linassier, P. Mary, G. Margueritte, E. Mascard, A. Moreau, J. Michon, C. Michot, F. Millot, Y. Musizzano, M. Munzer, B. Narciso, O. Oberlin, D. Orbach, H. Pacquement, Y. Perel, B. Petit, M. Peuchmaur, J.Y. Pierga, C. Piguet, S. Piperno-Neumann, E. Plouvier, D. Ranchere-Vince, J. Rivel, C. Rouleau, H. Rubie, H. Sartelet, G. Schleiermacher, C. Schmitt, N. Sirvent, D. Sommelet, P. Terrier, R. Tichit, J. Vannier, J.M. Vignaud and V. Verkarre. We also thank D. Darmon for technical assistance, S. Grossetete-Lalami for bioinformatic assistance, and V.R. Buchholz and E. Butt for critical reading of the manuscript.

AUTHOR CONTRIBUTIONS

T.G.P.G. coordinated and designed the study, performed all functional experiments, analyzed the sequencing data, performed bioinformatic analyses, wrote the paper, designed the figures and helped with grant applications. V. Bernard processed the sequencing data and performed bioinformatic analyses. P.G.-H. participated in the study design, cloned enhancer elements and contributed to data analysis. V.R. performed all sequencing experiments and helped analyze the bioinformatic data. D.S. contributed to the *in vivo* experiments, performed the ChIP-MiSeq experiments and provided experimental protocols. M.-M.A., F.C.-A., A.H.J. and S.Z. helped with functional experiments. O.M., F.T. and C.L. provided statistical advice and helped in the bioinformatic analyses. G. Perot assisted in generation of the shRNA constructs. M.-C.L.D., O.O. and P.M.-B. provided Ewing sarcoma samples and annotation. G. Pierron, S.R. and E.L. provided and prepared Ewing sarcoma samples. T.R.F. coordinated and supervised sequencing experiments. V. Boeva helped analyze ChIP-Seq data. J.A. provided the A673-TR-shEF1 and SK-N-MC–TR–shEF1 cell lines. A.S.V. performed principal-component analysis clustering of Ewing sarcoma subjects and controls. G.C.-T. and O.C. provided DNA from healthy controls. D.G.C. and S.J.C. provided genetic and statistical guidance. S.B., L.M.M., M.J.M. and S.J.C. provided data for the CCSS replication cohort and performed imputation analyses. P.C. provided advice on analyses concerning *EGR2* and laboratory infrastructure. O.D. initiated, designed and supervised the

study; provided biological and genetic guidance; analyzed the data; wrote the paper together with T.G.P.G.; and provided laboratory infrastructure and financial support. All authors read and approved the final manuscript.

COMPETING FINANCIAL INTERESTS

The authors declare no competing financial interests.

1. Delattre, O. *et al.* Gene fusion with an ETS DNA-binding domain caused by chromosome translocation in human tumours. *Nature* **359**, 162–165 (1992).
2. Gangwal, K. *et al.* Microsatellites as EWS/FLI response elements in Ewing's sarcoma. *Proc. Natl. Acad. Sci. USA* **105**, 10149–10154 (2008).
3. Guillon, N. *et al.* The oncogenic EWS-FLI1 protein binds *in vivo* GGAA microsatellite sequences with potential transcriptional activation function. *PLoS One* **4**, e4932 (2009).
4. Postel-Vinay, S. *et al.* Common variants near *TARDBP* and *EGR2* are associated with susceptibility to Ewing sarcoma. *Nat. Genet.* **44**, 323–327 (2012).
5. von Levetzow, C. *et al.* Modeling initiation of Ewing sarcoma in human neural crest cells. *PLoS One* **6**, e19305 (2011).
6. Tirode, F. *et al.* Mesenchymal stem cell features of Ewing tumors. *Cancer Cell* **11**, 421–429 (2007).
7. Delattre, O. *et al.* The Ewing family of tumors—a subgroup of small-round-cell tumors defined by specific chimeric transcripts. *N. Engl. J. Med.* **331**, 294–299 (1994).
8. Patel, M. *et al.* Tumor-specific retargeting of an oncogenic transcription factor chimera results in dysregulation of chromatin and transcription. *Genome Res.* **22**, 259–270 (2012).
9. Brohl, A.S. *et al.* The genomic landscape of the Ewing sarcoma family of tumors reveals recurrent *STAG2* mutation. *PLoS Genet.* **10**, e1004475 (2014).
10. Crompton, B.D. *et al.* The genomic landscape of pediatric Ewing sarcoma. *Cancer Discov.* **4**, 1326–1341 (2014).
11. Tirode, F. *et al.* Genomic landscape of Ewing sarcoma defines an aggressive subtype with co-association of *STAG2* and *TP53* mutations. *Cancer Discov.* **4**, 1342–1353 (2014).
12. Worch, J. *et al.* Racial differences in the incidence of mesenchymal tumors associated with *EWSR1* translocation. *Cancer Epidemiol. Biomarkers Prev.* **20**, 449–453 (2011).
13. Chung, C.C. & Chanock, S.J. Current status of genome-wide association studies in cancer. *Hum. Genet.* **130**, 59–78 (2011).
14. Dominy, J.E. Jr. *et al.* Discovery and characterization of a second mammalian thiol dioxygenase, cysteamine dioxygenase. *J. Biol. Chem.* **282**, 25189–25198 (2007).
15. Chandra, A., Lan, S., Zhu, J., Siclari, V.A. & Qin, L. Epidermal growth factor receptor (EGFR) signaling promotes proliferation and survival in osteoprogenitors by increasing early growth response 2 (EGR2) expression. *J. Biol. Chem.* **288**, 20488–20498 (2013).
16. Topilko, P. *et al.* Krox-20 controls myelination in the peripheral nervous system. *Nature* **371**, 796–799 (1994).
17. Mackintosh, C., Madoz-Gúrpide, J., Ordóñez, J.L., Osuna, D. & Herrero-Martín, D. The molecular pathogenesis of Ewing's sarcoma. *Cancer Biol. Ther.* **9**, 655–667 (2010).
18. Gao, C. *et al.* HEFT: eQTL analysis of many thousands of expressed genes while simultaneously controlling for hidden factors. *Bioinformatics* **30**, 369–376 (2014).
19. Radtke, I. *et al.* Genomic analysis reveals few genetic alterations in pediatric acute myeloid leukemia. *Proc. Natl. Acad. Sci. USA* **106**, 12944–12949 (2009).
20. Moffatt, M.F. *et al.* Genetic variants regulating *ORMDL3* expression contribute to the risk of childhood asthma. *Nature* **448**, 470–473 (2007).
21. Northcott, P.A. *et al.* Subgroup-specific structural variation across 1,000 medulloblastoma genomes. *Nature* **488**, 49–56 (2012).
22. Wang, K. *et al.* Integrative genomics identifies *LMO1* as a neuroblastoma oncogene. *Nature* **469**, 216–220 (2011).
23. GTEx Consortium. The Genotype-Tissue Expression (GTEx) project. *Nat. Genet.* **45**, 580–585 (2013).
24. Labalette, C. *et al.* Hindbrain patterning requires fine-tuning of early *krox20* transcription by Sprouty 4. *Development* **138**, 317–326 (2011).
25. Weisinger, K., Kayam, G., Missulawin-Drillman, T. & Sela-Donenfeld, D. Analysis of expression and function of FGF-MAPK signaling components in the hindbrain reveals a central role for FGF3 in the regulation of *Krox20*, mediated by Pea3. *Dev. Biol.* **344**, 881–895 (2010).
26. ENCODE Project Consortium. *et al.* An integrated encyclopedia of DNA elements in the human genome. *Nature* **489**, 57–74 (2012).
27. Riggi, N. *et al.* EWS-FLI1 utilizes divergent chromatin remodeling mechanisms to directly activate or repress enhancer elements in Ewing sarcoma. *Cancer Cell* **26**, 668–681 (2014).
28. Ernst, J. *et al.* Mapping and analysis of chromatin state dynamics in nine human cell types. *Nature* **473**, 43–49 (2011).
29. Maurano, M.T. *et al.* Systematic localization of common disease-associated variation in regulatory DNA. *Science* **337**, 1190–1195 (2012).
30. Ghislain, J. *et al.* Characterisation of cis-acting sequences reveals a biphasic, axon-dependent regulation of *Krox20* during Schwann cell development. *Development* **129**, 155–166 (2002).
31. 1000 Genomes Project Consortium. *et al.* An integrated map of genetic variation from 1,092 human genomes. *Nature* **491**, 56–65 (2012).
32. Robison, L.L. *et al.* The Childhood Cancer Survivor Study: a National Cancer Institute–supported resource for outcome and intervention research. *J. Clin. Oncol.* **27**, 2308–2318 (2009).
33. Edwards, S.L., Beesley, J., French, J.D. & Dunning, A.M. Beyond GWASs: illuminating the dark road from association to function. *Am. J. Hum. Genet.* **93**, 779–797 (2013).
34. Faye, L.L., Machiela, M.J., Kraft, P., Bull, S.B. & Sun, L. Re-ranking sequencing variants in the post-GWAS era for accurate causal variant identification. *PLoS Genet.* **9**, e1003609 (2013).
35. Surdez, D. *et al.* Targeting the EWSR1–FLI1 oncogene-induced protein kinase PKC-β abolishes Ewing sarcoma growth. *Cancer Res.* **72**, 4494–4503 (2012).
36. International HapMap 3 Consortium. *et al.* Integrating common and rare genetic variation in diverse human populations. *Nature* **467**, 52–58 (2010).
37. Robinson, J.T. *et al.* Integrative genomics viewer. *Nat. Biotechnol.* **29**, 24–26 (2011).

ONLINE METHODS

Cell culture. Ewing sarcoma cell lines A673, SK-N-MC, RDES and SK-ES1 were obtained from the American Type Culture Collection (ATCC); lines MHH-ES1 and TC-71 were from the German Collection of Microorganisms and Cell Cultures (DSMZ); lines EW1, EW3, EW7, EW16, EW18, EW23, EW24 and ORS were from the International Agency for Research on Cancer (Lyon, France); lines STA-ET-1, STA-ET-3, and STA-ET-8 were from the Children's Cancer Research Institute Vienna (kindly provided by H. Kovar); lines ES7, EW22 and POE were from the Institut Curie Research Centre (Paris, France); and line TC-32 was from the University of Nantes (kindly provided by F. Redini). A673-TR-shEF1 and SK-N-MC–TR–shEF1 harbor a doxycycline-inducible shRNA against *EWSR1-FLI1* (ref. 38). Neuroblastoma: SK-N-SH, IMR-32; breast cancer: MDA-MB-231; alveolar rhabdomyosarcoma: SJ-RH30 (from ATCC). Human MSC lines L87 and V54-2 were kindly provided by P. Nelson (University Hospital LMU)[39,40]. Cells were grown at 37 °C in 5% CO_2 in a humidified atmosphere in RPMI 1640 medium (Gibco) containing 10% FCS (Eurobio), 100 U/ml penicillin and 100 µg/ml streptomycin (Gibco). Cell line purity and authenticity were confirmed by deep sequencing of susceptibility loci and short tandem repeat profiling. Cells were checked routinely by PCR for the absence of mycoplasma.

Transient transfection. Cells were seeded at a density of 1×10^5 to 2×10^5 per well of a six-well plate in a volume of 2.1 ml medium. Cell numbers were adjusted accordingly for transfection in larger or smaller volumes, and cells were transfected with siRNA (15 nM) with RNAiMAX (Invitrogen). The Qiagen AllStars Negative Control non-targeting siRNA was used as a control. siRNAs are listed in the **Supplementary Data**. For transfection with plasmids, 3×10^5 cells per well of a six-well plate were seeded in 2.5 ml medium and transfected with Lipofectamine LTX and Plus Reagent (Invitrogen). The pCDH1-MCS1-Puro (pControl) (System Biosciences) and the pCDH1-EWSR1-FLI1 (pEWSR1-FLI1) vectors were described previously[3,35].

Doxycycline-inducible shRNA constructs. Negative-control and specific shRNAs against *EGR2* were purchased from Sigma-Aldrich (**Supplementary Data**) and cloned into the pLKO-Tet-On all-in-one system[41] (Addgene). Lentivirus was produced in HEK293T cells (from ATCC). SK-N-MC and POE cells were infected with a multiplicity of infection of 10 and selected for 7 d using 1–2 µg/ml puromycin (Invitrogen). Puromycin-resistant clones were grown from single cells. Knockdown efficacy was assessed in individual clones by quantitative real-time PCR (qRT-PCR) 96 h after the addition of doxycycline (1 µg/ml).

RNA extraction, reverse transcription and qRT-PCR. RNA was extracted with the Nucleospin II kit (Macherey-Nagel) and reverse-transcribed using the High-Capacity cDNA Reverse Transcription Kit (Applied Biosystems). PCRs were performed either using TaqMan assays with qRT-PCR Mastermix Plus without UNG (Eurogentec) or using SYBR green (Applied Biosystems). Oligonucleotides were purchased from MWG Eurofins Genomics (**Supplementary Data**). Reactions were run on an ABI/PRISM 7500 instrument and analyzed using the 7500 system SDS software (Applied Biosystems).

DNA microarrays. RNA from A673 and SK-N-MC cells was extracted 48 h after transfection with siRNA. RNA quality was checked with a Bioanalyzer (Agilent). Total RNA (200 ng) was amplified and labeled with the Affymetrix GeneChip Whole Transcript Sense Target Labeling Kit. Antisense copy RNA was hybridized on Affymetrix Human Gene 2.1 ST arrays. Data were normalized by means of Probe Logarithmic Intensity Error (PLIER) estimation and custom brainarray CDF (v16)[42], are compliant with the MIAME guidelines, and were deposited in the Gene Expression Omnibus (GEO; GSE62090).

eQTL analyses. Microarray data retrieved from GEO were normalized by robust multiarray averaging using custom brainarray CDF (v18)[42]. Accession codes are listed in the **Supplementary Data**. Matched genotype data for rs1848797 were retrieved from the series-matrix files of the original studies, except for the neuroblastoma and LCL data sets, for which genotypes were kindly provided by J. Maris (Children's Hospital of Philadelphia, Pennsylvania, USA) or by L. Liang (Harvard School of Public Health, Boston, Massachusetts, USA) and W. Cookson (Imperial College, London, UK). Additionally, the Broad GTEx database[23] was assessed for associations of *EGR2* and *ADO* expression with the genotypes at rs1848797 (data censoring: July 8, 2014; 13 normal tissue types with at least 60 samples per tissue type, amounting to 1,421 samples). *P* values of linear regressions are reported.

Between-group analysis (BGA). BGA was performed as described[35]. In total, 279 Ewing sarcomas (GSE34620, GSE34800, GSE12102, and unpublished data), together with 32 desmoplastic small-round-cell tumors (unpublished data), 52 medulloblastomas (GSE12992 and unpublished data), 64 neuroblastomas (GSE12460 and unpublished data), 121 rhabdomyosarcomas (E-TABM-1202 and unpublished data), 35 malignant rhabdoid tumors (unpublished data) and 25 osteosarcomas (GSE14827), were included in the BGA, which was carried out with the made4 R package[43]. All microarray data were generated on Affymetrix HG-U133Plus2.0 arrays and simultaneously normalized using the gcrma package version 2.18.1 in R.

Immunoblots. Immunoblots were done with rabbit polyclonal anti-EGR2 (1/2,000, PRB-236P, Covance), mouse monoclonal anti-FLI1 (1:5,000, clone 7.3)[44], rabbit polyclonal anti-FLI1 (1:250, RB-9295-PCL, Thermo Scientific), rabbit monoclonal anti-ADO (1:1,000, EPR6581, Abcam), mouse monoclonal anti–α-tubulin (1:10,000, DM1A, Sigma-Aldrich), and mouse monoclonal anti–β-actin (1:10,000, A-5316, Sigma-Aldrich). Then membranes were incubated with an anti-rabbit or anti-mouse immunoglobulin G (IgG) horseradish peroxidase–coupled secondary antibody (1:3,000, NA934 or NXA931, respectively; Amersham Biosciences). Proteins were detected by enhanced chemiluminescence (Pierce).

Sequence alignments. Mouse and human DNA sequences of *EGR2* enhancers were aligned using Clustal Ω (v1.2.0)[45].

Immunohistochemistry. Analyses were done on archived tumors derived from xenografted Ewing sarcoma cell lines (A673, TC-71, SK-ES1), an alveolar rhabdomyosarcoma cell line (SJ-RH30), and a neuroblastoma cell line (IMR-32) grown in immunocompromised mice. Sections were stained with polyclonal rabbit anti-EGR2 as the primary antibody (1:50, Covance, PRB-236P) and hematoxylin.

Proliferation assays. *xCELLigence.* Cells were counted in real time with an xCELLigence instrument (Roche/ACEA Biosciences) monitoring impedance across gold microelectrodes. 8.5×10^3 cells per well of a 96-well plate were seeded in 200 µl medium containing transfection reagents (hexaplicates per group). Medium and transfection reagents were refreshed after 48 h. For Coulter counting, cells were plated in six-well plates and transfected immediately after seeding with siRNA. After 96 h, cells (including supernatant) were harvested and counted in a Vi-CELL XR Cell Viability Analyzer (Beckman Coulter) (duplicates per group). For Resazurin assay, 3×10^3 to 5×10^3 cells per well of a 96-well plate were seeded in 100 µl medium containing the desired growth factor. After 72–96 h, Resazurin (Sigma-Aldrich) was added (20 µg/ml) and cells were incubated for another 2–6 h, depending on the cell line. Fluorescence signals proportional to the number of cells were recorded in a FLUOstar Omega plate reader (BMG labtech SARL).

Analysis of cell cycle and apoptosis. Cell cycle phases were analyzed using propidium iodide (PI) (Sigma-Aldrich). 96 h after transfection with siRNA, cells (including supernatant) were harvested, fixed in 70% ethanol at 4 °C, and stained with PI solution (40 µg/ml, with 100 µg/ml RNase A). For analysis of apoptosis, cells (including supernatant) were harvested 96 h after transfection and stained with the Annexin-V-FITC/PI Apoptosis Detection Kit II (Becton Dickinson). Samples were assayed on an LSR II flow cytometer (Becton Dickinson). Data were analyzed with FlowJo software (TreeStar).

Clonogenic growth assays. Assays were performed essentially as described[46]. Depending on the cell line, 1.5×10^3 to 3×10^3 cells per well of a 12-well plate were seeded in 1 ml medium containing 5% FCS for A673 cells and 10% FCS for SK-N-MC, EW7 and POE cells. Cells were transfected with siRNA 24 h after seeding and re-transfected every 96 h. After 9–14 d, colonies were methanol-fixed

and stained with crystal violet. Colony number and area were quantified on scanned plates with ImageJ. Relative clonogenicity is reported as the product of the colony number and the average colony size.

Spheroidal growth assays. 2×10^2 cells per well of a 96-well plate were seeded in 120 µl in an equal mix of 10% FCS–containing RPMI 1640 medium and AIM-V medium (Gibco) in plates covered with attachment-preventing poly-2-hydroxyethyl-metacrylate (20 mg/ml PolyHEMA, Sigma-Aldrich). Doxycycline (1 µg/ml) was added for the induction of *EGR2* knockdown. We used the following clones: SK-N-MC shControl#19, shEGR2_4#31, shEGR2_5#2, POE shControl21b, shEGR2_4#22, and shEGR2_5#2. After 9–11 d, spheres were documented by phase-contrast microscopy (four individual images per well; octaplicates per group). Images were analyzed with ImageJ. The relative sphere-formation capacity is reported as the product of the sphere number and the average sphere size.

DNA constructs and mutagenesis. Human elements mSat1, mSat2, MSE and BoneE were PCR cloned using the primers listed in the **Supplementary Data** into the pGL3-luc vector (Promega) upstream of the SV40 minimal promoter. T-to-A mutagenesis of mSat2 at rs79965208 was done with the QuickChange Mutagenesis Kit (Clontech).

Reporter assays and constructs. A673-TR-shEF1 and SK-N-MC–TR–shEF1 (ref. 38) were transfected with pGL3-luc vectors and *Renilla* pGL3-Rluc (ratio, 100:1). After 4 h, transfection media were replaced by media with or without doxycycline (1 µg/ml). Cells were lysed after 48 h and assayed with a dual luciferase assay system (Promega). *Firefly* luciferase activity was normalized to *Renilla* luciferase activity.

Chromatin immunoprecipitation. ChIP was done with rabbit polyclonal anti-FLI1 (C19-X, Santa Cruz Biotechnology) or a rabbit IgG control in MHH-ES1 cells using the iDeal ChIP-Seq Kit for Transcription Factors (Diagenode). DNA was sheared to an average size of 500 bp to enable mSat2 PCR amplification followed by deep sequencing in an Illumina MiSeq instrument (>42,000×). ChIP efficacy was validated by qRT-PCR using a *CCND1* EWSR1-FLI1 binding site[47] (positive control) and an intronic *CCND1* locus (negative control; **Supplementary Fig. 10**). Primers are listed in the **Supplementary Data**.

Xenotransplantation experiments and mice. 8×10^6 POE or 15×10^6 SK-N-MC cells containing either a doxycycline-inducible negative control shRNA (POE shControl#21b or SK-N-MC shControl#19) or a specific shRNA against *EGR2* (POE shEGR2_4#22 or SK-N-MC shEGR2_4#31) were injected subcutaneously in the flanks of 6-week-old female C.B-17/SCID mice (Charles River Laboratories) in an equal mix of PBS and Matrigel (BD Biosciences). When tumors reached a volume of 75–100 mm^3, mice were randomly assigned to either the control (5% sucrose in drinking water) or the treatment (doxycycline (2 mg/l) and 5% sucrose in drinking water) group. Tumor growth was monitored with a caliper every 2–3 d. Mice were killed once tumors reached a volume of 1,500 mm^3, calculated as $V = a \times b^2/2$, with a being the largest diameter and b the smallest. Doxycycline-induced *EGR2* knockdown was confirmed by qRT-PCR 72 h after the start of doxycycline treatment in aliquots of the injected cells that were grown in parallel *in vitro*. Experiments were conducted in accordance with the recommendations of the European Community (86/609/EEC), the French Competent Authority, and UKCCCR (guidelines for the welfare and use of animals in cancer research). The sample size was not predetermined.

Human samples. Ewing sarcoma patients from France have been referred to the Institut Curie Hospital for molecular diagnosis since 1990. All subjects included in this study had a specific *EWSR1-ETS* fusion. Constitutional DNA of adequate quality was available for 343 subjects. This study received approval by institutional review boards and ethics committees (Comité de Protection des Personnes Ile-de-France I). Consent was obtained through communication with patients or families either by the referring oncologists or by the Institut Curie Unité de Génétique Somatique. Genomic DNA was isolated from bone marrow or blood via proteinase K lysis and a phenol chloroform extraction method. We included control samples from 251 French subjects originally obtained as part of the Cancer Genetic Markers of Susceptibility (CGEMS) prostate cancer project[48]. All control subjects were male and recruited in the geographical areas close to Paris, Nancy and Brest through participation in a systematic health-screening program funded by the French National Health Insurance. All controls were determined to be unaffected by cancer through medical examination and blood tests for prostate-specific antigen. The sample size was not predetermined.

Analysis of population substructure. Principal-component analysis (PCA) was performed as described[4] to select genetically matching cases and controls for sequencing and association testing. To ensure genetic homogeneity in populations of affected subjects and controls, we used an EM-fitted Gaussian mixture clustering method assuming one cluster and noise to exclude isolated subjects (**Supplementary Fig. 6**). Noise was initialized by the NNclean function in the prabclus R package, which determines whether data points are noise or part of a cluster on the basis of a Poisson process model. This was followed by definition of the partition between the core of the data (one cluster) and the noise using the mclustBIC function of the mclust R package. Clustering was carried out in two dimensions for cases versus controls on the basis of the relative contribution of the first two PCA vectors.

DNA capturing and next-generation sequencing. *Illumina HiSeq2500 (non-repetitive regions).* DNA capturing of all three susceptibility loci[4] was done with a customized Nextera target-enrichment system (Illumina). For all loci, the given risk haploblock and the adjacent 5′ and 3′ haploblocks were captured, for a total target size of 993 kb (library size, 500 bp; 2,614 Nextera probes with a predicted average coverage of the target regions of 95%: chr1:11,023,000–11,088,000 (171 probes); chr10:64,252,000–64,967,000 (1,882 probes); chr15:40,203,000–40,416,000 (561 probes)). Repetitive regions such as GGAA microsatellites were omitted in the Nextera design. Constitutional DNA was captured from 343 Ewing sarcoma cases and 251 controls. In addition, DNA from 14 Ewing sarcoma cell lines was captured. Massive parallel-end deep sequencing was done in an Illumina HiSeq2500 instrument (rapid mode; 150/150 nt) yielding a median capturing rate of 91.35% with at least 10× across samples and target regions and a median read depth per sample of 217× (**Supplementary Fig. 6**).

Illumina MiSeq (GGAA microsatellites). The mSat2 region was amplified by PCR with the primers listed in the **Supplementary Data** and Phusion High-Fidelity DNA polymerase (Thermo Scientific). After barcoding (Fluidigm), massive parallel-end deep sequencing was done in an Illumina MiSeq instrument (300/300 nt). Paired-end reads were merged using SeqPrep tools with the default parameters (median coverage, 124×).

Variant calling, genotyping, and statistical assessment. HiSeq reads were mapped on hg19 (NCBI GhR36 build) using BWA 0.6.2 with up to 4% mismatches allowed. BAM files were preprocessed according to the recommendations of the Genome Analysis Toolkit (GATK) using Samtools 1.8 (ref. 49), Picard tools 1.97 and GATK2.2.16 (ref. 50). Variant calling was done with GATK, focusing on single-nucleotide variants (SNVs) supported by ≥2 identical alternative reads at positions with ≥10× in 90% of the samples. Genotype calling was done with the GATK DepthOfCoverage function. SNVs were defined as homozygous if the alternative allele ratio (AAR) was <0.2 or >0.8, whereas heterozygous SNVs were defined by an AAR within ± 2 s.d. of the mean AAR of the non-homozygous SNVs. SNVs that had a minor allele frequency of >0.05 and that did not depart from Hardy-Weinberg equilibrium in the entire cohort were considered for further analyses. Regional association results were plotted using LocusZoom[51]. The workflow is summarized in **Supplementary Figure 7**.

Association testing and analysis of LD. Statistical differences in genotype distributions were assessed with a logistic regression. Associations were adjusted for significant PCA eigenvectors (EV1, EV5 and EV6). *P* values were adjusted by false discovery rate. Significantly different SNVs were annotated with information available from the dbSNPv137 and RefGene databases using ANNOVAR v2013. LD and haplotype analyses were done with PLINK and HaploView[52,53] as described by Gabriel *et al.*[54]. Association testing conditional to rs79965208

doi:10.1038/ng.3363

was done with PLINK[53] with a logistic regression including significant PCA eigenvectors (EV1, EV5 and EV6) and the 'condition' command option.

Analysis of mSat2 MiSeq reads. To avoid mapping errors, we aligned raw reads on specific 'anchor' sequences (**Supplementary Data**) flanking mSat2. We determined the sequence between these anchors using a custom script designed to report the two alleles of each sample, taking into account a PCR-based slippage bias generating $n-1$ GGAA repeats co-occurring with n GGAA repeats and a lower PCR-amplification rate affecting long GGAA stretches (≥19 GGAA repeats). Only alleles supported by ≥10× were reported. Comparison of results with matched mSat2 Sanger sequences in 57 subjects showed an accuracy rate of our custom script and MiSeq analysis of 97.4%.

Replication of association results. A first replication of the initial rs79965208 association result was conducted in an independent sample of individuals of European descent, which was part of our preceding GWAS[4]. The pool of affected subjects included 156 individuals of European descent. Controls were 184 unaffected women from the French E3N cohort[55]. In this cohort, the mSat2 region containing rs79965208 was directly sequenced in an Illumina MiSeq instrument. A second replication of the association of rs79965208 with Ewing sarcoma was conducted in an independent sample of individuals of European descent from the United States. This group of affected subjects included 162 individuals identified from the Childhood Cancer Survivor Study (CCSS), a multi-institutional follow-up study of 5-year survivors of childhood cancer diagnosed between 1970 and 1986 (ref. 32). Subjects were genotyped on the Illumina HumanOmni5Exome array as part of a larger project within the CCSS, with 4,052,581 unique polymorphic loci and 5,324 unique samples from unrelated individuals of European descent passing quality control thresholds (missing rate < 0.1, locus genotype concordance > 0.99 in 539 blinded duplicate samples, sample missing rate < 0.08, sample heterozygosity of 0.11–0.16, and genotyped sex concordant with self-report). Controls were 435 individuals of European descent from the Division of Cancer Epidemiology and Genetics reference panel of cancer-free adults[56]. A region of ±1 Mb of rs79965208 was imputed using the 1000 Genomes Project Phase 3 reference panel in IMPUTE2 (ref. 57). The rs79965208 SNP was well imputed (info score = 0.952). Associations were assessed using logistic regression models and adjusted for significant PCA eigenvectors (EV1, EV2 and EV9). The sample size was not predetermined.

Analysis of allele-specific expression. Allele-specific *EGR2* expression was assessed via targeted RNA sequencing (Illumina HiSeq2500) in 45 individuals with Ewing sarcoma who were heterozygous in constitutional DNA for rs61865883 (located in the *EGR2* 3′ UTR), serving as transcribed allelic marker. Recurrent loss of heterozygosity at the *EGR2* locus was ruled out previously[4,11] and was further excluded by targeted DNA sequencing of 10 out of the 45 subjects for which matched tumor and constitutional DNA were available. For each of these 45 subjects, we statistically compared the raw rs61865883 allele fractions of 16 tumors heterozygous for rs79965208 (A/T) with those of 29 tumors that were homozygous for rs79965208 (A/A or T/T) using a parametric two-tailed Student's *t*-test.

Analysis of ChIP-Seq, DNase-Seq and FAIRE-Seq data. Publicly available data were retrieved from the GEO. *.bed files from Patel *et al.*[8] (GSE31838) were generated in FAIRE-Seq experiments in EW502 Ewing cells (GSM790218) and converted to hg19. ENCODE[26] SK-N-MC DNase-Seq (GSM736570) and RNA Pol II ChIP-Seq data (GSM1010793), together with the FAIRE-Seq data, were analyzed in the Nebula environment[58] using Model-based Analysis of ChIP-Seq v1.4.2 (MACS)[59] and converted to *.wig format for display in the UCSC Genome Browser[60]. Preprocessed ChIP-Seq data from Riggi *et al.*[27] (GSE61944) were converted from *.bigwig to *.wig format using the UCSC bigWigToWig conversion tool. Samples used were GSM1517544 SK-N-MC_shGFP_48h_FLI1, GSM1517553 SK-N-MC_shFLI1_48h_FLI1, GSM1517569 A673_shGFP_48h_FLI1, GSM1517572 A673_shFLI1_48h_FLI1, GSM1517548 SK-N-MC_shGFP_96h_H3K4me1, GSM1517557 SK-N-MC_shFLI1_96h_H3K4me1, GSM1517545 SK-N-MC_shGFP_48h_H3K27ac, and GSM1517554 SK-N-MC_shFLI1_48h_H3K27ac.

38. Carrillo, J. *et al.* Cholecystokinin down-regulation by RNA interference impairs Ewing tumor growth. *Clin. Cancer Res.* **13**, 2429–2440 (2007).
39. Conrad, C., Gottgens, B., Kinston, S., Ellwart, J. & Huss, R. GATA transcription in a small rhodamine 123(low)CD34(+) subpopulation of a peripheral blood-derived CD34(–)CD105(+) mesenchymal cell line. *Exp. Hematol.* **30**, 887–895 (2002).
40. Thalmeier, K. *et al.* Establishment of two permanent human bone marrow stromal cell lines with long-term post irradiation feeder capacity. *Blood* **83**, 1799–1807 (1994).
41. Wiederschain, D. *et al.* Single-vector inducible lentiviral RNAi system for oncology target validation. *Cell Cycle* **8**, 498–504 (2009).
42. Dai, M. *et al.* Evolving gene/transcript definitions significantly alter the interpretation of GeneChip data. *Nucleic Acids Res.* **33**, e175 (2005).
43. Culhane, A.C., Thioulouse, J., Perrière, G. & Higgins, D.G. MADE4: an R package for multivariate analysis of gene expression data. *Bioinformatics* **21**, 2789–2790 (2005).
44. Melot, T. *et al.* Production and characterization of mouse monoclonal antibodies to wild-type and oncogenic FLI-1 proteins. *Hybridoma* **16**, 457–464 (1997).
45. Sievers, F. *et al.* Fast, scalable generation of high-quality protein multiple sequence alignments using Clustal Omega. *Mol. Syst. Biol.* **7**, 539 (2011).
46. Franken, N.A.P., Rodermond, H.M., Stap, J., Haveman, J. & van Bree, C. Clonogenic assay of cells *in vitro*. *Nat. Protoc.* **1**, 2315–2319 (2006).
47. Boeva, V. *et al.* *De novo* motif identification improves the accuracy of predicting transcription factor binding sites in ChIP-Seq data analysis. *Nucleic Acids Res.* **38**, e126 (2010).
48. Yeager, M. *et al.* Genome-wide association study of prostate cancer identifies a second risk locus at 8q24. *Nat. Genet.* **39**, 645–649 (2007).
49. Li, H. *et al.* The Sequence Alignment/Map format and SAMtools. *Bioinformatics* **25**, 2078–2079 (2009).
50. McKenna, A. *et al.* The Genome Analysis Toolkit: a MapReduce framework for analyzing next-generation DNA sequencing data. *Genome Res.* **20**, 1297–1303 (2010).
51. Pruim, R.J. *et al.* LocusZoom: regional visualization of genome-wide association scan results. *Bioinformatics* **26**, 2336–2337 (2010).
52. Barrett, J.C., Fry, B., Maller, J. & Daly, M.J. Haploview: analysis and visualization of LD and haplotype maps. *Bioinformatics* **21**, 263–265 (2005).
53. Purcell, S. *et al.* PLINK: a tool set for whole-genome association and population-based linkage analyses. *Am. J. Hum. Genet.* **81**, 559–575 (2007).
54. Gabriel, S.B. *et al.* The structure of haplotype blocks in the human genome. *Science* **296**, 2225–2229 (2002).
55. Clavel-Chapelon, F. *et al.* E3N, a French cohort study on cancer risk factors. E3N Group. Etude Epidémiologique auprès de femmes de l'Education Nationale. *Eur. J. Cancer Prev.* **6**, 473–478 (1997).
56. Wang, Z. *et al.* Improved imputation of common and uncommon SNPs with a new reference set. *Nat. Genet.* **44**, 6–7 (2012).
57. Howie, B.N., Donnelly, P. & Marchini, J. A flexible and accurate genotype imputation method for the next generation of genome-wide association studies. *PLoS Genet.* **5**, e1000529 (2009).
58. Boeva, V., Lermine, A., Barette, C., Guillouf, C. & Barillot, E. Nebula—a web-server for advanced ChIP-seq data analysis. *Bioinformatics* **28**, 2517–2519 (2012).
59. Zhang, Y. *et al.* Model-based analysis of ChIP-Seq (MACS). *Genome Biol.* **9**, R137 (2008).
60. Meyer, L.R. *et al.* The UCSC Genome Browser database: extensions and updates 2013. *Nucleic Acids Res.* **41**, D64–D69 (2013).

The second European interdisciplinary Ewing sarcoma research summit – A joint effort to deconstructing the multiple layers of a complex disease

Heinrich Kovar[1,2,*], James Amatruda[3,*], Erika Brunet[4,*], Stefan Burdach[5,*], Florencia Cidre-Aranaz[6,*], Enrique de Alava[7,*], Uta Dirksen[8,*], Wietske van der Ent[9,10,*], Patrick Grohar[11,*], Thomas G. P. Grünewald[12,*], Lee Helman[13,*], Peter Houghton[14,*], Kristiina Iljin[15,*], Eberhard Korsching[16,*], Marc Ladanyi[17,*], Elizabeth Lawlor[18,*], Stephen Lessnick[19,*], Joseph Ludwig[20,*], Paul Meltzer[21,*], Markus Metzler[22,*], Jaume Mora[23,*], Richard Moriggl[24,25,*], Takuro Nakamura[26,*], Theodore Papamarkou[27,*], Branka Radic Sarikas[28,*], Francoise Rédini[29,*], Guenther H. S. Richter[5,*], Claudia Rossig[8,*], Keri Schadler[30,*], Beat W. Schäfer[31,*], Katia Scotlandi[32,*], Nathan C. Sheffield[28,*], Anang Shelat[33,*], Ewa Snaar-Jagalska[10,*], Poul Sorensen[34,*], Kimberly Stegmaier[35,*], Elizabeth Stewart[36,*], Alejandro Sweet-Cordero[37,*], Karoly Szuhai[38,*], Oscar M. Tirado[39,*], Franck Tirode[9,*], Jeffrey Toretsky[40,*], Kalliopi Tsafou[40,*], Aykut Üren[40,*], Andrei Zinovyev[9,41,42,*] and Olivier Delattre[9,*]

[1] Children's Cancer Research Institute, St. Anna Kinderkrebsforschung, Vienna, Austria

[2] Department of Pediatrics, Medical University Vienna, Vienna, Austria

[3] Departments of Pediatrics, Molecular Biology and Internal Medicine, University of Texas Southwestern Medical Center, Dallas, TX, USA

[4] Museum National d'Histoire Naturelle, INSERM U1154, CNRS 7196, Paris, France

[5] Children's Cancer Research Center and Department of Pediatrics, Klinikum rechts der Isar, Technical University and Comprehensive Cancer Center Munich (CCCM), Munich, Germany

[6] Unidad de Tumores Sólidos Infantiles, Área de Genética Humana, Instituto de Investigación de Enfermedades Raras, Instituto de Salud Carlos III, Madrid, Spain

[7] Institute of Biomedicine of Sevilla (IBiS), Virgen del Rocio University Hospital /CSIC/University de Sevilla, Department of Pathology, Seville, Spain

[8] University Children´s Hospital Muenster, Pediatric Hematology and Oncology, Muenster, Germany

[9] INSERM U830, Laboratoire de Génétique et Biologie des Cancers, Institut Curie, Paris, France

[10] Institute of Biology, Leiden University, Leiden, The Netherlands

[11] Van Andel Institute, Center for Cancer and Cell Biology and Helen DeVos Children's Hospital, Grand Rapids, MI, USA

[12] Laboratory for Pediatric Sarcoma Biology, Institute of Pathology of the LMU Munich, Munich, Germany

[13] Center for Cancer Rearch, NCI, NIH, Bethesda, MA, USA

[14] Greehey Children's Cancer Research Institute, University of Texas Health Science Center, San Antonio, TX, USA

[15] VTT Technical Research Centre of Finland Ltd, Espoo, Finland

[16] Institute of Bioinformatics, Faculty of Medicine, University of Muenster, Muenster, Germany

[17] Department of Pathology and Human Oncology and Pathogenesis Program, Memorial Sloan-Kettering Cancer Center, New York, NY, USA

[18] Department of Pediatrics and Department of Pathology, University of Michigan, Ann Arbor, MI, USA

[19] Center for Childhood Cancer and Blood Disorders, Nationwide Children's Hospital, and the Division of Pediatric Hematology/Oncology/BMT, The Ohio State University, Columbus, OH, USA

[20] Department of Sarcoma Medical Oncology, MD Anderson Cancer Center, Houston, TX, USA

[21] Genetics Branch, Center for Cancer Research, National Cancer Institute, Bethesda, MD, USA

[22] Pediatric Oncology and Hematology, University Hospital Erlangen, Erlangen, Germany

[23] Department of Pediatric Oncology, Sant Joan de Déu Hospital, Barcelona, Spain

[24] Ludwig Boltzmann Institute for Cancer Research, Vienna, Austria

[25] Institute of Animal Breeding and Genetics, University of Veterinary Medicine and Medical University, Vienna, Austria
[26] Division of Carcinogenesis, The Cancer Institute, Japanese Foundation for Cancer Research, Tokyo, Japan
[27] University of Glasgow, School of Mathematics and Statistics, Glasgow, UK
[28] CeMM Research Center for Molecular Medicine of the Austrian Academy of Sciences, Vienna, Austria
[29] INSERM UMR957, Université de Nantes, Nantes, France
[30] Department of Pediatrics Research, MD Anderson Cancer Center, Houston, TX, USA
[31] Department of Oncology and Children's Research Center, University Children's Hospital, Zurich, Switzerland
[32] CRS Development of Biomolecular Therapies, Experimental Oncology Lab, Rizzoli Institute, Bologna, Italy
[33] Department of Chemical Biology and Therapeutics, St. Jude Children's Research Hospital, Memphis,TN, USA
[34] Department of Molecular Oncology, British Columbia Cancer Research Centre, Vancouver, British Columbia, Canada
[35] Department of Pediatric Oncology, Dana-Farber Cancer Institute and Boston Children's Hospital, Boston, MA, USA
[36] Department of Developmental Neurobiology, St. Jude Children's Research Hospital, Memphis, TN, USA
[37] Division of Hematology and Oncology, Department of Pediatrics, Stanford University, Stanford, CA, USA
[38] Department of Molecular Cell Biology, Leiden University Medical Center, Leiden, The Netherlands
[39] Sarcoma Research Group, Molecular Oncology Laboratory, Bellvitge Biomedical Research Institute (IDIBELL), L'Hospitalet de Llobregat, Barcelona, Spain
[40] Department of Oncology, Georgetown University School of Medicine, Washington, DC, USA
[41] INSERM, U900, Paris, France
[42] Ecole des Mines ParisTech, Fontainbleau, France
[*] These authors have contributed equally to this work

Correspondence to: *Heinrich Kovar,* ***email***: *heinrich.kovar@ccri.at*

Keywords: Ewing sarcoma, epigenetics, development, therapy, microenvironment

Received: *October 20, 2015* ***Accepted***: *January 14, 2016* ***Published***: *January 18, 2016*

ABSTRACT

Despite multimodal treatment, long term outcome for patients with Ewing sarcoma is still poor. The second "European interdisciplinary Ewing sarcoma research summit" assembled a large group of scientific experts in the field to discuss their latest unpublished findings on the way to the identification of novel therapeutic targets and strategies. Ewing sarcoma is characterized by a quiet genome with presence of an *EWSR1-ETS* gene rearrangement as the only and defining genetic aberration. RNA-sequencing of recently described Ewing-like sarcomas with variant translocations identified them as biologically distinct diseases. Various presentations adressed mechanisms of EWS-ETS fusion protein activities with a focus on EWS-FLI1. Data were presented shedding light on the molecular underpinnings of genetic permissiveness to this disease uncovering interaction of EWS-FLI1 with recently discovered susceptibility loci. Epigenetic context as a consequence of the interaction between the oncoprotein, cell type, developmental stage, and tissue microenvironment emerged as dominant theme in the discussion of the molecular pathogenesis and inter- and intra-tumor heterogeneity of Ewing sarcoma, and the difficulty to generate animal models faithfully recapitulating the human disease. The problem of preclinical development of biologically targeted therapeutics was discussed and promising perspectives were offered from the study of novel *in vitro* models. Finally, it was concluded that in order to facilitate rapid pre-clinical and clinical development of novel therapies in Ewing sarcoma, the community needs a platform to maintain knowledge of unpublished results, systems and models used in drug testing and to continue the open dialogue initiated at the first two Ewing sarcoma summits.

INTRODUCTION

Ewing sarcoma is a rare, aggressive cancer of bone and soft tissues that presents most frequently in children and young adults. Progress in Ewing sarcoma therapy has reached a plateau with long-term overall survival rates less than 30% for patients with disseminated disease and 65-75% for patients who present without clinically overt metastases at diagnosis [1]. Using conventional multimodal treatment regimens, only minor improvements in outcome have been achieved during the last 30 years [2]. Therefore, more efficient and specifically targeted approaches are urgently required to combat this deadly disease. Such novel therapeutic strategies are expected to arise from a deeper biological understanding of the pathogenic mechanisms underlying the development, immune escape and metastatic spread of Ewing sarcoma. International Ewing sarcoma research, however, is fragmented and progress is slow due to the rarity of the disease (approximately 3 cases/million/year [3]). Two European framework program 7 (FP7) funded collaborative initiatives therefore put on their agenda activities to overcome this apparent bottleneck, although by different approaches. The research project ASSET ("Assessing and Striking the Sensitivities of Embryonal Tumors") follows a multi-disciplinary systems biology approach to identify vulnerabilities of the disease. The "European Network for Cancer research in Children and Adolescents" (ENCCA) facilitates and structures networking activities for prioritization of, access to and clinical research on innovative, biologically targeted drugs for the treatment of childhood cancer. However, regular exchange of knowledge and networking is required beyond European borders and beyond the tightly defined agenda of such projects to avoid redundancy and generate synergy in Ewing sarcoma research. In June 2015, four years after the first ENCCA funded Ewing sarcoma meeting [4] and jointly supported by ENCCA and ASSET, the "Second European Interdisciplinary Ewing Sarcoma Research Summit" assembled 77 researchers from Europe, Japan, the US and Canada to share exclusively unpublished results and to discuss future research directions and opportunities for clinical translation (Suppl. Table 1 for list of participants). It was the largest purely scientific Ewing sarcoma convention so far. Maybe it was the spirit of the venue at Institute Curie in Paris, where the *EWSR1-FLI1* fusion gene was discovered as the defining marker and driver of the disease almost 25 years ago, combined with the unique meeting format, that made it highly successful in bringing together colleagues and competitors in the field, fostering trustful exchange, open discussion, and the initiation of new promising collaborations. This review summarizes some exciting new insights into Ewing sarcoma biology presented at this meeting (Figure 1). Since speakers frequently used metaphors in their presentations, the chapters of this review are named accordingly (Figure 2).

THE MONSTER

In our nightmares and in horror movies, it is the unknown, the mysterious that threatens us in the shape of a dangerous monster. Ewing sarcoma remains such a monster, a "genetically engineered monster" with the *EWSR1-ETS* gene fusion as the major driver of its nefarious activities, as Paul Meltzer pointed out while introducing the topic of "Spatial and temporal genetic and non-genetic diversity of Ewing sarcoma" (Table 1). From recent sequencing studies it has become clear that with the exception of the well-known *EWSR1-ETS* gene fusions, which drive a complex tumor specific transcriptional program, the Ewing sarcoma genome is relatively quiet [5-9]. Franck Tirode provided an overview on the molecular heterogeneity of Ewing and Ewing-like tumors in a cohort of 130 sarcomas. By RNA sequencing he demonstrated that tumors with *FET-ETS* gene fusions involving *EWSR1* or *FUS* with members of the *ERG* (*FLI1, ERG*) or *PEA3* (*ETV1,* ETV4) subfamily of *ETS* transcription factor genes cluster tightly together in a homogenous group, separate from Ewing-like sarcomas with *EWSR1* fusions to non-*ETS* genes (i.e. *NFATC*, *POU5F1*, *SMARCA5*) and from those harboring the recently described *BCOR-CCNB3* or *CIC-DUX4* gene fusions.

Some of the mystery behind Ewing sarcoma pathogenesis and the inter-patient heterogeneity in its response to treatment may arise from non-genetic sources, such as the epigenome. Paul Meltzer stressed that the epigenetic states of cancer are generally abnormal, not fitting any healthy tissue, and thus, cancers deviate from physiologic epigenetic programs. In Ewing sarcoma, widespread epigenetic rewiring of gene regulatory regions was recently demonstrated to be induced by EWS-FLI11 [10, 11]. Knowledge about the exact mechanisms of epigenetic dysregulation may provide novel therapeutic opportunities. Stephen Lessnick reported on the preclinical testing of HCI2577, a second generation lysyl specific demethylase (LSD1) inhibitor, which they found to reverse the EWS-FLI1 transcriptional signature to a large extent and to cause apoptosis. However, based on previous results of the group on the anti-tumor effects of the first generation inhibitor HCI2509 [12], LSD1 inhibition affected both EWS-FLI1 activated and repressed genes that are bound by the fusion oncogene, the exact mechanism of functional interaction between EWS-FLI1 and LSD1 remains obscure.

Non-genetic variability may also be the basis for distinct treatment sensitivity. Paul Meltzer reported on differences in tumor transcriptomes of patients transiently responding or not to the R1507 IGF1R antibody in the SARC-011 trial. The molecular basis for resistance development may lie in genetic or non-genetic intra-tumor heterogeneity. Olivier Delattre introduced single

Table 1: Genetic and non-genetic sources of inter- and intra-tumor heterogeneity in Ewing sarcoma

Genetic	Germline genetic risk (susceptibility loci on chromosomes 1, 10, 15; metastasis loci?)
	Different EWSR1-transcription factor fusions
	Copy number variations (i.e. gains on chromosomes 8, 12, 1q; loss at 16p)
	Clonal complexity of tumor
	Therapy driven mutation/selection
Non-genetic	Plasticity of tumor/tumor stem cells
	Heterogenous epigenetic states (chromatin factors and DNA methylation)
	RNA metabolism (splicing, editing, degradation)
	Activity of non-coding RNAs (microRNAs, long noncoding RNAs, others)
	Metabolism (tissue site, microenvironment, stress and therapy driven)
	Proliferative states (dormancy)
	Micro-environment modification of tumor cells (i.e. immune system)
	Age and gender

cell transcriptome analysis to study variation and transitions in transcriptional programs in a population of Ewing sarcoma cells with fluctuations in EWS-FLI1 expression. Nathan Sheffield demonstrated the power of reduced representation bisulfite sequencing (RRBS) to study cell-to-cell heterogeneity in DNA methylation of a tumor. Neighboring CpG sites in a given genomic region often show concordant methylation status, but

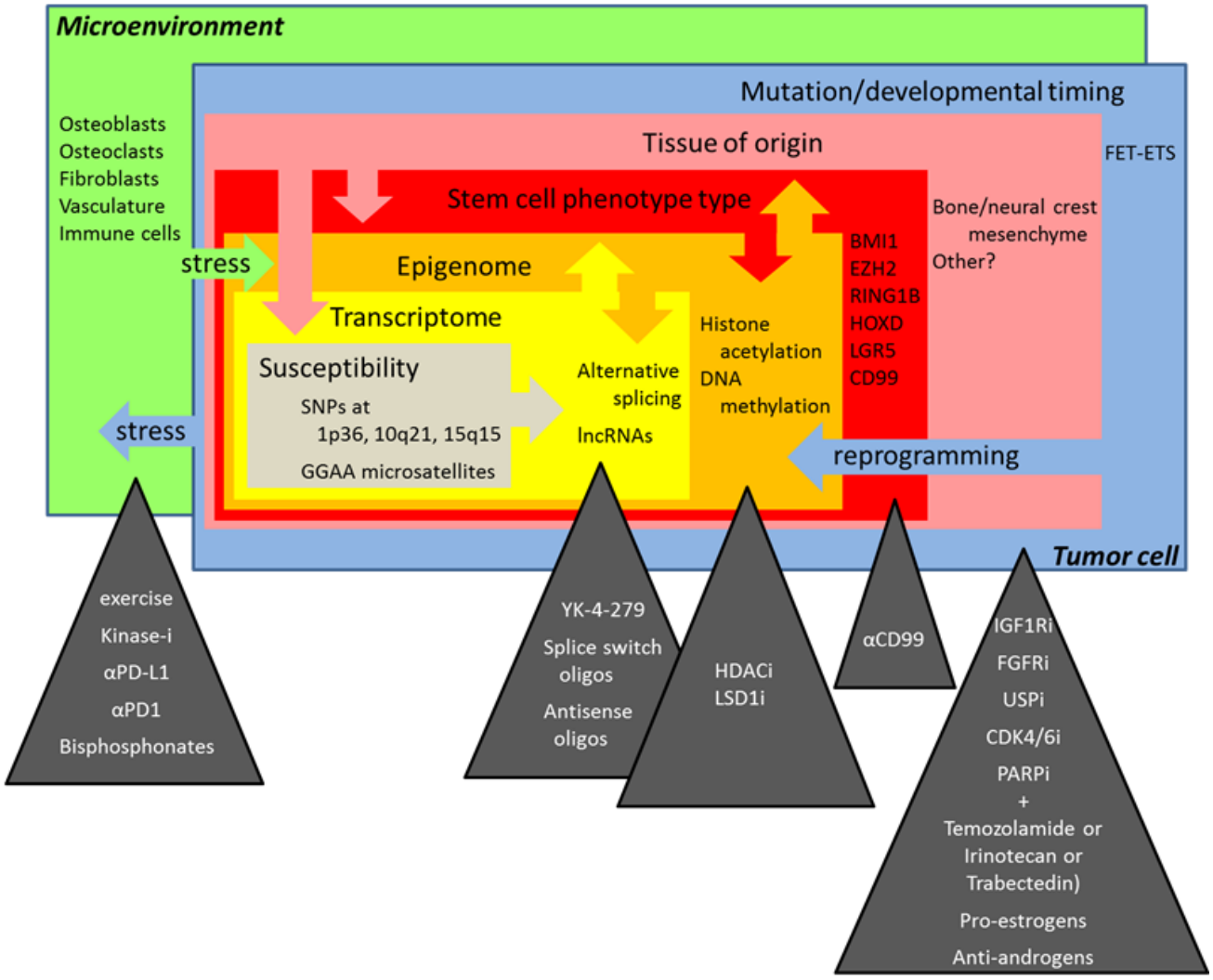

Figure 1: The multiple layers of complexity in Ewing sarcoma biology and novel treatment perspectives discussed at the "Second Interdisciplinary Ewing Sarcoma Research Summit".

the methylation of neighboring CpGs is occasionally not matching, leading to potentially disordered methylation patterns. Because each read may span several methylation sites and is derived from the sequencing of one DNA molecule, the comparison between methylation status at neighboring CpGs within a read can be used to assess intra-tumor heterogeneity. Nathan Sheffield demonstrated this phenomenon in a cohort of 140 Ewing sarcomas and normal mesenchymal stem cell samples, which are currently being explored for prognostic methylation patterns in a collaborative project between Austria, France and Germany.

Comparative methylation profiling between Ewing sarcoma and normal tissues also has the potential to uncover unknown tumor specific molecular traits. Using the Infinium 450K methylation array to study promoter methylation, Oscar Tirado´s group identified Ewing sarcoma specific inactivation of the *PTRF*/*Cavin-1* gene, which, when co-expressed with the EWS-FLI1 activated target gene Caveolin-1 (*CAV1*), induced TP53 dependent cell death. These results support the use of demethylating drugs for the treatment of Ewing sarcoma.

High-throughput sequencing technologies enable characterization of the genetic and epigenetic make-up and the transcriptional signature of tumors, and, by correlation analysis, how the one affects the other. Andrei Zinovyev described a computational method based on a Boolean mathematical model to predict genetic interactions and thus explain deviations of the phenotypic quantitative effect of multiple gene mutations from their simple additive effect as applied to Ewing sarcoma [13]. Theo Papamarkou discussed a novel mathematical method to also integrate so far poorly investigated RNA editing effects in gene regulatory networks based on RNA-seq data.

Several presentations addressed approaches to follow the tracks of the monster over time. Markus Metzler and Brian Crompton described methods for non-invasive detection of impending relapse based on the high-sensitivity detection of circulating tumor DNA in the plasma of Ewing sarcoma patients. Long-range PCR and capture sequencing methods are being applied to determine patient-specific genomic *EWSR1-FLI1* breakpoints which are subsequently used to detect tumor DNA shed in the circulation by digital PCR. Thus, Uta Dirksen presented first results from the "EFACT" (*EWSR1-FLI1* sequence

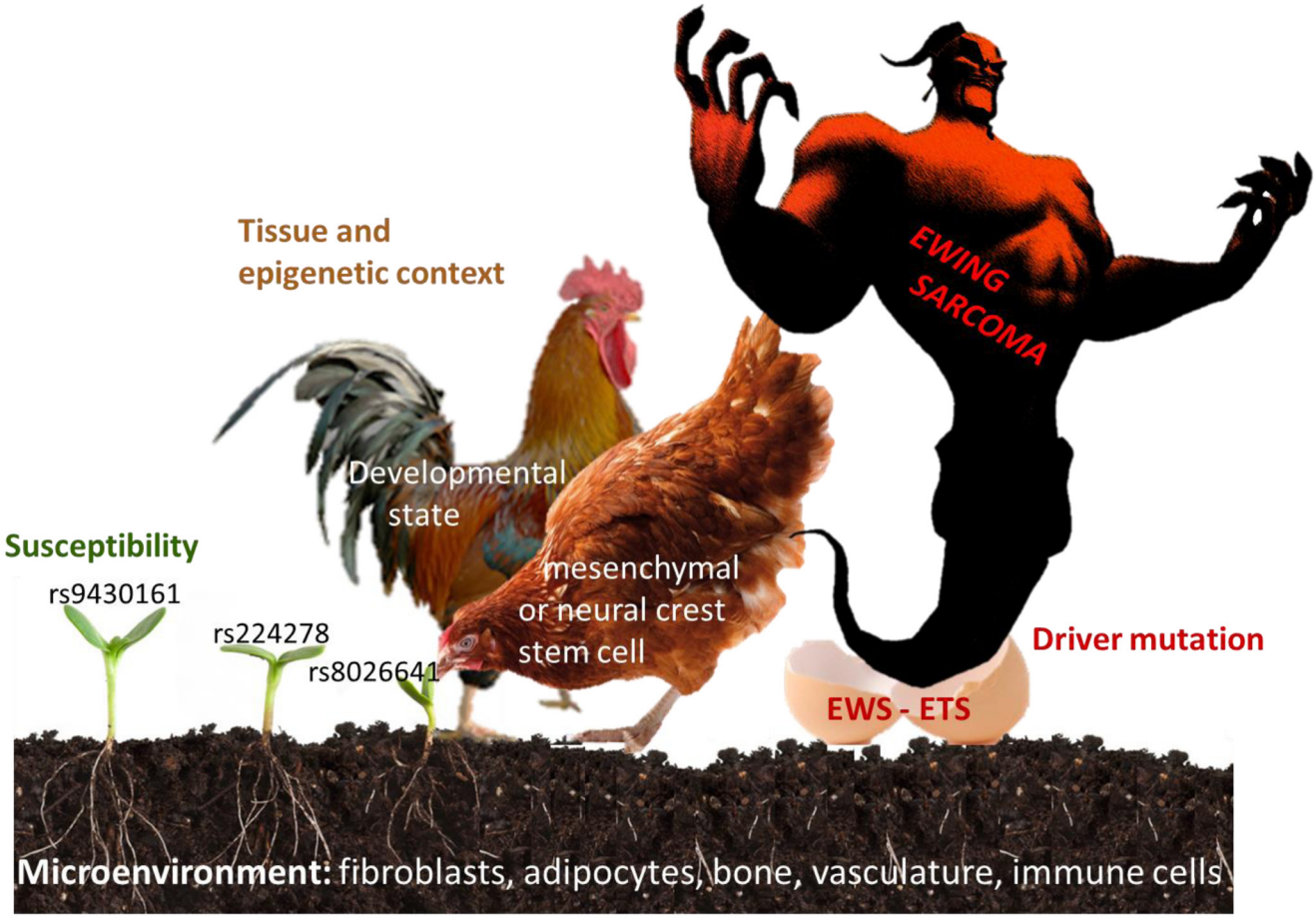

Figure 2: Factors involved in the pathogenesis of Ewing sarcoma. Seed (risk alleles at Ewing sarcoma susceptibility loci), soil (tissue microenvironment), hen (tissue of origin), rooster (developmental , epigenetic state), egg (driver mutation), monster (Ewing sarcoma).

analysis from ctDNA) study ancillary to the European clinical Ewing sarcoma trials Ewing2008 and Ewing 2012, while Marc Ladanyi presented data based on the MSK-IMPACT program at Memorial Sloan Kettering Cancer Center, which provided proof of principle for detection of circulating tumor (ct) DNA in the plasma preceding clinically overt relapse of Ewing sarcoma.

HEN AND EGG

While *Omics* technologies take a scan of Ewing sarcoma, the fully matured monster, and allow us to monitor its variability and plasticity, the egg from which it hatched remains unknown. Much of the difficulty in identifying the tissue of origin for Ewing sarcoma arises from the toxicity of *EWSR1-ETS* fusion genes to most cell types. This is probably the reason why most attempts to generate animal models of EWS-ETS driven oncogenesis have so far failed. The current view is that the disease arises from some mesenchymal or neural crest derived stem or progenitor cell. Erika Brunet reported that though it was possible to induce the *EWSR1-FLI1* gene rearrangement in adult mesenchymal stem cells by zinc finger nucleases or CRISPR/Cas9 mediated gene editing, the gene fusion was unstable and gradually counter-selected in this cell type. Using the latter genome editing approach, Marc Ladanyi also showed efficient induction of the *EWSR1-FLI1* gene rearrangement in HEK293 cells. Aykut Üren summarized a plethora of mostly unpublished (because unsuccessful) attempts from various labs to generate *EWS-ETS* transgenic tumor models in rodents and fish by either conditional tissue specific activation or topical administration of the fusion gene. Most of them led to no phenotype or embryonic lethality, tissue damage (i.e cardiomyopathy [14]) and/or developmental defects, but not tumorigenesis. These studies included expression of the gene fusion in osteoblast precursors, limb bud mesenchyme, neuronal tissue, or muscle, using a variety of promoters to drive the gene fusion (CMV, LTR, EWSR1, Rosa26, Pgk, Nse, dNEFL, TRE) and Cre lines to activate the transgene (Runx2Cre, OsxCre, Prx1Cre, Dermo1Cre, P0Cre, Col1a2Cre, Sox9Cre). Given that even in humans Ewing sarcoma incidence varies with ethnicity (the disease is particularly rare in Africans), it is possible that model organisms are not susceptible to this disease. Aykut Üren discussed several potential reasons for this assumption, including different gene splicing patterns and variations in the lengths of GGAA micro satellites, two features that may differentially affect EWS-FLI1 function and target gene expression in mice and men.

However, Richard Moriggl presented data from a Prx1Cre driven EWS-FLI1 mouse model established in his group, which implicates developmental timing of the gene fusion as an important factor in tumorigenesis. When activated (using a tamoxifen-inducible Cre recombinase) in a narrow time window around birth, EWS-FLI1 expression in the bone mesenchyme resulted in sarcomas that recapitulate the human Ewing sarcoma EWS-FLI1 transcriptional signature. Consistent with this finding, Takuro Nakamura described their recently published transplantation model of tumors arising from EWS-FLI1 transgenic embryonic superficial zone cells from the articular cartilage at an ERG and PTHLH expressing developmental stage [15], and compared it to an unpublished similarly constructed model of CIC-DUX4 induced tumorigenesis from the same cell type. He demonstrated that the *CIC-DUX4* gene fusion activates PEA3 and ERG family ETS transcription factors and, similar to EWS-FLI1, down-regulates apoptosis genes.

In zebrafish, James Amatruda reported on the use of transgenic EWS-FLI1 zebrafish for small-molecule and genetic screens, and a new model of CIC-DUX4-Ewing-like sarcomas. Wietske van der Ent discussed their attempts to generate a flexible transgenic zebrafish model of EWS-ERG induced tumorigenesis using the binary UAS/GAL4 system. Similar to mice, most tested fish tissues did not tolerate the fusion gene with one exception: Expression of GFP-tagged EWS-ERG in neuronal tissues led to developmentally impaired embryos with large amounts of GFP-positive transformed cells, which showed histological features similar to Ewing sarcoma. Transcriptomic and proteomic analysis of regulated gene expression in these embryos showed that there was an overlap with human and murine expression profiles linked to Ewing sarcoma development.

The notion that certain embryonal mesenchymal and neuronal tissues tolerate EWS-ETS gene expression in animal models, at least at defined developmental stages, is consistent with the current view that Ewing sarcoma arises from some potentially neural crest-derived mesenchymal or neuronal progenitor cells. Elizabeth Lawlor reviewed the published evidence for this hypothesis and put it into context with available knowledge on pluripotent adult stem cells. These cells express high levels of polycomb proteins to suppress a large number of differentiation genes. Among them are *EZH2* and *BMI-1* and, as Inmaculada Hernandez and Jaume Mora reported, *RING1B* (*RNF2*), which affects genes of heme biosynthesis, endothelial and neural development, and which they found to protect Ewing sarcoma cells from NFκB induced apoptosis through regulation of the sodium channel NaV1.6. Summarizing available evidence, Elizabeth Lawlor speculated that BMI-1 positive cells may provide the permissive environment for fusion gene activity, as has previously been reported for E2A-PBX1 in hematopoietic stem cells [16], and more recently demonstrated by her own group for EWS-FLI1 in neural crest derived stem cells (NCSC) [17]. The chimeric oncogene would then perpetuate the progenitor-like state by hijacking the developmental transcription program.

On the other hand, there are developmental genes which escape suppression by overexpressed polycomb proteins in Ewing sarcoma. It has previously been

demonstrated that posterior homeobox (HOX) cluster D genes are paradoxically highly expressed in this disease [18]. Günther Richter and Stefan Burdach studied the mechanism and consequences of this up-regulation. They presented preliminary data indicating that *HOXD10,11* and *13* genes are regulated via the EWS-FLI1 target DKK2, presumably involving the canonical WNT/β catenin pathway, to drive chondrogenic but not osteogenic differentiation. Knockdown of *HOXD* genes resulted in down-regulation of *RUNX2*, *PTHLH*, *BGLAP*, *PDGF-BB* and *MMP1* reducing contact independent growth and metastatic potential of Ewing sarcoma cells. Elizabeth Lawlor concluded that, when it comes to the hen and egg question of which is the limiting factor in Ewing sarcomagenesis, cell type/stage of origin or EWS-ETS activity, the two features are tightly intertwined and cannot be separated from each other.

SEED AND SOIL

In contrast to infectious diseases, where the affected patient´s tissues serve as host for the invading pathogens, cancer constitutes a host tissue in itself. It is, however, comprised of multiple cell types that influence each other, as Lee Helman pointed out in his introduction to the topic "Targeting the Ewing sarcoma ecosystem". Tumor-microenvironment interactions occur between multiple host cell types. Tumor infiltrating fibroblasts, adipocytes and immune cells alter their metabolism to adapt to the tumor environment where they create an immunosuppressive milieu. Lee Helman referred to a study that demonstrated the importance of the mitochondrial Krebs cycle in shaping the nuclear methylome of several cancers [19] and speculated that metabolic adaptations in tumor-microenvironment interactions may affect the epigenome of both tumor and infiltrating host cells. In addition, he pointed out that genotoxic treatments elicit DNA damage responses in healthy tissues leading to inflammatory responses that affect tumor cells and metastases. Steve Lessnick discussed the contrasting effects of normoxia and hypoxia on proteolytic cleavage and isoform expression of neuropeptide Y (NPY) with opposite consequences for cell proliferation and apoptosis (Tilan et al. 2013). Consequently, several talks addressed the interaction between the seed - the molecular underpinnings of Ewing sarcoma, and the soil - the tumor microenvironment.

Previously, the group of Franck Tirode demonstrated that sustained knockdown of EWS-FLI1 restores multipotency to Ewing sarcoma cell lines *in vitro* [20]. Expanding on this observation, Olivier Delattre reported that EWS-FLI1 silencing in the *in vivo* context of a mouse xenograft model resulted specifically in adipogenic differentiation of tumor cells. Similarly, Patrick Grohar observed replacement of the tumor tissue in Ewing sarcoma bearing mice by fat tissue of human origin upon treatment with PM01183, a second generation Trabectedin analog. This drug, which similar to UV distorts and breaks DNA strands, seems to inactivate EWS-FLI1 by driving it into the nucleolus. Thus, it appears that the tumor microenvironment has a profound effect on the differentiation route of Ewing sarcoma cells upon inactivation of the fusion gene *in vivo*. However, it is not clear if this effect resulted from the direct differentiation of Ewing sarcoma cells or due to the creation of a pro-adipogenic microenvironment.

Wnt/β-catenin signaling is one of the developmental pathways deregulated in Ewing sarcoma. In mesenchymal tumors it acts as a morphogen rather than driving proliferation. It has been demonstrated previously that activation of the Wnt pathway in Ewing sarcoma is potentiated by R-spondins, the ligands of the somatic stem cell surface receptor LGR5, which stabilizes β-catenin and functions as an oncogene in several human cancers [21]. Elizabeth Lawlor reported that while under standard *in vitro* growth conditions Wnt signaling is off and can only be activated upon EWS-FLI1 silencing and ligand addition, focal β-catenin staining is observed in primary tumors. Because LEF1/TCF is a transcriptional downstream effector of Wnt/ β-catenin signaling and its expression is associated with poor prognosis, Elizabeth Lawlor speculated about intra-tumor heterogeneity of EWS-FLI1 expression and the role of the tumor micro-environment in activating Wnt/ β-catenin and its role in promoting tumor cell motility and metastasis. In this context, the applicability of the tumor stem cell model to Ewing sarcoma was discussed by Eberhard Korsching.

In light of recent evidence that suggests the EWS-FLI fusion protein may act as a pioneer factor capable of eliciting broad sweeping epigenetic effects, novel *ex vivo* models may provide an innovative platform to determine how microenvironmental cues—and their downstream signaling cascades—contribute to and/or reinforce epigenetic changes linked to the aberrant EWS-FLI fusion. One way to study bidirectional feedback mechanisms that exist between Ewing sarcoma and its adjacent microenvironment is with *ex vivo* tissue engineered three-dimensional culture models. Such a model was pioneered by Joseph Ludwig´s laboratory. As recently published, in sharp contrast to Ewing sarcoma cells cultured upon flat tissue culture plastic ware, cells cultured on biologically inert poly(ε-caprolactone) (PCL) microfiber scaffolds placed within a flow perfusion bioreactor were hypersensitive to IGF-1R targeted monoclonal antibodies, which represent a promising class of precision-guided experimental drugs currently in evaluation in early phase clinical trials. Intriguingly, though improved nutrient delivery throughout the porous scaffolds contributed to cell survival within this preclinical model, heightened sensitivity to IGF-1R antibodies seemed to be mediated by physiological levels of shear stress that can be precisely regulated experimentally [22]. Similarly, Francoise

Rédini used novel mineralized scaffolds to investigate the vicious cycle between osteoclasts, bone stromal cells/osteoblasts and tumor cells in Ewing sarcoma progression by transcriptomic analysis. Results are integrated with differential gene expression patterns and therapy responses observed in patients and pre-clinical models of bone versus soft tissue Ewing sarcoma. Such an approach may also be useful to validate the potential influence of the stromal component on the prognostic transcriptional signature of Ewing sarcoma with respect to chemokine receptor expression CXCR7 and CXCR4 isoforms that differ in their affinity to antagonistic ligands CXCL12 and CXCL14, discussed by Karoly Szuhai.

Tumor growth beyond the reach of existing vasculature triggers cellular adaptations to overcome limiting nutrient and oxygen delivery. In addition, oncogenic activation and metabolic re-programming elicit cell intrinsic stresses. Under these conditions, metabolism is re-wired to support cellular energy homeostasis and to supply the building blocks for biomass [23]. One mechanism of energy preservation is selective withdrawal of mRNAs from translation by storage in ribonucleoprotein complexes, called stress granules. Poul Sorensen described that under oxidative stress up to 60% of mRNA gets entrapped in stress granules. He recently reported that the RNA binding protein YB-1 translationally activates expression of a number of stress-responsive proteins including HIF1α [24], and activates translation of the stress granule nucleator, G3BP1 [25]. He reported on proteomic approaches to define the composition of YB-1 containing stress granules, and the promising activity of several histone deacetylase inhibitors in preventing stress granule formation.

A so far unrecognized hint to a potential role of stress granules in the pathogenesis of Ewing sarcoma may arise from the functional analysis of genes in the vicinity of Ewing sarcoma susceptibility loci. A previously published genome-wide association study from the Delattre lab identified candidate risk loci on chromosomes 1, 10, and 15 [26]. The chromosome 1 susceptibility SNP rs9430161 is located in the vicinity of *TARDBP*, encoding an RNA binding protein that is structurally similar to and co-localizes with FUS and EWS to stress granules. Heinrich Kovar now reported on preliminary results generated by Dave Aryee suggesting that the chromosome 15 associated risk locus rs4924410 may affect the activity of a further stress granule associated protein, SRP14, via EWS-FLI1 dependent regulation of a novel long non-coding (lnc)RNA.

While these studies are still in their infancy, Thomas Grünewald summarized his recently completed study on the functional analysis of the chromosome 10 encoded Ewing sarcoma susceptibility locus, which he demonstrated to affect expression of the Ewing sarcoma growth regulatory *EGR2* gene through extension of an EWS-FLI1 bound enhancer-like GGAA microsatellite [27].

All together, these findings underline the context-specific role of EWS-ETS proteins in giving birth to the monster. It is clear that dysregulation of transcriptional programs by EWS-ETS driven wide-spread enhancer reprograming and promoter deregulation is a major factor shaping the biological and clinical characteristics of this monstrous disease. At the meeting, however, some less well characterized EWS-ETS activities and their potential roles in sarcomagenesis and progression were discussed.

Alejandro Sweet-Cordero reported that EWS-FLI1 deregulates the expression of >300 lncRNAs, some directly some indirectly. He presented data on two highly expressed Ewing sarcoma specific, EWS-FLI1 regulated lncRNAs, EWSAT1 [28] and EWSAT2 (lnc659). He demonstrated that lncRNA EWSAT1 is involved in EWS-FLI1 mediated gene repression whereas ongoing studies are directed at identifying the mechanism of EWSAT2. Importantly, knock-down of both lncRNAs interferes with tumor cell growth *in vitro* and *in vivo*.

TAMING THE MONSTER

To identify vulnerabilities of Ewing sarcoma, Kimberly Stegmaier presented the "Pediatric cancer dependencies project", which combines high-throughput shRNA and drug screens, super-enhancer profiling, and CRISPR/Cas9 mediated knockout on a multitude of cell lines *in vitro*. Using this approach, they identified the regulatory subunit of the protein phosphatase PP2A complex, STRN4, and the cyclin dependent kinase CDK4 as essential for Ewing sarcoma cell growth/survival. In fact, they found that the CDK4/6 inhibitor LEE011 (Novartis) has promising *in vitro* and *in vivo* cytostatic and cytotoxic activity on Ewing sarcoma cells [29].

Branka Radic Sarikas performed a synergy screen on selected FDA approved drugs and identified synergistic cytotoxic effects of IGF1R and protein kinase C inhibition in the presence of EWS-FLI1. Kristiina Iljin reported on the results of a drugable siRNA cell viability screen in an inducible EWS-FLI1 shRNA Ewing sarcoma cell line interrogating nearly 7000 genes with 4 siRNAs per gene for EWS-FLI1 dependencies, which was performed as part of the "ASSET" project. In addition, they also performed a small compound screen of >3000 agents comparing EWS-FLI1 on/off states in the same model. Integrating a variety of genomic data sets and mining the literature Kalliopi Tsafou developed an algorithm to link drug effects to genes. By this approach, she identified nodes for which several drugs scored high in the synthetic lethality screen with EWS-FLI1 expression in the Ewing sarcoma cell line A673. Among top hits were histone deacetylases. Consistent with this finding, Anang Shelat and Elizabeth Stewart reported exquisite sensitivity of Ewing sarcoma cells to the class I selective HDAC inhibitor OKI-5.

They also reported that adding a poly(ADP-ribose)

polymerase inhibitor such as Talazoparib or Olaparib to Irinotecan and dose-escalating Temozolomide yielded approximately 90% survival in Ewing sarcoma xenografted mice compared to 100% mortality in mice receiving Irinotecan and full-dose Temozolomide. Refering to a recently published study, they discussed the expression effect of the EWS-FLI1 target *SLFN11* on sensitivity to this drug combination [30]. Synergistic activity for combination treatment of patient derived xenografts with Olaparib and Trabectedin was reported by Enrique de Alava [31]. While PARP1 was previously demonstrated to regulate EWS-FLI1 expression and transcriptional activity [32], and Trabectidin reported to revert the EWS-FLI1 transcriptional signature [33], the de Alava study did not detect any effect of the Olaparib plus Trabectedin combination on EWS-FLI1 target gene expression at Trabectedin concentrations 5-10x lower than previously reported to suppress EWS-FLI1.

In addition to targeting hubs in the EWS-ETS downstream gene regulatory network , perturbation of the expression or functional activity of the gene fusion product itself is considered the holy grail from which innovative Ewing sarcoma specific therapies may arise. A siRNA screen performed in Lee Helman´s lab to identify genes whose depletion recapitulates the transcriptional effects of EWS-FLI1 knockdown, identified several components of the splicing machinery. In fact, knockdown of one of them, HNRNPH1, perturbed the correct splicing of primary EWS-FLI1 transcripts in cells with breakpoints in *EWSR1* intron 8 leading to an out-of-frame fusion product. An alternative approach to disrupt correct EWS-FLI1 RNA processing was presented by Marc Ladanyi, who showed *in vitro* data on treatment with splice-switching oligonucleotides to introduce premature polyadenylation from internal polyA sites of the fusion RNA. In addition, Jeff Toretsky´s group recently demonstrated that, in turn, altered RNA splicing is one of the EWS-ETS fusion protein´s oncogenic functions, which can be inhibited by the small molecule YK-4-279 [34]. Jeff Toretsky discussed the difficulty of pharmacologically targeting the EWS-ETS fusion protein introducing the concept of protein concentration dependent physical phase separation, potentially nucleated by local enrichment at GGAA microsatellites [35]. Although so far all attempts to map the exact binding site of the YK-4-279 compound along the fusion protein failed, and no influence on the EWS-FLI1 transcriptional signature was observed, results presented by Lee Helman and Jeff Toretsky encourage clinical evaluation of splicing inhibitors in Ewing sarcoma patients.

Alternatively, targeting EWS-ETS protein stability may provide a so far unexplored therapeutic option. EWS-FLI1 stability is regulated by K48 polyubiquitinylation and proteasomal degradation. Using a targeted shRNA screen interrogating 21 Ewing sarcoma expressed deubiquitinating enzymes, Beat Schäfer´s group identified ubiquitin-specific protease USP19 as an EWS-FLI1 regulatory enzyme, whose knockdown destabilizes EWS-FLI1 protein and may therefore serve as an attractive therapeutic target.

Pre-clinical drug validation requires studies in model organisms. In the absence of validated rodent models for most pediatric cancers, the "Pediatric Preclinical Testing Program" (PPTP) studied 67 drugs on 83 different xenograft mouse models, in all together 2134 drug/model comparisons. Peter Houghton reported that retrospective analysis of the results for any of 1000 randomly selected mice accurately predicted the response of the whole group in each comparison in 75% of cases. The predictive power of the response of a single mouse increased to 95%, if one deviation per group was allowed. Based on these results, he provocatively suggested to use a single mouse xenograft instead of 10 mice per patient sample or cell line in future pre-clinical drug efficacy tests. This strategy would lower costs and increase throughput, two key factors in *in vivo* drug screens. An attractive alternative to mice in this respect are zebrafish. James Amatruda presented a chemical suppressor screen in a *mitfa:EWS-FLI1* transgenic zebrafish model. EWS-FLI1 is well tolerated by melanocytes which increase in number due to oncogene expression. Drug-induced reduction in melanocytes can therefore be used as a surrogate readout for activity against EWS-FLI1 driven cell proliferation. Testing 1200 compounds, they identified activity for several kinase inhibitors, bisphosphonates and, interestingly, pro-estrogens and anti-androgens.

For an anti-cancer drug to be effective, it needs to reach its target via the blood stream. However, about 50% of tumor vessels are non-functional. Therefore normalization of the tumor vasculature should improve drug delivery. Keri Schadler reported that vascular shear stress, which is induced in endothelial cells by the blood flow in response to aerobic exercise, induces functional tumor vasculature and increases chemotherapeutic efficacy, as exemplified for doxorubicin. She presented data identifying a role for nuclear factor of activated T cells (NFAT) c1 and thrombospondin TSP1 in the normalization of the tumor vasculature.

Whole genome sequencing technologies have provided ultimate proof that cancers are vastly different from normal tissues and that some of these differences will be recognized by the immune system if immune checkpoints can be overcome. Identification of mechanisms by which tumor cells manipulate the immune system is of critical importance for developing strategies that reverse tumor-induced immunosuppression and sensitize tumor cells to lysis by preexisting or therapeutic effector cells. Cellular imunotherapies for Ewing sarcoma are under development but have not yet been effective. In many cancers, the number of mutations predicts response to checkpoint targeting drugs (i.e. anti-PDL1 and -PD1 antibodies). Since the mutational landscape of Ewing

sarcoma is relatively quiet, the question arises if this type of cancer is sensitive to immunotherapy. As a first step to address this problem, Claudia Rössig reported preliminary results on local expression of the immune-inhibitory ligand PD-L1 and the non-classical HLA molecule HLA-G in the Ewing sarcoma microenvironment, as determined by immunohistochemistry in pre-therapy tumor biopsies.

In addition to the *EWSR1-ETS* gene fusion, Ewing sarcoma is characterized by high CD99 expression. Katia Scotlandi explored the therapeutic potential of targeting this enigmatic surface glycoprotein. She presented new results on non-apoptotic tumor cell killing by the murine monoclonal antibody O662 and a human, CD99-directed single chain antibody. This type of cell death is initiated by HRAS and RAC-1 activation and dysregulation of micropinocytosis, and is insensitive to overexpression of anti-apoptotic Bcl2 family members and ERK activation. Dysregulation of RAS signaling in Ewing sarcoma may also be deduced from work presented by Florencia Cidre-Aranaz. She observed EWS-FLI1 mediated suppression of the fibroblast growth factor receptor (FGFR) antagonist sprouty 1 (SPRY1). FGFR1 has been recently demonstrated to be active in Ewing sarcoma [9]. SPRY1 antagonizes ERK activation of RAS and acts as a tumor suppressor in Ewing sarcoma cells reducing proliferation and migration when ectopically overexpressed. Florencia Cidre-Aranaz reported that increased SPRY1 expression was associated with a better relapse-free and overall survival, while low SPRY1 levels associated with increased metastasis in patients. These data may provide a rationale to consider therapeutic use of FGFR1 and RAS inhibitors in the treatment of Ewing sarcoma.

PROGRESS SINCE THE FIRST INTERDISCIPLINARY EWING SARCOMA RESEARCH SUMMIT

In-depth genome and transcriptome sequencing studies identified widespread dynamic inter- and intra-tumor heterogeneity of Ewing sarcoma down to the single cell level. The rapid expansion and spread of sophisticated novel next generation sequencing applications beyond RNA and genome analysis have provided unprecedented insights into chromatin dynamics. Most importantly, it has become clear that reprogramming of the epigenome and alternative RNA splicing downstream of EWS-FLI1 play central roles in Ewing sarcoma pathogenesis and may therefore provide novel therapeutic targets. As the epigenome serves the ultimate "receptor" for developmental and microenvironmental signaling cues, we have started to understand how tissue context, architecture, and metabolic state may influence tumor growth with implications for therapy response. For the first time, a mouse model of Ewing sarcoma is on the horizon based on developmentally tightly timed EWS-FLI1 expression in the bone mesenchyme, which has the potential of speeding-up preclinical drug development in the near future.

CONCLUSIONS

Ewing sarcoma remains a monstrous disease to patients, families, doctors and scientists. It hatches from the malicious activities of EWS-ETS fusion proteins as the egg, bred by some neural crest or mesenchyme derived stem cell at a defined developmental stage, as parental hen and rooster. Researchers at the ASSET/ENCCA meeting discussed the role of the soil - the microenvironment, and the seed - a susceptible genetic background, which are required to feed the chick to become the monster that is so difficult to tame. Laboratory data, both mature and preliminary, were presented in support of new treatment concepts in the war against Ewing sarcoma, including the use of epigenetic and specific pathway-directed drugs targeting the tumor and its microenvironment (Figure 1). To enable the next step along the path to clinical translation of these promising insights, pre-clinical compound testing in animal and/or 3D culture systems, it was recognized that the field would greatly benefit from an exchange platform to allow for sharing of cell lines and models, omic and linked clinical data, standard operating procedures and harmonization of protocols. The group agreed that the atmosphere of trust, openness and cooperativeness demonstrated at this meeting should facilitate the establishment of an international working group to put in place a common database that keeps memory of tested compounds and systems. This would be required for efficient prioritization of novel drugs for further pre-clinical and clinical development, which may hopefully lead to a major transition in the way patients with Ewing sarcoma are treated. Such a working group should also involve patient advocacy groups in the hope that they may help obtain sustained funding sources for this endeavor. With their support, ASSET and ENCCA tried to pave the way, but with termination of these projects in 2016, novel funding strategies are needed to keep up the fruitful momentum of the "Second European Interdisciplinary Ewing Sarcoma Research Summit".

ACKNOWLEDGMENTS AND FUNDING

We thank Anirah Amber and Nuno Andrade for excellent organization of the meeting. The conference was supported by the European Union's Seventh Framework Programme grants 261743(ENCCA) and 259348 (ASSET).

CONFLICTS OF INTEREST

There is no conflict of interest.

REFERENCES

1. Gaspar N, Hawkins DS, Dirksen U, Lewis IJ, Ferrari S, Le Deley MC, Kovar H, Grimer R, Whelan J, Claude L, Delattre O, Paulussen M, Picci P, Sundby Hall K, van den Berg H, Ladenstein R, et al. Ewing Sarcoma: Current Management and Future Approaches Through Collaboration. J Clin Oncol. 2015.
2. Gorlick R, Janeway K, Lessnick S, Randall RL, Marina N and Committee COGBT. Children's Oncology Group's 2013 blueprint for research: bone tumors. Pediatric blood & cancer. 2013; 60:1009-1015.
3. Esiashvili N, Goodman M and Marcus RB, Jr. Changes in incidence and survival of Ewing sarcoma patients over the past 3 decades: Surveillance Epidemiology and End Results data. J Pediatr Hematol Oncol. 2008; 30:425-430.
4. Kovar H, Alonso J, Aman P, Aryee DN, Ban J, Burchill SA, Burdach S, De Alava E, Delattre O, Dirksen U, Fourtouna A, Fulda S, Helman LJ, Herrero-Martin D, Hogendoorn PC, Kontny U, et al. The first European interdisciplinary ewing sarcoma research summit. Front Oncol. 2012; 2:54.
5. Brohl AS, Solomon DA, Chang W, Wang J, Song Y, Sindiri S, Patidar R, Hurd L, Chen L, Shern JF, Liao H, Wen X, Gerard J, Kim JS, Lopez Guerrero JA, Machado I, et al. The Genomic Landscape of the Ewing Sarcoma Family of Tumors Reveals Recurrent STAG2 Mutation. PLoS Genet. 2014; 10:e1004475.
6. Crompton BD, Stewart C, Taylor-Weiner A, Alexe G, Kurek KC, Calicchio ML, Kiezun A, Carter SL, Shukla SA, Mehta SS, Thorner AR, de Torres C, Lavarino C, Sunol M, McKenna A, Sivachenko A, et al. The genomic landscape of pediatric Ewing sarcoma. Cancer discovery. 2014; 4:1326-1341.
7. Lawrence MS, Stojanov P, Mermel CH, Robinson JT, Garraway LA, Golub TR, Meyerson M, Gabriel SB, Lander ES and Getz G. Discovery and saturation analysis of cancer genes across 21 tumour types. Nature. 2014; 505:495-501.
8. Tirode F, Surdez D, Ma X, Parker M, Le Deley MC, Bahrami A, Zhang Z, Lapouble E, Grossetete-Lalami S, Rusch M, Reynaud S, Rio-Frio T, Hedlund E, Wu G, Chen X, Pierron G, et al. Genomic landscape of Ewing sarcoma defines an aggressive subtype with co-association of STAG2 and TP53 mutations. Cancer discovery. 2014; 4:1342-1353.
9. Agelopoulos K, Richter GH, Schmidt E, Dirksen U, von Heyking K, Moser B, Klein HU, Kontny U, Dugas M, Poos K, Korsching E, Buch T, Weckesser M, Schulze I, Besoke R, Witten A, et al. Deep Sequencing in Conjunction with Expression and Functional Analyses Reveals Activation of FGFR1 in Ewing Sarcoma. Clin Cancer Res. 2015.
10. Riggi N, Knoechel B, Gillespie SM, Rheinbay E, Boulay G, Suva ML, Rossetti NE, Boonseng WE, Oksuz O, Cook EB, Formey A, Patel A, Gymrek M, Thapar V, Deshpande V, Ting DT, et al. EWS-FLI1 utilizes divergent chromatin remodeling mechanisms to directly activate or repress enhancer elements in Ewing sarcoma. Cancer Cell. 2014; 26:668-681.
11. Tomazou EM, Sheffield NC, Schmidl C, Schuster M, Schonegger A, Datlinger P, Kubicek S, Bock C and Kovar H. Epigenome Mapping Reveals Distinct Modes of Gene Regulation and Widespread Enhancer Reprogramming by the Oncogenic Fusion Protein EWS-FLI1. Cell reports. 2015.
12. Sankar S, Theisen ER, Bearss J, Mulvihill T, Hoffman LM, Sorna V, Beckerle MC, Sharma S and Lessnick SL. Reversible LSD1 inhibition interferes with global EWS/ETS transcriptional activity and impedes Ewing sarcoma tumor growth. Clin Cancer Res. 2014; 20:4584-4597.
13. Calzone L, Barillot E and Zinovyev A. Predicting genetic interactions from Boolean models of biological networks. Integrative biology : quantitative biosciences from nano to macro. 2015; 7:921-929.
14. Tanaka M, Yamaguchi S, Yamazaki Y, Kinoshita H, Kuwahara K, Nakao K, Jay PY, Noda T and Nakamura T. Somatic chromosomal translocation between Ewsr1 and Fli1 loci leads to dilated cardiomyopathy in a mouse model. Scientific reports. 2015; 5:7826.
15. Tanaka M, Yamazaki Y, Kanno Y, Igarashi K, Aisaki K, Kanno J and Nakamura T. Ewing's sarcoma precursors are highly enriched in embryonic osteochondrogenic progenitors. The Journal of clinical investigation. 2014; 124:3061-3074.
16. Sparmann A and van Lohuizen M. Polycomb silencers control cell fate, development and cancer. Nature reviews. 2006; 6:846-856.
17. von Levetzow C, Jiang X, Gwye Y, von Levetzow G, Hung L, Cooper A, Hsu JH and Lawlor ER. Modeling initiation of Ewing sarcoma in human neural crest cells. PLoS ONE. 2011; 6:e19305.
18. Svoboda LK, Harris A, Bailey NJ, Schwentner R, Tomazou E, von Levetzow C, Magnuson B, Ljungman M, Kovar H and Lawlor ER. Overexpression of HOX genes is prevalent in Ewing sarcoma and is associated with altered epigenetic regulation of developmental transcription programs. Epigenetics. 2014; 9:1613-1625.
19. Killian JK, Kim SY, Miettinen M, Smith C, Merino M, Tsokos M, Quezado M, Smith WI, Jr., Jahromi MS, Xekouki P, Szarek E, Walker RL, Lasota J, Raffeld M, Klotzle B, Wang Z, et al. Succinate dehydrogenase mutation underlies global epigenomic divergence in gastrointestinal stromal tumor. Cancer discovery. 2013; 3:648-657.
20. Tirode F, Laud-Duval K, Prieur A, Delorme B, Charbord P and Delattre O. Mesenchymal stem cell features of Ewing tumors. Cancer Cell. 2007; 11:421-429.
21. Scannell CA, Pedersen EA, Mosher JT, Krook MA, Nicholls LA, Wilky BA, Loeb DM and Lawlor ER. LGR5 is Expressed by Ewing Sarcoma and Potentiates Wnt/beta-Catenin Signaling. Front Oncol. 2013; 3:81.
22. Santoro M, Lamhamedi-Cherradi SE, Menegaz BA,

Ludwig JA and Mikos AG. Flow perfusion effects on three-dimensional culture and drug sensitivity of Ewing sarcoma. Proceedings of the National Academy of Sciences of the United States of America. 2015; 112:10304-10309.

23. Qiu B and Simon MC. Oncogenes strike a balance between cellular growth and homeostasis. Seminars in cell & developmental biology. 2015.

24. El-Naggar AM, Veinotte CJ, Cheng H, Grunewald TG, Negri GL, Somasekharan SP, Corkery DP, Tirode F, Mathers J, Khan D, Kyle AH, Baker JH, LePard NE, McKinney S, Hajee S, Bosiljcic M, et al. Translational Activation of HIF1alpha by YB-1 Promotes Sarcoma Metastasis. Cancer Cell. 2015; 27:682-697.

25. Somasekharan SP, El-Naggar A, Leprivier G, Cheng H, Hajee S, Grunewald TG, Zhang F, Ng T, Delattre O, Evdokimova V, Wang Y, Gleave M and Sorensen PH. YB-1 regulates stress granule formation and tumor progression by translationally activating G3BP1. The Journal of cell biology. 2015; 208:913-929.

26. Postel-Vinay S, Veron AS, Tirode F, Pierron G, Reynaud S, Kovar H, Oberlin O, Lapouble E, Ballet S, Lucchesi C, Kontny U, Gonzalez-Neira A, Picci P, Alonso J, Patino-Garcia A, de Paillerets BB, et al. Common variants near TARDBP and EGR2 are associated with susceptibility to Ewing sarcoma. Nature genetics. 2012.

27. Grunewald TG, Bernard V, Gilardi-Hebenstreit P, Raynal V, Surdez D, Aynaud MM, Mirabeau O, Cidre-Aranaz F, Tirode F, Zaidi S, Perot G, Jonker AH, Lucchesi C, Le Deley MC, Oberlin O, Marec-Berard P, et al. Chimeric EWSR1-FLI1 regulates the Ewing sarcoma susceptibility gene EGR2 via a GGAA microsatellite. Nature genetics. 2015; 47:1073-1078.

28. Marques Howarth M, Simpson D, Ngok SP, Nieves B, Chen R, Siprashvili Z, Vaka D, Breese MR, Crompton BD, Alexe G, Hawkins DS, Jacobson D, Brunner AL, West R, Mora J, Stegmaier K, et al. Long noncoding RNA EWSAT1-mediated gene repression facilitates Ewing sarcoma oncogenesis. The Journal of clinical investigation. 2014; 124:5275-5290.

29. Kennedy AL, Vallurupalli M, Chen L, Crompton B, Cowley G, Vazquez F, Weir BA, Tsherniak A, Parasuraman S, Kim S, Alexe G and Stegmaier K. Functional, chemical genomic, and super-enhancer screening identify sensitivity to cyclin D1/CDK4 pathway inhibition in Ewing sarcoma. Oncotarget. 2015; 6:30178-93. doi: 10.18632/oncotarget.4903.

30. Tang SW, Bilke S, Cao L, Murai J, Sousa FG, Yamade M, Rajapakse V, Varma S, Helman LJ, Khan J, Meltzer PS and Pommier Y. SLFN11 Is a Transcriptional Target of EWS-FLI1 and a Determinant of Drug Response in Ewing Sarcoma. Clin Cancer Res. 2015.

31. Ordonez JL, Amaral AT, Carcaboso AM, Herrero-Martin D, Del Carmen Garcia-Macias M, Sevillano V, Alonso D, Pascual-Pasto G, San-Segundo L, Vila-Ubach M, Rodrigues T, Fraile S, Teodosio C, Mayo-Iscar A, Aracil M, Galmarini CM, et al. The PARP inhibitor olaparib enhances the sensitivity of Ewing sarcoma to trabectedin. Oncotarget. 2015; 6:18875-18890. doi 10.18632/oncotarget.4303.

32. Brenner JC, Feng FY, Han S, Patel S, Goyal SV, Bou-Maroun LM, Liu M, Lonigro R, Prensner JR, Tomlins SA and Chinnaiyan AM. PARP-1 inhibition as a targeted strategy to treat Ewing's sarcoma. Cancer research. 2012; 72:1608-1613.

33. Grohar PJ, Segars LE, Yeung C, Pommier Y, D'Incalci M, Mendoza A and Helman LJ. Dual targeting of EWS-FLI1 activity and the associated DNA damage response with trabectedin and SN38 synergistically inhibits Ewing sarcoma cell growth. Clin Cancer Res. 2014; 20:1190-1203.

34. Selvanathan SP, Graham GT, Erkizan HV, Dirksen U, Natarajan TG, Dakic A, Yu S, Liu X, Paulsen MT, Ljungman ME, Wu CH, Lawlor ER, Uren A and Toretsky JA. Oncogenic fusion protein EWS-FLI1 is a network hub that regulates alternative splicing. Proceedings of the National Academy of Sciences of the United States of America. 2015; 112:E1307-1316.

35. Toretsky JA and Wright PE. Assemblages: functional units formed by cellular phase separation. The Journal of cell biology. 2014; 206:579-588.

Journal of Human Genetics (2016), 1–4

www.nature.com/jhg

SHORT COMMUNICATION

Familial retinoblastoma due to intronic LINE-1 insertion causes aberrant and noncanonical mRNA splicing of the *RB1* gene

Carlos Rodríguez-Martín[1], Florencia Cidre[1], Ana Fernández-Teijeiro[2], Gema Gómez-Mariano[1], Leticia de la Vega[1], Patricia Ramos[1], Ángel Zaballos[3], Sara Monzón[1,4] and Javier Alonso[1]

Retinoblastoma (RB, MIM 180200) is the paradigm of hereditary cancer. Individuals harboring a constitutional mutation in one allele of the *RB1* gene have a high predisposition to develop RB. Here, we present the first case of familial RB caused by a *de novo* insertion of a full-length long interspersed element-1 (LINE-1) into intron 14 of the *RB1* gene that caused a highly heterogeneous splicing pattern of *RB1* mRNA. LINE-1 insertion was inferred by mRNA studies and full-length sequenced by massive parallel sequencing. Some of the aberrant mRNAs were produced by noncanonical acceptor splice sites, a new finding that up to date has not been described to occur upon LINE-1 retrotransposition. Our results clearly show that RNA-based strategies have the potential to detect disease-causing transposon insertions. It also confirms that the incorporation of new genetic approaches, such as massive parallel sequencing, contributes to characterize at the sequence level these unique and exceptional genetic alterations.
Journal of Human Genetics advance online publication, 14 January 2016; doi:10.1038/jhg.2015.173

Retinoblastoma (RB, MIM 180200) is an embryonic neoplasm of retinal origin with an incidence of 1 in 15 000–20 000 live births.[1,2] Approximately 40% of the patients harbor a constitutional mutation in one allele of the *RB1* gene, which predisposes to develop RB.[3] Here, we report an RB family with two affected members that harbor an exceptional mutational event in the *RB1* gene leading to hereditary RB. The proband and his father were diagnosed with bilateral RB at the age of 4 and 18 months, respectively, and were referred to our laboratory to identify the mutation that predisposed to RB in this family. Research was approved by the institutional ethics committee of the Instituto de Salud Carlos III and written consent were obtained from all members of the family. Proband's blood DNA was first screened for mutations in *RB1* gene using a standard strategy (polymerase chain reaction (PCR) sequencing of all exons and promoter and multiplex ligation-dependent probe amplification),[4,5] but no causative mutations were identified. Thus, we subsequently analyzed *RB1* mRNA isolated from peripheral leukocytes to identify putative intronic mutations that could affect splicing.[6,7]

RB1 cDNA was reverse transcription-PCR amplified in three overlapping fragments (exons 1–8, 7–17 and 16–27). As shown in Figure 1a, reverse transcription-PCR of exons 7–17 showed a highly heterogeneous aberrant splicing pattern produced by skipping of exons 14, 15 or 16 and/or inclusion of cryptic exons of variable length (Figure 1b and Supplementary Figures S1A and H). BLAST analysis (http://blast.ncbi.nlm.nih.gov/Blast.cgi) of the cryptic exons showed a 98% homology of these sequences with the 5′ end of the long interspersed element-1 (LINE-1) transposons family[8] (Figure 1b).

We next performed a PCR assay with primers localized in the cryptic exons (LINE-1 sequences) and in the exon 14 of the *RB1* (Figure 2a) to confirm at the genomic level this mutation. This assay rendered a specific amplicon in the two affected members of the family (proband and his father) but not in the unaffected ones (proband's brother and father's parents), demonstrating that the mutation was a *de novo* event occurring for the first time in the proband's father.

To characterize the complete LINE-1 sequence inserted in the *RB1* gene, we performed a long-PCR assay from introns 13 to 15. Sequencing of the amplicon obtained by Roche/454 massive parallel sequencing confirmed that it contained a full-length LINE-1 (6.044 bp) and adjacent intronic and exonic sequences derived from *RB1* (Figure 2b). The complete sequence of the LINE-1 and surrounding *RB1* exons has been deposited in GenBank database under the accession number KU308246. According to this sequence

[1]Unidad de Tumores Sólidos Infantiles, Área de Genética Humana, Instituto de Investigación de Enfermedades Raras (IIER), Instituto de Salud Carlos III (ISCIII), Madrid, Spain; [2]Unidad de Gestión Clínica Intercentros de Oncología Pediátricas, Hospitales Universitarios Virgen Macarena y Virgen del Rocío, National Reference Unit for Retinoblastoma, Sevilla, Spain; [3]Unidad de Genómica, Centro Nacional de Microbiología, Instituto de Salud Carlos III, Madrid, Spain and [4]Centro de Investigación Biomédica en Red de Enfermedades Raras (CIBERER U758), Instituto de Salud Carlos III, Madrid, Spain
Correspondence: Dr J Alonso, Unidad de Tumores Sólidos Infantiles, Área de Genética Humana, Instituto de Investigación de Enfermedades Raras (IIER), Instituto de Salud Carlos III (ISCIII), Ctra. Majadahonda-Pozuelo Km 2, Majadahonda, Madrid 28220, Spain.
E-mail: fjalonso@isciii.es
Received 17 October 2015; revised 21 December 2015; accepted 25 December 2015

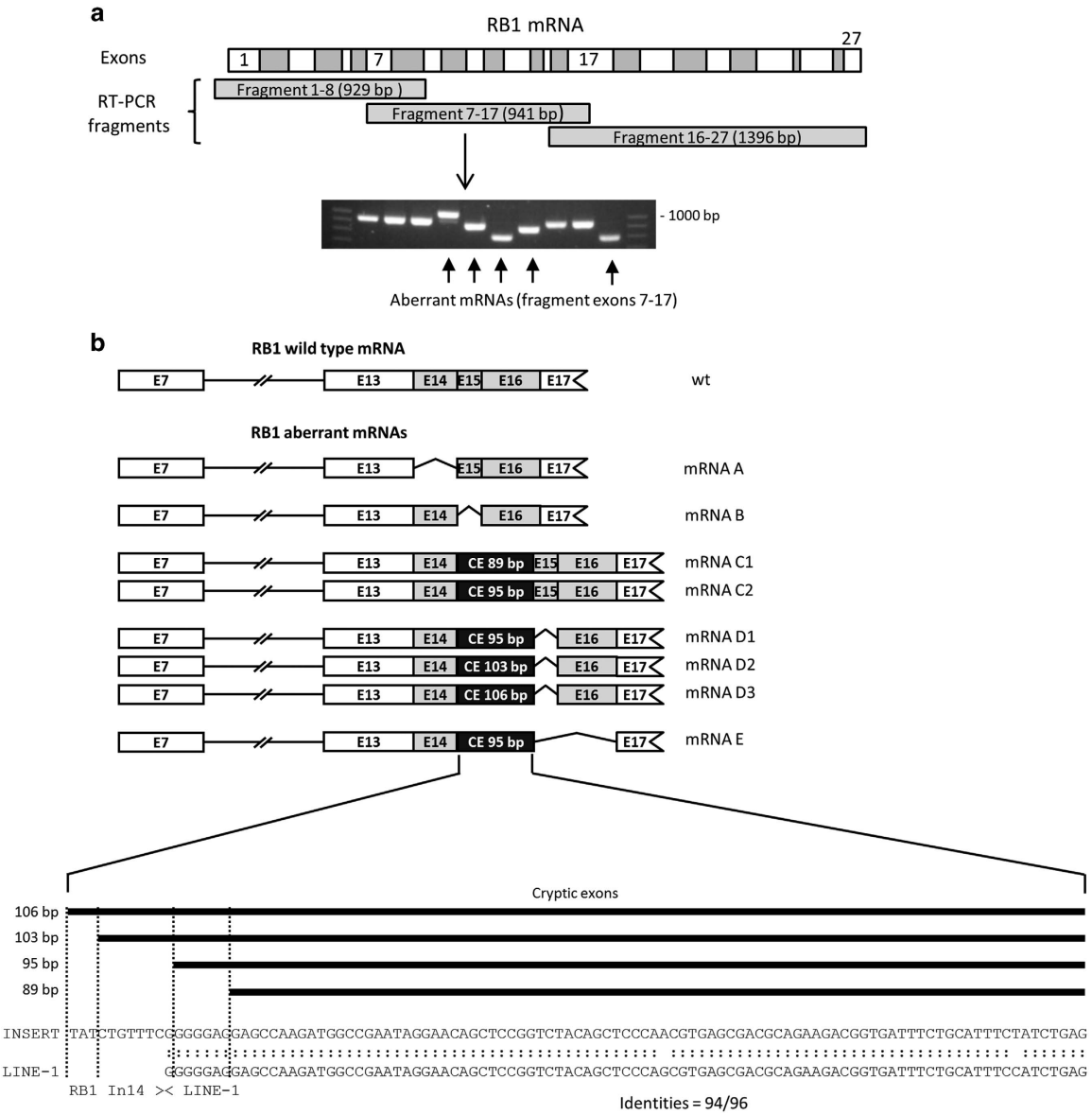

Figure 1 Characterization of retinoblastoma 1 (*RB1*) mRNA aberrant splicing in the retinoblastoma patient. (**a**) RNA isolated from peripheral blood leukocytes of the proband and his affected father were amplified by reverse transcription-polymerase chain reaction (RT-PCR) in three overlapping fragments. Amplicons obtained were then analyzed by gel electrophoresis, cloned in pGEM-T vector and sequenced to identify aberrant mRNA products. No aberrant mRNAs were observed in fragments covering exons 1–8 and exons 16–27. By contrast, 20% (11 out of 54) of the clones derived from cDNA fragments covering exons 7–17 showed an aberrant pattern. The figure shows representative PCR-amplified inserts derived from clones covering exons 7–17. Inserts which sizes differed from the expected correspond to aberrant mRNAs and are marked with an arrow. (**b**) Scheme of the different types of aberrant *RB1* mRNAs identified. The aberrant transcripts were produced by skipping of exons 14, 15 or 16 (gray boxes) or by integration of new cryptic exons (CE, black boxes) of variable length (89, 95, 103 and 106 bp), with or without additionally skipped exons. All cryptic exons shared a 89-nucleotide common sequence but had different 5′ end sequences. Each aberrant mRNA was predicted to codify a non-functional RB1 protein (i.e. truncated proteins with premature stop codons or aberrant mRNAs lacking in-frame exon 14). BLAST analysis of the cryptic exon sequences showed a high homology with the long interspersed element-1 (LINE-1) consensus sequence.

the LINE-1 was inserted at position chr13:48954187_48954188 (GRCh37/hg19 assembly), disrupting the intron 14/exon 15 boundary of the *RB1* gene (NM_000321.2:c.1390-2insL1) (Supplementary Figure S2).

We performed an *in silico* analysis using L1Xplorer tool (http://line1.bioapps.biozentrum.uni-wuerzburg.de/l1xplorer.php)[9] to characterize the functional elements of LINE-1 in detail. This analysis showed that 24 out of 25 parameters analyzed were conserved (Figure 2c), including the most characteristic domains of LINE-1 that are key for its function (5′-untranslated region, open reading frame-1 and open reading frame-2, the 66-bp intergenic spacer, a polyadenylation signal and a 33 bp 3′-A-tail).[10] This analysis suggest that this LINE-1 could potentially remain active and be capable of secondary retrotransposition events, as it has been previously reported in two other cases of full-length LINE-1 insertions (β-globin gene and retinitis pigmentosa-2 gene).[11] In agreement with this, the LINE-1 inserted in the *RB1* gene was highly homologous to one of the most active LINE-1s (hot LINE-1s) described in humans[12] (Figure 2c). An

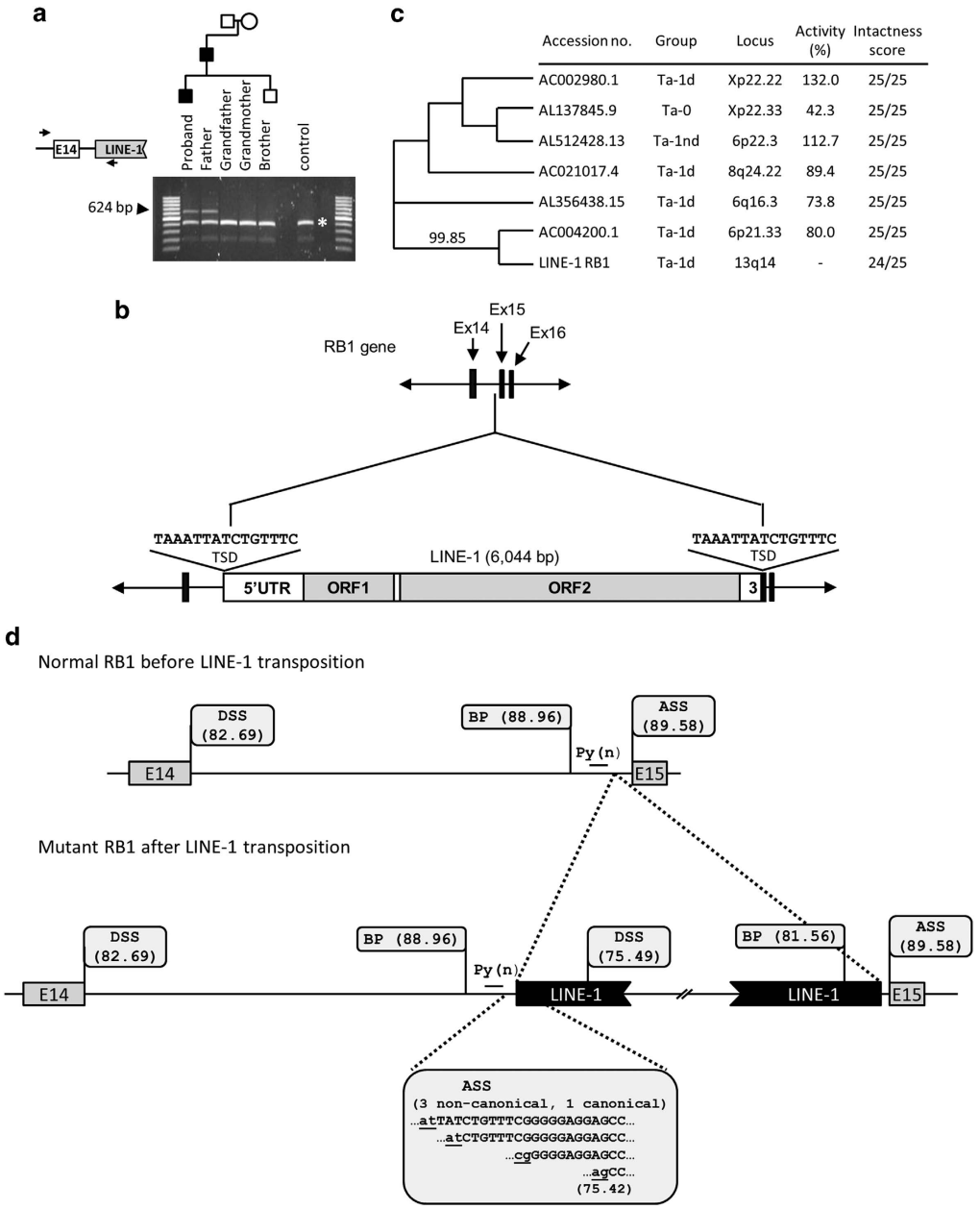

Figure 2 Comprehensive genomic characterization of long interspersed element-1 (LINE-1) retrotransposition in the retinoblastoma 1 (*RB1*) gene and its effects on consensus splicing motifs. (**a**) A PCR assay using a forward primer localized in intron 13 of *RB1*, close to exon 14, and a reverse primer derived from the LINE-1 fragment integrated in the aberrant transcripts, was designed to confirm the insertion of the LINE-1 at the genomic level. An amplicon with the expected size (arrowhead on the left) was detected in the affected members of the family (the proband and his father), but was not observed in the unaffected members (a proband's brother and the father's parents), indicating that this assay has diagnostic value. An unspecific amplicon (asterisk on the right) was observed in all DNA analyzed. DNA from an unrelated individual was used as control. (**b**) The scheme shows the complete genomic structure of the LINE-1 insertion in the context of the *RB1* gene. To obtain the complete sequence of the LINE-1, a long-PCR assay from intron 13–15 of *RB1* gene was performed. Next, the 6.7 kb amplicon obtained was sequenced by Roche/454 massive parallel sequencing. A total of 24 723 reads were obtained and assembled using gsAssembler v.2.8 software (Roche, Branford, CT, USA), obtaining a unique contig of 6655 bp, with a 243x median depth per nucleotide. This contig contained a full-length LINE-1 (6.044 bp) that conserved the key LINE-1s functional domains. Tandem segmental duplication (TSD)[8] repeats characteristic of LINE-1 retrotransposition are also shown. (**c**) DNA phylogenetic analysis (ClustalW-Phylogeny, http://www.ebi.ac.uk/)[18] carried out with the six more active LINE-1s in the human genome (hot LINE-1s)[12] and the LINE-1 characterized in this work. The new LINE-1 inserted in the *RB1* gene was highly homologous to a LINE-1 located in chromosome 6p21 (NCBI accession number AC004200.1). Percent identity between both LINE-1s is shown. Transposon activity as reported in Brouha *et al.*[12] is specified. Intactness score indicates the number of LINE-1 functional parameters tested by the L1Xplorer tool that are conserved versus the total of parameters analyzed. (**d**) Scheme representing the splicing motifs and their location before and after LINE-1 retrotransposition. Branch points (BP), Polypyrimidine tracks ((Py)n) and acceptor/donor splice sites (ASS, DSS) are indicated. Exonized sequences are shown in capital letters. BP and splice sites scores were calculated with Human Splice Finder tool and showed within parentheses when available.

alignment of both sequences with indication of the changes observed is shown in Supplementary Figure S3.

In an attempt to explain the different aberrant mRNAs observed, we analyzed in detail the impact of LINE-1 insertion on the consensus sequences involved in mRNA processing using the Human Splice Finder tool (HSF) (http://www.umd.be/HSF/).[13] Since the LINE-1 was inserted between the polypyrimidine track located in intron 14 and the AG dinucleotide of the acceptor site of exon 15, LINE-1 sequences replaced the original branch point and polypyrimidine track (Figure 2d). *In silico* analysis of the new context showed a new branch point with a high score (81.56) provided by the LINE-1 sequence that could be used during splicing of exon 15. However, a consensus polypyrimidine track was not found, which is expected to severely affect exon recognition. In agreement with this, nearly 50% of the aberrant mRNA species identified lacked exon 15.

As a consequence of the LINE-1 transposition, the polypyrimidine track and the high score branch point site situated in intron 14 were then placed upstream the LINE-1 itself (Figure 2d). Consequently, the cryptic exons detected used three noncanonical acceptor splice sites (AT, AT and CG) derived from intron 14 of *RB1* and one canonical acceptor splice site (AG) situated in the LINE-1 sequence (HSF score 75.42). Of note, although the canonical splice site was disrupted, the original branch point and polypyrimidine track placed upstream LINE-1 transposon were still strong enough to provoke the exonization of intronic/LINE-1 sequences. All cryptic exons used a single canonical GT donor splice site located at position 97 of the LINE-1 consensus sequence (HSF score 75.49). This splice donor site was also observed in two cases of partial LINE-1 exonization in genes *ABHD5* and *NF1* (neurofibromatosis type I).[14,15]

The RB case reported here indicates that while standard mutational screening are effective to detect the majority of the mutations causing familial RB,[16] *ad hoc* strategies should be achieve to resolve some cases. This study exemplified how an RNA-based mutation analysis in combination with massive parallel sequencing may be an effective method to identify retrotransposon insertions. In this line, all 18 pathogenic insertions of LINE-1s and Alu elements in the *NF1* gene reported by Wimmer *et al.*[15] were identified because they altered transcripts splicing.

We reported here the first case of familial RB caused by retrotransposition of a LINE-1 into *RB1* gene and provided a comprehensive analysis of the effects caused by this LINE-1 insertion on *RB1* mRNA splicing. Interestingly, until now only three cases of LINE-1 insertions have been associated to familial cancer: a case of familial adenomatous polyposis[17] and two cases of NF1,[15,17] which suggest that these mutations are probably underrepresented because these events may be overlooked by the most commonly used mutation detecting methods that rely on PCR amplification of small amplicons (i.e. exons from genomic DNA). We propose that in some cases a combination of RNA-based strategies and massive parallel sequencing can be useful to identify and characterize the causative mutation in hereditary diseases. The characterization of these rare events can help to design specific PCR assays to screen the presence of the mutation in the family, providing a simple genetic test for future screening of other first degree relatives (including prenatal testing).

Nucleotide data

The nucleotide sequence data reported is available in the GenBank database under the accession number KU308246.

CONFLICT OF INTEREST

The authors declare no conflict of interest.

ACKNOWLEDGEMENTS

This study was funded by grants of the Instituto de Salud Carlos III (PI12/00816 and RTICC RD12/0036/0027). CR-M was supported by a MINNECO contract. FC was supported by Asociación Pablo Ugarte and Miguelañez SA. SM was supported by a CIBERER contract. We greatly appreciate the collaboration of the RB patients, their parents and their families.

1 Lohmann, D. Retinoblastoma. *Adv. Exp. Med. Biol.* **685**, 220–227 (2010).
2 Dimaras, H., Kimani, K., Dimba, E. A., Gronsdahl, P., White, A., Chan, H. S. *et al.* Retinoblastoma. *Lancet* **379**, 1436–1446 (2012).
3 Valverde, J. R., Alonso, J., Palacios, I. & Pestana, A. RB1 gene mutation up-date, a meta-analysis based on 932 reported mutations available in a searchable database. *BMC Genet.* **6**, 53 (2005).
4 Alonso, J., Garcia-Miguel, P., Abelairas, J., Mendiola, M., Sarret, E., Vendrell, M. T. *et al.* Spectrum of germline RB1 gene mutations in Spanish retinoblastoma patients: phenotypic and molecular epidemiological implications. *Hum. Mutat.* **17**, 412–422 (2001).
5 Parsam, V. L., Kannabiran, C., Honavar, S., Vemuganti, G. K. & Ali, M. J. A comprehensive, sensitive and economical approach for the detection of mutations in the RB1 gene in retinoblastoma. *J. Genet.* **88**, 517–527 (2009).
6 Parsam, V. L., Ali, M. J., Honavar, S. G., Vemuganti, G. K. & Kannabiran, C. Splicing aberrations caused by constitutional RB1 gene mutations in retinoblastoma. *J. Biosci.* **36**, 281–287 (2011).
7 Dehainault, C., Michaux, D., Pages-Berhouet, S., Caux-Moncoutier, V., Doz, F., Desjardins, L. *et al.* A deep intronic mutation in the RB1 gene leads to intronic sequence exonisation. *Eur. J. Hum. Genet.* **15**, 473–477 (2007).
8 Ostertag, E. M. & Kazazian, H. H. Jr. Biology of mammalian L1 retrotransposons. *Annu. Rev. Genet.* **35**, 501–538 (2001).
9 Penzkofer, T., Dandekar, T. & Zemojtel, T. L1Base: from functional annotation to prediction of active LINE-1 elements. *Nucleic Acids Res.* **33**, D498–D500 (2005).
10 Beck, C. R., Garcia-Perez, J. L., Badge, R. M. & Moran, J. V. LINE-1 elements in structural variation and disease. *Annu. Rev. Genomics Hum. Genet.* **12**, 187–215 (2011).
11 Kimberland, M. L., Divoky, V., Prchal, J., Schwahn, U., Berger, W. & Kazazian, H. H. Jr. Full-length human L1 insertions retain the capacity for high frequency retrotransposition in cultured cells. *Hum. Mol. Genet.* **8**, 1557–1560 (1999).
12 Brouha, B., Schustak, J., Badge, R. M., Lutz-Prigge, S., Farley, A. H., Moran, J. V. *et al.* Hot L1s account for the bulk of retrotransposition in the human population. *Proc. Natl Acad. Sci. USA* **100**, 5280–5285 (2003).
13 Desmet, F. O., Hamroun, D., Lalande, M., Collod-Beroud, G., Claustres, M. & Beroud, C. Human Splicing Finder: an online bioinformatics tool to predict splicing signals. *Nucleic Acids Res.* **37**, e67 (2009).
14 Samuelov, L., Fuchs-Telem, D., Sarig, O. & Sprecher, E. An exceptional mutational event leading to Chanarin–Dorfman syndrome in a large consanguineous family. *Br. J. Dermatol.* **164**, 1390–1392 (2011).
15 Wimmer, K., Callens, T., Wernstedt, A. & Messiaen, L. The NF1 gene contains hotspots for L1 endonuclease-dependent de novo insertion. *PLoS Genet.* **7**, e1002371 (2011).
16 Price, E. A., Price, K., Kolkiewicz, K., Hack, S., Reddy, M. A., Hungerford, J. L. *et al.* Spectrum of RB1 mutations identified in 403 retinoblastoma patients. *J. Med. Genet.* **51**, 208–214 (2014).
17 Miki, Y., Nishisho, I., Horii, A., Miyoshi, Y., Utsunomiya, J., Kinzler, K. W. *et al.* Disruption of the APC gene by a retrotransposal insertion of L1 sequence in a colon cancer. *Cancer Res.* **52**, 643–645 (1992).
18 Larkin, M. A., Blackshields, G., Brown, N. P., Chenna, R., McGettigan, P. A., McWilliam, H. *et al.* Clustal W and Clustal X version 2.0. *Bioinformatics* **23**, 2947–2948 (2007).

Supplementary Information accompanies the paper on Journal of Human Genetics website (http://www.nature.com/jhg)